



PHD

Synthesis and thermal studies of boron-containing heterosiloxanes, and their relevance to ceramic formation

Behebehani, Haider S. J.

Award date:
1994

Awarding institution:
University of Bath

[Link to publication](#)

Alternative formats

If you require this document in an alternative format, please contact:
openaccess@bath.ac.uk

Copyright of this thesis rests with the author. Access is subject to the above licence, if given. If no licence is specified above, original content in this thesis is licensed under the terms of the Creative Commons Attribution-NonCommercial 4.0 International (CC BY-NC-ND 4.0) Licence (<https://creativecommons.org/licenses/by-nc-nd/4.0/>). Any third-party copyright material present remains the property of its respective owner(s) and is licensed under its existing terms.

Take down policy

If you consider content within Bath's Research Portal to be in breach of UK law, please contact: openaccess@bath.ac.uk with the details. Your claim will be investigated and, where appropriate, the item will be removed from public view as soon as possible.

SYNTHESIS AND THERMAL STUDIES OF
BORON-CONTAINING HETEROSILOXANES, AND THEIR
RELEVANCE TO CERAMIC FORMATION

A thesis submitted by **Haider S J Behebehani** for the degree of
Doctor of Philosophy of the University of Bath

1994

Attention is drawn to the fact that the copyright of this thesis rests with its author. This copy of the thesis has been supplied on condition that anyone who consults it is understood to recognise that its copyright rests with its author and that no quotation from the thesis and no information derived from it may be published without the prior written consent of the author.

This thesis may be made available for consultation within the University of Bath library and may be photocopied or lent to other libraries for the purpose of consultation.



UMI Number: U602098

All rights reserved

INFORMATION TO ALL USERS

The quality of this reproduction is dependent upon the quality of the copy submitted.

In the unlikely event that the author did not send a complete manuscript and there are missing pages, these will be noted. Also, if material had to be removed, a note will indicate the deletion.



UMI U602098

Published by ProQuest LLC 2014. Copyright in the Dissertation held by the Author.
Microform Edition © ProQuest LLC.

All rights reserved. This work is protected against
unauthorized copying under Title 17, United States Code.



ProQuest LLC
789 East Eisenhower Parkway
P.O. Box 1346
Ann Arbor, MI 48106-1346

UNIVERSITY OF CATH
LIBRARY
21 17 MAY 1994
PHD
5079849

DEDICATION

This thesis is dedicated to my parents and my wife with my son
abudallah for their support during the course of this study

ACKNOWLEDGEMENT

I would like to express my thanks and appreciation to Dr. B J Brisdon and Prof B McEnaney for their supervision and advice throughout the course of this study.

I also would like to record my thanks to the staff of the School of Chemistry especially to Dr. M Mahon for carrying out the x-ray crystallography measurements. I am also grateful to Dr. S Parker for his assistance in using the crystal modelling computer program. Also I would like to thank the staff of the School of Materials Science in the University of Bath for their assistance during the course of this work.

LIST OF COMPOUNDS

compound 1	$\text{Me}_2(\text{HO})\text{SiOSi}(\text{OH})\text{Me}_2$
compound 2	$\text{Ph}_2(\text{HO})\text{SiOSi}(\text{OH})\text{Ph}_2$
compound 3	$\text{Ph}_2(\text{HO})\text{SiOSi}(\text{Ph}_2)\text{OSi}(\text{OH})\text{Ph}_2$
compound 4	$[\text{PhBO}]_3^*$
compound 5	$\text{c-Cy}(\text{HO})_2\text{SiOSi}(\text{OH})_2\text{c-Cy}$
compound 6	$\text{c-Cy}_6\text{Si}_6\text{O}_9$
compound 7	$\text{c-Cy}_7\text{Si}_7\text{O}_9(\text{OH})_3$
compound 8	$[\text{c-Cy}_7\text{Si}_7\text{O}_{12}\text{B}]_2$
compound 9	$[\text{Ph}_2\text{B}_2\text{O}_4\text{Si}_2\text{Ph}_4]^*$
compound 10	$[\text{PhBO}_3\text{Si}_2\text{Ph}_4]^*$
compound 11	$[\text{MeBO}_3\text{Si}_2\text{Me}_4]^*$
compound 12	$[\text{PhBO}_3\text{Si}_2\text{Me}_4]^*$
compound 13	$[\text{Me}_2\text{B}_2\text{O}_4\text{Si}_2\text{Ph}_4]^*$
compound 14	$\text{Ph}_2(\text{H})\text{SiOB}(\text{Ph})\text{OSi}(\text{H})\text{Ph}_2$
compound 15	$\text{Ph}_3\text{SiOB}(\text{OSiPh}_3)\text{OSiPh}_3$
compound 16	$\text{Ph}_3\text{SiOB}(\text{Ph})\text{OSiPh}_3$
compound 17	$\text{Ph}_3\text{SiOB}(\text{Me})\text{OSiPh}_3$
compound 18	$\text{Ph}_2(\text{H})\text{SiOB}(\text{Me})\text{OSi}(\text{H})\text{Ph}_2$
compound 19	$[\text{Me}_2\text{Si}(\text{BPhNH})_2\text{NH}]^*$
'compound 20'	$[(\text{MeSi})(\text{PhMeSi})_y]_n$

* cyclic

LIST OF TABLES

1.1	Atomic properties of silicon and carbon	4
1.2	Average bond energies and calculated ionic character of selected silicon and carbon bonds	4
1.3	Structural units of poly(organosiloxanes)	6
1.4	Properties and application of poly(diorganosiloxanes)	24
2.1	Bond energies	35
3.1	Methods for sintering ceramics	61
3.2	Properties of special ceramics	61
5.1	Fractional atomic coordinates and thermal parameters (Å) for $\text{Cy}_6\text{Si}_6\text{O}_9$, compound 6	120
5.2	Selected bond lengths (Å) and bond angles (°) for $\text{Cy}_6\text{Si}_6\text{O}_9$, compound 6	122
5.3	Comparative geometric data for organosiloxanes and related compounds	
5.4	Fractional atomic coordinates and thermal parameters (Å) for $\text{Ph}_2(\text{HO})\text{SiOSi}(\text{Ph}_2)\text{OSi}(\text{OH})\text{Ph}_2$, compound 3	131
5.5	Selected bond lengths (Å) and bond angles (°) for $\text{Ph}_2(\text{HO})\text{SiOSi}(\text{Ph}_2)\text{OSi}(\text{OH})\text{Ph}_2$, compound 3	132
5.6	Fractional atomic coordinates and thermal parameters (Å) for $\text{PhB}(\text{Ph}_3\text{SiO})_2$, compound 16	137
5.7	Selected bond lengths (Å) and bond angles (°) for $\text{PhB}(\text{Ph}_3\text{SiO})_2$, compound 16	138
5.8	Comparative geometric data for $\text{PhB}(\text{Ph}_3\text{SiO})_2$ (compound 16) and related compounds	139
5.9	Fractional atomic coordinates and thermal parameters (Å) for $\text{Me}_2\text{Si}(\text{PhBNH})_2\text{NH}$, compound 19	143
5.10	Selected bond lengths (Å) and bond angles (°) for $\text{Me}_2\text{Si}(\text{PhBNH})_2\text{NH}$, compound 19	144
5.11	Comparative geometric data for $\text{Me}_2\text{Si}(\text{PhBNH})_2\text{NH}$ (compound 19) and related compounds	145
6.1	Experimental conditions for the pyrolysis process using thermogravimetric analysis	151
6.2	Analysis of the solid residue from the heat treatment up to 1400°C of $\text{Ph}_2\text{B}_2(\text{OSiPh}_2)_2\text{O}_2$ and $\text{PhB}[(\text{OSiPh}_2)_2\text{O}]$ (compounds 9 and 10 respectively)	174

6.3 Quantitative results of B_4C microcrystals
present in the solid residue from the heat treatment at
1700°C of $Ph_2B_2(OSiPh_2)_2O_2$ and $PhB(OSiPh_2)_2O$
(compounds 9 and 10 respectively) with standard B_4C
crystals by SEM probe analyser

178

LIST OF FIGURES

1.1	Thermal gravimetric analysis, (TGA) of a silanol terminated polymer	22
1.2	Effect of thermal degradation on the molecular weight of silanol terminated PDMS	22
3.1	Structural changes accompanying the manufacture of a sintered product	59
3.2	Powder synthesis methods	59
3.3	Forming methods of ceramics	59
3.4	Functions and applications of fine ceramics	62
3.5	Schematic representation of a commercial process for producing partially stabilised zirconia powder by a coprecipitation process	65
3.6	Schematic of the three types of sintering	68
3.7	Schematic of the various sol-gel processing routes	72
3.8	Typical reaction pathway for producing an alkoxide gel	72
3.9	Organosilicon-derived ceramic fibre and composite main routes to silicon carbide	76
5.1	The asymmetric unit of $\text{Cy}_6\text{Si}_6\text{O}_9$, compound 6	118
5.2	The sesquisiloxanes cage of $\text{Cy}_6\text{Si}_6\text{O}_9$, compound 6 showing the crown configuration of the Si_4O_4 rings	119
5.3	The asymmetric unit of $\text{Ph}_2(\text{HO})\text{SiOSi}(\text{Ph}_2)\text{OSi}(\text{OH})\text{Ph}_2$, compound 3	128
5.4	The dimer arrangements in $(\text{HO})\text{Ph}_2\text{SiOSiPh}_2\text{OSiPh}_2(\text{OH})$ and $(\text{HO})^t\text{Bu}_2\text{SiOSiMe}_2\text{OSi}^t\text{Bu}_2(\text{OH})$ (a and b respectively), viewed orthogonal to the approximate planes of the individual molecules	129
5.5	The dimer arrangements in $(\text{HO})\text{Ph}_2\text{SiOSiPh}_2\text{OSiPh}_2(\text{OH})$ and $(\text{HO})^t\text{Bu}_2\text{SiOSiMe}_2\text{OSi}^t\text{Bu}_2(\text{OH})$ (a and b respectively), viewed perpendicular to the approximate planes of the individual molecules	130
5.6	The asymmetric unit of $\text{PhB}(\text{Ph}_3\text{SiO})_2$, compound 16	136
5.7	The asymmetric unit of $\text{Me}_2\text{Si}(\text{PhBNH})_2\text{NH}$, compound 19	142
6.1	Schematic diagram of the main components of the SETARAM TGA-92 equipment	150
6.2	Weight losses versus time for $\text{Ph}_2\text{B}_2(\text{OSiPh}_2)_2\text{O}_2$,	

	PhB[(OSiPh ₂) ₂ O] and PhB(OSiPh ₂ H) ₂ (compounds 9, 10 and 14 respectively) heated at 220°C	157
6.3	Mass spectrum of the volatile product from Ph ₂ B ₂ (OSiPh ₂) ₂ O ₂ , compound 9 heated at 220°C for 3 hours	158
6.4	Infra-red spectrum of the final residue heated at 220°C from Ph ₂ B ₂ (OSiPh ₂) ₂ O ₂ , compound 9	159
6.5a	Thermogravimetric analysis of Ph ₂ B ₂ (OSiPh ₂) ₂ O ₂ , compound 9, from room temperature to 1200°C in a stream of helium	165
6.5b	Thermogravimetric analysis of Ph ₂ B ₂ (OSiPh ₂) ₂ O ₂ , compound 9, from room temperature to 1200°C in a stream of air	166
6.6a	Thermogravimetric analysis of PhB[(OSiPh ₂) ₂ O], compound 10, from room temperature to 1200°C in a stream of helium	167
6.6b	Thermogravimetric analysis of PhB[(OSiPh ₂) ₂ O], compound 10, from room temperature to 1200°C in a stream of air	168
6.7	Scanning electron micrographs of amorphous SiC from Ph ₂ B ₂ (OSiPh ₂) ₂ O ₂ , compound 9, pyrolysed to 1200°C under an inert atmosphere	169
6.8a	Energy dispersive x-ray analysis of the 1200°C solid residue formed under an inert atmosphere for Ph ₂ B ₂ (OSiPh ₂) ₂ O ₂ , compound 9	170
6.8b	Energy dispersive x-ray analysis of the 1200°C solid residue formed under an air atmosphere for Ph ₂ B ₂ (OSiPh ₂) ₂ O ₂ , compound 9	171
6.9	Energy dispersive x-ray analysis of the 1200°C solid residue formed under an inert atmosphere for PhB[(OSiPh ₂) ₂ O], compound 10	172
6.10	Thermogravimetric analysis of poly(boradiphenylsiloxane) and poly(boradimethylsiloxane) in a stream of nitrogen gas	173
6.11	Scanning electron micrographs of microcrystalline SiC from Ph ₂ B ₂ (OSiPh ₂) ₂ O ₂ , compound 9, pyrolysed to 1700°C under an inert atmosphere	181
6.12	Scanning electron micrographs of microcrystalline SiC from PhB[(OSiPh ₂) ₂ O], compound 10, pyrolysed to 1700°C under an	

	inert atmosphere	182
6.13	Energy dispersive x-ray analysis of the microcrystalline SiC present in the final solid residue from $\text{Ph}_2\text{B}_2(\text{OSiPh}_2)_2\text{O}_2$, compound 9, heated to 1700°C	183
6.14	Energy dispersive x-ray analysis of the microcrystalline SiC present in the final solid residue from $\text{PhB}[(\text{OSiPh}_2)_2\text{O}]$, compound 10, heated to 1700°C	184
6.15	Energy dispersive x-ray analysis of standard SiC	185
6.16	Scanning electron micrographs of large crystals of B_4C over a microcrystalline SiC matrix formed from $\text{Ph}_2\text{B}_2(\text{OSiPh}_2)_2\text{O}_2$, compound 9, pyrolysed to 1700°C	186
6.17	Scanning electron micrographs of large crystals of B_4C over a microcrystalline SiC matrix formed from $\text{PhB}[(\text{OSiPh}_2)_2\text{O}]$, compound 10, pyrolysed to 1700°C	187
6.18	Energy dispersive x-ray analysis of the large crystals of B_4C embedded on a microcrystalline matrix of SiC in the residual decomposition product of $\text{Ph}_2\text{B}_2(\text{OSiPh}_2)_2\text{O}_2$, compound 9, pyrolysed to 1700°C	188
6.19	Energy dispersive x-ray analysis of the large crystals of B_4C embedded on a microcrystalline matrix of SiC in the residual decomposition product of $\text{PhB}[(\text{OSiPh}_2)_2\text{O}]$, compound 10, pyrolysed to 1700°C	189
6.20	Whisker of B_4C present in the final residual decomposition product of $\text{Ph}_2\text{B}_2(\text{OSiPh}_2)_2\text{O}_2$, compound 9, heated at 1700°C	190
6.21	Scanning electron micrograph of B_4C in a SiC matrix above a computer generated model of B_4C space group $\text{R}_3\text{-MH}$	191
6.22	Phase diagram of SiC and BC	192
6.23	Segregation of the final residual decomposition product from $\text{Ph}_2\text{B}_2(\text{OSiPh}_2)_2\text{O}_2$, compound 9, heated to 1700°C	193
6.24	EDX spectra showing the oxygen concentration at the centre and edge of the dark line of segregation in the final residue of $\text{Ph}_2\text{B}_2(\text{OSiPh}_2)_2\text{O}_2$, compound 9, heated at 1700°C	194
6.25	EDX spectra showing the carbon concentration at the centre	

	and edge of the dark line of segregation in the final residue of $\text{Ph}_2\text{B}_2(\text{OSiPh}_2)_2\text{O}_2$, compound 9, heated at 1700°C	195
6.26	Thermogravimetric analysis up to 1700°C of the residual decomposition product of $\text{Ph}_2\text{B}_2(\text{OSiPh}_2)_2\text{O}_2$, compound 9, then heated to 1200°C in an air stream	196
6.27	Energy dispersive x-ray analysis of the solid residue heated at 1700°C from $\text{Ph}_2\text{B}_2(\text{OSiPh}_2)_2\text{O}_2$, compound 9, then heated to 1200°C in an air stream	197
6.28	Thermogravimetric analysis of $(\text{Me}_2\text{SiO})_3$ in a stream of He	201
6.29	Thermogravimetric analysis of $(\text{Ph}_2\text{SiO})_3$ in a stream of He	202
6.30	Thermogravimetric analysis of $(\text{PhBO})_3$ in a stream of He	203
6.31	Thermogravimetric analysis of $\text{PhB}(\text{OSiPh}_3)_2$, compound 16, to 600°C in a stream of He	204
6.32	Thermogravimetric analysis of $\text{PhB}(\text{OSiPh}_2\text{H})_2$, compound 14, to 800°C in a stream of He	205
6.33	Thermogravimetric analysis of $\text{Me}_2\text{Si}(\text{PhBNH})_2\text{NH}$, compound 19 to 800°C in a stream of He	206
6.34	Thermogravimetric analysis of $(\text{MePhSi})_n(\text{Me}_2\text{Si})_m$, compound 20, to 800°C in a stream of He	209
6.35	Energy dispersive x-ray analysis of the solid residue from $(\text{MePhSi})_n(\text{Me}_2\text{Si})_m$, compound 20, heated at 800°C under an inert atmosphere	210
6.36	Scanning electron micrographs of microcrystalline SiC from $(\text{MePhSi})_n(\text{Me}_2\text{Si})_m$, compound 20, pyrolysed to 1700°C under an inert atmosphere	211
6.37	Thermogravimetric analysis of $\text{Cy}_6\text{Si}_6\text{O}_9$, compound 6, heated from room temperature to 600°C in a stream of He	213
6.38	Energy dispersive x-ray analysis of the residue present after heating of $\text{Cy}_6\text{Si}_6\text{O}_9$, compound 6, heated at 700°C	214
6.39	Energy dispersive x-ray analysis of microcrystalline SiO_2 from $\text{Cy}_6\text{Si}_6\text{O}_9$, compound 6, pyrolysed to 1700°C under an inert atmosphere	215
6.40	Scanning electron micrograph of the residue from $\text{Cy}_6\text{Si}_6\text{O}_9$,	

compound 6, Pyrolysed to 1700°C under an inert atmosphere

216

ABSTRACT

Cyclic heterosiloxanes $[\text{RB}(\text{OSiR}^*_2)\text{O}]_2$ and $\text{RB}[(\text{OSiR}^*_2)\text{O}]_2$; ($\text{R}, \text{R}^* = \text{Me or Ph}$) containing eight- and six-membered rings with 1:1 and 2:1 silicon to boron ratios respectively, which were prepared via the reaction of $\text{RB}(\text{OH})_2$ ($\text{R} = \text{Me or Ph}$) with diphenylsilandiol or 1,1,3,3-tetraphenyl(or tetramethyl)-1,3-dihydroxy-1,3-disiloxane, have been characterised by infrared, ^1H , ^{13}C and ^{29}Si NMR spectroscopies and by mass spectrometry. On thermolysis of the phenyl analogues, ring-opening polymerization and ring-ring transformations occur below 220°C for these strained ring compounds yielding volatile $(\text{PhBO})_3$ together with polymeric borasiloxanes which provide novel silicon carbide precursors. Heat treatment to 1400°C yields an amorphous glassy phase containing carbon, boron, silicon and oxygen. Upon further heating to 1700°C microcrystalline silicon carbide (SiC) is formed together with a few large crystals of boron carbide (B_4C). The identities of the intermediate and final residues of the pyrolysis process have been determined using x-ray diffraction and scanning electron microscopy with energy dispersive x-ray analysis for qualitative measurement, and an electron probe analyser for quantitative measurements.

Linear borosiloxanes $\text{RB}(\text{OSiPh}_n\text{H}_{3-n})_2$; ($\text{R} = \text{Ph, or Me } n = 2 \text{ or } 3$) and $\text{B}(\text{OSiPh}_3)_3$ were prepared by the reaction of $\text{B}(\text{OMe})_3$ or $\text{PhB}(\text{OH})_2$ with triphenylsilanol or diphenylchlorosilane, and their thermolytic behaviour examined. Only compounds with Si-H residues are able to cross-link easily on thermolysis and form polymeric borasiloxanes. The other non-strained linear compounds volatilise completely below 500°C . The cyclic heterosilazane $\text{Me}_2\text{Si}(\text{NHBPh})_2\text{NH}$, containing a six-membered ring, was prepared via the reaction of 2,2,4,4,6,6-hexamethylcyclotrisilazane with dichlorophenylborane. Unlike the cyclic heterosiloxanes above, this compound does not decompose on heating but totally volatilises below 300°C .

The hexacyclohexyl-hexasiloxane, $c\text{-Cy}_6\text{Si}_6\text{O}_9$, and the heptacyclohexyl-heptasiloxane-1,6,7-triol, $[(c\text{-C}_6\text{H}_{11})_7\text{Si}_7\text{O}_9(\text{OH})_3]$, were prepared by controlled hydrolysis of cyclohexyltrichlorosilane. The triol was used to synthesise a

boron containing silsesquioxane, $[(c\text{-C}_6\text{H}_{11})_7\text{Si}_7\text{O}_{12}\text{B}]_2$, by reaction with BI_3 . Thermolysis of $c\text{-Cy}_6\text{Si}_6\text{O}_9$ up to 1700°C under an inert atmosphere forms crystalline silica, whereas under similar conditions $(\text{Ph}_2\text{SiO})_n$ (where $n = 3$ or 4) volatilises.

For comparative purposes a phenylmethyilsilane-dimethylsilane copolymer was thermolysed under similar conditions in order to prepare silicon carbide from an oxygen free polymeric source.

Compound 3, $\text{Ph}_2(\text{HO})\text{SiOSi}(\text{Ph}_2)\text{OSi}(\text{OH})\text{Ph}_2$, compound 6, $c\text{-Cy}_6\text{Si}_6\text{O}_9$, compound 16, $\text{PhB}(\text{Ph}_3\text{SiO})_2$ and compound 19 $\text{Me}_2\text{Si}(\text{PhBNH})_2\text{NH}$, were all characterised for the first time by single crystal x-ray diffraction studies, and their main structural features were discussed in relation to their chemical reactivity.

CONTENTS

Contents

Title and copyright	i
Dedication	ii
Acknowledgement	iii
List of compounds	iv
List of tables	v
List of figures	vii
Abstract	xii
Contents	xiv
Abbreviations	xvii

CHAPTER ONE: Introduction to Siloxanes

1.1	Summary	1
1.2	General consideration	1
1.2.1	Synthesis of poly(organosiloxanes)	10
1.2.2	Properties and applications of poly(organosiloxanes) and their derivatives	16
1.3	References	25

CHAPTER TWO: Introduction to Heterocyclosiloxanes

2.1	Summary	28
2.2	Inorganic ring systems	29
2.3	Structure and bonding in heterocyclic systems containing silicon and boron	33
2.3.1	Heterocycloboroxanes	38
2.3.2	Heterocyclosilazanes	40
2.3.3	Heterocyclosiloxanes	44
2.3.4	Borocyclosiloxanes	49
2.4	References	53

CHAPTER THREE: Introduction to Ceramics and Preceramic Polymers

3.1	Summary	56
-----	---------	----

3.2	General consideration of ceramic materials	57
3.3	Conventional routes to ceramics	63
3.3.1	Precipitation from solution	63
3.3.2	Powder mixing techniques	66
3.3.3	Fusion route to ceramics	66
3.3.4	Ceramic sintering and fabrication	67
3.3.5	Sol-gel techniques	70
3.4	Preceramic polymers (PCP)	73
3.4.1	Silicon-carbon ceramic precursors	77
3.4.2	Silicon-nitrogen ceramic precursors	83
3.4.3	Boron-containing ceramics	86
3.5	References	88

CHAPTER FOUR: Synthesis of Linear and Cyclic Heterosiloxanes

4.1	Summary	91
4.2	Synthetic procedures	92
4.2.1	Preparation of silanols	92
4.2.2	Preparation of silsesquioxanes	95
4.2.3	Synthesis of a silsesquioxanes containing boron	99
4.2.4	Synthesis of heterocyclosiloxanes containing boron	101
4.2.5	Synthesis of linear heterosiloxanes containing boron	106
4.2.6	Synthesis of heterocyclosilazanes containing boron	109
4.2.7	Synthesis of a methylphenylsilane-dimethylsilane copolymer	112
4.3	References	114

CHAPTER FIVE: Structural Characterisation of Model Compounds

5.1	Summary	115
5.2	The structure of hexa(cyclo-hexylsilsesquioxane)	115
5.3	The structure of hexaphenyl-1,3,5-trisiloxane -1,5-diol	124
5.4	The structure of 1,1,1,3,5,5,5-heptaphenyl-3-bora 1,5-siloxane	133
5.5	The structure of 2,2-dimethyl-4,6-diphenyl -1,3,5-triaza-2-sila-4,6-diboracyclohexane	140
5.6	References	147

CHAPTER SIX: Thermolysis of Heterocyclic siloxanes and Related Materials

6.1	Summary	148
6.2	Experimental	148
6.2.1	Low temperature heat treatment	148
6.2.2	Intermediate heat treatment	149
6.2.3	High temperature heat treatment	149
6.3	Results and discussion of the thermolysis processes	153
6.3.1	Low temperature heat treatment of $[\text{PhB}(\text{OSiPh}_2)\text{O}]_2$ and $[\text{PhB}(\text{OSiPh}_2)_2\text{O}]$	153
6.3.2	Intermediate heat treatment of $[\text{PhB}(\text{OSiPh}_2)\text{O}]_2$ and $[\text{PhB}(\text{OSiPh}_2)_2\text{O}]$	160
6.3.3	High temperature heat treatment of $[\text{PhB}(\text{OSiPh}_2)\text{O}]_2$ and $[\text{PhB}(\text{OSiPh}_2)_2\text{O}]$	176
6.4	Thermolysis of other compounds containing Si, C, B and O or N	198
6.5	Thermolysis of a phenylmethylsilane-dimethylsilane copolymer	207
6.6	Thermolysis of silsesquioxanes	212
6.7	Conclusions	217
6.8	Future work	220
6.9	References	222

Appendix I: Safety and reagents

Appendix II: Instrumentation

Appendix III: Supplementary x-ray crystallographic data for compounds 6, 3, 16 and 19.

ABBREVIATIONS

br	broad
b.p.	boiling point
Bu	butyl
CDCl ₃	deuterated chloroform
c-Cy	cyclohexyl
D	difunctional
d	doublet
DMF	N,N-dimethylformamide
en	1,2-diaminoethane
Et	ethyl
GC	gas chromatography
GLC	gas liquid chromatography
h	hour
I	spin isotope
ⁱ Pr	isopropyl
IR	infrared
J	joule
K	kelvin
kJ	kilojoule
l	litre
M	monofunctional
m	medium/multiple
Me	methyl
MHz	megahertz
min	minute
mm/Hg	millimetre of mercury
Mn	molecular weight (weight average)
m.p.	melting point
MS	mass spectrum
MW	molecular weight
NMR	nuclear magnetic resonance
Pa	pascal
PDMS	poly(dimethylsiloxane)
Ph	phenyl
ppm	part per million

py	pyridine
Q	tetrafunctional
q	quartet
R	alkyl group
s	singlet/strong
SEM	scanning electron microscopy
T	trifunctional
t	triplet
TGA	thermogravimetric analysis
THF	tetrahydrofuran
TMS	tetramethylsilane
UV	ultraviolet
v	very
w	weak
X	halide
Å	angstrom
(°)	degree
°C	degree celsius
δ	chemical shift

CHAPTER ONE

INTRODUCTION TO SILOXANES

1.1 SUMMARY

Poly(organosiloxanes) as a generic type are intermediate in composition between the purely inorganic silicates, and organic polymers with a mainly carbon-backbone, and they comprise the only class of semi-inorganic polymer to date which has achieved great commercial importance. Their properties, which reflect their hybrid composition in many respects are reviewed in this chapter. In 1943 the first commercial products based on linear poly(dimethylsiloxanes), $(\text{Me}_2\text{SiO})_n$, were developed by hydrolysis of dichlorodimethylsilane, subsequently specific properties were optimized by controlled cross-linking or by replacing some or all of the methyl groups on the silicon atoms by other substituents. The unique properties possessed by these materials are highly dependent upon the bonding properties and characteristics of the backbone of the polymer, as well as the nature of the substituents. Another class of silanes which has attracted considerable recent attention include polycyclic and cage siloxanes, the silsesquioxanes, based on the $(\text{RSiO}_{3/2})$ repeated unit.

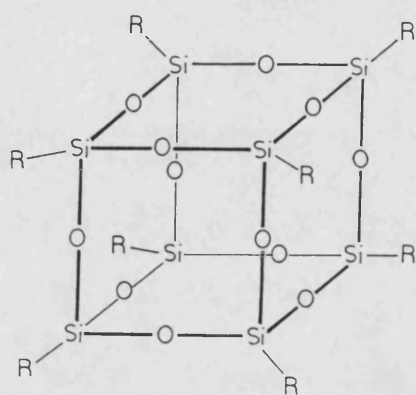
1.2 GENERAL CONSIDERATION

Silicon, a second row element of group IV, has many chemical properties which differ significantly from those of carbon, and a direct comparison of their respective atomic and bonding properties of relevance to this study is instructive¹ (Tables 1.1 and 1.2), and show in particular the exceptional strength of the Si-O and Si-F linkages. The first organosilicon compounds were prepared in 1860 via the reaction of diethylzinc with silicon tetrachloride by Friedel, Crafts and Ladenburg². The availability of the Grignard reaction in 1900 led to the synthesis of a wide variety of organochlorosilanes, from which siloxanes may be obtained by hydrolysis. Polymeric siloxanes were identified by 1937, and in 1940, several groups of investigators focused their attention on various aspects of the synthesis and characterization of polysiloxanes. It was discovered that the thermal and

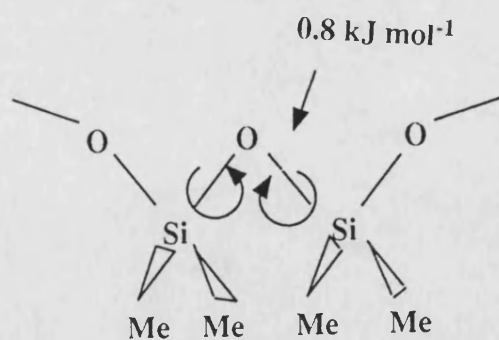
thermoxidative stability of these polymers was far greater than that of most of the common organic polymers, and that their dielectric properties were suitable for high temperature materials³. In 1943 the first commercial products based on poly(dimethylsiloxanes) were developed. These remain the most common of the industrial silicone polymers, as the molecular weight of the material is easily controlled to produce oligomers through to high molecular weight materials. Specific properties can be optimized by controlled cross-linking, by replacing some or all of the methyl groups on the silicon atoms by other substituents or by introducing finely divided solids such as silica into the polymers.

Polysiloxanes have in general high thermal and chemical stabilities, and are resistant to moisture, sunlight, oxygen and ozone, with the nature of the siloxane bonds being an important factor. The basic structural characteristics of polysiloxanes are also dependent on the Si-O bond, which is partially ionic because of the relatively large difference in the electronegativities of silicon and oxygen, (1.8 and 3.5 respectively on the Pauling scale⁴). It may also exhibit very limited double bond character, associated with the overlap of the vacant low energy silicon d-orbitals with the filled p-orbitals of oxygen, which enables oxygen to backdonate its lone-pair electrons and create a partial $d\pi-p\pi$ bond in addition to the normal σ bond, but recent work has cast doubt on this concept⁵. The Si-O bond lengths in siloxanes have been found to vary between 1.63 to 1.66 Å in different compounds⁶. These values are about 10% smaller than the value of 1.83 Å, calculated for a normal σ bond distance between the silicon and oxygen atoms⁷. Thus the siloxane linkage is a strong bond, as reflected in thermochemical data giving Si-O bond energies in the range 420-490 kJ mol⁻¹. The O-Si-O bond angles in siloxanes are normally between 108 and 120°, whilst C-Si-C angles between 106 and 118° are close to the values expected for the angles between essentially single Si(sp³)-C bonds. Values determined for the Si-O-Si angles range from 104 to almost 180°, with angles between 144 and 150° being the most often reported⁸ as illustrated in (I) and are indicative of the minimum energy configuration⁵. This very wide range of bond angles indicates that the

Si-O-Si bond is readily deformed and in general, rotation about the siloxane bond occurs relatively freely, as in the fragment of a dimethylsiloxane polymer⁹ shown in (II). These fundamental characteristics of the siloxane bonds are responsible for many of the important properties of PDMS, including in particular, its pronounced thermal and chemical stability.



(I)



(II)

Table 1.1

Atomic properties of silicon and carbon

Atomic properties	Carbon	Silicon
electronic configuration	[He]2s ² 2p ²	[Ne]3s ² 3p ²
atomic radius	66 pm	106 pm
covalent radius	77 pm	117 pm
effective nuclear charge (Clementi)	3.14	4.29
electronegativity (Pauling)	2.5	1.8

Table 1.2

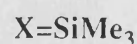
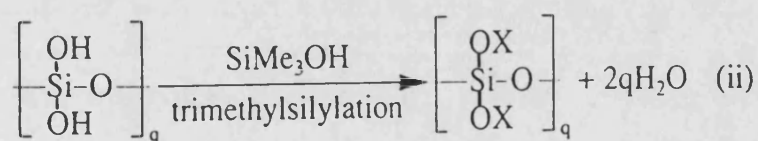
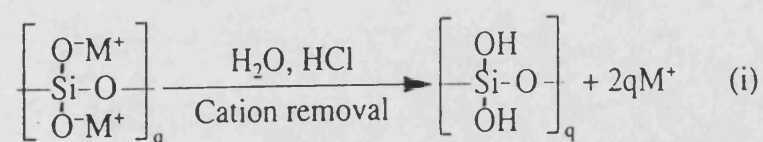
Average bond energies and calculated ionic character of selected silicon and carbon bonds

Silicon Bond	Bond Energy kJ/mol	Ionic Character ^a %	Carbon Bond	Bond Energy kJ/mol	Ionic Character ^a %
Si-Si	226	-	C-Si	301	12
Si-C	302	12	C-C	348	-
Si-H	326	3	C-H	339	4
Si-O	485	51	C-O	355	22
Si-N	355	30	C-N	304	7
Si-F	582	70	C-F	484	43
Si-Cl	391	30	C-Cl	338	7
Si-Br	309	22	C-Br	284	3
Si-I	234	12	C-I	213	0
Si=Si	318	-	C=C	610	-

^a According to Pauling

In general terms, the name silicone is applied to an organosiloxane polymer having silicon atoms bound to each other through oxygen atom links, with the silicon valances not associated with oxygen being saturated by organic groups. It encompasses commercial products containing polymers of various lengths and degrees of cross-linking such as rubbers, resins, oils. The term siloxane is used in systematic terminology.

Their formal derivation from silicates by replacement of one or more oxygen atoms by R groups to form mono-, di-, tri- and tetrafunctional siloxane units is shown in Table 1.3. Indeed, attempts have been made recently to achieve the synthesis of siloxanes directly from mineral silicate materials by trimethylsilylation as shown in the equations below¹⁰:



If the polyorganosiloxane product remains the same size as the silicate anion, that is the value of q remains unchanged. Then the technique allows the original silicate structure to be determined. The polyorganosiloxane products produced above have a general formula Q_xM_y ($\text{Q} = \text{SiO}_4$) and ($\text{M} = \text{Me}_3\text{SiO}_{1/2}$).

Table 1.3

Structural units of poly(organosiloxanes)

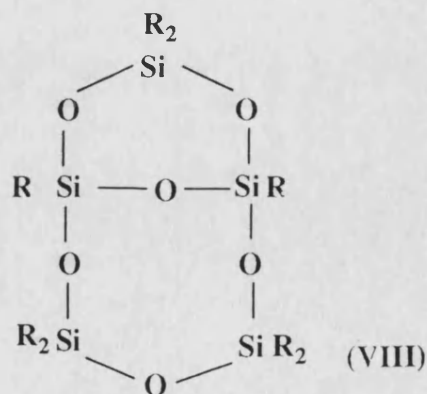
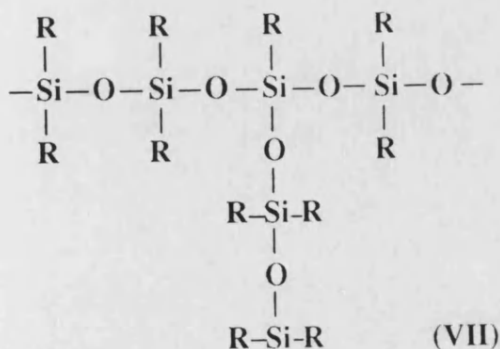
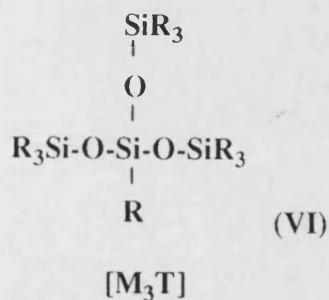
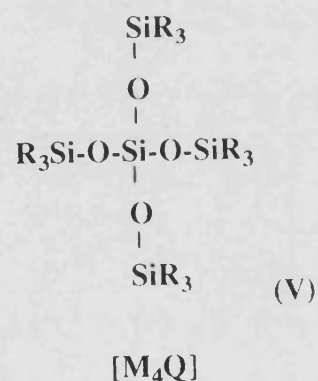
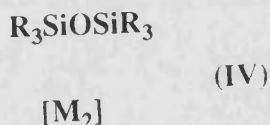
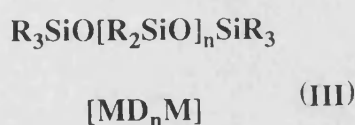
Structural Formula	Functionality and symbol
$\begin{array}{c} \text{R} \\ \\ \text{R}-\text{Si}-\text{O} \\ \\ \text{R} \end{array}$	monofunctional (M)
$\begin{array}{c} \text{R} \\ \\ \text{O}-\text{Si}-\text{O} \\ \\ \text{R} \end{array}$	Difunctional (D)
$\begin{array}{c} \text{O} \\ \\ \text{O}-\text{Si}-\text{O} \\ \\ \text{R} \end{array}$	Trifunctional (T)
$\begin{array}{c} \text{O} \\ \\ \text{O}-\text{Si}-\text{O} \\ \\ \text{O} \end{array}$	Tetrafunctional (Q)

The symbols M, D, T and Q (Table 1.3) have been used to good effect in representing clearly the structures of complex polymer and cage siloxanes. By analogy with organic polymers, siloxanes can be distinguished according to their structural types.

- (i) Linear polysiloxanes correspond to the structural type MD_nM . Oligomeric polysiloxanes having definite low molecular weights which can be isolated by crystallisation or distillation may be prepared by insertion of difunctional units into a hexaorganodisiloxane (III) to give siloxanes of formula (IV). The nature of the organic substituents R largely determines the physicochemical behaviour of linear poly(organosiloxanes) of comparable molecular weights, since only weak intermolecular forces act between siloxane chains which are protected by alkyl substituents. High molecular weight polymers with small aliphatic groups e.g. $R = Me$ are fluids at room temperature, but even small oligomers containing aromatic substituents are solids, e.g. hexaphenyldisiloxane m.p. $226^\circ C$. Modification of linear polysiloxanes can be achieved by insertion of silicon-functional and/or organofunctional atoms into the chain, or by variation of one or both of the organic substituents on silicon. There may be differences in the reactivity between functional groups substituted in D or M units in a polymer (III), and those of the same groups present in monomers (IV). This can be attributed to the effect of steric factors, molecular coiling or substituent inductive effects, transmitted to a limited extent through neighbouring linkages. The average Si-C bond is about 20% longer than the C-C bond, which lowers the steric hindrance in the hydrolysis reactions of organosilicon compounds. For example, Me_3Si- or $t-Bu_3Si-$ groups are not strongly sterically hindering groups in this type of reactions, and both $(Me_3Si)_4C$ and $t-Bu_3SiF$ are stable compounds. However, steric effects are not completely absent and can influence the reactivity of silicon compounds to some extent. Thus, for example, the methylchlorosilanes are

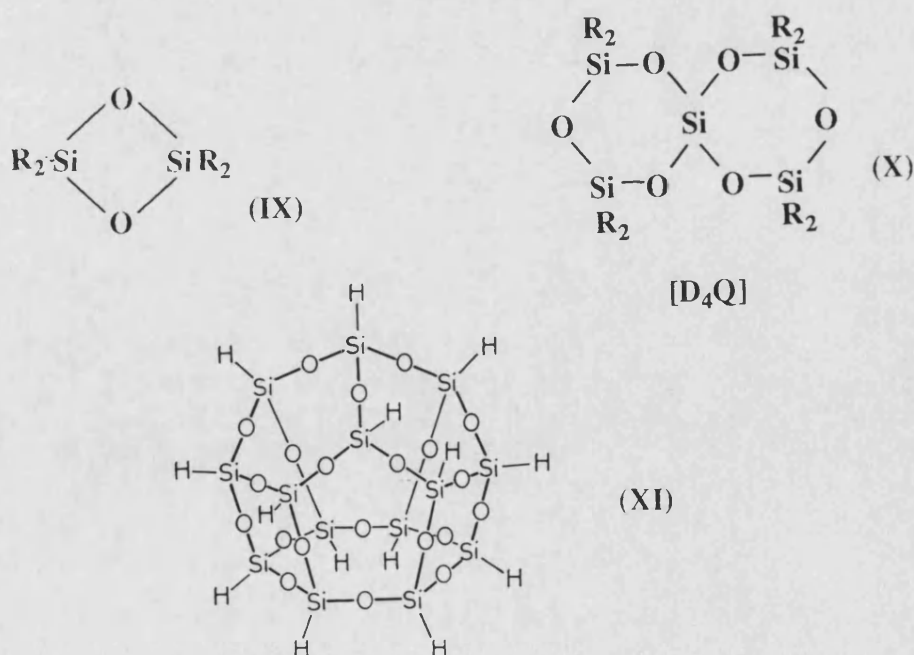
very reactive, but substitution of the methyl groups by larger alkyl or aryl groups generally decreases the reactivity. Similarly within a homologous series of alkylsilanols, the stability of the Si-OH group increases with the size of the alkyl group, and oligomerisation may be entirely prevented.

- (ii) The combination of mono- and tri- or tetra-functional siloxane units leads to low molecular weight structures such as (V) and (VI). Branched-chain polysiloxanes which contain a minimum of one trifunctional T or tetrafunctional Q siloxane unit serve as centres of branching within chain or ring siloxanes (VII) and (VIII). Only relatively few examples are known¹ of oligomeric organosiloxanes of this structural type, which permit branching effects on physicochemical behaviour to be studied.



(iii) A large number of cyclic polysiloxanes have been isolated and characterised.

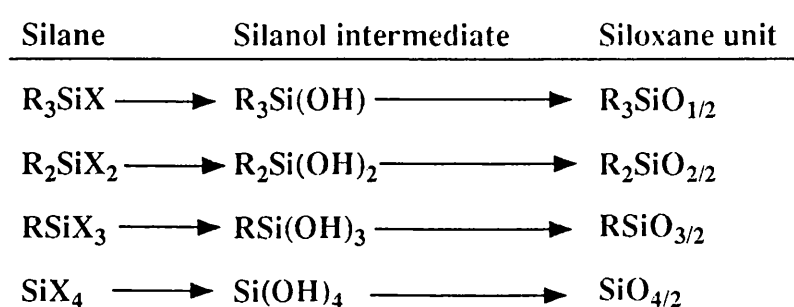
The difunctional D units gives closed rings in combination with one another, and $(R_2SiO)_n$ rings are of great commercial importance as precursor to high molecular weight silicone copolymers¹¹. Examples of rings with 3-15 siloxane units have been obtained by condensation of silandriols, and several cyclic siloxanes have been the subject of x-ray crystallography, with the smallest cyclic molecule being the highly strained dimer containing just two siloxane units¹² (IX). Trifunctional siloxane units combining with one another give molecules cross-linked randomly in three dimension. Under certain conditions small cage like structures, with 4-12 siloxane units which can be interpreted as being polycyclic, have also been obtained¹³. Spirocyclic systems have Q units at the point of linkage which distinguishes them from polycyclic systems such as (X). The tetrahedral coordination of oxygen atoms around a silicon centre in a Q unit, results in the alternate ring planes being perpendicular to one another. A further sub-group of cyclic polymers built up of T units oligomerise to form spherocycles and other polymers (XI)¹⁴.



(iv) Cross-linked polymers consisting of 2- or 3-D networks of linear or cyclic molecules cross-linked by T or Q units have also been characterised¹¹. Besides combinations of two different units of siloxanes, it is also possible to use combinations of three or four different types to construct a particular molecular type. Generally, the D unit is used for chain and ring formation, the M unit as a chain stopper or regulator, and the T or Q units as cross-linking centres.

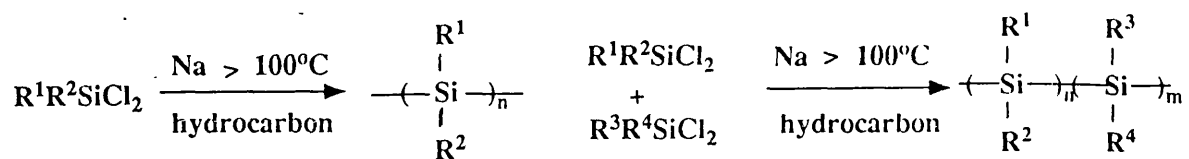
1.2.1 Synthesis of Poly(organosiloxanes)

There are numerous methods available for synthesising poly(organosiloxanes) from monomeric silicon functional organosilanes¹¹. By virtue of simplicity and economy, the most frequently used process involves hydrolysis but other methods use alcohols, alkoxysilanes and inorganic oxides as the source of oxygen for siloxane bond formation¹⁵. The hydrolysis reaction leads initially to silanols, but in view of the instability of many silanols, condensation frequently take place spontaneously, with respect to siloxane bond formation and the elimination of water. The structural siloxane units M, D, T and Q defined previously may be obtained from functionalised silanes accordingly:



Polysilanes as well as polysiloxanes can be synthesized from organochlorosilanes. Thus treatment of diorganodichlorosilane with sodium metal in a hydrocarbon diluent at temperatures above 100°C, yields polysilanes as mixtures of cyclic and linear materials.

Either homopolymers or copolymers can be made because the substituents R^1 - R^4 can be a wide variety of aryl and alkyl groups¹⁶.

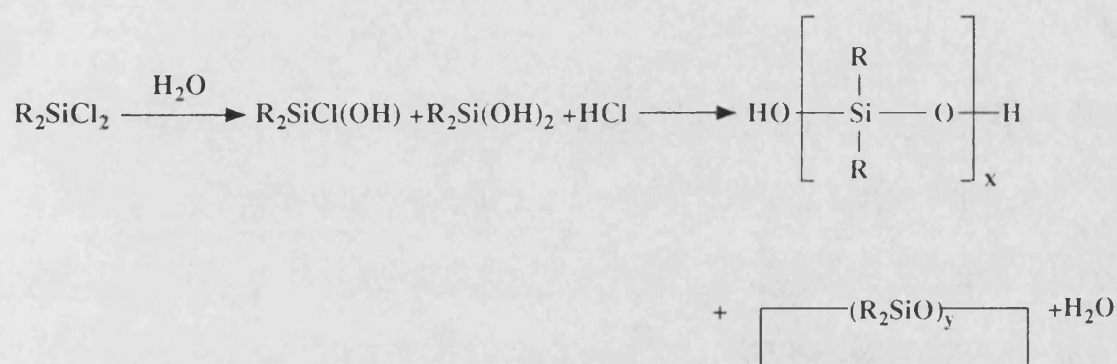


When mixtures of silanes having different functionalities are hydrolysed, the method and conditions used have significant effects on the resultant siloxane with respect to oligomer size and structure. The rate of hydrolysis of SiX bonds (X=halogen) increases with polarity of the Si-X bond and with the number of X atoms or groups bonded to each silicon in the molecule. The rate is also affected by the size and type of organic groups present, since ease of nucleophilic attack by water molecules, and hence scission of the Si-X bond, is diminished with increasing steric hindrance. Thus, phenyl substituted chlorosilanes hydrolyse at a slow rate compared to their methylchlorosilane counterparts. Another consideration that may affect hydrolysis is the nature of the Si-C bond, which is relatively weakly polar, and more sensitive to acids formed during halosilanes hydrolysis than normal C-C bonds^{17,18}.

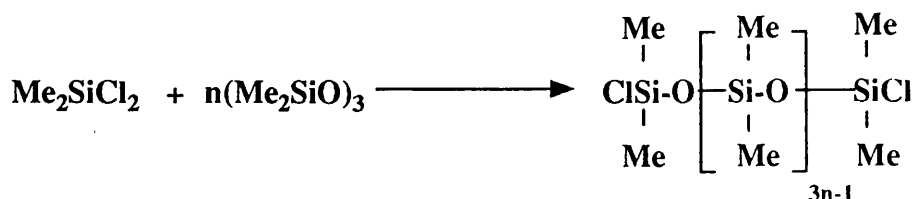
When all these factors have been considered, a suitable method is chosen which must facilitate hydrolysis and condensation to a homo- or copolymer. If different components of the siloxane mixture have very different rates of hydrolysis and/or self-condensation, then a copolymer will not be formed. Sequencing long chain siloxanes is often a major problem but is of commercial importance.

The commercial hydrolysis reaction consists essentially of mixing one or more organohalosilanes (R_nSiX_{4-n}) with excess water and judging the dilution accordingly to prevent strong hydrochloric acid (<20%) from being formed, although this accelerates the self-condensation of silanols. The exothermic reaction is usually cooled and organic solvents, typically toluene, diethyl ether and dibutyl ether, which are either immiscible or

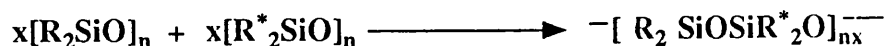
slightly miscible with water and yet show no reactivity toward the halosilane, are often used for dilution, product distribution and separation purposes, since the hydrolysis products are extracted by the solvent and are protected from attack by the strong aqueous acid generated. Dilution of the siloxane phase will promote intramolecular over inter-molecular condensation, and when difunctional silanes such as dimethyldichlorosilane are used low molecular weight poly(cyclosiloxanes) are formed preferentially¹⁹. However, when dimethyldichlorosilane is hydrolysed in water alone, a mixture of linear siloxanediols and cyclosiloxanes are produced, i.e.



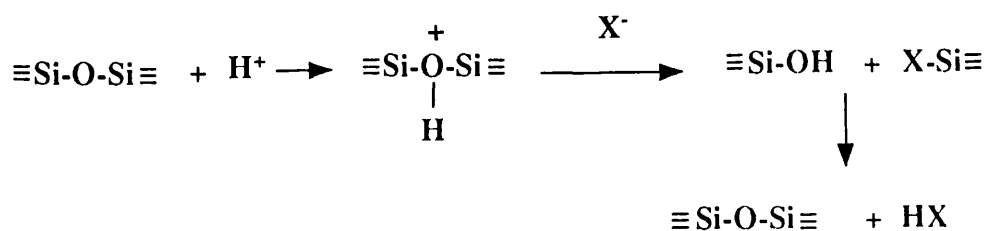
For reactions in which the number of moles of chlorosilane are greater than those of water, polysiloxanes with terminal chlorine atoms are formed. As well as hydrolytic methods of preparing polysiloxanes, other polymerisation procedures utilising thermal, acid and base catalysis, which convert low molecular weight polyorganosiloxanes into high molecular weight products are available. Thus low molecular weight cyclic diorganosiloxanes will rearrange to give high molecular weight polymers when heated to 250-300°C in a closed system. Temperature limits are governed by the cleavage sensitivity of the Si-C bond and on the susceptibility of the organic groups to thermal decomposition. High temperatures and pressures increase the yield of high molecular weight products. If mixed systems such as poly(diorganocyclosiloxanes) and dimethyldichlorosilane are heated in a closed system, then polymerisation and ring opening can give the following types of products.



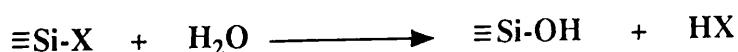
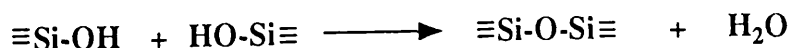
Two organosiloxanes having different substituents and molecular weights can be copolymerised to form only a high molecular weight polysiloxane having a gaussian molecular weight distribution.



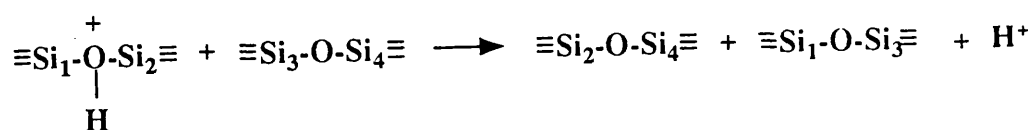
This process involves equilibration of the mixture of polysiloxanes so that cleavage and re-forming of siloxane bonds occurs, so bringing the system to a state of maximum thermodynamic stability based essentially on entropy consideration. Acids and bases are frequently employed as catalysts to accelerate this process and to moderate the reaction conditions. When siloxane bonds are cleaved, the high energy intermediate complexes so formed, spontaneously change to yield low energy polymers, and for every decrease in size of the larger siloxane molecules there is a simultaneous increase in the size of the smaller molecules. The initial step in an acid catalysed polymerisation reaction involves attachment of a proton to the oxygen atom of a siloxane bond to form an oxonium complex. This intermediate is unstable and is susceptible to nucleophilic attack. On decomposing through cleavage of the Si-O link, Si-OH and Si-X bonds react further to regenerate the acid and form a new siloxane linkage. A series of bond scissions and reformations follow to form a polysiloxane chain as a result of a favourable energy gradient.



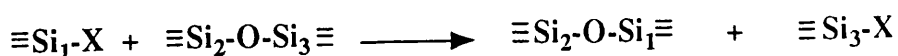
Alternatively, two silanol groupings may condense to form a new siloxane linkage with the elimination of water which can promote further silanol group production through hydrolysis of an Si-X bond, i.e.



An alternative mechanism may occur which involves nucleophilic attack on the oxonium complex by a siloxane oxygen of an unprotonated molecule to form a new siloxane linkage, i.e.



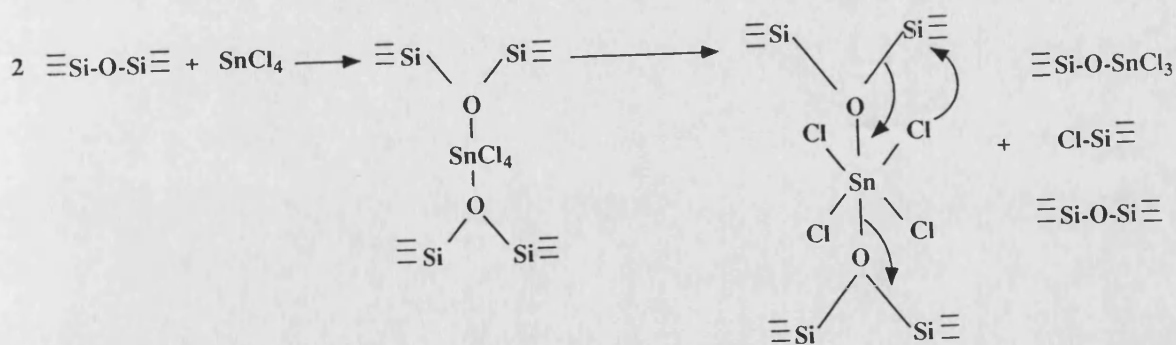
Strong acids are frequently used as catalysts, and acid equilibration of polysiloxanes with organohalosilanes proceeds by an exchange reaction, whereby the silicon atoms of the halosilane become incorporated into the siloxane chain, i.e.



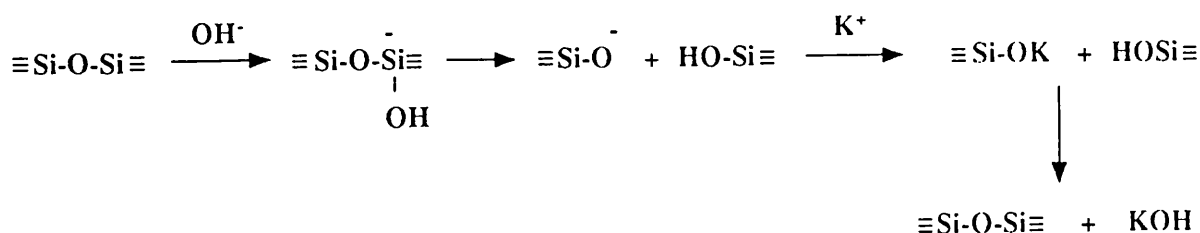
The nature of the substituents strongly influence the reactivity of the Si-O-Si bond in acid catalysis. Increasing the size of the aliphatic substituent decreases the reactivity.

Thus methyl-siloxanes equilibrate and polymerise more quickly than siloxanes with aromatic substituents. Similarly, electron acceptor substituents will decrease reactivity towards acid catalysis. On completion of polymerisation, catalyst removal is generally necessary to prevent any redistribution reaction during the polymer heat ageing process. This can be achieved by careful washing or extraction with water, or by filtration followed by neutralisation.

Lewis acids of the Friedel Crafts type are known to cleave siloxane linkages, and if the reactions involved are reversible then siloxane bond redistribution will occur. The mechanism illustrated below is similar to that of a protic acid, where an oxygen atom of the siloxane initially acts as an electron donor towards the catalyst. The key feature here is the instability of the adduct formed between the siloxane and Lewis acid which decomposes to regenerate the catalyst and a new Si-O bond¹¹.



Polymerisation by base-catalysed reactions are now thought to proceed via ion pairs or charge separated ion pairs in which the cation interacts with oxygens of the siloxanes. These ion pairs dissociate to provide a low concentration of unassociated ion pairs prior to propagation. As with acid catalysts base catalysts promote cleavage and rearrangement of siloxane bonds, leading to polymer formation and regeneration of the catalyst. This process is illustrated in the scheme below:

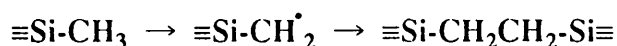


Thus the extent of these reactions are sensitive to the nature of the cation, and to the presence of species more basic than siloxanes that can complex competitively with the cation. As for acid catalysis, the choice of solvent can influence the rate of rearrangement. Increasing the polarity of the solvent results in the formation of a higher concentration of Si-O^- ions, and a fast attainment of equilibrium. Base catalysts can be removed by analogous methods to those described for acid catalyst.

1.2.2 Properties and Application of Poly(organosiloxanes) and their Derivatives

Poly(organosiloxanes) are of increasing interest in science and even more in technology arise mainly from the nature, physical and chemical characteristics of the siloxane Si-O bond which have been discussed earlier in this chapter. These characteristics include a high thermal and oxidative stability, good electrical properties, low surface energy, high hydrophobicity, U.V resistance, a good chemical resistance, film forming ability, water repellent properties, high permeability to many gases, and biocompatibility.

Despite the good overall stability of poly(organosiloxanes), two types of reaction can contribute to severe property changes. Free radical homolytic cleavage of Si-O, Si-C, or C-H bonds can occur, for example on long exposure to air, leading to cross-linking.



More serious degradation occurs under these conditions in the presence of water or alcohol, particularly if traces of acids or bases are generated. The silanol intermediates yield a mixture of linear and cyclic materials by the mechanisms described earlier.

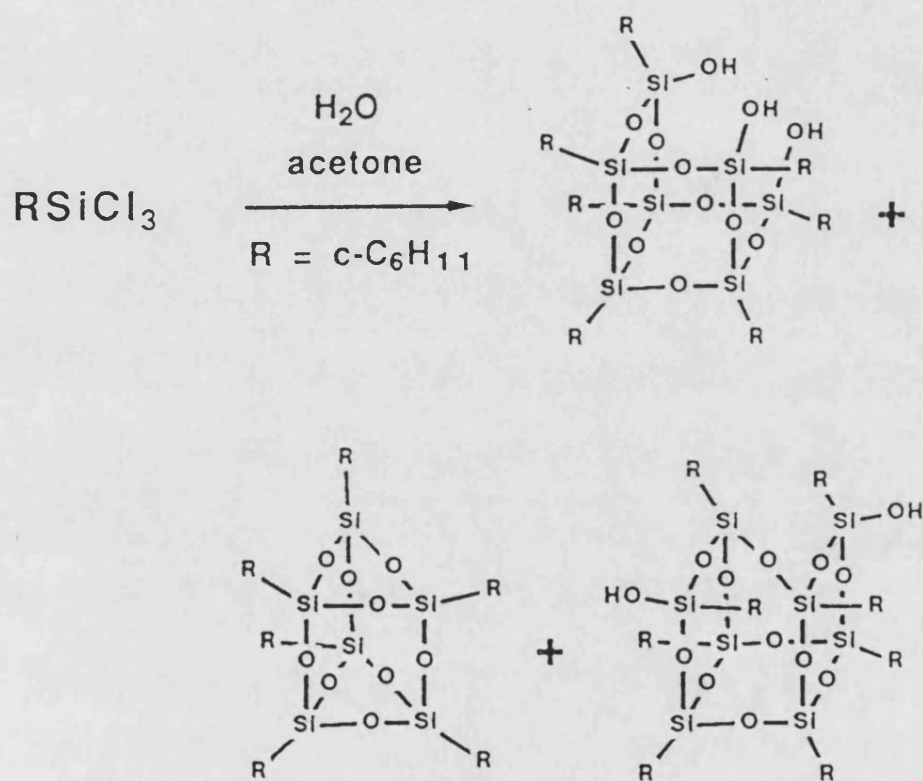
Nevertheless, silicones have numerous applications, many of which are dependent upon their water repellency. Thus silicone elastomers can be used as insulation on wires. Even when the insulation is exposed to high temperatures, properly controlled systems burn to a non-conducting ash, which means that the degraded material may continue to function as insulation in a suitably designed cable²⁰.

The mechanical properties of silicones can also be tailored for many purposes by proper use of cross-linking chemistry. A lightly cross-linked linear siloxane polymer has a low modulus and is quite weak when compared with other polymers and materials. Amorphous silica particles are frequently used to increase tensile strength and also raise the modulus. Recent developments have shown that on rearrangement of cross-links, unique properties can be achieved. The nature of organic substituents strongly affect the electrical properties with hydrocarbon side groups such as *n*-octyl giving resistivities and dielectric constants similar to those of hydrocarbon fluids, whereas very polar groups such as nitrophenyl increase the dielectric constant. The high diffusivity of silicones, combined with high transparency and biological inertness, gives rise to several interesting applications^{21,22} as indicated in Table 1.4.

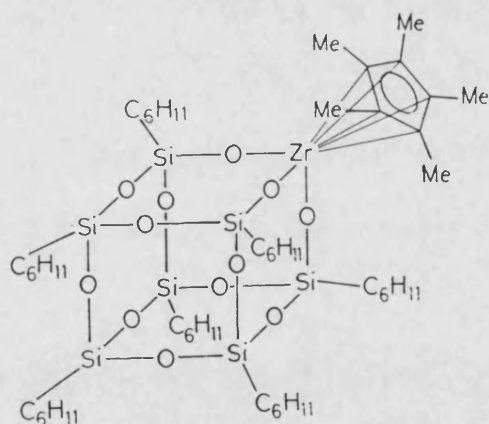
The chemistry of cyclosiloxanes has some biological implications and interest. Thus 2,6-cis-diphenylhexamethylcyclotetrasiloxane has been reported to have oestrogenic antigonadotropic activity in some mammalian species²³. Since (Me₂SiO)₄ is a component

of a lotion for skin care, the toxic and allergenic properties of common cyclosiloxanes have been studied in detail. Other silicon containing compounds exhibit biological activities which are a function of size, configuration and silicon substituents, e.g. trimethylsilanol is a central nervous system depressant. These bio-activities are not always predictable from structure/reactivity considerations, and silicon-containing compounds should always be treated with respect.

Two other classes of siloxanes which are of importance are branched and ladder polymers composed of trifunctional (T) units. Poly(phenylsilsesquioxanes) are used for the preparation of molecular orientation-controlling layers of liquid-crystal display devices. Silsesquioxanes ($\text{RSiO}_{1.5}$)_n are polycyclic, cage-like siloxanes; these compounds have attracted the attention of both academic and industrial laboratories, owing to their interesting properties and possible applications. For example, the addition of oligomeric methylsilsesquioxanes increases the arc resistance of phenyl-formaldehyde resins, and poly(methylsilsesquioxane) based composite materials have a high tensile strength and a low water sorption. The methods of synthesis and structure of silsesquioxanes have been thoroughly investigated. Ethylcyclodisiloxanes and ethylcyclotrisiloxanes, containing silsesquioxane units, were prepared by cohydrolysis of EtSiCl_3 and EtHSiCl_2 ²⁴. The cyclohexylsilanetriol, formed in dilute aqueous acetone solution by the hydrolysis of cyclohexyltrichlorosilane, condenses to give an easily isolated dimer, a trimer and a tetramer. Further condensation gives a resinous mixture which very slowly converts to three crystalline species²⁵:



Alkoxysilanes can also be used as starting materials. Thus poly(methylsilsesquioxanes) have been prepared by hydrolysis of MeSi(OMe)_3 in the presence of Ca(OH)_2 ²⁶. Much attention has been paid to the physical properties of organosilsesquioxanes, especially their surface properties and thermal behaviour. For example, $\text{Cy}_7\text{Si}_7\text{O}_9(\text{OH})_3$ has been used as an idealised model for silica surface sites. Its close-range geometric similarity to known SiO_2 morphologies makes it the best model for silica that has been developed to date²⁷⁻³⁰. The relatively unstable poly(phenylsilsesquioxanes) undergo thermal changes due to cross-linking. The nature of the organic substituents has a predominant influence on the mass spectral fragmentation of organosilsesquioxanes. For methyl and ethyl derivatives only, cleavage of the alkyl-silicon bonds occurs, whereas for vinyl derivatives Si-O bonds are broken. Also in three dimensions the vertex-deficient cuboides of $\text{R}_7\text{Si}_7\text{O}_9(\text{OH})_3$ analogues (where $\text{R} = \text{c-C}_5\text{H}_9$, $\text{c-C}_6\text{H}_{11}$, $\text{c-C}_7\text{H}_{13}$)²⁷, can be capped by a range of transition^{28,29} and main group element fragments³⁰, to form analogues of silica-supported metal catalysts.



Besides a high thermal stability, this cluster has excellent solubility in organic solvents. Feher and his coworkers have utilised the enhanced reactivity of the incomplete-condensed silsesquioxane $(\text{c-C}_6\text{H}_{11})_7\text{Si}_7\text{O}_9(\text{OH})_3$ towards main groups and transition-metal halide complexes to provide an alternative route for the preparation of

metallasilsesquioxanes. For example, the reaction of $(\text{c-C}_6\text{H}_{11})_7\text{Si}_7\text{O}_9(\text{OH})_3$ with Me_5Sb is much faster than the reactions of Me_5Sb with silanols containing fewer than three mutually hydrogen-bonded siloxy groups.

The unusually high thermal and thermo-oxidative stability of poly(organosiloxanes) is another important property. Whilst most polymers containing C-C single bond main-chain units begin to degrade at temperatures above 250°C , rigorously purified polysiloxanes are stable under high vacuum or in an inert atmosphere to at least $350\text{-}400^\circ\text{C}$. This difference is directly attributable to the greater strength of the Si-O bond relative to the C-C bond, as discussed earlier. Macfarlane³¹ measured the changes in the molecular weight of PDMS on extended exposure to isothermal heating (Figure 1.1). In silanol terminated polymers, they found that above 160°C the molecular weight first increased with time to reach a maximum value and then decreased as the polymer degraded to small ring compounds which volatilized as shown in Figure 1.2.

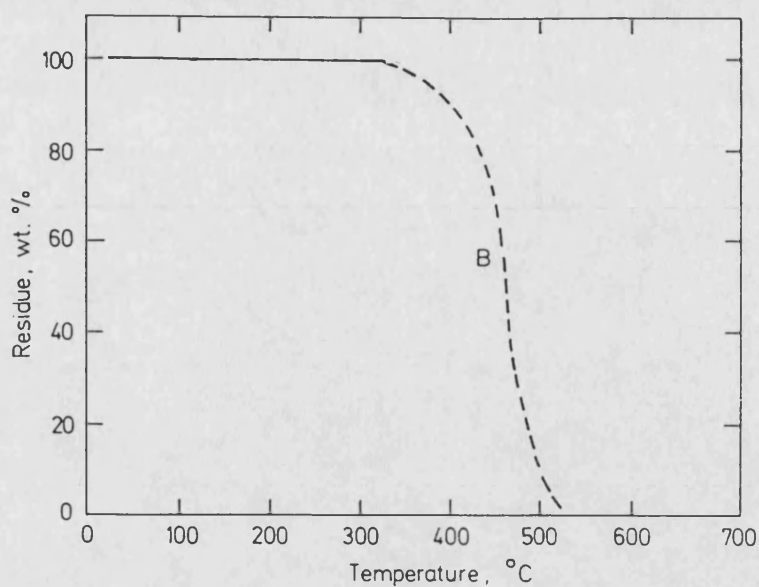


Figure 1.1 Thermal gravimetric analysis, (TGA) of a silanol terminated polymer

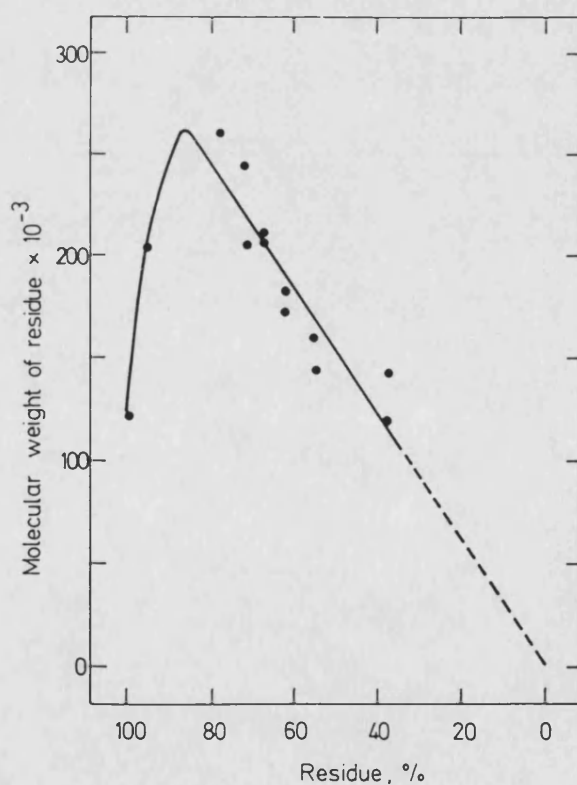


Figure 1.2 Effect of thermal degradation on the molecular weight of silanol terminated PDMS

The initial increase in molecular weight was attributed to silanol condensation reactions between end-groups which leads to a considerable broadening of the molecular weight distribution. The activation energy of this reaction was 35.6 kJ mol^{-1} ³² in good agreement with the usual value obtained for the silanol condensation reaction³³. Subsequent degradation results in a linear decrease in molecular weight with the extent of volatilization, which indicates that the volatile cyclic products are formed in a step-wise fashion. An investigation of the degradation of trimethylsilyl end-capped poly(dimethylsiloxanes) by thermal gravimetric analysis revealed that this process started in argon at about $390\text{--}410^\circ\text{C}$, with an activation energy measured in vacuum of $159 \pm 12.5 \text{ kJ mol}^{-1}$ and $180 \pm 12.5 \text{ kJ mol}^{-1}$ ³⁴. Considering that the values obtained correspond to less than one half of the siloxane bond dissociation energy of *ca* 490 kJ mol^{-1} , it was concluded that depolymerisation of the polysiloxanes was governed mainly by molecular structural and kinetic factors rather than by bond energies. To account for this surprisingly low activation energy for the polysiloxane depolymerisation reaction, a mechanism was proposed by which siloxane bond rearrangement occurs through the formation of an intramolecular, cyclic, four-centre transition state, which is involved in the rate determining step of the polysiloxane degradation process, as shown below:

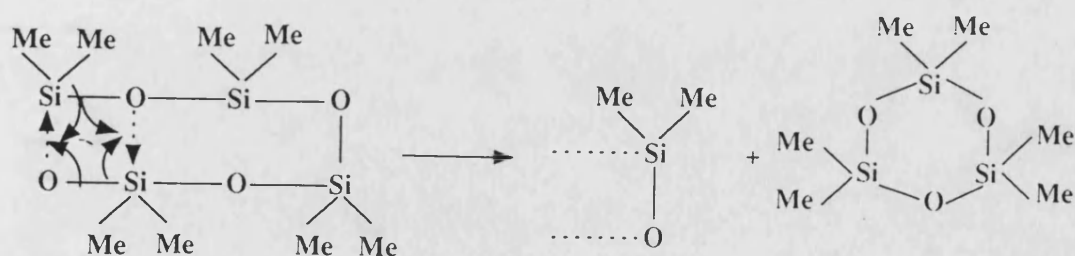


Table 1.4

Properties and application of poly(diorganosiloxanes)

<u>Property</u>	<u>Application</u>
Thermal stability and U.V. resistance	Oil seals, oven gaskets, insulators, paints, cathode ray tube, gas turbines and roof coating.
Surface behaviour and release characteristics	Non-spreading lubricant, antifoam agent, protective coating pigments, space heaters and skin coating for high speed aircraft.
Adhesive properties and viscosity	Construction of jet planes and rockets, brake fluids, liquid spring, toys and sound damping.
Chemical stability and biocompatibility	Blood transfusion tubing, gaskets in chemical reactors, conveyor belting in the foodstuff industry, medical applications in plastic surgery and drug carriers.
High permeability	Continuous drug release, gas separation technology, contact lenses, selective liquid extractants and fibre coating.

1.3 REFERENCES

1. J Emsley, *The Elements*, Oxford University Press, 1989, 172; J M Zeigler and F W G Fearon, *Silica-Based Polymer Science: A Comprehensive Resource*. ACS Series 224, Washington, USA, 1990, 45; F O Stark, J R Falender and A P Wright, *Comprehensive Organometallic Chemistry*, Ed. G Wilkinson, F G Stone and E W Abel, Pergamon Oxford, 1982, **2**, 324.
2. C Friedel and J M Crafts, *Ann Chim Phys*, 1870, **19**, 334; A Ladenburg, *Ann Chim*, 1871, **159**, 259.
3. J F Hyde and R C Delong, *J Am Chem Soc*, 1941, **63**, 1194.
4. L Pauling, *The Nature of the Chemical Bond*, Third Ed., Cornell University Press, Ithaca, New York, 1960, 322.
5. S Shambayati, J F Blake, S G Wierschke, W L Jorgensen and S L Schreiber, *J Am Chem Soc*, 1990, **112**, 697.
6. K Yamasaki, A Kotera and M Yokoi, *J Chem Phys*, 1950, **18**, 1414.
7. R A Shaw, *J Chem Soc*, 1957, 2831.
8. V E Shklover and Y T Struchkov, *J Organomet Chem*, 1987, **322**, 269.
9. J E Mark, *Macromolecules*, 1978, **11**, 627.
10. P R Hayes, D Kendrick and J R Parsonage, *Chemistry and Industry*, 1993, **4**, 125..
11. W Noll, *Chemistry and Technology of Silicones*. Academic Press, New York and London, 1968, references therein.
12. M J Michalczyk, M J Fink and K J Haller, *Organometallics*, 1986, **5**, 531.
13. M Veith, *Chem Rev*, 1990, **90**, 3.
14. E Lukevics, O Pudova and R Sturkovich, in *Molecular Structure of Organosilicon Compounds*, Ellis Horwood, Chichester, UK, 1989, 196.
15. V E Shklover and Y T Struchkov, *J Organomet Chem*, 1987, **322**, 269.
16. R West, L D David and P I Djurovich, *Am Chem Soc Bull*, 1983, **62**, 825; R West, R D Miller and D Hofer, *J Polym Sci Polym Lett Ed*, 1983, **21**, 819 (and references

therein).

17. C Eaborn and R Damja, *J Organomet Chem*, 1985, **290**, 267.
18. N Buttrus, C Eaborn, P Hitchcock, P D Lickiss and A D Taylor, *J Organomet Chem*, 1986, **309**, 25.
19. R Gewald, U Scheim and R Lang, *J Organomet Chem*, 1993, **446**, 79.
20. I M Mayotic, *Plastic Insulation Materials*, 1966.
21. K E Polmanteer and C W Lentz, *Rubber Chem Technol*, 1957, **48**, 810.
22. U Deschler, P Kleinschmint and P Panster, *Angew Chem Ind Ed Engl*, 1986, **25**, 236.
23. T A Aire and F I Ikegwuonu, *IRCS Med Sci Libr Compend*, 1979, **7**, 186.
24. J M Sosa, *Macromolecules*, 1980, **13**, 1260.
25. J Brown and L A Vogt, *J Am Chem Soc*, 1965, **87**, 4313.
26. M D Romanova and I A Metkin, *Zh Prikl Khim*, 1981, **54**, 212.
27. F J Feher, T A Budzichowski, R L Blanski, K J Weller and J W Ziller, *Organometallics*, 1991, **10**, 2526.
28. F J Feher, D Newman and J Walzer, *J Am Chem Soc*, 1989, **111**, 1741.
29. F J Feher and T A Budzichowski, *Organometallics*, 1991, **10**, 812; F J Feher and R L Blanski, *J Chem Soc, Chem Commun*, 1990, 1614; F J Feher, S L Gonzales and J W Ziller, *Inorg Chem*, 1988, **27**, 3440; F J Feher, *J Am Chem Soc*, 1986, **108**, 3850.
30. F J Feher, J F Walzer and R L Blanski, *J Am Chem Soc*, 1991, **113**, 3618; F J Feher and D Newman, *J Am Chem Soc*, 1990, **112**, 1931; F J Feher, T A Budzichowski and K J Weller, *J Am Chem Soc*, 1989, **111**, 7288; F J Feher and J Weller, *Organometallics*, 1990, **9**, 2638; F J Feher, T A Budzichowski and J W Ziller, *Inorg Chem*, 1992, **31**, 5100.
31. N Grassie and I G Macfarlane, *Euro Polym J*, 1978, **14**, 875.
32. T H Thomas and T C Kendrick, *J Polym Sci, Part A-2*, 1969, **7**, 537.
33. S P Moulik and B N Ghosh, *J Indian Chem Soc*, 1963, **40**, 907.

34. A H Frazer, High Temperature resistant polymers, New York Chichester: Interscience, 1968.

CHAPTER TWO

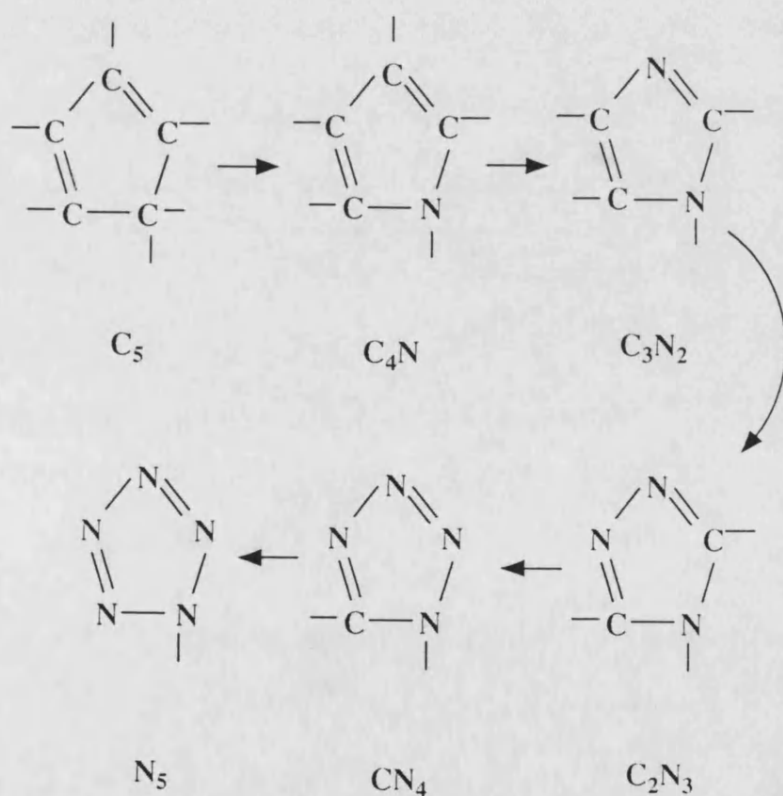
INTRODUCTION TO HETEROCYCLICSILOXANES

2.1 SUMMARY

The incorporation of one or more heteroatoms into cyclic siloxanes or silazanes will modify the structure and properties of the ring, in a way which will be highly dependent upon the bonding properties and characteristics of the backbone of the compound, as well as the nature of the heteroatom substituents. These considerations are briefly reviewed in this chapter. Introduction of one or more small heteroatoms such as boron into a six- or eight-membered siloxane ring would be expected to increase the ring strain present in these molecules, and therefore facilitate ring-opening polymerization to polyheterosiloxanes. This is a key consideration in this study which seeks to prepare compounds with properties that complement and extend those of conventional siloxane polymer systems, for possible use as preceramic polymer precursors to silicon carbide.

2.2 INORGANIC RING SYSTEMS

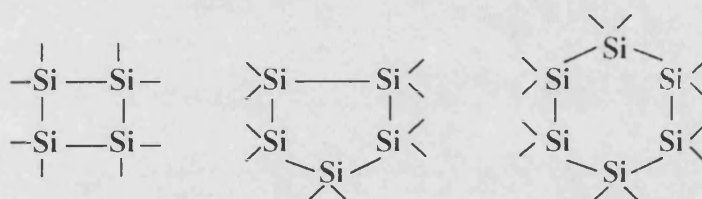
Cyclic ring and cluster structures, consisting of entirely carbon atoms, are the basis of a vast area of organic chemistry. Partial replacement of carbon by heteroatoms leads to an extensive group of heterocycles and cage molecules, while full replacement of carbon produces inorganic ring and cage systems with totally different properties. For example starting from cyclopentadiene, successive replacement of CH by its isoelectronic equivalent nitrogen, produces pentazole:



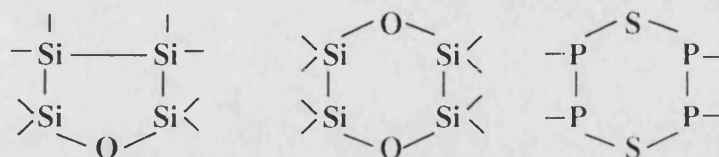
Inorganic ring systems have a long history¹, and representative examples are now known for every non-metal. However, the development of inorganic ring chemistry has occurred in the shade of more spectacular achievements (for example in coordination and organometallic chemistry). Inorganic homo- and heterocycles were in the past studied mostly in relation to the chemistry of specific elements such as sulphur, phosphorus, silicon and boron, which were noted for their tendency towards catenation, and these are used to illustrate the ring classifications below.

Inorganic rings can be classified conveniently according to their composition and structure into the following types:

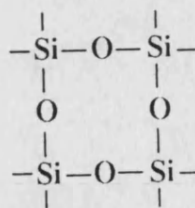
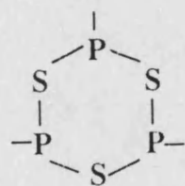
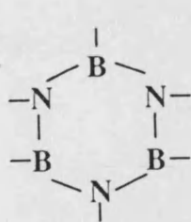
(a) Homocycles containing identical atoms, $(A)_n$:



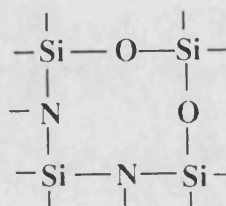
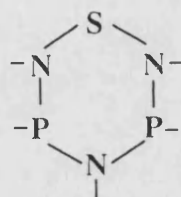
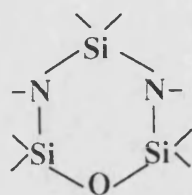
(b) Heterocycles formed by insertion of a heteroatom into a parent homocyclic system whilst preserving bonds between like atoms, A_mB_n , where $m \neq n$:



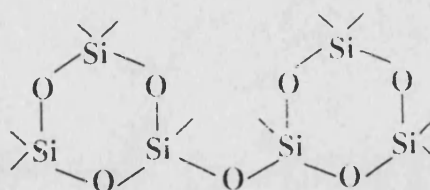
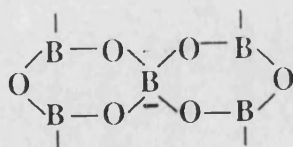
(c) Heterocycles formed by regular alternation of two different elements containing repeat units or atom pairs, $(AB)_n$. This type is of particular importance in inorganic heterocyclic chemistry:



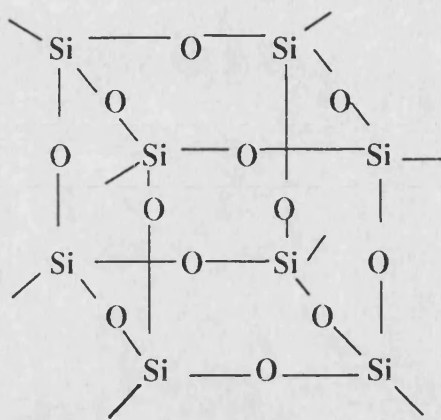
- (d) Mixed types of heterocycles, in which the regular alternation is disturbed by introducing a third element. These heterocycles are formed from different units or atom pairs $A_m B_p C_n$:



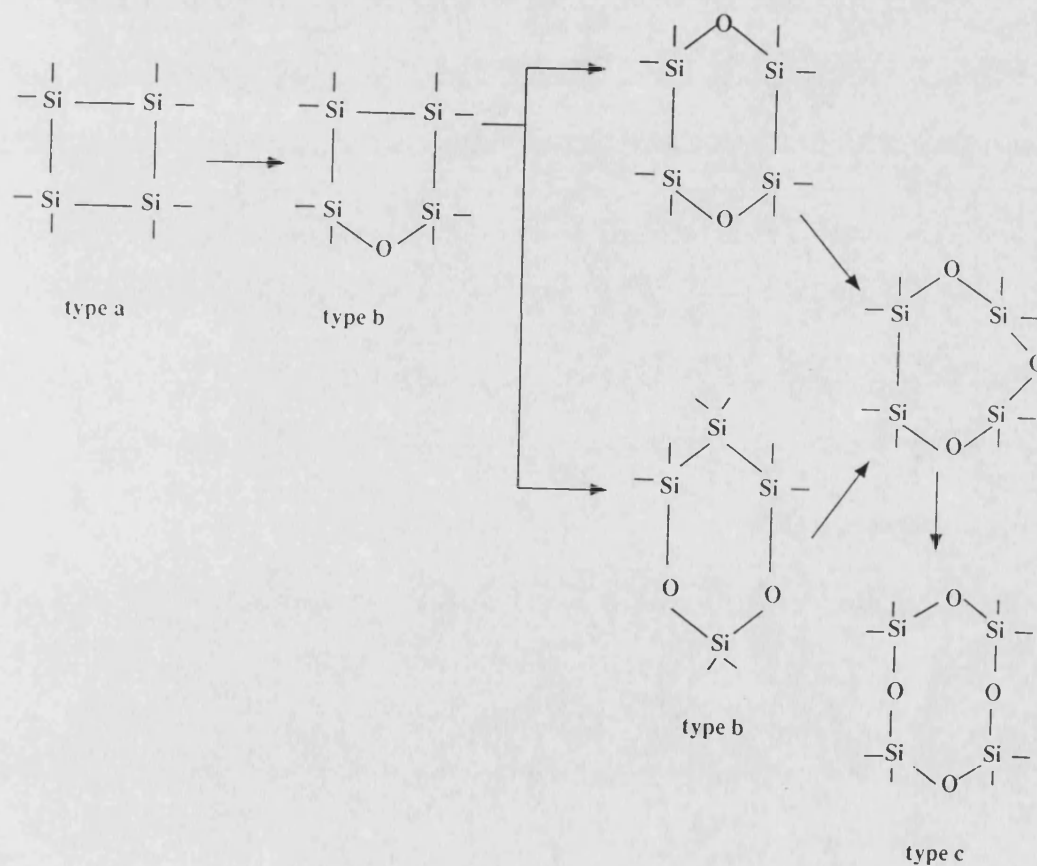
Types (a) and (d) are known mainly for non-metallic elements in combination with main group elements. Polycyclic systems are often formed by connection of monocyclic units via bridges (bridged rings), by one common atom (spirocyclic systems), or by two or more common atoms (fused rings):



Particularly interesting examples of polycyclic systems are provided by cage-structures, consisting of several rings connected in a finite, three-dimensional molecular skeleton:



The various types of inorganic rings are inter-related. Thus the transition from homocyclic systems to heterocycles formed by regular alternation occurs formally via successive insertion of heteroatoms:

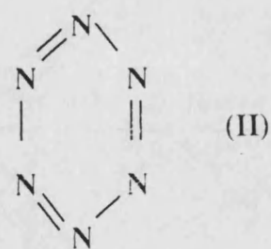
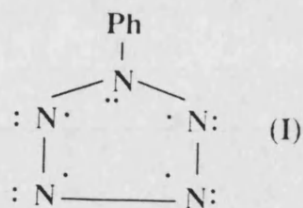


2.3 STRUCTURE AND BONDING IN HETEROCYCLIC SYSTEMS CONTAINING SILICON AND BORON

The main group elements, which are commonly involved in the formation of ring systems are listed below:

B	C	N	O
Al	Si	P	S
Ga	Ge	As	Se
In	Sn	Sb	

Electronegativity can be used to compare qualitatively several important properties of the elements. A simple comparison of the electronegativities of carbon and the surrounding elements, shows that carbon occupies a central position between the most electronegativity element, fluorine $\chi_F = 4.0$ on the Pauling scale², and the least electronegativity element, caesium $\chi_{Cs} = 0.7$. Therefore carbon shows little tendency unless bonded to a very electropositive element to form ionic bonds, and instead forms extensive homoatomic chains and rings. When saturated such compounds are quite inert to either electrophilic or nucleophilic attack. The elements with an electronegativity greater than that of carbon, do not form stable homonuclear chain and rings without additional stabilizing factors. This is exemplified by oxygen and nitrogen, which show little tendency to form homo-rings or chains containing more than four oxygen or eight nitrogen atoms. Even such short chains are very unstable. Cyclopentaazadiene (I) exhibits some stability due apparently to the presence of a sextet of π -electrons within the ring, and to conjugation with the phenyl group. Cyclohexaazatriene, which may be formed by the photolysis of cis-diazidobis(triphenylphosphine)platinum(II) in ethanol or THF, was tentatively assigned the structure shown in (II)³.



Catenated species of oxygen and nitrogen tend to rearrange to very short-chain species, which are more favoured electronically. The ability of oxygen and nitrogen to form stable multiple bonds with themselves due to the favourable 2p-2p bonding interactions as in $\text{O}=\text{O}$, $\text{N}\equiv\text{N}$ or $\text{R}-\text{N}=\text{N}-\text{R}$, favours the destabilization of larger rings or chains with lower bond orders. Elements with an electronegativity less than that of carbon have only a small tendency to form catenated molecules, and these are unstable towards the action of oxidizing reagents. Electron-poor elements of the first row elements readily form cage structures rather than rings as in icosahedral B_{12} units. This maximizes the bonding effects of the valency electrons. Heavier elements with sufficient valence electrons to form catenated or multiply bonded species such as Si, Ge, Sn, P and As, favour homocyclic and linear species containing 4-8 atoms, but their stability does not compare with that of homocyclic carbon compounds. Multiply bonded dinuclear species, $\text{R}_2\text{M}=\text{MR}_2$, have also attracted considerable attention, particularly for Si, and both P and As form $\text{M}\equiv\text{M}$ molecules at elevated temperatures.

The bond energy of a heteronuclear species contains a term determined by the differences between the electronegativities of the elements forming the linkage²:

$$D_{\text{PAB}} = D_{\text{npA}} + D_{\text{npB}} + 23.06 (x_{\text{A}} - x_{\text{B}})^2$$

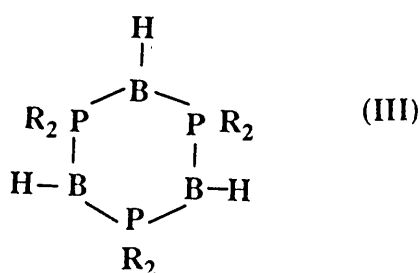
where D_{pAB} is the bond energy of the polar heterogeneous bond (A-B), D_{npA} and D_{npB} are the non-polar contributions to the bond energy from the elements A and B, x_{A}

and x_B are the electronegativities of the elements A and B. Thus, linkages between different elements will in general have higher bond energies than their homologues, (Table 2.1) which tends to promote chain and ring formation. It is not surprising therefore that the most stable inorganic heterocycles and polymers are formed by alternation of two elements, A and B, having electronegativities greater and less than that of carbon.

Table 2.1 Bond energies

Homogeneous bonds		Heterogeneous bonds					
Si—Si	209	Si—O	423	Si—N	301	Si—S	255
Ge—Ge	167	Ge—O	402	Ge—N	276	Ge—S	234
Sn—Sn	142	Sn—O	389	Sn—N	264	Sn—S	222
N—N	134	N—O	184				
P—P	209	P—O	352	P—N	251	P—S	230
As—As	159	As—O	352	As—N	234	As—S	209
Sb—Sb	142	Sb—O	342	Sb—N	234	Sb—S	205
O—O	142						
S—S	209	S—O	255	S—N	193		
Se—Se	176	Se—O	230	Se—N	243	Se—S	201

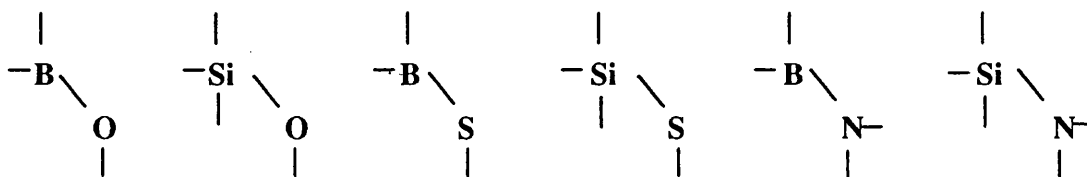
Other important factors which strongly influence the stability and the structures of ring systems are the presence on one element of vacant orbitals, and on the other of low energy electron pairs. Thus electron delocalization, donor-acceptor and other electronic and steric features⁴ can enhance stability. Such factors explain in part the high stability and inertness of cyclophosphinoborines (III), in which both boron and phosphorus are less electronegative than carbon, but boron can accept electron density from phosphorus, so making the system more stable than simple electronegativity considerations would predicted.



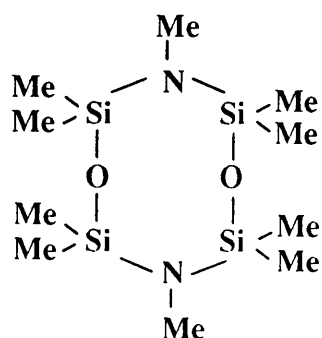
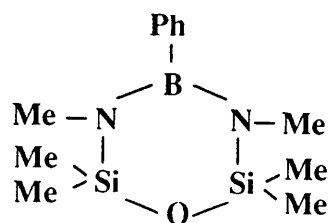
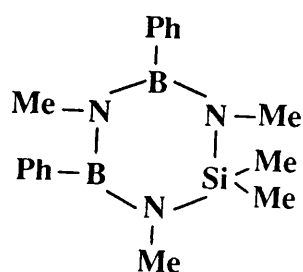
The particular stability of carbon in its sp^3 hybridization state may be a further factor responsible for the great ability of carbon to catenate. The absence of free orbitals and lone electron pairs makes a saturated C-C bond very unreactive. It is a reasonable expectation that in inorganic ring formation, each element will exhibit its most stable and characteristic hybridization state, as in non-cyclic compounds. Therefore, if there are two different structures, which both satisfy simple valency rules, one involving a non-characteristic hybridization state and a cyclic one involving only atoms in their characteristic hybridization states, the cyclic arrangement will be preferred. This explains the instability of the multiple-bond compounds of some element with oxygen, nitrogen or sulphur. Thus no monomeric compounds containing any of the following multiple bonds are stable:



In such compounds boron and silicon would have the uncharacteristic hybrid states sp and sp^2 respectively. Polymerization or cyclization of monomers containing such multiple bonds gives compounds (cyclic or polymers) containing the units below, in which every element exhibits its stable hybridization state for the given valency. This explains why in reactions involving silicon and boron where monomers with double bonds might be expected, only their cyclic or linear polymers are isolated under normal conditions. The same is expected for compounds of composition R_n-E-O , $R_n-E-N-R$ and R_n-E-S , where $E = Al, Ga, In, Sn, Pb$ etc.

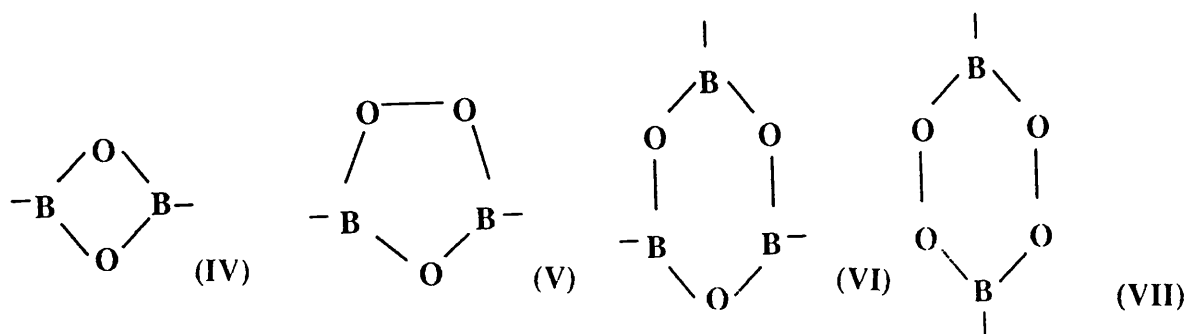


Introducing an appropriate heteroatom into a homocycle should give a heterocycle of comparable or higher stability, and replacing an element A by an element C in a heterocycle $(AB)_n$ formed by regular alternation, should give rise to a new heterocycle if the pair A-C has similar electronegativities and its characteristic hybridizations are preserved. Similarly, the element B can be replaced by D as appropriate. Therefore, it can be concluded that if two heterocycles $(AB)_n$ and $(CD)_n$ are known, one should be able to prepare the intermediate heterocycles $A_nB_mD_{n-m}$. In this way, transition series of heterocycles may be obtained, having intermediate composition between two heterocycles with one common element. A few such series have already been completed⁵:



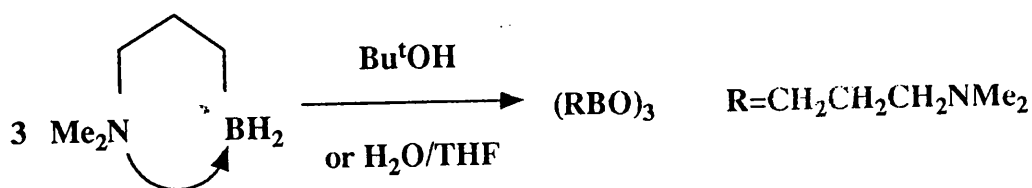
2.3.1 Heterocycloboroxanes

Boron-oxygen heterocycles of various ring sizes are known, the regular six-membered B_3O_3 (VI) ring showing the greatest stability and yielding many derivatives:



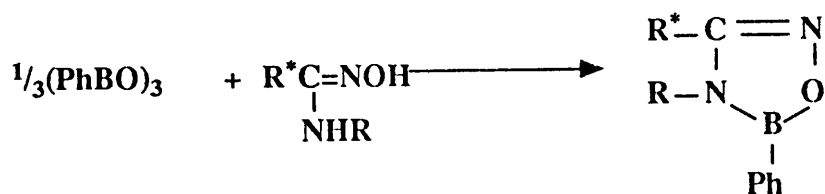
In many compounds boron may become four-coordinate by addition of supplemental groups, such as hydroxyl groups. The four-membered ring (IV) and six-membered ring (VII) are in fact known only with three-coordinate boron. The parent six-membered ring compound $(HBO)_3$, contains a planar B_3O_3 ring and is stable only in the gaseous phase. In the condensed state it is thermodynamically unstable at room temperature and disproportionates into B_2O_3 , but it provides the parent skeleton for an extensive class of boron-oxygen heterocyclic derivatives, whose chemistries were established before 1970. Most of the progress achieved in the following decade relates to the preparative and structural chemistry of cyclic borates derived from the B_3O_3 ring. Grignard reagents have been much used in the preparation of cyclotriboroxanes. Thus these reagents react with trialkoxyboranes to give cyclotriboroxanes⁶, and aryl derivatives are formed in the reaction of refluxing alkyl or aryl halides with magnesium in THF in the presence of boron⁷. The dehydration of boronic acid $RB(OH)_2$, also provides a convenient method for the preparation of organocycloboroxanes⁸. Finally, many organoboron compounds containing B-H bonds can be converted to cyclotriboroxanes because of the stability of the B-O linkage. Thus substituted diboranes $(RBH_2)_2$ hydrolyse to $(RBO)_3$ and refluxing 1,1-dimethyl-1,2-azaboralidine with t-butanol or in wet THF also affords

cyclotriboroxanes.



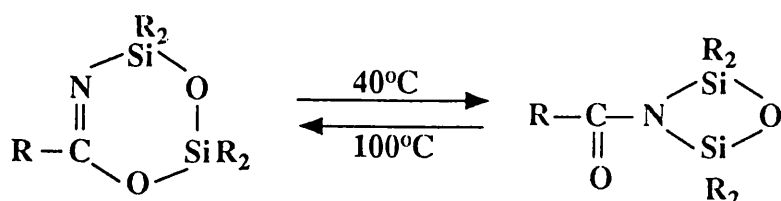
There are two basic types of transformation of cyclotriboroxanes. In one the B_3O_3 ring is preserved, and in the other the ring is cleaved. Addition reactions affording 1:1 adducts occur between cyclotriboroxanes and various nucleophiles by donation from nitrogen, oxygen or phosphorus to boron. An increase in the size of the organic group on boron reduces the acceptor properties of the boron atom. Another such reaction involves insertion which has been investigated in considerable detail⁹. This reaction takes place during oxidation with various reagents, when alkyl and aryl cyclotriboroxanes are converted to alkoxy and aroxy derivatives.

The cleavage of the B_3O_3 ring with organic functional derivatives containing mobile hydrogen can be used for preparative purposes in the synthesis of organoboron compounds. For example, the reaction with amidoximes gives five-membered rings¹⁰.

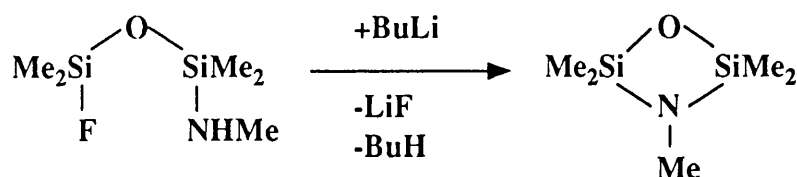


2.3.2 Heterocyclosilazoxanes

Cyclosilazoxanes are heterocycles, usually with 4-12 ring atoms formed by partial replacement of NR in the cyclosilazane rings by oxygen. The parent compound contains the four-membered Si_2NO ring system shown below¹¹. NMR analysis of pentamethyldisiladioxazine showed that the Si_2NO ring which predominates in polar solvents at low temperatures, rearranges to a six-membered ring completely at 100°C in benzonitrile¹¹.



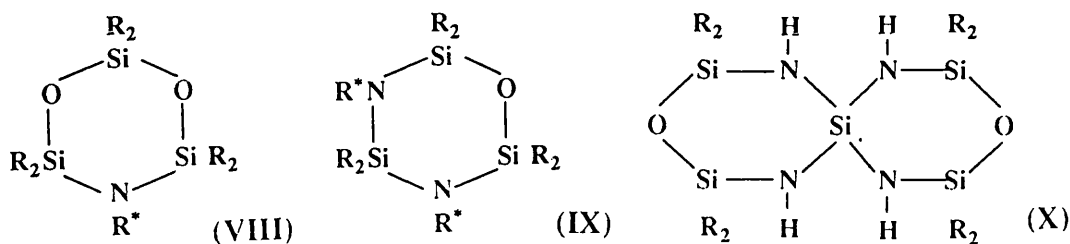
The bis(isopropyltrimethylsilyl)amino-substituted Si_2NO ring has also been prepared by cyclization of 1-fluoro-3-aminodisiloxane with BuLi ¹².



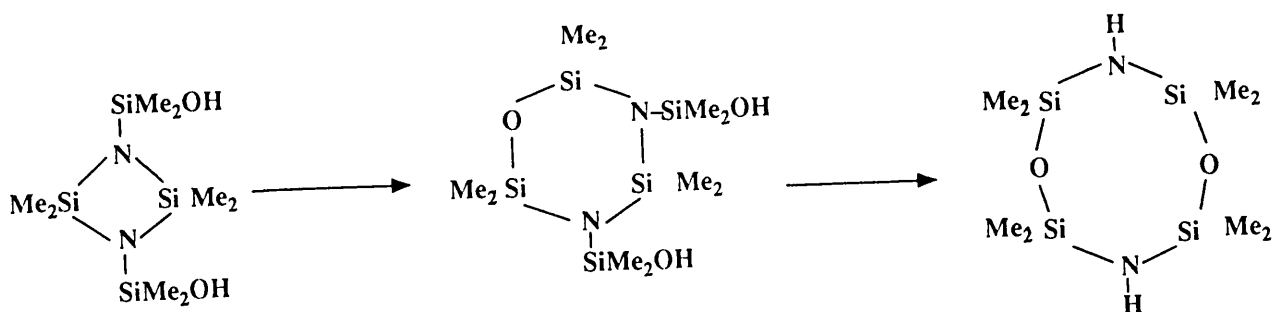
Larger ring systems are commonly prepared by one of the three general routes involving (a) ring closure of linear compounds, (b) partial hydrolysis of cyclic precursors, and (c) insertion reactions. These are exemplified below.

Treatment of $\text{O}(\text{SiMe}_2\text{NHMe})_2$ with dihalosilane RR^*SiX_2 , after metalation or in the presence of Et_3N , leads to ring closure, with formation of a six-membered $\text{Si}_3\text{N}_2\text{O}$ ring. The use of a dipolar solvent (DMF) is necessary for the formation of the cyclic compound (VIII) in the reaction of aniline with $\text{O}(\text{SiMe}_2\text{Cl})_2$, otherwise linear oligomers are the only products¹³. The reaction of $(\text{Me}_2\text{SiNH})_3$ with Me_2SiCl_2 in wet dioxane¹⁴, led

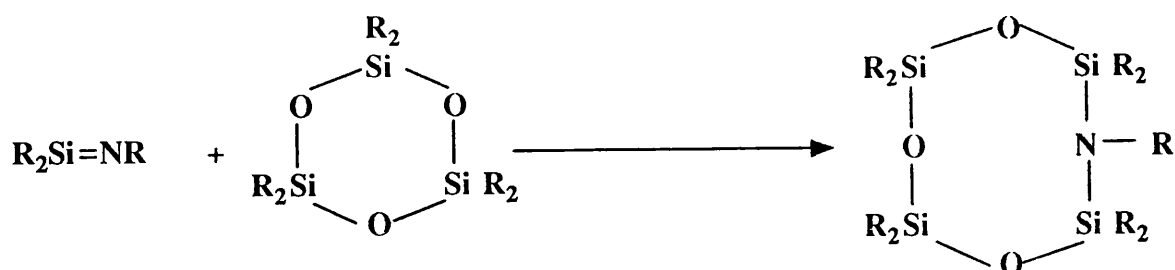
to the formation of (VIII) and (IX). Spirocyclic compounds containing silazoxane rings can also be prepared using this methodology. Thus the spiro-silazoxane (X) is formed as an isomeric mixture by cyclization of the dilithium derivatives $[\text{R}_2(\text{NHLi})\text{Si}]_2\text{O}$ with SiCl_4 ¹⁵.



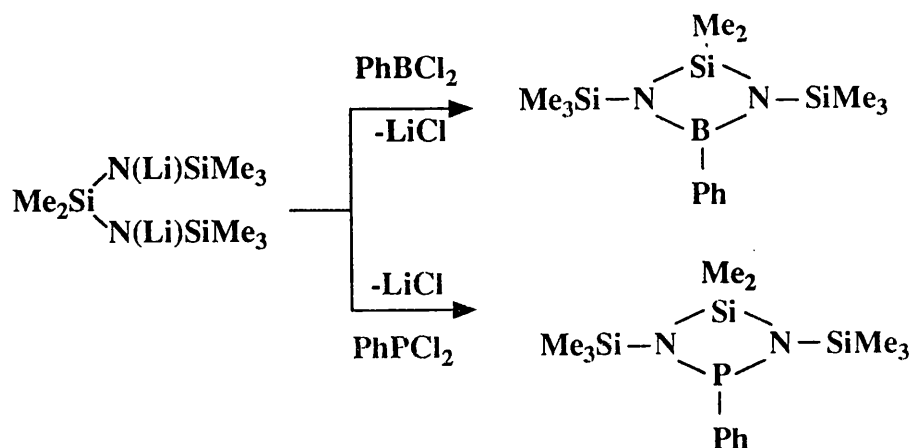
Hydrolysis is another frequently used method for the preparation of cyclosilazoxanes. Thus hydrolysis of the cyclodisilazane $\text{Me}_4\text{Si}_2\text{N}_2\text{H}(\text{SiMe}_3)$ gave a bis(trimethylsilyl)-substituted eight-membered ring $\text{Si}_4\text{N}_2\text{O}_2$, this ring also resulted from a rearrangement of a four-membered ring compound containing silanol substituents. The eight-membered ring has been shown to exhibit a chair conformation¹⁶.



Another interesting method of preparing cyclotetrasilazatrioxanes is via the reaction of monomeric silaimines $\text{R}_2\text{Si}=\text{NR}$ (generated by the gas-phase pyrolysis of the corresponding silylazides), with hexamethylcyclotrisiloxane $(\text{Me}_2\text{SiO})_3$ ¹⁷. The fragment inserts into the Si-O link of the strained cyclotrisiloxane resulting in ring expansion.

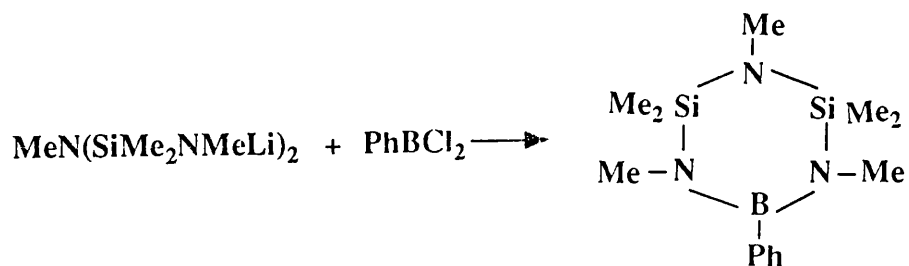


In principle a large number of heterocyclic silazanes are possible by replacing one or more of the Si atoms in cyclosilazanes with another heteroatom, e.g. boron, germanium, phosphorus, arsenic and sulphur. To date there are very few reports concerning such compounds. Four-membered cyclobora- and cyclophosphasilazanes have been prepared however, by the reaction of N,N'-dilithiumoctamethyltrisilazanes with phenylboron dichloride¹⁸.

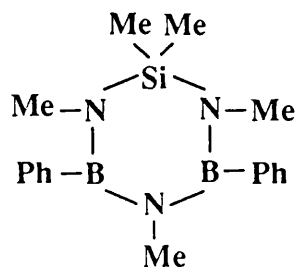


Other lithium-terminated oligomeric silazanes of potential interest for similar syntheses are known, including $\text{LiN(R)Si(R}_2\text{)NRLi}$ and $(\text{LiNRSiR}_2)_2\text{NR}$ ¹⁹. Thus, six-membered rings containing silicon, nitrogen and boron or germanium have been obtained by the reaction of dilithium diaminodisilazane with phenylboron dichloride or

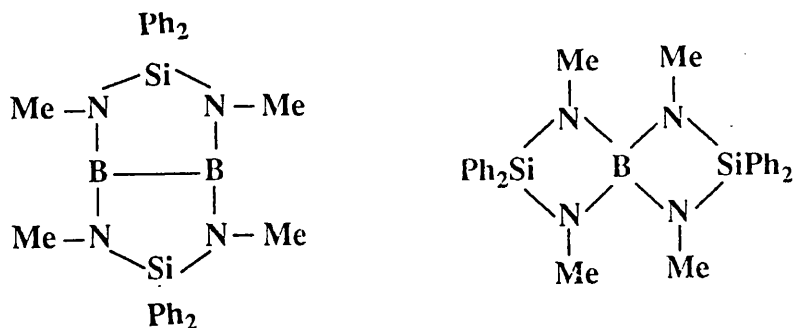
diphenylgermanium dihalide²⁰.



The molecular structures of six-membered ring compounds containing 2:1 and 1:2 Si to B ratios have been determined⁵. The Si-N-B fragments are almost planar and no unexpected geometric parameters were observed in either structure.



An alternative method of generating cycloheterosilazanes involves homofunctional condensation of different amino derivatives. Heating bis(dimethylaminodiphenylsilane) with tetrakis(dimethylamino)diboron yields, after elimination of dimethylamine, a B-N-Si compound with one of the two structures shown below, based on infrared and ¹H NMR evidence²¹.



Rings with four different elements, namely Si, N, B and O, have also been obtained. These include the six-membered system, $\text{Si}_2\text{N}_2\text{BO}$, obtained in the reaction of $\text{O}(\text{SiR}_2\text{NRLi})_2$ with phenyl boron dichloride, and the six-membered $\text{Si}_2\text{NO}_2\text{B}$ ring compound afforded by the reaction of $\text{PhB}(\text{OH})_2$ with $\text{MeN}(\text{SiMe}_2\text{Cl})_2$ in the presence of Et_3N ²².

2.3.3 Heterocyclosiloxanes

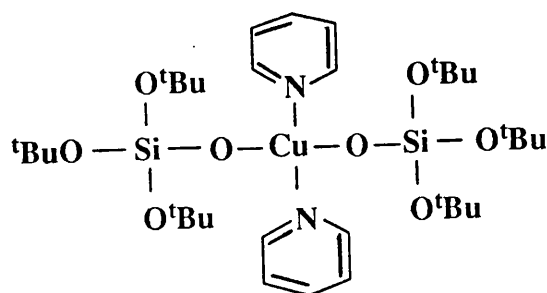
Interest in the chemistry of cyclosiloxanes, their structure, physical properties and reactivity, has been stimulated by the development of their applications. Not only have the organic substituents on silicon been varied²³, but the basic skeleton can be modified by partial replacement of silicon atoms by other atoms groups. From the industrial viewpoint, organocyclosiloxanes are important since in the presence of acidic or basic catalysts they undergo polymerisation to produce silicone fluids and elastomers which have been discussed earlier. Introduction of main chain substituents may lead to novel materials with other useful properties and applications.

Although heterosiloxanes have been known for over 30 years¹, structural characterisation of these species is relatively recent. The largely intractable nature of high molecular weight polymers has focused attention on small molecule model systems. Substituted heterocyclosiloxanes, with some silicon atoms of the siloxane units replaced by other elements, most frequently boron, phosphorus, aluminium and several transition

metals, have received some attention. In this review only recent examples of heterocyclosiloxanes containing selected transition metals forming different ring size compounds, and main group elements of relevance to this study will be explored. Borocyclosiloxanes will be discussed in more detail, due to their involvement in this study.

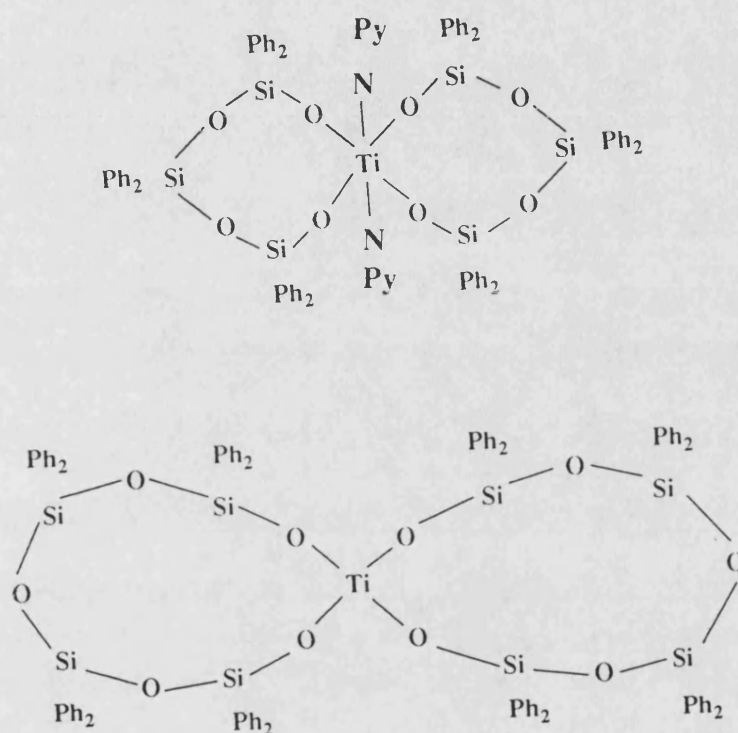
Heterocyclosiloxanes containing transition metals

The recent preparation and structure determination of the copper(II) siloxide complex $\{\text{Cu}[\text{OSi}(\text{O}^t\text{Bu})_3]_2(\text{py})_2\}$ (py= pyridine) show below typifies attempts to isolate and characterise silicon analogues of metal alkoxides²⁴. The structure of this complex consists of well-separated monomeric units with square planar coordination. No monomeric copper analogues with monodentate alkoxy or aryloxy ligands has been structurally characterized, but a related compound having two aryloxy legends and two nitrogen donors per copper atom, $[\text{Cu}(\text{OPh})_2(\text{en})]_2 \cdot 2\text{PhOH}$, is dimeric with bridging phenoxy groups²⁵. Schmidbaur has also reported a series of copper(I) compounds, $[\text{CuOSiMe}_3]_4$ and $(\text{Me}_3\text{P})_x\text{CuOSiMe}_3$ ($x = 1-3$), that are polymeric with bridging siloxide ligands²⁶.



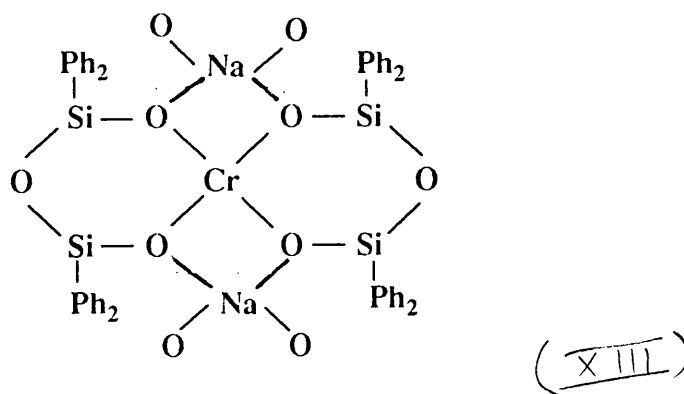
Cyclic and oligomeric systems represent further Si-O-M aggregation (M = transition metal), and the structures of two cyclo-titanosiloxanes, $\text{cis}-(\text{py})_2\text{Ti}[\text{OSiPh}_2(\text{OSiPh}_2)_2\text{O}]_2 \cdot 2\text{PhMe}$ (XI) and $\text{Ti}[\text{OSiPh}_2(\text{OSiPh}_2)_3\text{O}]_2$ (XII), which contain $\text{TiSi}_n\text{O}_{2n+2}$ ($n = 3, 4$) heterocycles with 8- and 10-membered rings, have been reported. They were synthesized by the reaction of dilithium tetraphenyldisiloxanediolate

$\text{Ph}_4\text{Si}_2\text{O}(\text{OLi})$ and titanium tetrachloride in the presence of pyridine, and by the reaction of diphenylsilanediol and tetraisopropoxytitanium respectively^{27,28}.



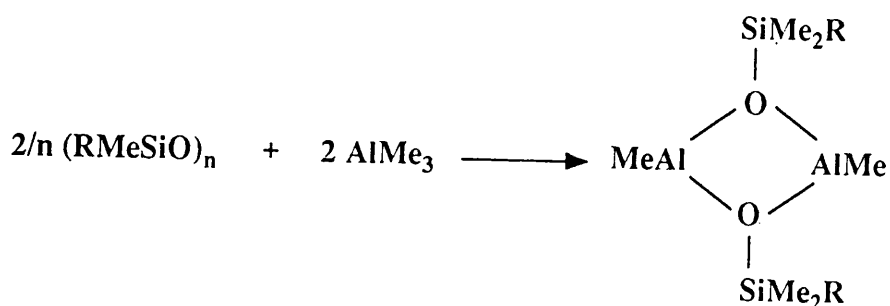
X-ray crystallographic studies of $\text{cis}-(\text{py})_2\text{Ti}[\text{OSiPh}_2(\text{OSiPh}_2)_2\text{O}]_2 \cdot 2\text{PhMe}$ show a distorted octahedral geometry about the central titanium atom, with the titanasiloxane rings adopting an almost planar conformations. The Si-O(Si) bond lengths and Si-O-Si angles are close to those in the tetrahedral compound $\text{Ti}[\text{OSiPh}_2(\text{OSiPh}_2)_3\text{O}]_2$, and the Ti-O bond lengths and Ti-O-Si angles are 1.87 Å and 180° respectively, and indicate very strong bonds due to the $\text{O} \rightarrow \text{Ti}$ π -bonding. This would explain the high thermal stability of these compounds, even though the ring strain in these heterocycles is expected to be high. Recently $[\text{Cr}\{(\text{OSiPh}_2\text{OSiPh}_2)-\text{Na}(\text{THF})_2\}_2]$ (XIII) has been synthesized and structurally characterized, and in combination with trimethyl aluminium it may be used as a precatalyst for the polymerisation of ethene to linear polyethylene²⁹. The angles at silicon atoms are close to regular tetrahedral values. The siloxane rings are coplanar and the geometry at the

chromium site is consequently square planar. The siloxane framework in the structure (XIII) is flexible enough to accommodate a range of metal stereochemistries at the spiro atom sites, The Si-O-Si angles are relatively small [mean: 128.0] and this probably indicates some degree of ring strain.



Heterocyclosiloxane containing main group element

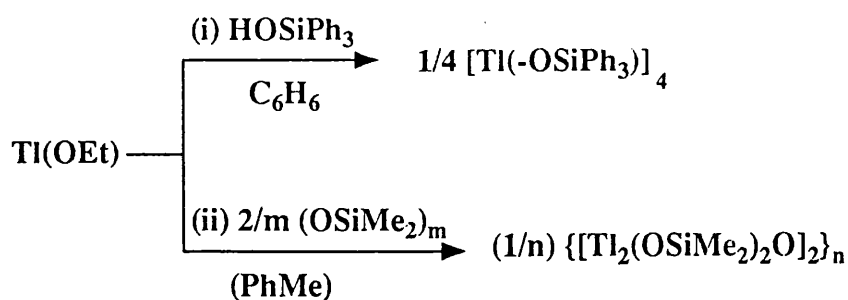
Heterocyclic compounds containing main group III elements such as Al, Tl and B are more common and will be discussed here. Germanium is also included because of its similarity to silicon. The reaction of Me_6Al_2 with poly(organosiloxanes), $(\text{R}_2\text{SiO})_n$ leads to rupture of the silicon-oxygen framework via attack by the electron poor metal on the oxide bridges and yields the novel dimeric aluminium siloxides $[\text{Me}_2\text{Al}(\text{OSiMe}_2\text{R})_2]_2^{30}$, (where $\text{R} = \text{Me}, n\text{-C}_{18}\text{H}_{37}, \text{CH}_2\text{CH}_2\text{CF}_3$ and Ph).



$\text{R} = \text{Me}, n\text{C}_{18}\text{H}_{37}, \text{CH}_2\text{CH}_2\text{CF}_3, \text{Ph}$

The structure of this compound ($R = \text{Ph}$) has been confirmed by x-ray crystallography, and show a planar Al_2O_2 ring system with the siloxy phenyl rings in the anti-conformation. It has been suggested that the nature of the siloxane polymer end-blocking unit, such as SiMe_3 , may play a role in determining the products. For example, the addition of Al_2R_6 to $\text{HO}(\text{R}_2\text{SiO})\text{H}$ results in initial formation of $-\text{SiOAlR}_2$ end-blocked polymers³⁰, whereas the interaction of Al_2Me_6 with the cyclic trisiloxane $(\text{Me}_2\text{SiO})_3$ in which no end-blocking unit is present, results in the formation of the 1:1 Lewis acid-base adduct $\text{Me}_3\text{Al}[(\text{OSiMe}_2)_3]$ ³⁰. Anhydrous aluminium chloride is also able to split the siloxane bond, and it reacts with $(\text{Me}_2\text{SiO})_4$ at 120°C to form an aluminocyclosiloxane $\text{ClAl}(\text{Me}_2\text{Si})_2\text{O}_3$, which is catalytically active in the rearrangement of hydrocarbons and can also be used as a catalyst in the alkylation of benzene by propane³¹.

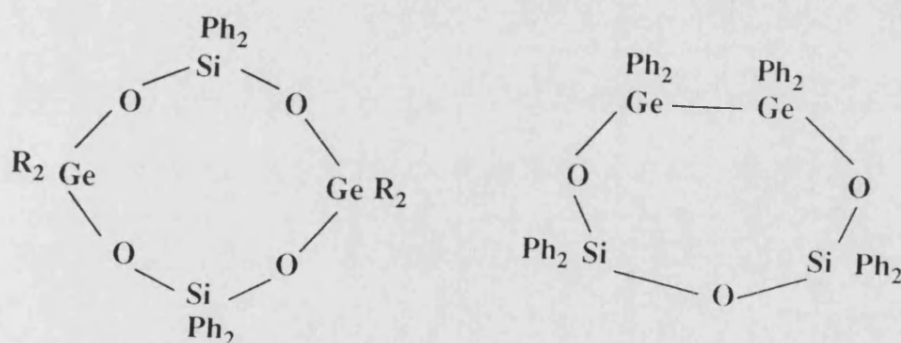
Other heterocyclicsiloxane ring systems containing thallium have been reported recently³². Thus the reaction of $\text{Tl}(\text{OEt})$ with $(\text{R}_2\text{SiO})_n$ in PhMe or $\text{Ph}_3\text{Si}(\text{OH})$ at ambient temperature instantly yields the ladder polymer $\{[\text{Tl}_2(\text{OSiMe}_2)_2\text{O}]_2\}_n$.



It is suggested that each of these reactions proceeds by nucleophilic attack of OEt^- at a silicon atom in HOSiPh_3 or $(\text{OSiMe}_2)_n$. The degradation of a silicone to a disiloxane as shown above is very important in this type of reaction. The structures of the ladder polymer contains TlOSiOSiOTl fragments linked into rings by $\text{O}:\rightarrow\text{Tl}$ interactions. Further $\text{O}:\rightarrow\text{Tl}$ coordination links the rings into a polymeric array, centred on Tl_4O_4

cubes. Both structures in the reaction scheme above comprise a tetrahedral arrays of thallium atoms with four oxygens centred over each triangular face, each approximately equidistant from the three metal centres, which leads to the Tl_4O_4 cuboids. The high Lewis acidity of Tl(I) dictates the lattice structure of this species³².

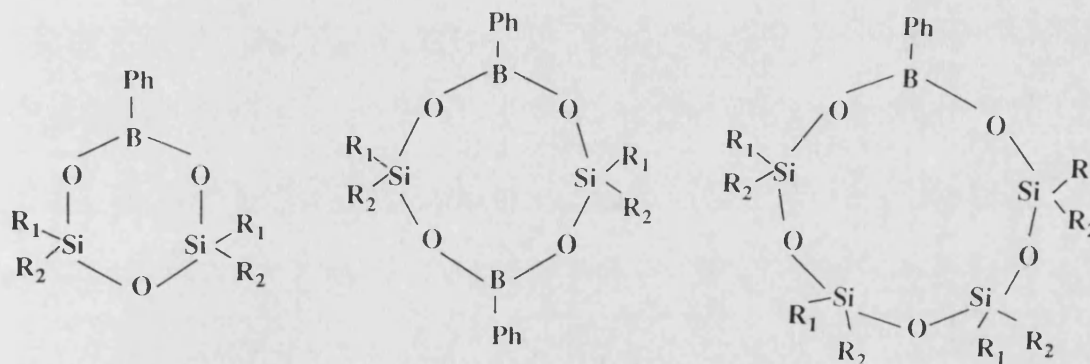
Non-planer eight-membered Si-O-Ge rings are present in $[\text{R}_2\text{Ge}(\text{OSiPh}_2)\text{O}]_2$ (where $\text{R} = \text{Me}, \text{Ph}$), which are synthesised by treatment of diorganogermaniumdihalides with diphenylsilandiol. These rings are more puckered than those of cyclotetrasiloxane³³. Interestingly, a seven-membered Si-O-Ge ring with a Ge-Ge bond occurs in $(\text{Ph}_8\text{Ge}_2\text{Si}_2\text{O}_3)$, which is produced by the reaction of $\text{ClPh}_2\text{Ge-GePh}_2\text{Cl}$ with $\text{Ph}_2\text{Si}(\text{OH})_2$. The ring is slightly puckered and has a twisted conformation³⁴.



2.3.4 Borocyclosiloxanes

The Si-O-B based heterocycles are of particular interest in the context of this work, and studies of these compounds provides a valuable insight into how the presence of different skeletal atoms influences ring opening polymerization, which could provide a route to new inorganic polymers with interesting and potentially useful properties. These compounds are important from the viewpoint of their reactivity and also their quasi-aromatic character³⁵. Rings of general formula $\text{B}_n\text{Si}_m\text{O}_{n+m}$ will incorporate $2(n+m)$ -electrons from the oxygen lone pairs, which can be delocalized through the vacant p-orbitals on B or d-orbitals on Si. Such heterocycles will then be aromatic by the Huckel criterion if $(n + m = 3)$, and antiaromatic when the sum is 4.

A range of cyclic siloxanes containing boron atom of different ring sizes (6-10) were isolated by Manners and his coworker³⁶. Six-membered ring compounds $(\text{PhBO})(\text{RR}^*\text{SiO})_2$ ($\text{R} = ^* = \text{Me}$ or Ph ; $\text{R} = \text{Me}$, $\text{R}^* = \text{Ph}$) were prepared by the reaction of the dichlorotetraorganodisiloxanes with phenylboronic acid in the presence of Et_3N as an acid acceptor. Similar procedures using the appropriate α,ω -dichlorosiloxanes $\text{ClMe}_2\text{Si}(\text{OSiMe})_n\text{OSiMe}_2\text{Cl}$ ($n = 1$ or 2) give eight and ten-membered rings $(\text{PhBO})(\text{Ph}_2\text{SiO})_3$ and $(\text{PhBO})(\text{MeSiO})_4$ respectively.



The x-ray crystal structure of $(\text{PhBO})(\text{Ph}_2\text{SiO})_2$ confirmed the presence of a six-membered BSi_2O_3 planar ring, and analysis of the structural data indicates that the structural consequences of replacing a silicon atom (covalent radius 1.17 Å) by boron atom (covalent radius 0.80 Å) are very significant. This causes an appreciable decrease of 0.26 Å in the distance between the two oxygen atoms in the $2\text{Si}-\text{O}(\text{B})$ bond compared to the situation in $(\text{Ph}_2\text{SiO})_3$ ³⁷. This contraction can be readily appreciated by noting the non-parallel nature of the $\text{Si}-\text{O}(\text{B})$ bonds. The enforced decrease in the oxygen distance leads to a marked contraction of the bond angles to $[127.1^\circ]$ compared to the value of $[131.8^\circ]$ in cyclohexaphenyltrisiloxane. The presence of appreciable angle strain in the

six-membered ring containing Si-O-B is further emphasized by a consideration of the much larger Si-O-Si bond angles found in unconstrained, linear disiloxanes such as $\text{Me}_3\text{SiOSiMe}_3$ [148.8°] or in essentially unstrained cyclic siloxanes such as $(\text{Ph}_2\text{SiO})_4$ [152.3 and 167.4°]³⁸. Another important feature of the six-membered ring in $(\text{Ph}_5\text{Si}_2\text{BO}_3)$ is the significant widening of the O-B-O bond angles to [120.8°] compared to the analogous value of [118°] in the $\text{Ph}_3\text{B}_3\text{O}_3$ ³⁹. In addition the structure of $(\text{Ph}_3\text{BO}_2\text{Si})_2$ which contains an eight-membered planar ring with a 1:1 silicon to boron ratio has been recently determined⁴⁰. The pattern of bond angles about oxygen across the planar eight-membered ring is remarkably uniform. Only in tricyclic $\text{Me}_{12}\text{Si}_8\text{O}_{10}$ containing two Si_3O_3 rings fused to opposite points of a near planar Si_4O_4 unit (Σ internal angles = 1072.4°) is equality of the O-Si-O angles observed ($159.1(9)^\circ$)⁴¹, while the M_3O_3 rings are almost invariably planar. This is not the case for the M_4O_4 systems where planarity is relatively rare. The non-planar rings, typified by the $(\text{Si}_2\text{Ge}_2\text{O}_4)$ ³³ system discussed earlier, incorporate uniform angles about oxygen atoms in contrast to the planar species. It would appear that in the planar species, the majority of the ring strain is concentrated at a limited number of sites, rather than being evenly distributed.

Interestingly, the strain induced in the eight-membered Si_4O_4 by substitution of two boron atoms is more pronounced than the single substitution on going from $\text{Ph}_6\text{Si}_3\text{O}_3$ to $\text{Ph}_5\text{Si}_2\text{BO}_3$, as reflected in the changes in angles of the oxygen atoms. Thus, the maximum angular changes at oxygen on going from $\text{Ph}_6\text{Si}_3\text{O}_3$ to $\text{Ph}_5\text{Si}_2\text{BO}_3$ is 4.5° , while the analogous angles change by 7.3° from $\text{Ph}_8\text{Si}_4\text{O}_4$ to $\text{Ph}_6\text{Si}_2\text{B}_2\text{O}_4$ ⁴⁰.

Ring-opening polymerization represents a powerful synthetic route to a variety of organic polymers such as polyamides, polyethers, polycycloolefines, and most recently, polyacetylenes and polycarbonates⁴². In view of the abundance and the structural diversity of known cyclic inorganic compounds, ring opening polymerization might be expected to provide access to a similar or even broader range of inorganic macromolecules⁴³. However, although the polymerization behaviour of cyclic siloxanes and cyclic phosphazenes has been well explored and the ring opening polymerization of species such

as $[\text{Me}_2\text{SiO}]_n$ ($n = 3, 4$) and $[\text{NPCl}_2]_3$ provides routes to two of the most important inorganic polymer systems, the polysiloxanes and polyphosphazenes, relatively few other inorganic ring systems have been studied in detail^{44,45}. During the course of this work, the ring-opening polymerization reactions on heat treatment of heterocyclosiloxanes containing boron with 1:1 and 2:1 silicon to boron ratio were studied and are discussed in Chapter 6.

2.4 REFERENCES

1. I Haiduc, *The Chemistry of Inorganic Ring Systems*, Wiley-Interscience, London, 1970, Part 1 and references therein.
2. L Pauling, *The Nature of the Chemical Bond*, Cornell University Press, Ithaca, New York, 1960, 322.
3. O Chalvet and J Kaufman, *J Am Chem Soc*, 1965, **87**, 399.
4. K Ya Syrkin, *Usp Khim*, 1962, **31**, 398.
5. E Hanecker and H Noth, *Z Naturforsch*, 1985, **40b**, 717.
6. R Van Veen and F Bickelhaupt, *J Organomet Chem*, 1972, **43**, 214.
7. S W Breuer and F A Broster, *Tetrahedron Lett*, 1972, **22**, 2193.
8. R A Bowie and O C Musgrave, *J Chem Soc C*, 1966, 566.
9. A G Davies, K U Ingold and B P Robert, *J Chem Soc B*, 1971, 698.
10. A Dornow and K Fischer, *Chem Ber*, 1966, **99**, 68.
11. B Dejak and Z Lasocki, *J Organomet Chem*, 1972, **44**, C39.
12. W Clegg, U Klingebiel and G M Sheldrick, *Z Naturforsch*, 1982, **37b**, 423.
13. Z Lasocki and M Witekowa, *Synth React Inorg Metalorg Chem*, 1974, **4**, 231
14. E P Lebedev, V G Zavada and A D Fedorov, *Zh Obshch Khim*, 1979, **49**, 151.
15. R P Bush and C A Pearce, *J Chem Soc*, 1969, 808.
16. D R Parker and L H Sommer, *J Organomet Chem*, 1976, **110**, C1.
17. K A Andrianov, A B Zachernyuk and E A Zhdanova, *Dokl Akad Nauk SSSR*, 1974, **214**, 325.
18. W Fink, *Chem Ber*, 1963, **96**, 1071.
19. K Lienhard and E G Rochow, *Angew Chem Int Ed Engl*, 1963, **75**, 638.
20. U Wannagat, *Pure Appl Chem*, 1966, **13**, 263.
21. R L Wells and R W Nelson, *Inorg Nucl Chem letters*, 1965, **1**, 149.
22. U Wannagat and G Eisele, *Z Naturforsch*, 1978, **33b**, 475.
23. M G Vorankov, E A Maletina and V K Raman, *Comprehensive Review*, Harwood

- Acad, 1988.
24. A K McMullen, T D Tilley, A L Rheingold and S J Geib, *Inorg Chem*, 1989, **28**, 3772.
 25. F Calderazzo, F Marchetti and G Amico, *J Chem Soc Dalton Trans*, 1980, 1419.
 26. H Schmidbaur, J Adlkofer and A Shiotani, *Chem Ber*, 1972, 723.
 27. V A Zeitler and C A Brown, *J Am Chem Soc*, 1957, **79**, 4618; M A Hossain, M B Hursthouse and M A Mazid, *J Chem Soc, Chem Commun*, 1988, 1305.
 28. M B Hursthouse and M A Hossain, *Polyhedron*, 1984, **3**, 95.
 29. M Motevalli, M Sanganee, P Savage and S Shah, *J Chem Soc Chem Commun*, 1993, 1132.
 30. A W Apblett and A R Barron, *Organometallics*, 1990, **9**, 2137.
 31. N N Belov and I M Kolesnikov, *Zh Fiz Khim*, 1982, **56**, 2103.
 32. S Harvey, M F Lappert and C L Raston, *J Chem Soc, Chem Commun*, 1988, 1216.
 33. H Puff, M P Bockmann, T R Kok and W Schuh, *J Organomet Chem*, 1984, **268**, 197.
 34. H Puff, P Nauroth, T R Kok and W Schuh, *J Organomet Chem*, 1985, **281**, 141.
 35. P P Power, *J Organomet Chem*, 1990, **400**, 49.
 36. D A Foucher, A J Lough and I Manners, *J Organomet Chem*, 1991, **414**, C1.
 37. G N Bokii, N G Zakharova and T Y Struchov, *Zh Strukt Khim*, 1972, **13**, 291
 38. J M Barrow, V Ebsworth and M Harding, *Acta Crystallogr*, 1979, **B35**, 2093.
 39. P C Brock, P R Minton and K Niedenza, *Acta Crystallogr*, 1987, **C43**, 1775.
 40. B J Brisdon, M F Mahon, K C Molloy and P J Schofield, *J Organomet Chem*, 1992, **436**, 11.
 41. E Lukevics, O Pudova and R Sturkovich, in *Molecular Structure of Organosilicon Compounds*, Ellis Horwood, Chichester, UK, 1989, 196.
 42. K J Saegusa, *Ring Opening Polymerization*, Eds; Elsevier, New York, 1984.
 43. I Haiduc, I Sowerby, *The Chemistry of Inorganic Homo- and Heterocycles*, Eds; Academic Press, Tronto, 1987, **1**, 109.

44. J M Zeigler and J M G Fearon, Silicon Based Polymer Science: A Comprehensive Resource. ACS Series 224, Washington, USA, 1990, 194.
45. M Cypryk, Y Gupta and K Matyjaszewski, J Am Chem Soc, 1991, **113**, 1046.

CHAPTER THREE

INTRODUCTION TO CERAMICS AND PRECERAMIC POLYMERS

3.1 SUMMARY

In this chapter the general methods of forming and fabrication of ceramics together with their main properties and functions will be discussed briefly, with the production of ceramic materials containing Si-C-B-O-N through preceramic polymer precursors being highlighted. Ceramic materials have traditionally been prepared from structurally simple starting materials. As a result, their structural features are relatively difficult to control or modify in a systematic fashion. Many polymeric organic and organometallic materials, on the other hand, can be designed and synthesized in a more controlled fashion by proceeding in a step-wise manner, i.e. by polymerizing these monomers in a subsequent reaction step. Successful polymer pyrolysis requires (i) identifying a suitable polymer, (ii) devising an efficient preparative route, (iii) effecting polymer characterisation (yield, molecular weight, purity, etc), and (iv) developing pyrolysis conditions that will yield a quantity and quality of the desired ceramic. Ceramic yield is typically measured by the weight of the ceramic product as a percentage of the starting polymer weight. The quality of the ceramic product is a function of polymer composition, structure, and processing conditions and is reflected in the composition of the product. Making ceramics by the pyrolysis of organometallic polymers, or other precursors, has begun to attract considerable attention; such processing shows great promise for producing improved ceramics and resultant expanded and new ceramic applications.

3.2 GENERAL CONSIDERATION OF CERAMIC MATERIALS

The initial material of this section is drawn from general reviews of standard texts on ceramic materials^{A1}. Initially, the majority of ceramics were based on clay, the word ceramic being derived from the Greek word Keramos, the word for objects made of fired clay. This includes pottery and porcelain, glass and enamel, bricks and refractories, cement and concrete. Added to these were carbon materials, electrical and thermal insulators, and grinding and sharpening tool materials. A common characteristic of these traditional ceramics was that they were based on natural raw materials, with an inherent variation in composition, characteristics and manufacturing processes. Many of these traditional ceramics were located on either the silica-clay or the alumina-silica-magnesia systems. Advanced (fine) ceramics were developed for specific properties, especially mechanical, electrical/electronic, thermal or optical properties. They differ from the traditional ceramics in that they use highly refined raw materials, with rigorously controlled composition and characteristics, and strictly controlled manufacturing processes. The common features of ceramics are high heat resistance, electrically insulating or semi-conducting, with various magnetic and dielectric properties, strong resistance to deformation and low toughness. The range of microstructures found in ceramics stems from the fact that they generally arise from the sintering of particles, frequently involving the presence of a liquid phase, rather than from cooling from the molten state. Two major consequences often arise from this, the presence of significant porosity and thick grain boundary regions.

Industrial materials are classified into classes which reflect differences in chemical bonding. Almost all ceramics are compounds of the electropositive and electronegative elements and ionic bonding, but in some cases covalent or metallic bonding occurs. Because of their extensive ionic and/or covalent bonding many ceramics have a high melting point, high hardness, high Young's modulus, and good resistance to abrasion and

wear. However, many potential uses are precluded by their brittleness and poor thermal shock resistance. This brittleness, or lack of toughness, arises because the bonding, unlike that in metals, does not allow a region of plastic deformation to develop at a crack tip and dissipate the energy and so blunt crack growth.

The ionic ceramics are generally compounds of metallic ions and non-metallic ions, most commonly the oxide ion. The resulting crystal structures approximate to the most efficient packing of the constituent ions, with ions of opposite charge being as close together as possible. The covalent ceramics are generally compounds of two non-metals, but also includes the element carbon, which forms very directional bonds, generally giving chains, sheets or 3D networks of the constituent atoms.

Up to now porcelain, refractories, etc., have been made using crushed natural minerals, but in order to make use of the specific functions of fine ceramics, high purity and extremely fine powders are necessary before the raw material is sintered. Figure 3.1 shows the structural changes accompanying the manufacture of a sintered product. So new methods have been developed for the synthesis of base materials.

These methods, which produce refined base powders that comply with the limits summarized in Figure 3.2.

In sintered ceramics which includes the majority of ceramics, it is difficult to use the melting-pouring-hardening methods employed with metals and plastics, and injection moulding requires malleability. Therefore, methods for shaping and then sintering powders are often used. Depending on shape and required characteristics, numerous powder forming processes have been developed. The five main ones are illustrated in Figure 3.3.

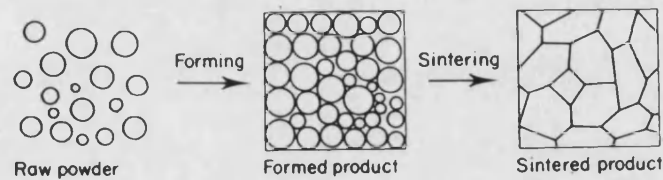


Figure 3.1 Structural changes accompanying the manufacture of a sintered product

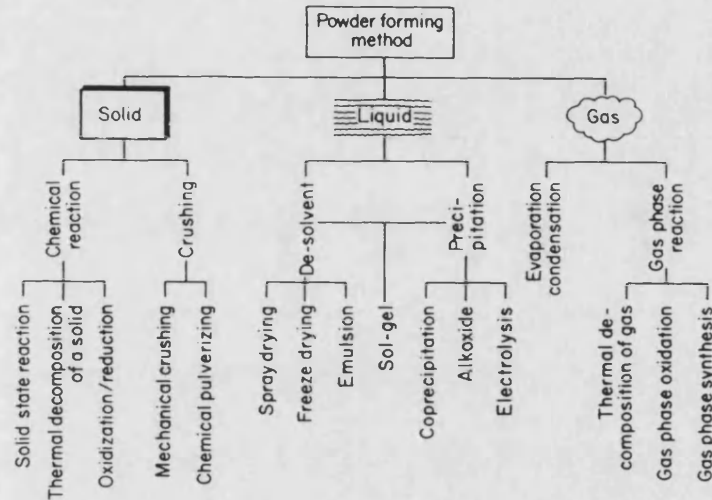


Figure 3.2 Powder synthesis methods

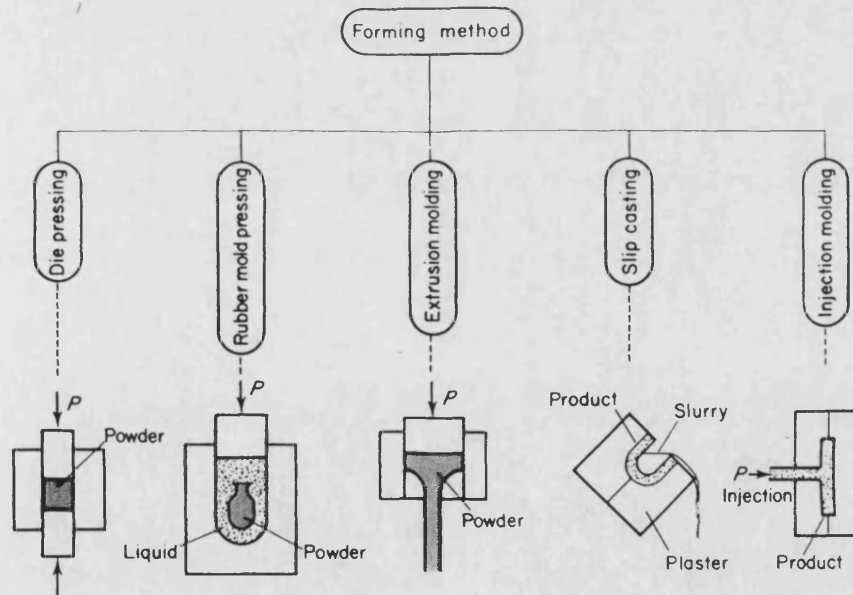


Figure 3.3 Forming methods of ceramics

Ceramics have a wide range of characteristics, so there are a variety of sintering methods. The main processes are shown in Table 3.1. Usually, ceramics are oxides or non-oxides composed of metallic and non-metallic elements. Therefore, there are many kinds of ceramics with function in many fields.

Figure 3.4, from S Saito¹, summarises the field under the headings of function, properties and application. Finally, it is perhaps useful to summarise the properties which make fine ceramics of such potential and actual use to engineers Table 3.2.

Table 3.1 Methods for sintering ceramics

- | | |
|----------------------------------|-------------------------------|
| ○ Standard pressure sintering | ○ Reaction-sintering |
| ○ Hot pressing | ○ Post-reaction sintering |
| ○ Hot isostatic pressing | ○ Recrystallization sintering |
| ○ Atmospheric pressure sintering | ○ Chemical vapor deposition |
| ○ Ultra-high pressure sintering | |

Table 3.2 Properties of special ceramics

<u>Structural</u>	<u>Functional</u>
High hardness	Piezoelectric effect
High stiffness	Pyroelectric effect
High corrosion resistance	Optoelectric effect
High strength (compression)	Dielectric properties
Low density	Temp. dependent resistivity
Low thermal expansion	Voltage sensitive resistivity
Low friction	Superconduction
Low toughness	
Wide range of thermal conductivity	

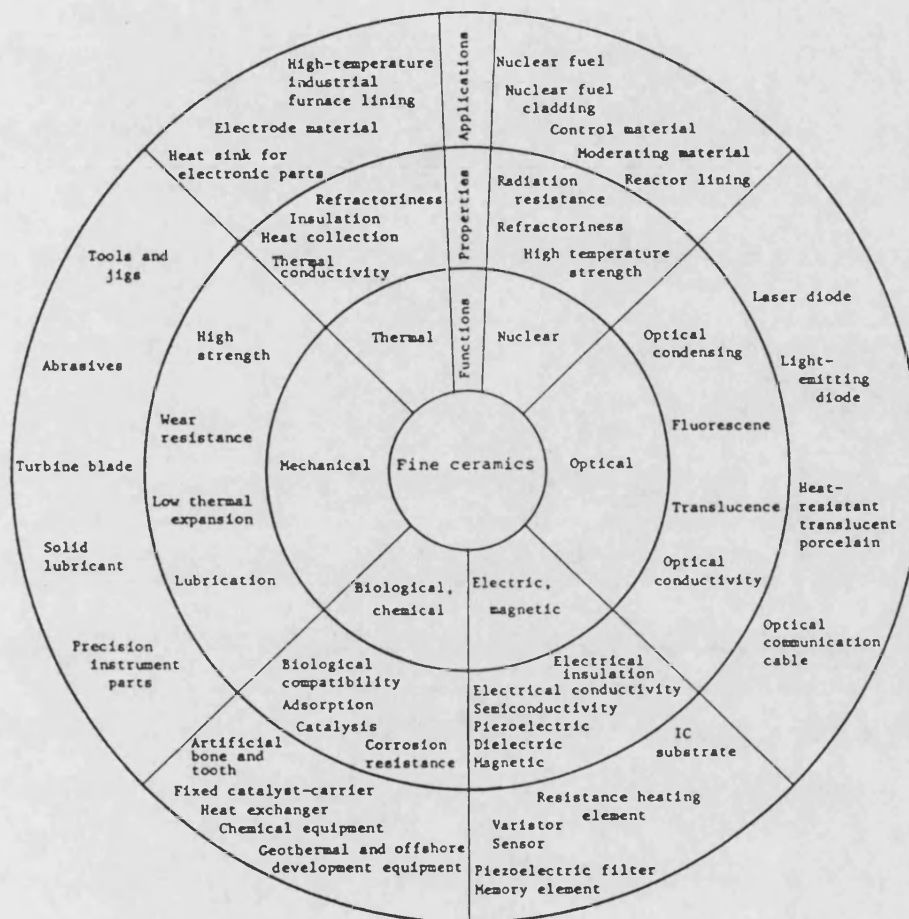


Figure 3.4 Some functions and applications of fine ceramics, (from Japan Fine Ceramics Assoc., Survey of Trends in Development of Fine Ceramics Technologies and Situation of Development of Related Equipment, April 1983)

3.3 CONVENTIONAL ROUTES TO CERAMICS

There are many conventional routes for synthesis of traditional and advanced ceramics on both the laboratory and industrial scale. At the same time there is increasing demand for alternative routes to ceramic materials that impart superior properties compared with those attainable from conventional syntheses. A brief review of the main conventional routes to ceramic will be discussed, to provide a background to the fabrication route of principal interest in this study of the conversion of polymer to ceramics.

3.3.1 Precipitation from Solution

Alumina occurs as the mineral bauxite and is refined in the Bayer process whereby ore is initially dissolved under pressure in sodium hydroxide so that solid impurities (SiO_2 , TiO_2 , Fe_2O_3) separate from sodium aluminate solution. This solution is seeded with crystals ($\alpha\text{-Al}_2\text{O}_3 \cdot 3\text{H}_2\text{O}$), after neutralisation with CO_2 gas. Temperature, alumina supersaturation and amount of seed affect the particle size during crystallization but, as for other precipitation reactions, the product is agglomerated.

Another important example is zirconyl chloride which is obtained from the product of fusion between zircon and sodium hydroxide. The manufacturing route for producing partially stabilised zirconia powder, involving precipitation from this chloride solution is shown in Figure 3.5. Problems can arise when two or more components are coprecipitated. Thus different species do not always deposit from solution at the reaction pH, while washing procedures can selectively remove a precipitated component as well as dissolve entrained electrolyte. The difficulty in maintaining chemical homogeneity is serious as inhomogeneities have a deleterious effect on the mechanical and electrical properties of ceramics. Because precipitation results in agglomerated powders, grinding, dry-milling or wet-milling with water or non-aqueous liquid are used for particle size reduction so that powder compacts will sinter to near theoretical density. These comminution processes can

introduce impurities into the ceramic from the grinding media, while high temperatures are required for densification.

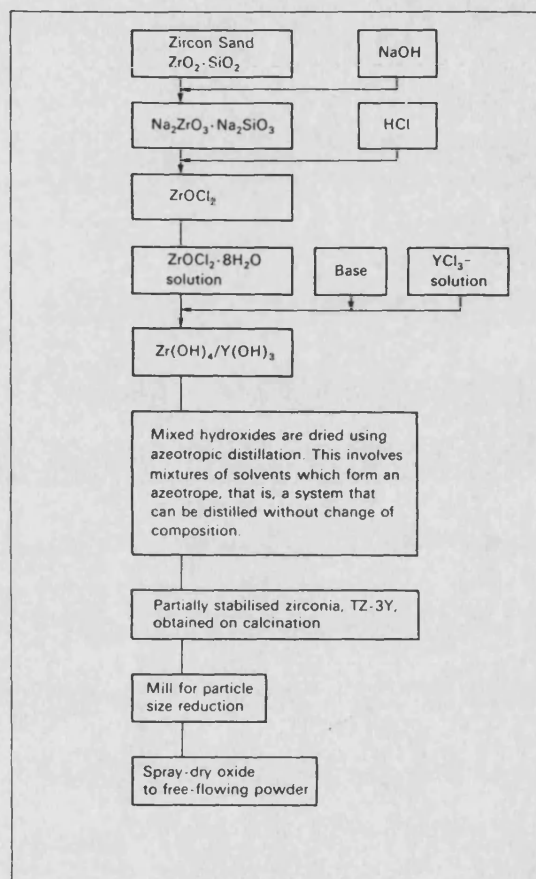


Figure 3.5

Schematic representation of a commercial process for producing partially stabilised zirconia powder by a coprecipitation process, (Toya Soda Company, 1984)

3.3.2 Powder Mixing Techniques

Multi component oxide powders are synthesized from conventional mixing techniques by initially blending together starting materials, usually metal oxides and carbonates, after which the mixtures are ground or milled. Comminuted powders are then calcined, sometimes after compaction, and the firing sequence may be repeated several times with intermediate grinding stages. As for coprecipitation, impurities can be introduced into the ceramic from the grinding operation; grinding also results in angular-shaped powders. Several problems are associated with mixing powders. High temperatures required for reaction between components can result in loss of volatile oxides, while milling may not comminute powders sufficiently for complete reaction to occur on calcination. It is difficult to obtain reproducible, uniform distributions of material in ball-milled powders, especially when one fraction is present in small amounts as occurs in electroceramics whose properties are often controlled by grain boundary phases containing minor quantities of additives.

3.3.3 Fusion Route to Ceramics

Fusion techniques are used for traditional ceramics such as window glass and advanced ceramics such as abrasive grains. These methods are limited by the melting point of reactants, while high temperatures can lead to loss of volatile oxides, for example PbO, from the melt. Glass ceramics were discovered in 1964 and are polycrystalline materials made by controlled crystallization of glasses. In these techniques, the reactants are mixed as powders and melted, after which nucleating agents are added. These promote nucleation at temperatures with corresponding viscosities between 10^{10} - 10^{11} Pas, which are usually about 50K above the softening temperatures of the glass. The temperature is then raised until crystallization occurs and the microstructure is developed.

3.3.4 Ceramic Sintering and Fabrication

Solid ceramic bodies are generally produced by using the process of powder compaction followed by firing at high temperature. Sintering or powder densification occurs during this heat treatment and is associated with joining together of particles, volume reduction, decrease in porosity and increase in grain size. The aim of these techniques is to produce microstructures suitable for particular applications. Hence a fine-grained distribution is required for strength, controlled grain size is necessary where optical properties such as translucency are required.

Sintering processes can be sub-divided into three categories. These are:

Solid-state sintering: no liquid is produced at any stage during solid-state sintering. All densification is achieved by changes in particle shape and size.

Liquid-phase sintering: the composition of the greenbody and the processing conditions are such that some liquid forms. This allows particle rearrangement, but insufficient liquid is produced to fill all the greenbody porosity.

Viscous flow sintering: sufficient liquid is formed to fill all the green state porosity and bind the particles together. This means that about 20% of the greenbody needs to melt.

The ease of forming fully dense materials increases with the amount of liquid that is formed during sintering. Any liquid that is formed and not consumed during processing will solidify to form a grain boundary or matrix phase. This will preclude the use of the ceramic at elevated temperature since the grain boundary phase will soften leading to problems with creep. Thus, solid-state sintering is the preferred route for the production of ceramics for high temperature applications. For some materials most notably silicon nitride, solid-state sintering routes have not been found and these materials must be liquid-phase sintered. Viscous flow sintering is used extensively in the fabrication of traditional ceramics, Figure 3.6.

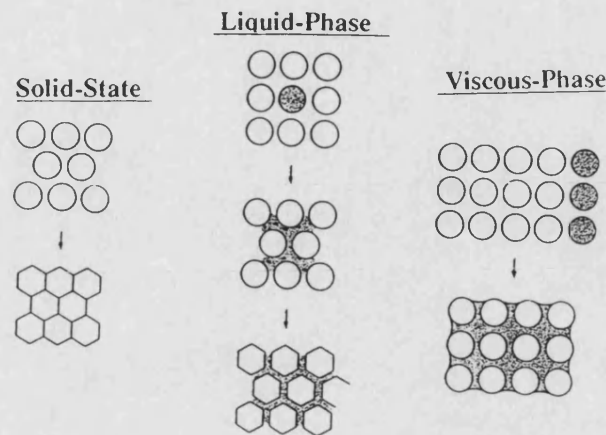


Figure 3.6 **Schematic of the three types of sintering**

The solid-state sintering is sub-divided into three stages, the initial stage in which the density increases by a few percent, the intermediate stage during which the majority of the densification takes place and the final stage corresponding to a slight increase to give the final density. There is no clear demarcation between the three stages but certain phenomena are associated with each one.

Initial stage: Grain boundaries form between the particles and the neck region grows. The sharp re-entrant angles at the points of contact are rounded off. The start of densification is detected when the centres of the particles begin to approach one another. In this stage the ratio of the radius of the circle of contact to the particle size is less than 0.3.

Intermediate stage: The open interconnected porosity decreases significantly and with time porosity may become closed (isolated pores) and grain growth may begin.

Final stage: When the porosity level is below about 8%, open porosity becomes geometrically unstable. Isolated pores decrease in volume, the larger ones more slowly than the smaller ones which might disappear completely. Grains grow and grain boundary area decreases. The gas trapped inside porosity will limit the end density.

Liquid-phase sintering is a sintering where the densification kinetics are much more rapid than for solid-state sintering and thus the process is a more economical way of producing dense products. Also, it is possible to densify materials that cannot be solid-state sintered, such as silicon nitride, since the method includes two stages which are not dependent on lattice vacancy concentration, although the final stages of densification still require solid-solid interactions. The major disadvantage is the poor high temperature performance of the product due to the residual grain boundary phase. The majority of the densification takes place immediately after melting. It is important that the liquid is able to wet the ceramic particles to allow them to slide over one another and thus rearrange to a denser structure. Further densification occurs as a result of the solid powder dissolving in the liquid, under the influence of pressure at the contact points, and reprecipitating elsewhere. As the solid particles are brought together the liquid is squeezed out and the final stages of densification occur by solid-solid interactions. On cooling the liquid solidifies as film or matrix. Conversion of this phase to crystalline form, as in the post-sinter treatment of sialons, or removal of the liquid prior to solidification are of interest as they will remove the major limitation of the technique.

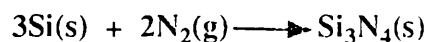
There are various other ways of producing a dense ceramic which do not involve forming a greenbody and then sintering:

Hot pressing (HP); Where the powder is placed in a mould and sintered under pressure at high temperatures. This method is used with Si_3N_4 , SiC , Al_2O_3 , etc. It is best suited to material that can be solid-state sintered, since liquid phases would tend to be squeezed out causing inhomogeneities. Applying pressure increases the driving force for densification. The densification kinetics are increased due to particle rearrangement and particle flow. Thus it is possible to decrease the sintering time and reduce the sintering temperature, resulting in less grain growth. Hot pressed products have lower levels of porosity than solid-state sintered specimens which, coupled with the smaller grain size, results in stronger material.

Hot isostatic pressing (HIP); While hot pressing is carried out with pressure along

a single axis, this method uses gas pressure (commonly argon) to obtain isostatic pressure, which increase greatly the driving force for densification, lowering sintering temperature by 25-30% and decreasing the need for additives. Recently the effects of HIP treatment to the change in final densities and microstructures of sintered silicon nitride were analysed in terms of the types and amounts of sintering additives, and pre-HIP sintering conditions².

Reaction sintering/reaction bonding; Reaction sintering and reaction bonding are two terms for a process in which the ceramic is made at the same time as densification is occurring. Silicon nitride and silicon carbide can be produced this way. Reaction sintered Si₃N₄ is made by heating a greenbody of silicon powder in a nitriding atmosphere. The following reaction takes place:



During the reaction the compact increases in weight but the dimension changes by less than 0.1%. The product is never fully dense since open porosity is required to transport the gas to all parts of the greenbody to ensure complete reaction.

3.3.5 Sol-gel Techniques

Sol-gel processing has attracted much interest for the preparation of powders, coatings and cast shapes. The process encourages the intimate mixing of components, produces materials that are sinter-active, and hence easier to convert to dense products, and is versatile in terms of end product³. Powders can be produced, but it is also possible to make coatings, fibres and monoliths without the need to make a powder first. The words sol-gel refer to the two physico-chemical states that arise during processing.

The sol can be a true sol i.e. a colloidal dispersion of a solid phase in a liquid phase or sol can be an abbreviation for solution. Solutions of metal-organic compounds, namely alkoxides, are frequently used in sol-gel processing. During the sol-gel transition the particles or macromolecules cross-link and form a structure that immobilises the

remaining solvent. This gives a gelatinous mass, known as a gel. The drying of the gel is crucial in determining the morphology of the end product. For coatings, fibres and monolithic bodies the gel must not break up and factors affecting stress development have been much discussed³, but for powder production the gel can be more friable. Powders can also be made by peptising an aggregated sol (Figure 3.7).

Sol-gel processing of colloids involves the dispersion of the starting material to form a sol followed by the removal of water and/or anions to form a gel. The sol-gel transition is usually reversible. The first major application of sol-gel processing of colloids was the production of mixed (Th,U)O₂ fuels for thermal reactors. A more recent development is the manufacture of Saffil fibres. These are 95 wt% Al₂O₃, 5 wt% SiO₂.

Mixing on the molecular level can be achieved through the sol-gel processing of alkoxides, these are metal-organic compounds with the general formula M(OR)_{*z*}, where M is a metal ion and R is an alkyl group. Gels are formed from solutions of alkoxides by hydrolysis and polymerisation Figure 3.8.

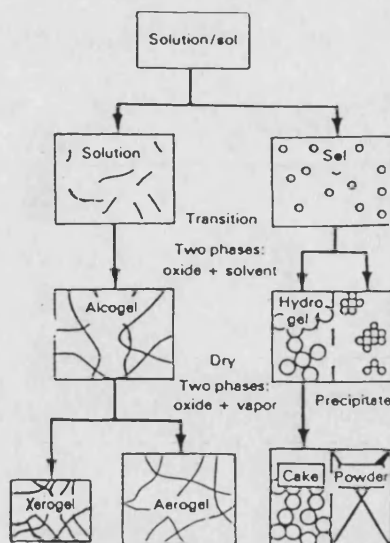


Figure 3.7 Schematic of the various sol-gel processing routes

Initial hydrolysis



Polymerisation

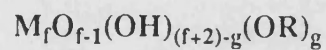
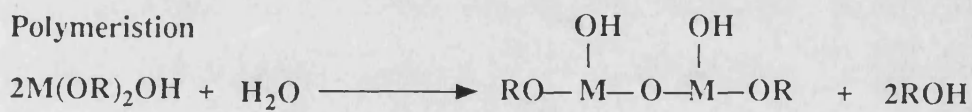


Figure 3.8 Typical reaction pathway for producing an alkoxide gel, (Yoldas 1973)

3.4 PRECERAMIC POLYMERS (PCP)

The special requirements of preceramic polymers are based on the requirements for the specific ceramic application. Heat engines and similar applications require structural ceramics stable in combustion atmospheres above 1200°C. Examination of the thermodynamic stabilities of these ceramic systems is helpful. Currently, most ceramics derived from preceramic polymers are silicon-based. Ceramics with varying Si:C:N:O ratios can be prepared by processing preceramic polymers. A calculation of the vapour pressure of all species found in Si-C-N-O systems showed that N₂, CO, and SiO are the most prevalent species at 1200°C with vapour pressures of (22.5, 7.5 and 0.0075 mm Hg), respectively⁴. Therefore, for highest thermal stability, the oxygen content of silicon carbide-based ceramics should be minimized, but at the same time, a large excess of free carbon should be avoided because ceramics with high free carbon content have poor oxidation resistance. Additionally, structural ceramics require high elastic modulus, and as this is a function of the concentration of covalent bonds per unit volume, elastic modulus decreases with increasing oxygen content over carbon. This can be explained in terms of Young's moduli for SiC, Si₃N₄ and SiO₂ of 412, 300, 70 GPa respectively. The oxidative stability of a series of ceramics which were produced by pyrolysis of silsesquiazanes [RSi(NH)_{3/2}]_x at 1200°C, was examined⁵. The ceramics with more than 35-40 wt% free carbon oxidized completely to silica after 12 hours at 1200°C in air, whereas, those with less than 25% carbon content contained only about 2% oxygen after the same heat treatment. This indicates that a large excess of carbon should be avoided. Structural ceramics require high elastic modulus and high flexural strength.

The strength of ceramic materials is determined by the law of brittle fracture expressed by the Griffith relationship:

$$\sigma_f = A(\gamma E/c)^{1/2}$$

where σ_f is the failure stress, A a flaw shape factor, γ the fracture surface energy, E

Young's modulus, and c effective size of the flaw. The size and shape of flaws determine the strength and depend on processing; γ and E are material-dependent parameters. Fracture toughness of monolithic ceramic materials is also governed by E and γ .

The brittle nature of ceramics can be overcome by forming a composite of ceramic fibres in a ceramic matrix⁶. The ceramic fibres can be made from preceramic polymers. The toughness of ceramic composites is controlled by the interaction of the fibres with the matrix. The composite derives its toughness from an energy-absorbing mechanism involving the separation of fibres from the matrix prior to fracture. Therefore, it is important in the design of ceramic-fibre precursors to consider the effects of the ceramic on the matrix-fibre interface.

The extremely high softening point precludes the moulding of complex shapes and fibres from the melt. Sintering aids used to densify SiC and Si₃N₄ powders usually compromise properties such as strength at high temperatures and oxidation resistance because of the formation of low melting glassy phases at grain boundaries. The process for reaction-sintered silicon carbide ceramic invariably leaves silicon in the pores of the Si-C body which causes weakening, especially above the melting point of silicon. The usefulness of reaction bonded silicon-nitride ceramics is limited to thin parts because thick sections of these ceramics are plagued by porosity; furthermore, the nitriding cycle takes several days to a week for completion. High temperature ceramic coatings may prolong the life of engineering systems, but matching of thermal expansion, adhesion and surface stresses between the coating and the substrate need to be resolved first.

Because of these difficulties, attention is focusing on new chemical routes employing organometallic and inorganic polymers as precursors. Controlled pyrolysis of these polymers has revealed several promising directions such as formation of fibres, ultra-fine powders, thin films and layer structures, and high strength, light weight monolithics and composites^{7,8}.

The route illustrated in Figure 3.9 is similar to the controlled pyrolysis of organic polymers such as polyacrylonitrile to produce carbon fibres. Organometallic preceramic

polymers offer several ways to overcome the fundamental problems of shaping ceramics: traditional low temperature processing techniques are used to form complex shapes such as fibres and yarns; fabricated shapes are converted to ceramic forms at lower temperatures than those of traditional ceramic processing. This is possible because the Gibbs free energy of formation of organometallic compounds is favourable. Pure starting materials and assured homogeneous mixing improve the uniformity and reliability of the final product. Novel ceramic alloys with a wide range of properties are conceivable because the organometallic starting materials are mixed at the atomic level. Additives, such as sintering aids, may be more effective when they are part of the precursor polymer.

Relatively little is known of the chemical processes by which polymers are converted to ceramics. IR, thermal gravimetric analysis (TGA), and x-ray data have been used to study the gross features of the conversion process in some cases⁹, but generally spectroscopic investigations have been limited. Considering the complex polymer structures that serve as precursors, and even more complex, amorphous, intractable structures that are intermediates in the pyrolysis process, it is clear that mechanistic studies pose a formidable challenge. Despite a lack of detailed chemical knowledge, the production of silicon-based ceramics via a polymer pyrolysis route has been commercialised. High ceramic yield is needed for low shrinkage upon pyrolysis and for minimum cost. For fibre spinning or other shaping operations, the polymer must be tractable, i.e. moderate softening temperature or solvent solubility. The polymer must undergo cross-linking reactions after it is shaped to avoid deformation during pyrolysis. In general branched-ring (polycyclic or cage) polymers with low molecular weight provide the desired tractability and favourable pyrolysis with high ceramic yield. Most effective silicon-based preceramic polymers developed thus far are in this category. For high quality ceramic fibres with high mechanical strength, high polymer purity and lack of spinning-induced imperfections are essential.

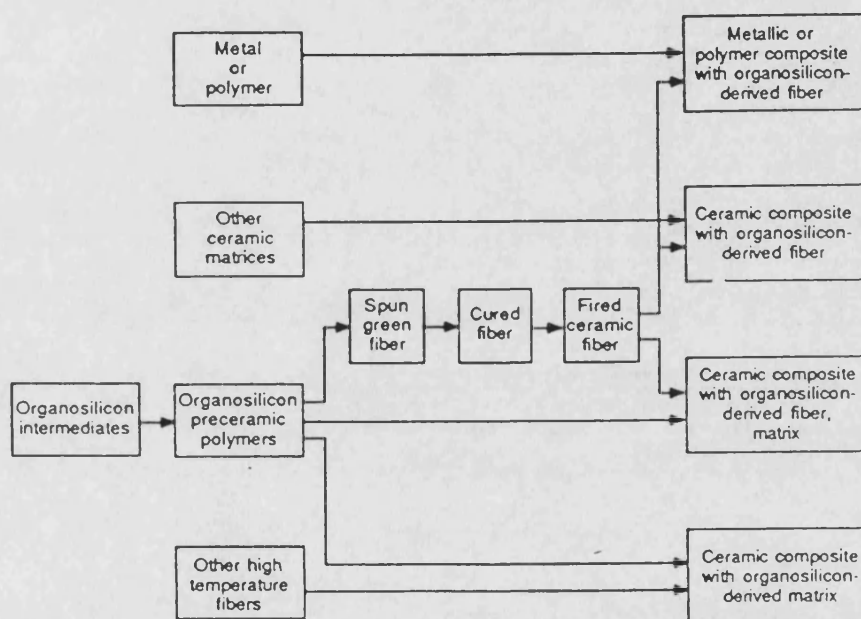


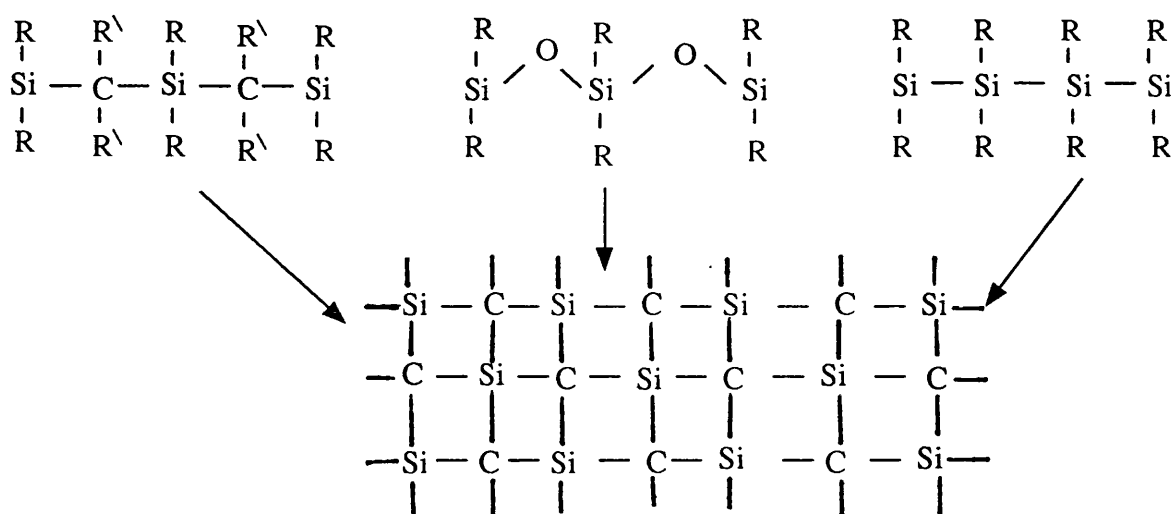
Figure 3.9 Organosilicon-derived ceramic fibre and composite main routes to silicon carbide

3.4.1 Silicon-Carbon Ceramic Precursors

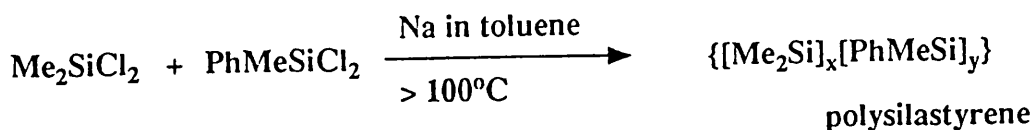
Two classes of organosilicon polymers can be converted into silicon carbide (SiC) ceramics by appropriate thermal treatment¹⁰. Their generic names are polycarbosilanes and polycarbosiloxanes (see chapter 1). The structural backbone of polycarbosilanes contain chains of silicon and carbon and is represented simply by the structure -Si-C-Si. The polycarbosiloxanes also contain oxygen, but the terminals of the polymer are hindered by the introduction of suitable siloxane and/or organic group.

The actual chemical structure, the molecular sizes and the molecular size distribution of the organosilicon polymers are determined by the chemical nature of the starting compounds and the processing parameters. Both classes of organosilicon polymers can produce SiC on thermal treatment in an inert atmosphere. Polycarbosilanes produce amorphous SiC at approximately 800°C or less depend on the thermal history of the materials, and subsequently crystalline SiC at higher temperature. On the other hand, the SiC from polycarbosiloxanes¹¹ remains amorphous up to about 1500°C and completely converts to crystalline SiC at about 1700°C¹².

The rheological properties of polycarbosilane and its pyrolytic behaviour which determine its usefulness as a binder can be related to molecular structure and molecular weight distribution. Therefore, an understanding of chemical nature and pyrolytic behaviour is important in designing the plan of investigations. The pyrolytic conversion of polycarbosilane and polycarbosiloxane into SiC ceramics is not a simple process. The complexities arise mainly as a result of simultaneous polymerisation, decomposition and degradation reactions. Some studies¹³ have reported on the pyrolytic conversion of the polycarbosilane to produce SiC, but the mechanism of polymer pyrolysis has not been clearly understood.



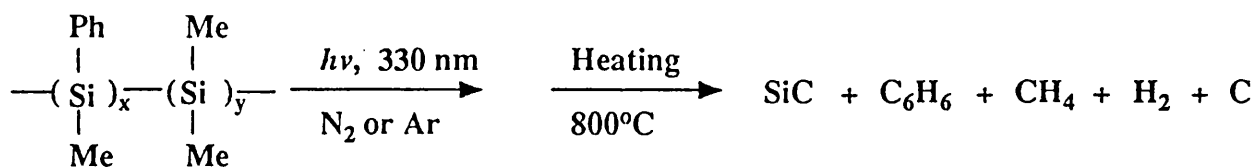
The conversion of polysilane polymers to silicon carbide is based on permethylpolysilanes¹⁴, derived from readily available $(\text{CH}_3)_2\text{SiCl}_2$; this process was commercialised in Japan by the Nippon Carbon Co Ltd. to produce high strength silicon carbide fibre. Thermal decomposition of linear permethylpolysilanes, or the cyclic $[(\text{CH}_3)_2\text{Si}]_6$, in an autoclave at $450\text{--}470^\circ\text{C}$ yields a polycarbosilane⁸. A 3-5% polyborodiphenylsiloxane catalyst allows this process to proceed at lower temperatures and atmospheric pressure¹⁵. The polycarbosilanes obtained were purified by solvent extraction to remove high molecular weight fractions followed by thermal treatment to remove low molecular weight species. The purified polycarbosilanes produced with a 50-60 wt% yield are yellowish-brown glassy solids with an average M_n of 1000-2000. They are soluble in common organic solvents and suitable for melt spinning into fine (10-20 μm diameter) fibres. Small amounts of $(\text{C}_6\text{H}_5)_2\text{SiCl}_2$ added to $(\text{CH}_3)_2\text{SiCl}_2$ facilitate the spinning of polycarbosilane, producing fibres with improved mechanical strength¹⁶. A modification of polycarbosilane was reported that contained phenyl pendant groups in the polymer chain¹³. This was effected through the use of phenylmethyldichlorosilane as a comonomer with Me_2SiCl_2 :



The structure of polycarbosilane has been studied in detail by NMR (^1H , ^{13}C and ^{29}Si), IR, UV spectra, and intrinsic viscosity measurements; these studies support a planar structure containing both linear and ring segments¹⁷.

Heating polycarbosilanes in vacuum to 550°C volatilizes lower molecular weight species and increases the molecular weight of the residue with the evolution of H_2 and CH_4 . Further heating to 800°C converts the organic polymer to an inorganic structure. The largest volume of gas (H_2 , CH_4) is evolved between 600 and 800°C with the formation of network and three-dimensional structures¹⁸. At 800°C the material becomes almost black. Little gas evolution occurs between 800 and 1100°C , and the material is essentially amorphous. The gas evolved between 1100 and 1200°C is hydrogen, and x-ray diffraction shows the amorphous product changing to crystalline $\beta\text{-SiC}$ ¹⁸. The elemental composition of the pyrolysed polycarbosilanes at 1300°C shows the nonstoichiometric nature of the ceramic with oxygen and excess carbon.

The carbosilane resulting from thermolysis of the copolymer, designed to contain a small percentage of $(\text{C}_6\text{H}_5)\text{SiMe}$ groups, was shown to have better spinnability than polycarbosilane so that precursor fibres of lower diameter were obtained. SiC fibres of higher strength and Young's modulus resulted upon pyrolysis of polysilastyrene, this polymer is photoreactive and undergoes chain scission when its solution or solid samples are exposed in air to UV radiation. Exposure of solid polysilastyrene to uv in an inert atmosphere results in cross-linking which increases rigidity, infusibility, and insolubility in organic solvents¹⁹. The cross-linked polymer was converted to SiC by pyrolysis at $10^\circ\text{C}/\text{min}$ in thermogravimetric analyser; char yield at 800°C is 30% (theoretical 45%)²⁰.

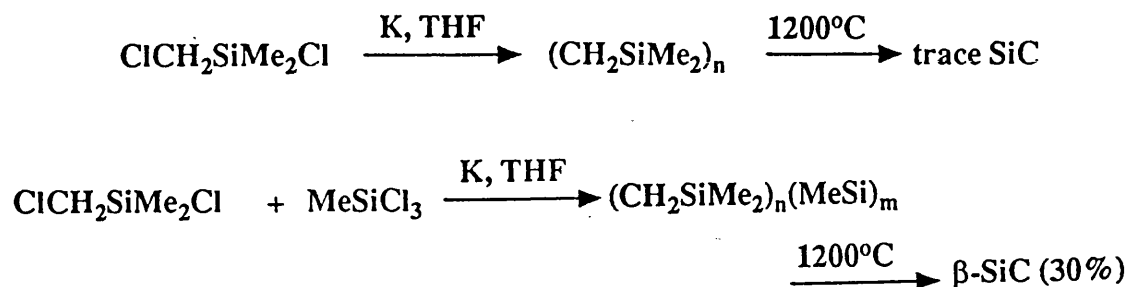


Fibres can be hand-drawn from molten polysilastyrene with a softening point of 200°C. These fibres are cross-linked by uv radiation in a nitrogen atmosphere and pyrolysed in a vacuum furnace by slowly heating to 1100°C and holding at this temperature for 30 minutes. The ceramic fibres retain their shape, but contract in length by 40%; the char yield in this experiment is only 15%. X-ray diffraction indicates these glossy black fibres to be amorphous: scanning electron microscopy (SEM) revealed hollow fibres, suggesting only surface cross-linking²⁰. Prolonged uv exposure, however, produces a fully cross-linked fibre. With recognition of the importance of cross-linking for ceramic fibre production and other applications, several new polysilanes with different functionalities have been synthesized^{21,22}. These functionalities undergo catalytic, thermal, oxidative, or photochemical cross-linking.

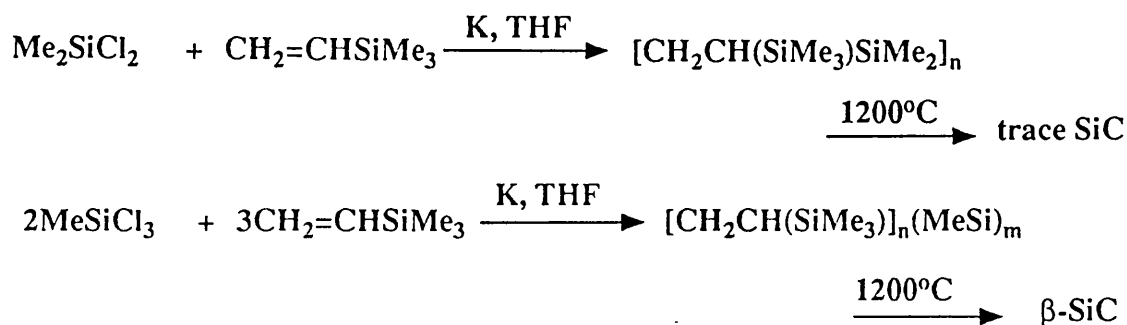
Methylphenylpolysilanes are used to strengthen Si₃N₄ ceramics. The ceramic body is soaked in the polymer and pyrolysed again, resulting in the formation of SiC in the pores of Si₃N₄ and increased strength²³. Branched polymethylsilanes, useful as binders of inorganic heat-resistant materials, are prepared by treating methylchlorosilanes with methyl Grignard reagent to increase the methyl content and reduced the chlorine content; subsequent heating with an alkali metal gives polysilanes. The structure and extent of cross-linking is determined by the Si-Cl content of the disilane.

Schilling et al²⁴ focused on branched polycarbosilane preceramic polymers with the preparation of tractable solid polycarbosilanes via the potassium dechlorination of mixtures of vinylmethylchlorosilanes or methyltrichlorosilane with other silane monomers. A comparison of SiC yields from similar linear and branched polycarbosilane is illuminating. Thus, the potassium dechlorination of ClCH₂SiMe₂Cl yields in THF a

linear polymer, which upon pyrolysis gives a negligible yield of SiC. In contrast, when $\text{ClCH}_2\text{SiMe}_2\text{Cl}$ is copolymerised with MeSiCl_3 , the resulting branched polycarbosilane is an effective SiC precursor, yielding 30% SiC on unconfined pyrolysis:



Similarly, Me_2SiCl_2 reacts with vinyltrimethylsilane to give linear polymer. The linear polymer, $[\text{CH}_2\text{CH}(\text{SiMe}_3)\text{SiMe}_2]_n$ produces SiC in negligible quantities on pyrolysis. However, when trifunctional MeSiCl_3 was substituted for difunctional Me_2SiCl_2 , the resultant branched polymer gave a 40% yield of SiC:



Polycarbosilanes can be melt-spun into continuous fibres at 250-350°C. The fibre is cross-link by oxidation of Si-H structures by heating (110-190°C) in air and pyrolysed to 1100-1200°C under N_2 or vacuum to black SiC fibres⁸. Pyrolysis in ammonia gives colourless fibres close to the composition of silicon oxynitride²⁵. Formation of Si_3N_4 whiskers by pyrolyzing polycarbosilane in an ammonia atmosphere has also been claimed²⁶. Ammonia plays a key role in eliminating organic groups from the polycarbosilane.

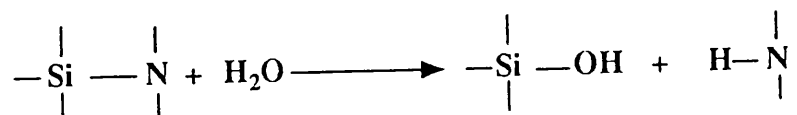
SiC fibre from polycarbosilanes (Nicalon fibres) 10-20 μm diameter, has excellent

tensile strength of 2500-3300 MPa and elastic or Young's modulus of 180-200 GPa; these properties are retained above 1000°C. It resists acid and alkali attack and oxidation. Yield and chemical nature of the ceramic produced from Nicalon precursor depend on the pressure and the atmosphere of the pyrolysis²⁷. The mechanical properties of SiC fibres remain essentially unchanged upon neutron irradiation. The chemical structure, microstructure, and morphology of Nicalon fibres have recently been studied in detail by elemental analysis, x-ray diffraction, IR, Raman, ²⁹Si NMR, and electron spectroscopy for chemical analysis²⁸. The elemental composition indicates both oxygen and excess carbon. A trace of nitrogen was probably acquired during processing under nitrogen. Nicalon fibre is an amorphous silicon oxycarbide containing 30-35 vol% of silicon carbide as microcrystalline β -SiC. The covalent chemical bonding in Nicalon fibre approaches a random distribution, i.e. silicon atoms are linked together through carbon and oxygen in random fashion. This is supported by a ²⁹Si NMR study which shows five signals corresponding to SiC₄, SiC₃O, SiC₂O₂, SiCO₃, and SiO₄ bondings. The excess carbon, according to a Raman study, is present as graphitic microcrystallites, which are embedded in a continuous glassy phase and thus not exposed to oxidation. This may explain the high oxidation resistance of Nicalon fibre in spite of the excess carbon content²⁸. Above 1200°C in vacuum, helium, or argon, coarse SiC grains crystallize with the loss of CO, SiO and N₂ (if present). This reduces the tensile strength of the ceramic fibres²⁹. In addition to the excellent mechanical properties and high oxidation and chemical resistance, Nicalon fibre is easily wet by liquid resins and metals at temperatures used to make composite materials. Thus Nicalon fibres are used to reinforce plastics, metals³⁰, glass^{31,32}, oxides³³ and nonoxide ceramics³⁴ matrices to form high performance composite materials. Polycarbosilanes are also used to synthesize sinterable β -SiC powders¹⁶, flaky β -SiC³⁵ and dense sintered SiC bodies³⁶. These polymers serve as sintering aids and binders for SiC and Si₃N₄ powders to produce sintered mouldings with high strength and oxidation resistance. These mouldings can be further densified and strengthened by impregnation with more polycarbosilanes and refiring. Other uses include high

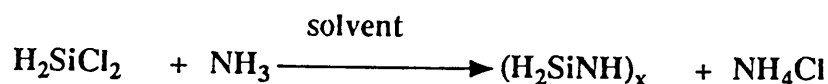
performance SiC coatings and as reactive binders for Fe-13Cr alloy powders to produce an oxidation-resistance sintered composite.

3.4.2 Silicon-Nitrogen Ceramic Precursors

Less work has been reported on the synthesis and characterisation of Si-N back-bone polymers compared to their Si-C analogues. An important reason for this is the lability of the Si-N bond with respect to the reaction with atmospheric moisture.



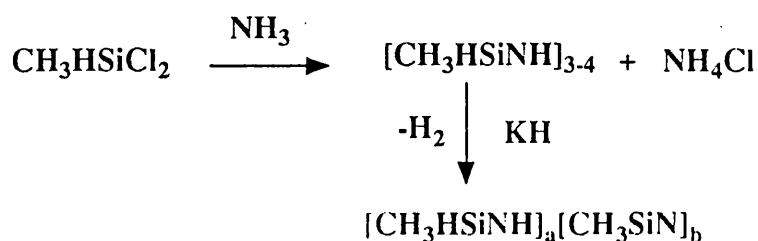
Such reactivity brings about obvious handling difficulties and results in oxygen incorporation in the polymer, which leads to the formation of SiO₂ on pyrolysis. Although this expected reactivity is found for a number of Si-N polymers, some materials display surprisingly high hydrolytic stability. This feature may prompt a growth of interest in this area. Polymers containing a predominantly Si-N microstructure have been known for many years, but as for Si-C polymers it is only recently that Si-N polymers have been prepared with a view to conversion to ceramic materials. The reaction of ammonia with silicon tetrachloride produces insoluble, cross-linked silicon diimide, Si(NH)₂³⁷, which is the basis of the commercial process developed by Ube Industries Ltd. for the preparation of silicon nitride powders. Also one other important silicon nitride precursor is formed by treating dichlorosilane with ammonia in an organic solvent³⁸, with benzene as solvent. Unstable polymers are produced in benzene which gelled within a few hours at room temperature. Reaction in more polar solvents such as chloromethane and ether produced polymers stable up to 3 days at room temperature. Preparation in heptane or pyridine gives more stable wet-spinnable polymers³⁹.



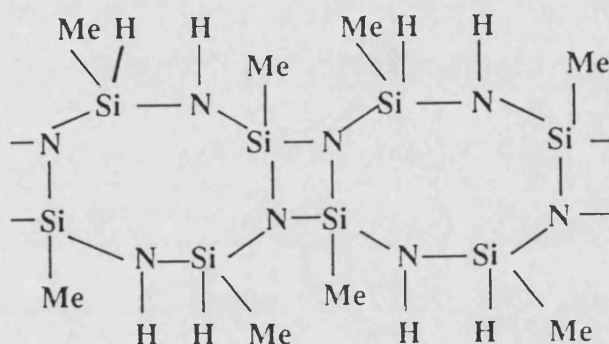
Pyrolysis at 1200°C of the gelled polymer obtained from polar solvents gave 69% char yield. Thermogravimetric analysis (TGA) showed that most of the weight loss occurred by 450°C; mass spectral analysis of the pyrolysis gases revealed that ammonia was the primary gas evolved up to 400°C. Above 400°C (H₃Si)₂NH was produced, giving evidence for significant Si-H/Si-N bond redistribution. X-ray powder patterns for the polymer pyrolysed at 1150°C revealed the presence of α- and β-Si₃N₄ as well as elemental silicon. The polymer was investigated as an infiltrate for ceramic matrix composites⁴⁰.

Treatment of methyltrichlorosilane with ammonia in methylene chloride gives methylsilsesquiazanes. The ammonium chloride is filtered and leaves a methylene chloride solution of methylsilsesquiazanes, which are presumably polycyclic moieties terminated with SiNH₂. Pyrolysis of the resultant fibre at 1200°C in nitrogen for 3 hours produces an amorphous ceramic fibre. This fibre contains approximately 50% silicon nitride and 50% silicon carbide, and has a tensile strength of up to 115 MPa and an elastic modulus of 10 GPa. In a similar fashion, phenyltrichlorosilane treated with ammonia produces phenylsilsesquiazane which is dry spun with the aid of polystyrene into 15 μm-diameter fibres and pyrolysed at 1200°C in nitrogen. The fibres contain 35% silicon carbide, 35% silicon nitride and 30% carbon. The yield of tractable polymer was significantly influenced by the size of the R group⁴¹.

A preceramic polymer can also be prepared by ammonolysis of MeSi(H)Cl₂, followed by polymerisation of the resulting cyclic silazanes catalysed by potassium hydride⁴².

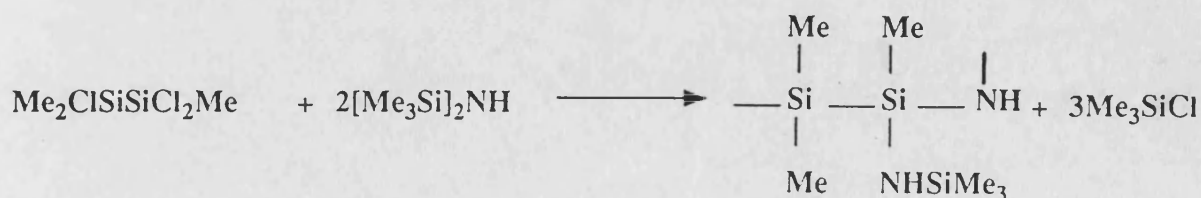


Cyclic and linear silazanes are produced in the first step; the average molecular weight is about 300. Pyrolysis of this mixture gives a low ceramic yield. Strong bases that deprotonate SiNHSi structures catalyse the second step. Hydrogen is lost with the formation of trifunctional SiN₃ and Si₃N moieties. The catalysts were destroyed by addition of methyl iodide. The molecular weight increases to 1180 during the second step. The empirical formula of [CH₃Si(H)NH]_{0.39}[CH₃Si(H)NCH₃]_{0.04}[CH₃Si(H)N]_{0.75} is suggested, and based on elemental analysis and ¹H NMR evidence, the following structure has been proposed:

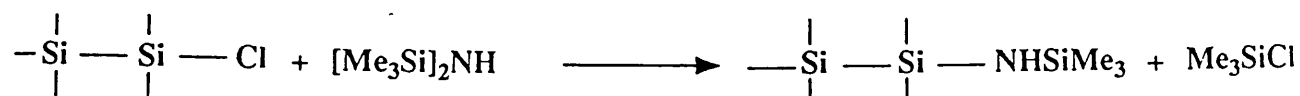


The ceramic yield from TGA analysis at 1000°C in nitrogen is ca 80-85%. Pyrolysis in nitrogen at 1400°C produces methane, hydrogen and traces of ammonia. The resulting char shows only broad x-ray diffraction peaks for Si₃N₄; chemical analysis indicates Si_{1.0}N_{0.88}C_{0.5}O_{0.04}³⁹.

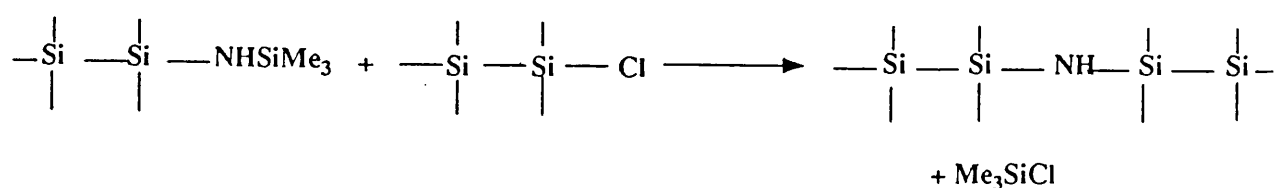
Heating methylchlorosilanes with hexamethyldisilazane gives methylpolydisilazanes through Si-Cl/Si-N redistribution⁴³:



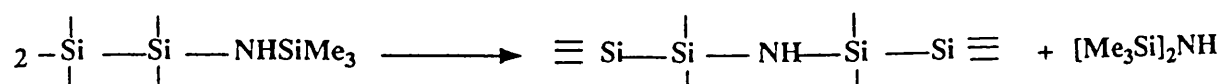
These polymerisation are more complex than this simple reaction indicates. The analysis of the early stages shows that the reaction proceeds first by Si-Cl/Si-N exchange:



followed by condensation of chlorosilanes with trimethylsilylamino silanes:



As the temperature is increased during polymerisation, trimethylsilylamino groups condense to form hexamethyldisilazane:



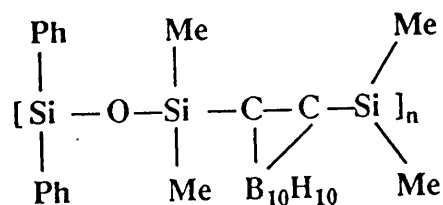
Infrared analysis revealed residual SiCl, even up to 230°C, and indicated that SiCH₂Si and Si₃N moieties are generated at the higher polymerisation temperatures.

3.4.3 Boron-Containing Ceramics

The search for suitable low temperature polymer synthesis and fabrication routes to high technology ceramics of boron, aluminium, and a few transition metals is showing some promise⁴⁴. Boron-containing systems provide one of the important routes and are related to this work in which the role of boron was studied. Polyborophenylsiloxanes ($M_n = 500-1000$) are prepared by the polycondensation of boric acid or trimethylborate with phenylsilanes⁴⁵. A resinous product was thus obtained by heating boric acid with Ph₂SiCl₂

in butyl ether at 100°C for 18 hours under nitrogen, followed by heating at 300°C for 1 hour under reduced pressure⁴⁶. Infrared analysis reveals the $--[Ph_2SiOB(O)_2]--$ structural unit. The polymer is more stable to hydrolysis than an analogous polymer prepared with Me_2SiCl_2 ⁴⁷. Pyrolysis of the resinous product in nitrogen at 1000°C gives an amorphous ceramic (46% char yield, $Si_{1.0}C_{2.47}B_{0.38}O_{0.57}H_{0.34}N_{0.01}$), which upon further heating to 1700°C in argon yields mainly β -SiC, glassy carbon, and some B_4C ⁴⁶. The ease of handling polyborodiphenylsiloxanes and their capability of conversion to predominately β -SiC makes these polymers useful as binders for SiC and Si_3N_4 ⁴⁸, where there is no dimensional change on sintering. Also these polymers are useful for joining SiC bodies⁴⁹. The polymer solutions were made highly viscous by evaporating the solvent and were then applied to the polished surfaces of two SiC bodies as a layer (1mm thick). The SiC bodies were then pressed firmly together, so that the bonding agent was sandwiched between them and heated to 1500°C at 100°C/h in an nitrogen stream, without hot-pressing. After a holding period of 1 hour, they were cooled gradually to room temperature. The joint strength was measured in three-point bending at room temperature with a testing machine which shows superior to carbon polymer. As a catalyst, the polymer allows polycarbosilane synthesis at lower temperatures and atmospheric pressure.

Carborane-siloxane polymers were developed as a high temperature substitute for polydialkyl(aryl)siloxanes because of their appreciable resistance to depolymerisation. Dexsil polymer has the following structure:



Pyrolysis at atmospheric pressure under an inert atmosphere yields a ternary ceramic consisting of SiC, B_4C and SiO_2 ¹³. The bulky carborane rings promote cross-linking, resulting in a high ceramic yield of 60%.

3.5 REFERENCES

- A1. N Ichinose, Introduction to Fine Ceramics Application in Engineering, J Wiley and Sons Ltd, 1987; D Segal, Chemical Synthesis of Advanced Ceramic Materials, Cambridge University Press, 1989; F W Wong, S Doswell and M De Malherbe, VDI Verlag, 1986; S Somiya, Advanced Ceramics II, Elsevier, 1989; I J McColm, Ceramic Science for Materials Technologists, Leonard Hill, New York, 1983.
1. S Saito, Fine Ceramics, Elsevier New York, Amsterdam, London, 1988.
 2. S Kim and S Baik, J Am Ceram Soc, 1991, **74**, 1735.
 3. E J Brinker and J W Scherer, Sol-gel Science, Academic Press, 1990.
 4. Y K Rao and H G Lee, Trans Br Ceram Soc, 1983, **82**, 123.
 5. G T Burns, T P Angelotti and J Chandra, J Mater Sci, 1987, **22**, 2609.
 6. K M Prewo and J J Brennan, J Mater Sci, 1980, **15**, 463.
 7. R W Rice, Am Ceram Soc Bull, 1983, **62**, 889.
 8. S Yajima, Am Ceram Soc Bull, 1983, **62**, 893.
 9. S Yajima, K Okamura and Y Hasegawa, J Mater Sci, 1981, **16**, 1349.
 10. B E Walker, R W Rice and P F Becher, Am Ceram Soc Bull, 1983, **62**, 916.
 11. R Wills, R Markle and S Mukherjee, Am Ceram Soc Bull, 1983, **62**, 904.
 12. V Iteine, C Cheng and R Needs, J Am Ceram Soc, 1991, **74**, 2630.
 13. C L Schilling, J P Wesson and T C Williams, Am Ceram Soc Bull, 1983, **62**, 912.
 14. S Yajima, J Hayashi and M Omori, Chem Lett, 1975, 931; R D Miller and J Michl, Chem Rev, 1989, **89**, 1359.
 15. S Yajima, J Hayashi and M Omori, Nature, 1976, **261**, 683.
 16. S Yajima, Phil Trans Roy Soc, 1980, **A294**, 419.
 17. D C Apperley and R K Harris, J Am Ceram Soc, 1991, **74**, 777.
 18. Y Hasegawa and K Okamura, J Mater Sci, 1983, **18**, 3633.
 19. R C West, J Organomet Chem, 1986, **300**, 327.

20. R C West, L D David and P I Djurovich, Am Ceram Soc Bull, 1983, **62**, 899.
21. C L Schilling and T C Williams, Polym Prepr Am Chem Soc Div Polym Chem, 1984, **25**, 1.
22. R C West, I Nozue and P Trefonas, Polym Prepr Am Chem Soc Div Polym Chem, 1984, **25**, 4.
23. K S Mazdiasni, R C West and L D David, J Am Ceram Soc, 1978, **61**, 504.
24. C L Schilling, J P Wesson and T C Williams, Am Ceram Soc Bull, 1983, **62**, 912.
25. K Okamura, M Sato, Y Hasegawa and T Amano, Chem Lett, 1984, 2059.
26. T Ishikawa, H Teranishi and H Ickawa, UK Pat 2178417, Feb 11 1987.
27. J J Pomeau, D Abbe and J Jamet, Emergent Process Methods for High Technology Ceramics, Plenum Press, New York, 1984.
28. J Lipowitz, H A Freeman, H A Goldberg and R T Chen, Adv Ceram Mater, 1987, **2**, 122.
29. K L Luthra, J Am Ceram Soc, 1986, **69**, C-231.
30. S Yajima, K Okamura and T Hayase, J Mater Sci, 1980, **15**, 2130.
31. K M Prewo, J J Bennan and G K Layden, Am Ceram Soc Bull, 1986, **65**, 305.
32. M A Herron and S H Risbud, Am Ceram Soc Bull, 1986, **65**, 342.
33. B Bender, D Shadwell, C Bulik and D Lewis, Am Ceram Soc Bull, 1986, **65**, 363.
34. L J Schioler and J J Stiglich, Am Ceram Soc Bull, 1986, **65**, 286.
35. T Hatta, H Ueno and T Hamamatu, US Pat 4,465,647, Aug 14 1984.
36. K Koga and S Nagano, US Pat 4,105,455, Aug 8 1978.
37. K S Mazdiasni and C M Cook, J Am Ceram Soc, 1973, **56**, 628.
38. D Seyferth, G H Wiseman and C Prudhomme, J Am Ceram Soc, 1983, **66**, C13.
39. T Isoda and M Arai, Chem Abstr, 1986, **104**, 3634.
40. R West and L David, J Am Ceram Soc, 1978, **61**, 504.
41. G T Burns, T P Angelotti and G Chandra, J Mater Sci, 1987, **22**, 2609.
42. G H Wiseman D R Wheelar and D Seyferth, Organometallic, 1986, **5**, 146.
43. R Baney, J Gaul and T Hilty in R Davis eds, Materials Science Research, Plenum

Press, 1984, **17**, 253.

44. S Sakka and T Yoko, Ceramic International, 1991, **17**, 217.
45. S Yajima, K Okamura and J Hayashi, U S Pat, 4,152,509, 1979.
46. S Yajima, J Hayashi and K Okamura, Nature, 1977, **266**, 521.
47. R L Vale, J Chem Soc, 1960, 2252.
48. S Yajima, T Shishido and M Hamano, Nature, 1977, **266**, 522.
49. S Yajima, K Okamura and T Shishido, Am Ceram Soc Bull, 1981, **60**, 259.

CHAPTER FOUR

SYNTHESIS OF LINEAR AND CYCLIC HETEROSILOXANES

4.1 SUMMARY

This chapter contains details of the experimental procedures used for the preparative chemistry carried out in this study. A series of cyclic heterosiloxanes $[\text{RB}(\text{OSiR}^*_2)\text{O}]_2$ and $\text{RB}[(\text{OSiR}^*_2)_2\text{O}]$, ($\text{R}, \text{R}^* = \text{Me or Ph}$) containing 8- and 6-membered rings respectively, have been synthesised by the reaction of $\text{RB}(\text{OH})_2$ with diphenylsilandiol or 1,1,3,3-tetraphenyl(tetramethyl)-1,3-dihydroxy-1,3-disiloxane. Linear borosiloxanes $\text{RB}(\text{OSiPh}_n\text{H}_{3-n})_2$; ($\text{R} = \text{Ph, Me}$); $n = 2$ or 3 and $\text{B}(\text{OSiPh}_3)_3$ were prepared by the reaction of $\text{B}(\text{OMe})_3$, $\text{PhB}(\text{OH})_2$ or $\text{MeB}(\text{OH})_2$ with triphenylsilanol or diphenylchlorosilane. A boron-containing silsesquioxane $\{[(\text{c-C}_6\text{H}_{11})_7\text{Si}_7\text{O}_{12}\text{B}]_2\}$ has been synthesised by the reaction of $[(\text{c-C}_6\text{H}_{11})_7\text{Si}_7\text{O}_9(\text{OH})_3]$ with BI_3 . The cyclic heterosilazane $\text{Me}_2\text{Si}[\text{NHBC}_6\text{H}_5]_2\text{NH}$ was isolated from the reaction of 1,1,3,3,5,5-hexamethylsilazane with PhBCl_2 .

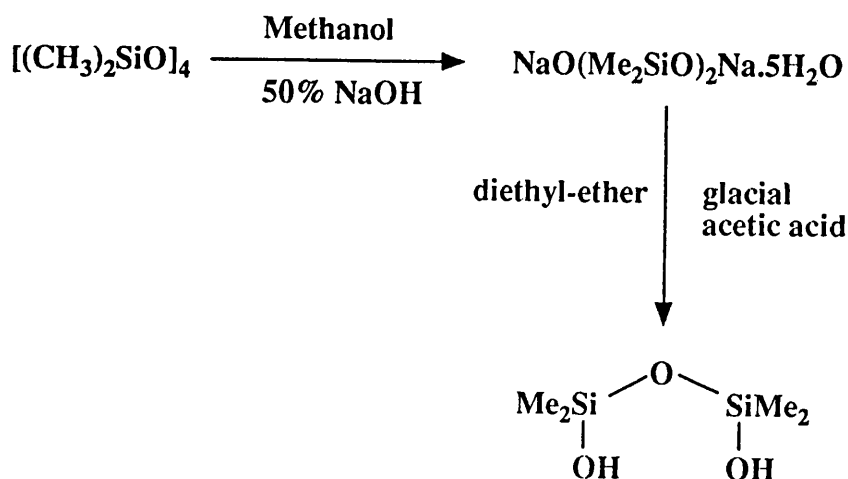
These compounds have in general been characterised by a combination of techniques including ^1H , ^{13}C and ^{29}Si nuclear magnetic resonance, infrared spectroscopy, elemental micro analysis and mass spectrometry. X-ray crystal structure determinations of $\text{Ph}_2(\text{HO})\text{SiOSiPh}_2\text{OSi}(\text{OH})\text{Ph}_2$, $(\text{c-C}_6\text{H}_{11})_6\text{Si}_6\text{O}_9$, $\text{PhB}(\text{OSiPh}_3)_2$ and $\text{Me}_2\text{Si}(\text{NHBPh})_2\text{NH}$ have been carried out by Dr. Mahon in the school of Chemistry University of Bath, and are described in the next chapter.

4.2 SYNTHETIC PROCEDURES

4.2.1 Preparation of Silanols

Preparation of Tetramethyldisiloxane-1,3-diol (Compound I)

Tetramethyldisiloxane-1,3-diol was prepared by a modification of a literature method¹. To 0.1 mole, (29.6g) of octamethylcyclotetrasiloxane was added 0.4 mole, (32g) of 50% aqueous NaOH. After adding approximately 25 ml of methanol, the mixture was stirred and gradually heated to boiling. More methanol was added in small amounts during this time until the reaction mixture became homogeneous. After cooling water suction was applied to remove the solvent and any uncombined water. The remaining powdery solid represented essentially a quantitative yield of $\text{NaO}(\text{Me}_2\text{SiO})_2\text{Na} \cdot 5\text{H}_2\text{O}$. This salt, (0.16 mole, 50g) was added in powder form in small portions to a stirred mixture of diethyl ether (500 ml) and glacial acetic acid (0.33 mole, 20g). As the added salt dissolved, a precipitate of sodium acetate formed. pH paper was used to follow the course of the reaction to the neutral point. The solids were filtered and the filtrate concentrated under water vacuum. This gave a mixture of an oil and needle-like crystals (18g), from which the oil was removed by washing with petroleum ether (20 ml). Crystals of tetramethyldisiloxane-1,3-diol remained (12.8g). 44%; m.p 64°C. Analysis, found (calculated for $\text{C}_4\text{H}_{14}\text{Si}_2\text{O}_3$): C 28.9(28.8); H 8.33(8.2)%; ^1H NMR spectrum $\delta(\text{CDCl}_3)$: 0.151-0.188m (12H, Me), 4.40s (2H, OH); ^{29}Si NMR spectrum: -10.52ppm.



Preparation of Tetraphenyldisiloxane-1,3-diol (Compound 2) and Hexaphenyltrisiloxane-1,5-diol (Compound 3)

Dichlorodiphenylsilane (0.15 mole, 37.9g) was added dropwise at room temperature over a 45 minute period to a stirred mixture of ammonium carbonate (0.21 mole, 20.1g), diethyl ether (150 ml), and water (0.15 mole, 2.7g). The mixture was then heated under reflux for 12 hours, cooled and then stirred with 100 ml water and the ethereal phase separated, dried overnight using anhydrous sodium sulphate, and evaporated to dryness. Extraction of the residue several times by cold benzene (40 ml) (CARE) left pure $\text{Ph}_2\text{Si}(\text{OH})_2$ (8.1g), 25%; m.p 130°C . Analysis, found (calculated for $\text{C}_{12}\text{H}_{12}\text{SiO}_2$): C 66.7(66.8); H 5.52(5.35)%. Oligomeric silanols and cyclic siloxanes, were recovered on evaporation of the combined extracts. Washing this residue successively with a 1:5 and a 1:1 benzene/petroleum ether ($80\text{-}100^\circ\text{C}$) mixture (120 ml) yielded crude tetraphenyldisiloxane-1,3-diol, which was recrystallised from 5:1 benzene/petroleum ether mixture to yield the pure product, (8.3g); m.p 108°C . Fractional crystallisation of the combined extracts yielded hexaphenyltrisiloxane-1,5-diol which was finally recrystallised from 1:1 benzene/petroleum ether mixture to give the pure product.

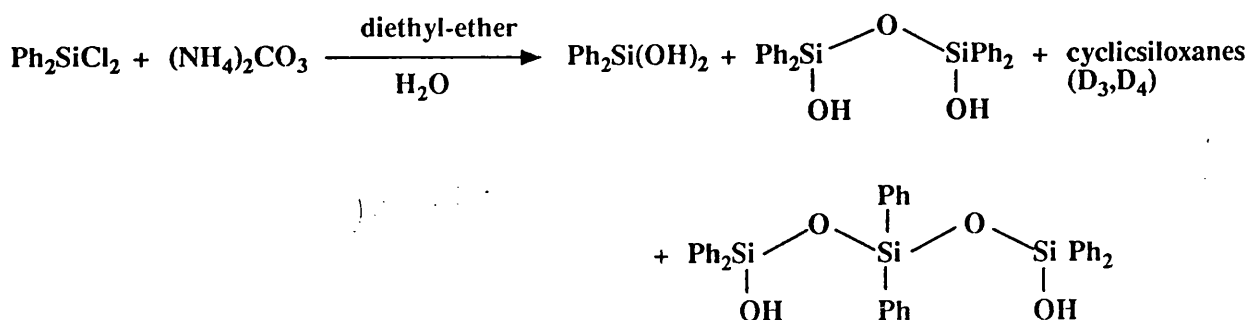
Tetraphenyldisiloxane-1,3-diol: Analysis, found (calculated for $\text{C}_{24}\text{H}_{22}\text{Si}_2\text{O}_3$): C 69.5 (69.8); H 5.3 (5.3)%. ^1H NMR spectrum $\delta(\text{CDCl}_3)$: 4.10s (2H, vbr, -OH), 7.20-7.56m (20H, - C_6H_5); ^{29}Si NMR spectrum: -36.04ppm; Mass spectral data (70eV E.I, m/z): 414 (M^+), 337 (M-Ph), 319 (M-Ph- H_2O).

Hexaphenyltrisiloxane-1,5-diol: Analysis, found (calculated for $\text{C}_{36}\text{H}_{32}\text{Si}_3\text{O}_4$): C 70.6 (70.4); H 5.22 (5.26)%. ^1H NMR spectrum $\delta(\text{CDCl}_3)$: 5.42s (2H, brs, OH), 7.20-7.56m (30H, - C_6H_5); ^{29}Si NMR spectrum: -36.5, -44.0ppm; Mass spectral data (C.I, m/z): 594 (cyclo- $\text{Ph}_6\text{Si}_3\text{O}_3$), 517 ($\text{M}^+\text{-Ph-H}_2\text{O}$), 437 ($\text{M}^+\text{-Ph-H}_2\text{O-PhH}$).

A cube shaped crystal of approximate dimensions 0.25 x 0.25 x 0.35 mm was selected for data collection.

crystal data: $\text{C}_{36}\text{H}_{32}\text{Si}_3\text{O}_4$, $M_r = 612.8$ triclinic, space group $P\bar{1}$, $a = 9.934(3)$, $b =$

13.299(3), $c = 14.4,59(4)$ Å. $\alpha = 65.92(2)$, $\beta = 82.95(3)$, $\gamma = 73.16(3)^\circ$, $U = 1669.2$ Å³, $Z = 2$, $D_x = 1.23$ gcm⁻³, Mo-K α , $\lambda = 0.71069$ Å, $\mu(\text{Mo-K}\alpha) = 1.40\text{cm}^{-1}$, $F(000) = 644$. Data were measured at room temperature on a Hilger and Watts Y290 four-circle diffractometer in the range of $2 < \Theta < 22^\circ$ using ω - 2Θ scans, covering the range h -10 \rightarrow 0, k -13 \rightarrow 13, l -14 \rightarrow 14. Cell dimensions were based on 12 accurately centered reflections with $14 < \Theta < 17^\circ$. 4382 Reflections were collected of which 2186 were unique and observed with $I > 3\sigma(I)$. A standard reflection measured after every 50 reflections showed no systematic crystal decay throughout data collection. Data were corrected for Lorentz and polarization effects but not for absorption. The structure was solved by conventional Patterson methods and refined using full matrix least squares based on F , using the SHELX suite of programs^{2,3}. Atomic scattering factors were taken from the *International Tables for X-ray Crystallography*⁴. In the final least squares cycles the silicon and oxygen atoms along with those carbons which exhibited high isotropic thermal parameters in the penultimate least squares refinement (C_{4-6} , $8-12$, $21-23$, $27-29$, and $32-36$) were treated anisotropically. All other atoms were treated isotropically. The hydrogen atom, H_4 , was located and refined at a fixed distance of 1.03 Å from O_4 , with its isotropic thermal parameter fixed at 0.05 Å². The remaining hydrogen were included at calculated positions (C-H: 1.08 Å) with a common, fixed thermal parameter ($U = 0.05$ Å²). Final residuals after 10 cycles of least squares were $R = R_w = 0.0657$ for unit weights. Max. final shift was 0.012. The max. and min. residual densities were 0.14 and -0.12 eÅ⁻³ respectively. Tables of fractional atomic coordinates and thermal parameters, anisotropic temperature factors, bond lengths and angles and intramolecular and intermolecular distances are available as supplementary data in Appendix III.



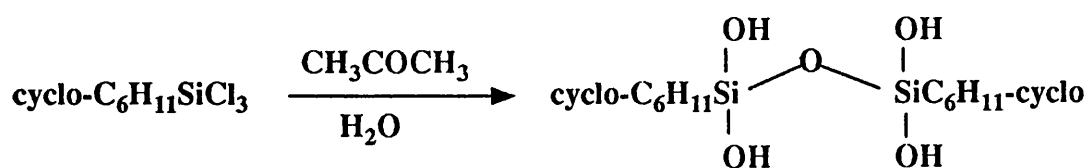
Preparation of Cyclotriphenylboraxine (Compound 4)

Phenylboronic acid (0.01 mole, 1.22g) was heated in refluxing sodium-dried benzene (CARE), (25 ml) for 5 hours. Water formed during the course of the reaction was removed using a Dean and Stark apparatus, and the reaction mixture was then allowed to cool to room temperature and solid residue removed by filtration. The solvent was removed from the filtrate under water vacuum and the residue recrystallised from diethyl ether to yield cyclotriphenylboraxine (0.75g, 73%); m.p 206°C. Analysis, found (calculated for $\text{C}_{18}\text{H}_{15}\text{B}_3\text{O}_3$): C 69.9(69.0); H 4.8(4.7)%. ^1H NMR spectrum $\delta(\text{CDCl}_3)$: 7.49-7.63m (9H, *m,p*- $\text{C}_6\text{H}_5\text{B}$), 8.23-8.26m (6H, *o*- $\text{C}_6\text{H}_5\text{B}$); Mass spectral data (70eV *E.I.*, *m/z*): 312 (M^+), 208 (M-PhBO), 104 (M-2PhBO).

4.2.2 Preparation of Silsesquioxanes

Preparation of -1,3-Dicyclohexyl disiloxane-tetraol (Compound 5)

This compound was prepared by a modification of a literature method⁵. Cyclohexyltrichlorosilane (0.6 mole, 13g) was dissolved in acetone (50 ml) and the solution added dropwise to cold water (600 ml). After 4 days at room temperature, filtration gave 1,3-dicyclohexyl-disiloxane-tetraol (6.5g, 71%); m.p 205°C. Analysis, found (calculated for $\text{C}_{12}\text{H}_{26}\text{Si}_2\text{O}_5$): C 47.3(47.0); H 8.8(8.5)%. ^1H NMR spectrum $\delta(\text{CDCl}_3)$: 0.73s (2H, *c*- C_6H_{11}), 1.22s (10H, *c*- C_6H_{11}), 1.71-1.78d (10H, *c*- C_6H_{11}), 4.41br (4H, HOSi); ^{29}Si NMR spectrum: -50.48ppm.



Preparation of Hexacyclohexyl-hexasiloxane (Compound 6) and Heptacyclohexyl-heptasiloxane-1,3,7-triol (Compound 7)

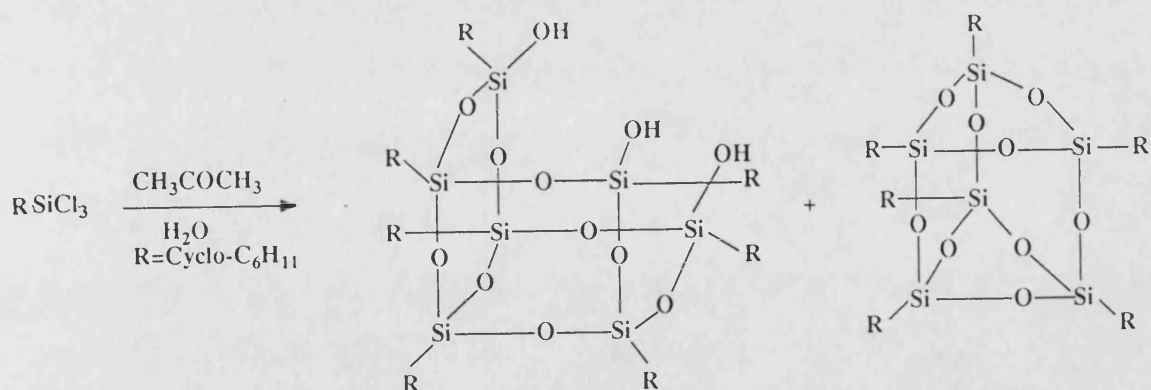
In a remarkable reaction first reported by Brown and Vogt⁵ in 1965, the trisilanol above is prepared by the hydrolytic condensation of cyclohexyltrichlorosilane (c-C₆H₁₁SiCl₃) in aqueous acetone. Cyclohexyltrichlorosilane (0.11 mole, 25g) was dissolved in acetone (500 ml), water (125 ml) was added, and the mixture was allowed to stand for 4 months. The crystalline precipitate was filtered, rinsed with acetone, and dried to give 2.3g of an approximately 2:1 heptacyclohexyl-heptasiloxane-1,6,7-triol and hexacyclohexyl-hexasiloxane mixture respectively. The later compound was isolated from this mixture by treatment with pyridine⁶. The reaction mixture was stirred with 5 times its weight of pyridine for 30 minutes. The insoluble hexamer was collected, washed with a small amount of pyridine, and dried overnight at 25°C in a fume hood. Recrystallization from boiling chloroform afforded pure compound 6 (1.4g, 10%); m.p 251°C. Analysis, found (calculated for C₃₆H₆₆Si₆O₉): C 53.2(53.2); H 8.4(8.2); I.R spectrum: 1049 cm⁻¹ (Si-O-Si). ¹H NMR spectrum δ(CDCl₃): 0.83m (6H, vbr, c-C₆H₁₁) 1.26-1.30m (24H, vbr, c-C₆H₁₁) 1.73-1.77m (36H, vbr, c-C₆H₁₁); ¹³C NMR spectrum: 27.3s, 26.6s, 26.1s (2:1:2 for CH₂), 22.6s (CH); ²⁹Si NMR spectrum: -56.5ppm. Mass spectral data (70 eV E.I, m/z): 811 (M⁺), 729 (M-C₆H₁₁).

A crystal of approximate dimensions 0.3 x 0.3 x 0.4 mm was used for data collection for the structure determination. These were formed recrystallisation of 0.1g of compound 6 from chloroform (10 ml).

crystal data: $C_{36}H_{66}Si_6O_9$, $M = 811.4$ monoclinic, $a = 10.810(1)$, $b = 18.756(3)$, $c = 21.424(3)$ Å, $\beta = 93.78(2)^\circ$, $U = 4334.5$ Å³, space group $P2_1/n$, $Z = 4$, $D_c = 1.24$ gcm⁻³, $\mu(\text{Mo-K}\alpha) = 2.3\text{cm}^{-1}$, $F(000) = 1752$. Data were measured at room temperature on a CAD4 automatic four-circle diffractometer in the range $2 < \Theta < 24^\circ$. 7018 reflections were collected of which 4372 were unique with $I > 3\sigma(I)$. Data were corrected for Lorentz and polarization effects but not for absorption. The structure was solved by direct methods and refined using the SHELX suite of programs^{2,3}. The asymmetric unit consisted of two unique molecule halves (refined in blocks) and the remainder of each molecule was generated by reflection through a mirror plane. Interestingly, a similarly unusual way of generating the asymmetric unit was also observed in $(\text{PhCH}_2)_8\text{Si}_8\text{O}_{12}$, in which the content of the unit cell (P1) were generated by two independent half-molecules sitting either side of the center of symmetry⁷. In both independent halves of the title compound a number of atoms ($\text{Si}_1, \text{Si}_3, \text{O}_2, \text{O}_4, \text{O}_6, \text{C}_1, \text{C}_4, \text{C}_{11}$, and C_{14} in molecule 1 and $\text{Si}_5, \text{Si}_7, \text{O}_8, \text{O}_{10}, \text{O}_{12}, \text{C}_{21}, \text{C}_{24}, \text{C}_{31}, \text{C}_{34}$ in molecule 2, were seated on the mirrors with appropriate occupancies 0.50. In the final least squares cycles all the silicon and oxygen atoms were allowed to vibrate anisotropically. Hydrogen atoms were included at calculated positions in all cases except for those bonded to carbon atoms laying on mirror planes. In these cases the relevant hydrogens with half site-occupancy were located in the penultimate difference Fourier and refined at fixed distances [1.08Å] from the parent atoms. Final residuals after 14 cycles of blocked matrix least squares were $R = R_w = 0.0861$ for unit weights. Maximum final shift/esd was 0.040. The maximum and minimum residual densities were 0.31 and -0.244 eÅ⁻³ respectively. Tables of fractional atomic coordinates and thermal parameters, anisotropic temperature factors, bond lengths and angles and intramolecular and intermolecular distances are available as supplementary data in Appendix III.

Isolation of Heptacyclohexyl-heptasiloxane-1,6,7-triol: The pyridine extract from the solution referred to above was carefully poured into 5 times its volume of ice-cooled

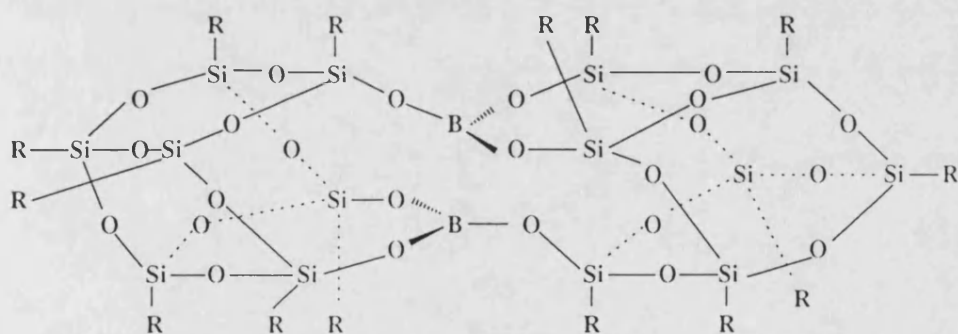
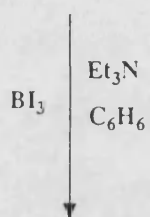
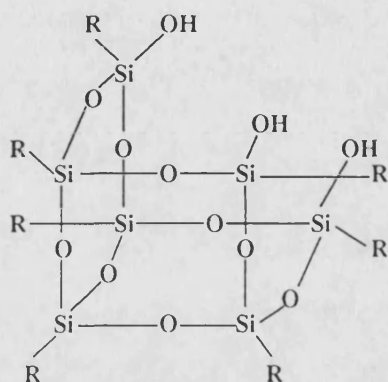
aqueous HCl (1 ml of conc. HCl/ml of pyridine). Any large clumps of precipitated product were broken up as finely as possible. It was essential to remove any mechanically entrained pyridine, pyridine-hydrochloride or HCl before continuing. This was accomplished by very finely pulverizing the solid, stirring with a large excess of water, collecting the product on a Buchner funnel, and then washing with copious amounts of water. The product was dried overnight at 40-50°C and then dissolved in a minimum amount of hot diethyl ether. Small microcrystals of compound 7 were formed (3.5g, 25%); m.p 269°C. Analysis found (calculated for $C_{42}H_{80}Si_7O_{12}$): C 51.8(52.1) H 8.2(8.31); I.R spectrum: 1107 (Si-O-Si), 3152 cm^{-1} (OH); 1H NMR spectrum $\delta(CDCl_3)$: 0.72m (7H, c- $C_6H_{11}Si$); 1.22m (35H, vbr, c- $C_6H_{11}Si$); 1.72m (35H, vbr c- $C_6H_{11}Si$); 7.26m (3H, vbr, SiOH); ^{13}C NMR spectrum: 27.5s, 26.9s, 26.6s (2:1:2 for CH_2), 23.8s, 23.5s, 23.1s (3:3:1 CH); ^{29}Si NMR spectrum: -60.3s, -68.2s, -69.7s ppm (3:1:3). Mass spectral data (70eV E.I, m/z): 973 (M^+), 871 ($M-C_6H_{11}-H_2O$), 789 ($M-C_6H_{11}-C_6H_{10}-H_2O$).



4.2.3 Synthesis of a Silsesquioxane Containing Boron

Synthesis of [(c-C₆H₁₁)₇Si₇O₁₂B]₂ (compound 8)

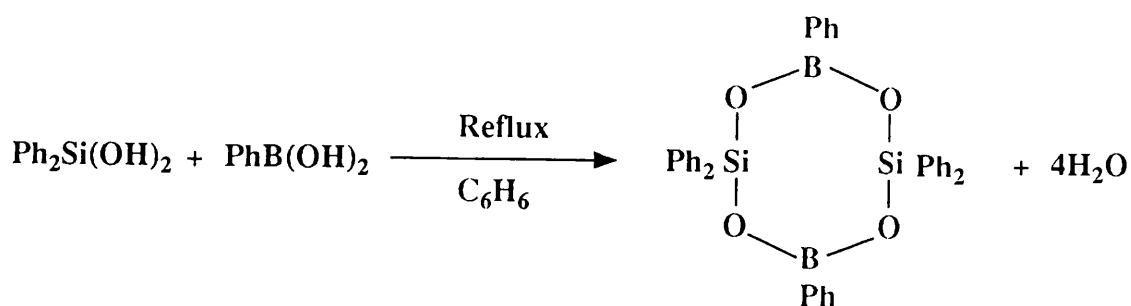
Borontriiiodide (0.0031 mole, 0.5g) was added with vigorous stirring to a solution of heptacyclohexylsiloxane-1,3,7-diol (0.0013 mole, 1.25g) and triethylamine (0.01 mole, 1.0g) in benzene (CARE) (50 ml) at room temperature. The solution was stirred for 3 hours, filtered to remove [Et₃NH]I, and then evaporated in vacuo (25°C, 0.01 Torr) to afford an amorphous white foam. Extraction with warm toluene, filtration to remove any unreacted diols and/or residual [Et₃NH]I, and cooling overnight yielded large colourless crystals which were collected by filtration, washed with toluene (5 ml) and dried in vacuum. This yielded the pure product Compound 8, (0.6g, 48%). Concentration of the mother liquors to half of the original volume afforded an additional amount of the known product after 2 days at -15°C. Analysis. found (calculated for C₈₄H₁₅₄Si₁₄O₂₄B₂): C 51.4(50.9); H 7.91(7.8)%. ¹H NMR spectrum δ(CDCl₃): 0.73m (7H, vbr, c-C₆H₁₁Si), 1.21m (35H, br, c-C₆H₁₁Si), 1.72m (35H, br, c-C₆H₁₁Si); ¹³C NMR spectrum: 23.12s, 23.51s, 23.82s for CH; 26.54s, 26.66s, 26.88s, 27.55s, for CH₂. ²⁹Si NMR spectrum: -60.02s, -67.55s, -67.97s, -68.16s, -69.58s ppm.



4.2.4 Synthesis of Heterocyclosiloxanes Containing Boron

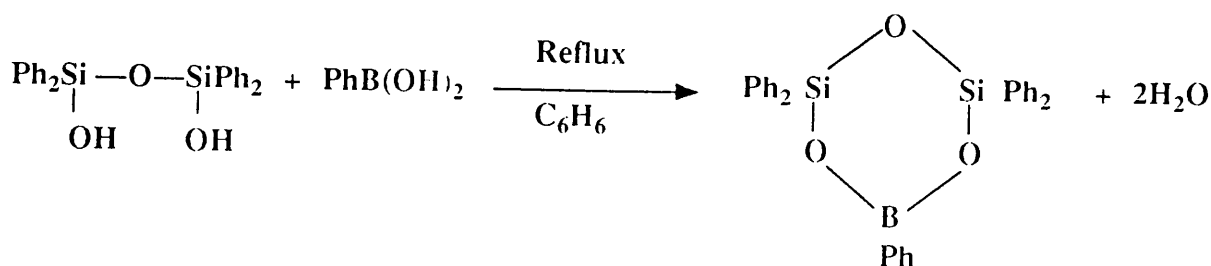
Synthesis of Cyclo-1,1,3,5,5,7-hexaphenyl-3,7-dibora-1,5-disiloxane (Compound 9)

The structure of $(\text{Ph}_2\text{B}_2\text{O}_4\text{Si}_2\text{Ph}_4)$ which contain an eight-membered ring with 1:1 boron to silicon ratio has been determined in these laboratories by B.Brisdon and his coworkers⁸. A mixture of diphenylsilanediol (0.01 mole, 2.16g) and phenylboronic acid 0.01 mole, (1.22g) were heated together in sodium-dried refluxing benzene (CARE) (20 ml) for 4 hours. Water formed during the course of the reaction was removed using a Dean and Stark apparatus. The reaction mixture was allowed to cool and any solid residues removed by filtration. The solvent was distilled off under reduced pressure and the solid residue recrystallised from 1:3 diethyl ether/petroleum-ether (60-80°C). to yield compound 9 (2.4g, 78%); m.p 158°C. Analysis, found (calculated for $\text{C}_{24}\text{H}_{22}\text{Si}_2\text{B}_2\text{O}_3$): C 71.5(71.1); H 4.9(4.8)%. I.R: 1321 (B-O-Si), 1128 cm^{-1} (Si-O-Si); ^1H NMR spectrum $\delta(\text{CDCl}_3)$: 7.40-7.66m (18H, *m,p*- C_6H_5); 7.84-7.88m (8H, *o*- $\text{C}_6\text{H}_5\text{Si}$), 8.20-8.23m (4H, *o*- $\text{C}_6\text{H}_5\text{B}$); ^{13}C NMR spectrum: 127.9s, 128.0s, 130.6s, 131.3s, 134.0s, 135.6s (*o,m,p*- $\text{C}_6\text{H}_5\text{Si}$, $\text{C}_6\text{H}_5\text{B}$); ^{29}Si NMR spectrum: -44.68ppm. Mass spectral data (70eV E.I. *m/z*): 604 (M^+), 527 (M^+-Ph), 500 (M^+-PhBO), 423 ($\text{M}^+-\text{Ph}_2\text{BO}$).



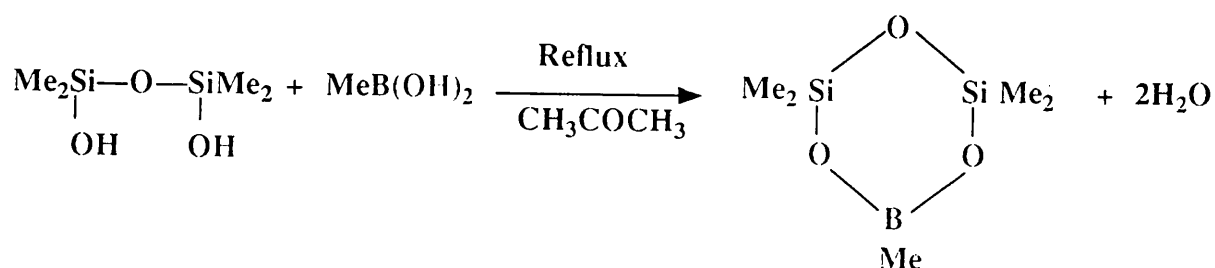
Synthesis of Cyclo-1,1,3,5,5-pentaphenyl-3-bora-1,5-disiloxane (Compound 10)

The structure of (PhBO₃Si₂Ph₄) which contains an six-membered ring with 1:2 boron to silicon ratio has been determined firstly by I.Manners⁹. The preparative method used in these laboratories is slightly different from this. A mixture of 1,1,3,3-tetraphenyldisiloxane-1,3-diol (0.005 mole, 2.07g) and phenylboronic acid (0.005 mole, 0.60g) were heated together in sodium-dried refluxing benzene (CARE) (20 ml) for 6 hours with continuous removal of water by use of a Dean and Stark apparatus. The mixture was allowed to cool and solid residues removed by filtration. The solvent was distilled off under reduced pressure and the solid residue recrystallised from 1:3 diethyl ether/petroleum ether 60-80°C. This procedure yielded pure compound 10 (1.1g, 83%); m.p 151°C. Analysis, found (calculated for C₃₀H₂₅BSi₂O₃): C 72.0(71.9); H 5.0(5.1)%. I.R: 1320s and 980s (B-O-Si), 1109 cm⁻¹ (Si-O-Si). ¹H NMR spectrum δ(CDCl₃): 7.23-7.64m (15H, *m,p*-C₆H₅), 7.84-7.87m (8H, *o*-C₆H₅Si), 8.21-8.25m (2H, *o*-C₆H₅B); ¹³C NMR spectrum: 127.7s, 128.0s, 129.8s, 130.7s, 131.6s, 132.9s, 134.4s, 135.6s (*o,m,p*-C₆H₅Si, C₆H₅B); ²⁹Si NMR spectrum: -31.0ppm. Mass spectral data (70eV *E.I.*, *m/z*): 500 (M⁺), 423 (M⁺-Ph), 319 (M⁺-Ph₂OB).



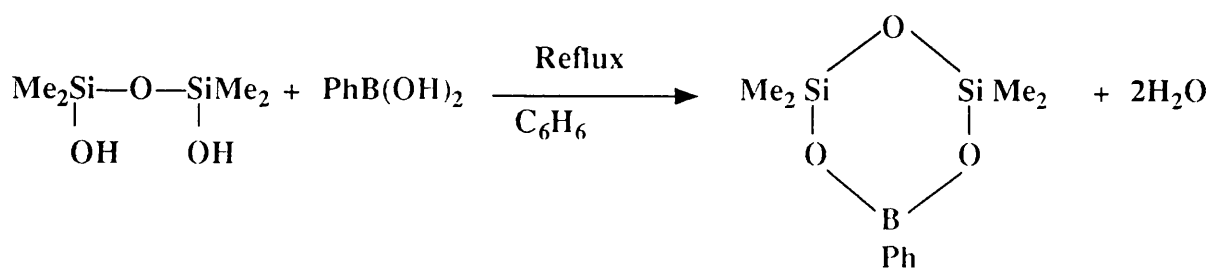
Synthesis of Cyclo-1,1,3,5,5-pentamethyl-3-bora-1,5-disiloxane (Compound 11)

Tetramethyldisiloxane-1,3-diol (0.01 mole, 1.66g) and methylboronic acid (0.01 mole, 0.60g) were heated in acetone (25 ml) for 6 hours. The solvent was removed under water vacuum, the resulting oil was then taken up in dry diethyl ether, and remaining water was removed by anhydrous sodium sulphate. After filtration, the solvent was evaporated, leaving the product as a colourless fluid, (1.2g, 63%). Analysis, found (calculated for $C_5H_{15}BSi_2O_3$): C 31.7(31.6); H 8.3(7.9)%. I.R spectrum: 1315s, 1250 (B-O-Si), 1040vs cm^{-1} (Si-O); 1H NMR spectrum $\delta(CDCl_3)$: 0.10-0.21t (12H, Me_2Si), 0.22-0.26t (3H, MeB); ^{13}C NMR spectrum: 0.48-0.58d (MeSi), 1.03 (MeB); ^{29}Si NMR spectrum: -17.6ppm. Mass spectral data (*Iso-but C.I.*, m/z): 191 (M^+), 175 ($M-CH_3$), 149 ($M-CH_3BO$).



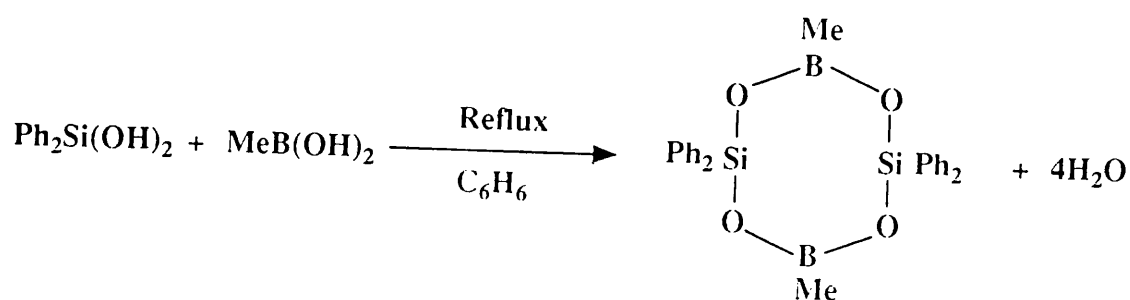
Synthesis of Cyclo-1,1,5,5-tetramethyl-3-phenylbora-1,5-disiloxane (Compound 12)

Tetramethyldisiloxane-1,3-diol (0.01 mole, 1.66g) and phenylboronic acid (0.01 mole, 1.21g) were heated together in dry refluxing benzene (CARE) (50 ml) for 5 hours. Water formed during the course of the reaction was removed using a Dean and Stark apparatus. On cooling the solvent was removed under reduced pressure, A semi-solid formed containing the product which was purified by vacuum distillation; b.p 80°C, 0.7mmHg. This procedure yielded compound 12 (0.95g, 38%). Analysis, found (calculated for $C_{10}H_{17}Si_2BO_3$): C 47.6(47.8); H 6.7(6.8)%; I.R spectrum: 1317vs (B-O-Si), 1064vs cm^{-1} (Si-O); 1H NMR spectrum $\delta(CDCl_3)$: 0.32-0.35m (12H, Me_2Si), 7.38-7.52m (3H, *m,p*- C_6H_5B), 7.82-8.31m (2H, *o*- C_6H_5B); ^{13}C NMR spectrum: 0.25s ($MeSi$), 27.0s (*o*- C_6H_5B), 130.5s, 134.5s (*m,p*- C_6H_5B); ^{29}Si NMR spectrum: -3.09ppm. Mass spectral data (70eV E.I, m/z): 252 (M^+), 237 (M^+-Me), 221 (M^+-MeO).



Synthesis of Cyclo-1,1,5,5-tetraphenyl-3,7-dimethyldibora-1,5-disiloxane (Compound 13)

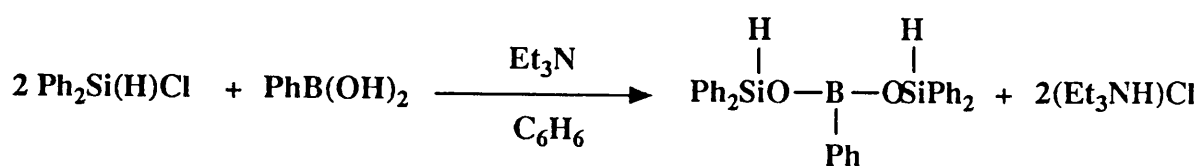
Diphenylsilandiol (0.005 mole, 1.08g) and methylboronic acid (0.005 mole, 0.30g) were heated together in sodium-dried benzene (CARE) (50 ml) for 5 hours. Water formed during the course of the reaction was removed using the method above. The reaction mixture was allowed to cool and any solid residue removed by filtration. The solvent was distilled from the filtrate under reduced pressure. This procedure yielded compound 13 (1.0g, 85%); m.p 110°C. Analysis, found (calculated for $C_{26}H_{26}Si_2B_2O_4$): C 65.3(64.8); H 5.4(5.2)%. I.R: 1336s (B-O-Si), 1130-1118s cm^{-1} (Si-O-Si); 1H NMR spectrum $\delta(CDCl_3)$: 0.034-0.27s (6H, 2MeB), 7.25-7.34m (12H, *m,p*- C_6H_5Si), 7.50-7.60m (8H, *o*- C_6H_5Si).



4.2.5 Synthesis of Linear Heterosiloxanes Containing Boron

Synthesis of 1,1,3,5,5-pentaphenyl-3-bora-1,5-dihydridotrisiloxane (Compound 14)

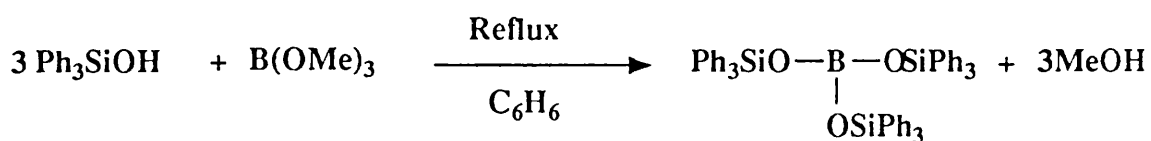
Phenylboronic acid (0.005 mole, 0.605g) was dissolved in sodium-dried benzene (CARE) (40 ml). A few drops of triethylamine were added to the mixture which was then heated gently under a N₂ atmosphere. Diphenylchlorosilane (0.01 mole, 2.18g) was added and a precipitate of (NEt₃H)Cl formed on addition. The mixture was stirred at 60°C for 2 hours, and then cooled and solid removed by filtration. The solvent was removed under reduced pressure and the solid residue was collected (2.1g, 43%). Attempts were made to recrystallise the solid formed by this procedure using a mixture of 1:1 hexane-diethyl ether, which produced a small twinned crystals in low yield (25%). Analysis, found (calculated for C₃₀H₂₇Si₂BO₂): C 73.3(74.2) ; H 5.6(5.6)%. I.R spectrum: 1346vs and 1305vs (B-O-Si), 1118s and 1093vs (Si-O), 2125vs cm⁻¹ (Si-H). ¹H NMR spectrum δ(CDCl₃): 5.6s (2H, Si-H), 7.29-7.40m (15H, *m,p*-C₆H₆), 7.53-7.57dd (8H, *o*-C₆H₅Si), and 8.22-8.25dd (2H, *o*-C₆H₅B).



Synthesis of 1,1,1,3,3,3,5,5,5-nonaphenyl-bora-1,3,5-trisiloxane (Compound 15)

Triphenylsilanol (0.015 mole, 4.14g) was dissolved in toluene (50 ml), and the mixture stirred at 60°C under N₂ atmosphere. Trimethylborate (0.005 mole, 0.52g) was added dropwise to the mixture, and the reaction refluxed overnight. On cooling a solid residue was first filtered off and the solvent removed under water vacuum. The crude product was recrystallised from the minimum amount of dichloromethane to yield

compound 15, (7.6g, 60%); m.p 130-132°C. Analysis; found (calculated for $C_{60}H_{45}Si_3BO_3$): C 77.6(77.7); H 5.4(5.4)%; I.R spectrum: 1365s, 1354s and 1313vs (B-O-Si), 1118vs and 1107vs cm^{-1} (Si-O); 1H NMR spectrum $\delta(CDCl_3)$: 7.14-7.64m (45H, *o,m,p*- C_6H_5Si); ^{29}Si NMR spectrum: -21.2ppm. Mass spectral data (*Iso-but. C.I.*): 759 (M-Ph), 681 (M-2Ph), 604 (M-3Ph), 559 (M-3PhSiO), 501 (M-3PhSi₂O₃).



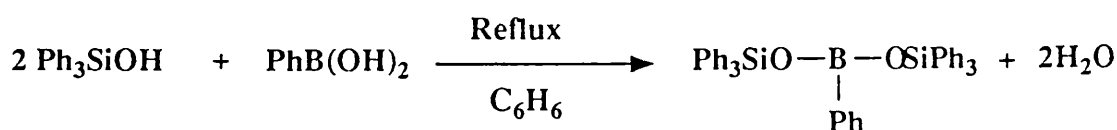
Synthesis of 1,1,1,3,5,5,5-heptaphenyl-3-bora-1,5-disiloxane (Compound 16)

Triphenylsilanol (0.01 mole, 2.76g) and phenylboronic acid (0.005 mole, 0.605g) were heated together in refluxing sodium-dried benzene (CARE) (50 ml) for 4 hours. Water formed during the course of the reaction was removed using a Dean and Stark apparatus. The reaction mixture was allowed to cool and solid deposits removed by filtration. The solvent was evaporated under reduced pressure and the residue recrystallised from the minimum amount of dichloromethane to yield compound 16 (3.2g, 50%); m.p 125°C. Analysis: found (calculated for $C_{48}H_{35}Si_2BO_2$): C 79.3(79.1); H 5.5(5.5)%. I.R spectrum: 1309vs, 1288s (B-O-Si), 1118vs cm^{-1} (Si-O). 1H NMR spectrum $\delta(CDCl_3)$: 7.18-7.68m (*o,m,p*- C_6H_5Si and *o,m*- C_6H_5B), 7.85-7.89m (*p*- C_6H_5B); ^{29}Si NMR spectrum: -16.7 and -12.4ppm; Mass spectral data (*Iso-but. C.I. m/z*): 561 (M-Ph), 365 (M- Ph_3SiO), 322 (M- $Ph_3Si_2O_2$), 305 (M- $Ph_3Si_2O_3$), 277 (M- $Ph_3Si_3O_3$), 199 (M- $Ph_4Si_3O_3$).

A crystal of approximate dimensions 0.3 x 0.3 x 0.4 mm was used for data collection for the structure determination.

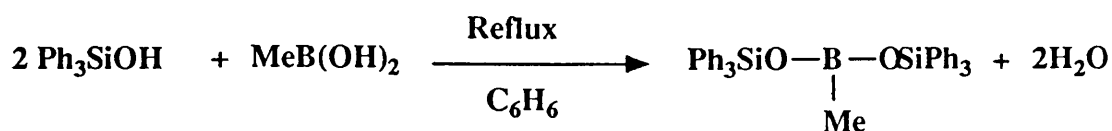
crystal data: $C_{48}H_{35}Si_2BO_2$, M = 638.8 monoclinic, $a = 18.666(4)$, $b = 9.685(2)$, $c = 19.837(6)$ Å, $\beta = 99.58$, $U = 3536.1$ Å³, space group $P2_1/c$, Z = 4, $D_c = 1.2$ gcm⁻³,

$\mu(\text{Mo-K}\alpha) = 0.99 \text{ cm}^{-1}$, $F(000) = 1344$. Data were measured at room temperature on a CAD4 automatic four-circle diffractometer in the range $2 \leq \Theta \leq 24^\circ$. 6108 reflections were collected of which 3327 were unique with $I \geq 3\sigma(I)$. Data were corrected for Lorentz and polarization effects but not for absorption. The structure was solved by Direct methods and refined using the SHELX suite of programs^{2,3}. In the final least squares cycles all atoms except for O_1 and O_2 were allowed to vibrate anisotropically. Hydrogen atoms were included at calculated positions. Final residuals after 7 cycles of least squares were $R = 0.0544$, $R_w = 0.0629$, for a weighting scheme of $\omega = 2.0099/[\sigma^2(F) + 0.002683(F)^2]$. Maximum final shift/esd was 0.038. The maximum and minimum residual densities were 0.12 and $-0.10 \text{ e}\text{\AA}^{-3}$ respectively. Tables of fractional atomic coordinates and thermal parameters, anisotropic temperature factors, bond lengths and angles and intramolecular and intermolecular distances are available as supplementary data in Appendix III.



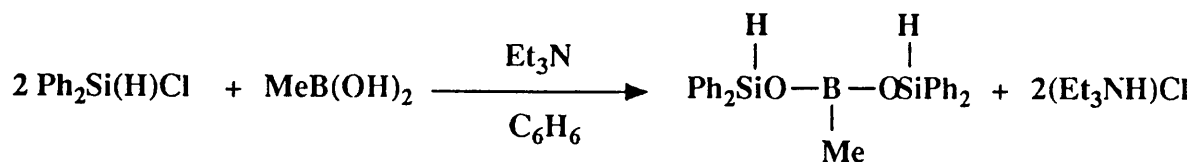
Synthesis of 1,1,1,5,5,5-hexaphenyl-3-methyl-3-bora-1.5-disiloxane (Compound 17)

Triphenylsilanol (0.01 mole, 2.76g) and methylboronic acid (0.005 mole, 0.3g) in sodium-dried benzene (CARE) (40 ml) were refluxed for 6 hours under a N_2 atmosphere. Water formed during the course of the reaction was removed using a Dean and Stark apparatus. The reaction mixture was allowed to cool and solid residues removed by filtration. The solvent was removed under vacuum, and the crude product recrystallised from the minimum amount of diethyl-ether. This procedure yielded compound 17 (2.9g, 50%); m.p 109°C . Analysis, found (calculated for $\text{C}_{37}\text{H}_{33}\text{Si}_2\text{BO}_2$): C 76.9(77.2); H 5.7(5.7)%. I.R spectrum: 1331vs and 1311vs (B-O-Si), 1118vs and 1107s cm^{-1} (Si-O); ^1H NMR spectrum $\delta(\text{CDCl}_3)$: 0.16s (3H, BMe), 7.25-7.65m (30H, *o,m,p*- $\text{C}_6\text{H}_5\text{Si}$); ^{13}C NMR spectrum: 127.7s, 127.9s, 129.8s, 130.1s, 135.0s, 135.2s (*o,m,p*- $\text{C}_6\text{H}_5\text{Si}$).



Synthesis of 1,1,5,5-tetraphenyl-3-methyl-3-bora-1,5-dihydridodisiloxane (Compound 18)

Methylboronic acid (0.005 mole, 0.3g) was dissolved in sodium-dried benzene (CARE) (40 ml). A few drops of triethylamine were added to the mixture, and after heating under N₂ atmosphere 0.01mole, (2.18g) of diphenylchlorosilane were added gradually, resulting in a precipitate of (NEt₃H)Cl. The mixture was stirred at 60°C for 3 hours after the addition. After cooling the reaction mixture solid residues were removed by filtration. The solvent was removed under water vacuum leaving the product as a viscous liquid (2.85g, 68%). Analysis found (calculated for C₂₅H₂₅Si₂BO₂): C 68.0(68.2); H 5.20(5.21)%. I.R spectrum: 2123vs (Si-H), 1349vs and 1307vs (B-O-Si), 1120vs and 1100s cm⁻¹ (Si-O). ¹H NMR spectrum δ(CDCl₃): 0.25s (3H, BMe), 5.5s (2H, SiH), 7.29-7.45m (12H, *m,p*-C₅H₆Si), 7.57-7.59d (8H, *o*-C₅H₆Si).



4.2.6 Synthesis of Heterocyclosilazanes Containing Boron

Synthesis of 2,2-dimethyl-4,6-diphenyl-1,3,5-triaza-2-sila-4,6-diboracyclohexane (Compound 19)

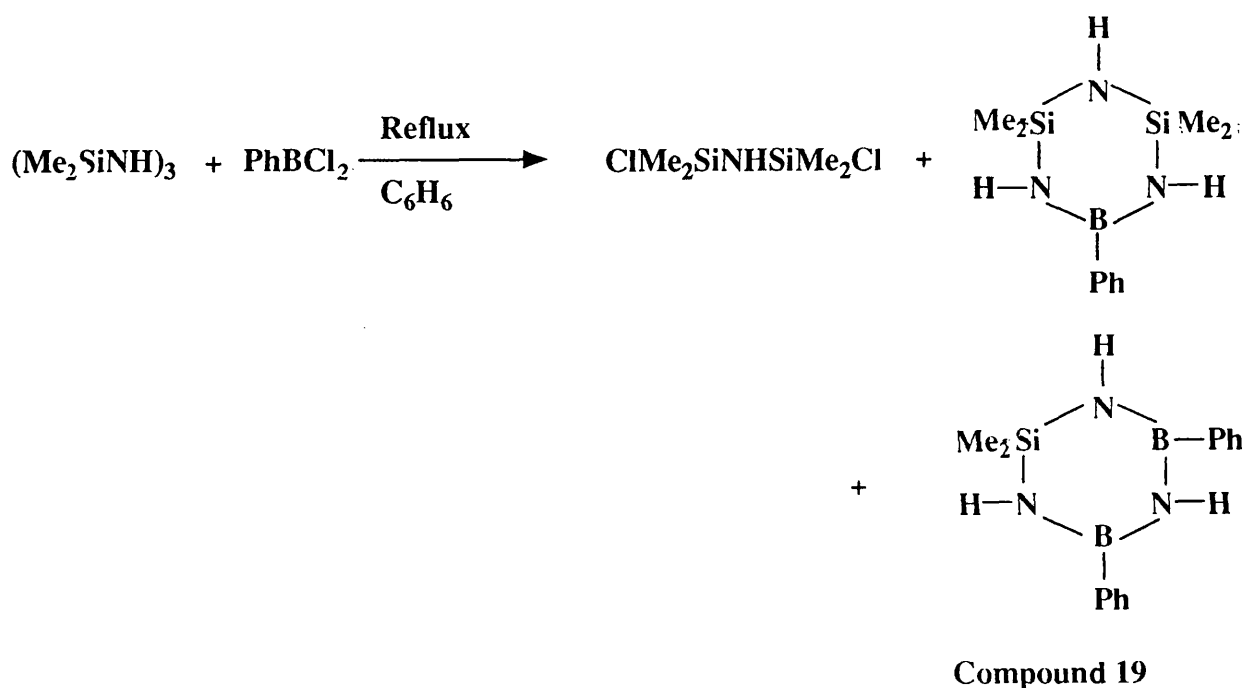
A solution of 2,2,4,4,6,6-hexamethylcyclotrisilazane (0.078mole, 17.1g) were mixed in benzene (CARE) (300 ml) then treated dropwise while vigorously stirred with phenylboron dichloride (0.0625 mole, 9.9g). After the exothermic reaction had died down, the reaction mixture was heated for 3 hours under reflux, then cooled and the solvent evaporated in vacuum leaving a mixture of products. Distillation gave in the initial fraction a mixture of 1,3-dichloro-1,1,3,3-tetramethyldisilazane, ClMe₂SiNHSiMe₂Cl, and

2,2,4,4-tetramethyl-6-phenyl-1,3,5-triaza-2,4-sila-6-boracyclohexane, $\text{PhB}(\text{SiMe}_2\text{NH})_2\text{NH}$ at 130°C , 0.01 Torr. Compound 19, 2,2-dimethyl-4,6-diphenyl-1,3,5-trisilaza-2-sila-4,6-diboracyclohexane, $\text{Me}_2\text{Si}(\text{BPhNH})_2\text{NH}$ was recovered at $140\text{--}170^\circ\text{C}$, 0.01 Torr, and after solidifying was recrystallised from n-heptane as colourless crystals; (2.4g, 25%), m.p $102\text{--}104^\circ\text{C}$. Analysis, found (calculated for $\text{C}_{14}\text{H}_{19}\text{B}_2\text{N}_3\text{Si}$): C 60.3(60.2); H 6.86(6.85); N 15.06(14.15)%. I.R: 3427s, 3410s, 3395s (N-H), 3072s, 3049s, 3011s (C-H aromatic), 2926vs, 2895vs (C-H aliphatic) 1599vs, 1572w, 1498s (C=C) 1441vs (br, BN), 1381vs (br, BPh) 864vs (SiN) 788s (SiC) $702\text{--}698\text{vs cm}^{-1}$ (B-N out of plane). ^1H NMR spectrum $\delta(\text{CDCl}_3)$: 0.12m (6H, (Me_2Si)), 2.95s (2H, 2NH), 4.58 (1H, NH), 7.10-7.87m (10H, $2\text{C}_6\text{H}_5\text{B}$); ^{13}C NMR: 3.98s $(\text{CH}_3)_2\text{Si}$, 127.1s, 127.7s, 127.9s, 129.4s, 130.8s, 131.5s (*o,m,p*- $\text{C}_6\text{H}_5\text{B}$); ^{29}Si NMR spectrum: -1.23ppm. Mass spectral data (*Iso-but. C.I*, *m/z*): 280 (M^+), 264 ($\text{M}^+ - \text{CH}_3$), 247 ($\text{M}^+ - \text{CH}_3\text{NH}_3$).

A crystal of approximate dimensions 0.9 x 0.6 x 0.2 mm was used for data collection.

crystal data: $\text{C}_{14}\text{H}_{16}\text{B}_2\text{N}_3\text{Si}$, $M = 276$ monoclinic, $a = 10.911(7)$, $b = 14.066(7)$, $c = 11.738(7)$ Å, $\beta = 114.98(4)$, $U = 1633.0$ Å³, space group $P2_1/c$, $Z = 4$, $D_c = 1.12$ gcm⁻³, $\mu(\text{Mo-K}\alpha) = 1.33$ cm⁻¹, $F(000) = 580$. Data were measured at room temperature on a CAD4 automatic four-circle diffractometer in the range $2 \leq \Theta \leq 22^\circ$. 2233 reflections were collected of which 1320 were unique with $I \geq 3\sigma(I)$. Data were corrected for Lorentz and polarization effects and also for linear crystal decay of 30.77 % in the x-ray beam. No absorption correction was applied. The structure was solved by Direct methods and refined using the SHELX suite of programs^{2,3}. In the final least squares cycles all atoms were allowed to vibrate anisotropically. Hydrogen atoms were included at calculated positions except in the case of H_1 , H_2 and H_3 (attached to N_1 , N_2 and N_3 respectively) which were located in an advanced difference Fourier and refined at a fixed distance of 1.00 Å from the relevant parent atoms. Final residuals after 8 cycles of least squares were $R = 0.0417$, $R_w = 0.0477$, for a weighting scheme of $\omega = 1.0000/[\sigma^2(F) + 0.002968(F)^2]$.

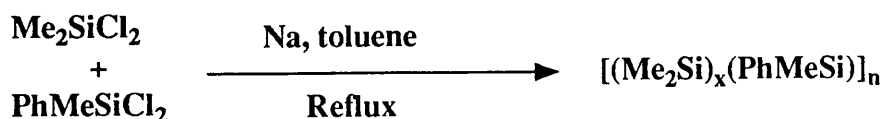
Maximum final shift/esd was 0.090. The maximum and minimum residual densities were 0.05 and -0.06 eÅ⁻³ respectively. Tables of fractional atomic coordinates and thermal parameters, anisotropic temperature factors, bond lengths and angles and intramolecular and intermolecular distances are available as supplementary data in Appendix III.



4.2.7 Synthesis of Phenylmethyilsilane-dimethylsilane Copolymer

Synthesis of Phenylmethyilsilane-dimethylsilane Copolymer (compound 20)

In 1983, Yajima and his coworkers¹⁰ reported that copolymers of phenylmethyilsilane and dimethylsilane units were formed with an approximately 1:1 ratio. To chunks of sodium (0.575 mole, 13.23g) suspended in toluene (150 ml) was added 100 μ l oleic acid to aid in dispersion of the sodium. The toluene was refluxed and a high speed stirrer used to create a sodium dispersion. The heating mantle was removed and the dispersion in toluene was allowed to cool down to 70°C, whereupon a mixture of PhMeSiCl₂ (0.14 mole, 26.3g) and Me₂SiCl₂ (0.14 mole, 17.8g) was added dropwise with stirring quickly enough to maintain the reaction mixture at gentle reflux. The solution turned from gray to dark blue. After the addition was complete, the heating mantle was replaced and the reflux was maintained for 7 hours. At the end of this period the reaction mixture was cooled down, and quenched by adding methanol (150 ml) dropwise over 20 minutes and then water (200 ml). The organic layer was separated, dried, and the solvent evaporated to yield a yellowish grease containing phenylmethyilsilane-dimethylsilane copolymer (15.3g, 64%). Analysis, found (calculated for C₉H₁₄Si₂): C 60.6(59.9); H 7.8(7.75); ¹H NMR spectrum δ (CDCl₃): 0.14-0.63brm (MeSi), 7.25-7.42brm (PhSi). The NMR spectrum data are similar to the chemical shifts for a (PhMeSi)_n homopolymer¹¹, the relative areas of the two peaks in compound 20 indicated a (Me₂Si)₁(PhMeSi)_{1.3} ratio.



Attempts were also made to synthesise heterocyclicsiloxanes containing boron with other substituents on boron via the reaction of $\text{Ph}_2\text{Si}(\text{OH})_2$ with $\text{B}(\text{OR})_3$ ($\text{R} = \text{Et}$ or $n\text{-Bu}$). The final products were impure due to the presence of unreacted starting materials, and attempts at purification using distillation or column separation were unsuccessful.

4.3 REFERENCES

1. J I Harris, J Chem Soc, 1963, 5879.
2. G M Sheldrick, 1976, SHELX76, A Computer Program for Crystal Structure Determinations, University of Cambridge, England.
3. G M Sheldrick, 1986, SHELX86, A Computer Program for Crystal Structure Determinations, University of Gotingen.
4. International Tables for X-ray Crystallography, 1974, **IV**, Birmingham: Kynoch Press.
5. J F Brown and L H Vogt, J Am Chem Soc, 1965, **87**, 4313.
6. F J Feher, D A Newman and J F Walzer, J Am Chem Soc, 1989, **111**, 1741.
7. F J Feher and T A Budzichowski, J Organomet Chem, 1989, **373**, 153.
8. B J Brisdon, M F Mahon, K C Molloy and P J Schofield, J Organomet Chem, 1992, **436**, 11.
9. D A Foucher, A J Lough and I Manners, J Organomet Chem, 1991, **414**, C1.
10. R West, L D David and P I Djurovich, Am Ceram Soc Bull, 1983, **62**, 899.
11. L D David, Ph.D Thesis; University of Wisconsin-Madison, 1981.

CHAPTER FIVE

STRUCTURAL CHARACTERISATION OF MODEL COMPOUNDS

5.1 SUMMARY

Several of the compounds synthesised during the course of this work have been structurally analysed and their significant structural features are compared below with those of related compounds. The crystal structures of *cyclo*-(C₆H₁₁)₆Si₆O₉ (Compound 6), which contains two 6-membered Si₃O₃ rings joined co-facially, Ph₂(HO)SiOSi(Ph₂)OSi(OH)Ph₂ (Compound 3) which contains a cyclic H-bonded ring skeleton, the linear derivative PhB(Ph₃SiO)₂ (Compound 16) and *cyclo*-Me₂Si(PhBNH)₂NH (Compound 19) which exhibits a B₂N₃Si ring system have been determined at room temperature by Dr Mahon in the School of Chemistry using a Hilger and Watts Y-290 four-circle diffractometer or a CAD 4 automatic four-circle diffractometer. All the crystallography experimental data are given in Chapter 4.

5.2 THE STRUCTURE OF HEXA(CYCLO-HEXYLSESQUISILOXANE)

Spherical sesquisiloxanes (RSiO_{1.5})_n are an important class of compounds due to their unique structural features. The first sesquisiloxanes were prepared by Scott in 1946 by the hydrolysis of organotrichlorosilanes^{1,2}. The general insolubility of this class of compounds has however, prevented extensive structural analysis. Of the eight organosilsesquisiloxanes structures defined crystallographically, six [R= Me, Et, Ph, PhCH₂, vinyl, allyl] are analogous octameric species (R₈Si₈O₁₂)^{3,4}. Higher oligomers are confined to the decamer and dodecamer, Me₁₀Si₁₀O₁₅⁵ and Ph₁₂Si₁₂O₁₈⁶, the inorganic species (Me₃SiO)₁₂Si₁₂O₁₈ and (Me₃SiO)₁₄Si₁₄O₂₁ (two isomers)⁷. As no structures have been reported for smaller, potentially strained, organosilicon oligomers (N<8), the structure of compound 6 was determined in order to provide a direct comparison with the known silicate systems, [Me₄N⁺]₆[Si₆O₁₅⁶⁻].36.5H₂O⁸, [Ni(en)₃²⁺]₃[Si₆O₁₅⁶⁻].26H₂O⁹,

and $[\text{Me}_3\text{SiO}]_6\text{Si}_6\text{O}_9$ ¹⁰.

The hydrolysis of cyclohexyltrichlorosilane in acetone has been reported to lead to the formation of three condensed sesquisiloxanes derivatives containing 6-, 7- and 8-silicon centres, $\text{Cy}_6\text{Si}_6\text{O}_9$, $\text{Cy}_7\text{Si}_7\text{O}_9(\text{OH})_3$ and $\text{Cy}_8\text{Si}_8\text{O}_{11}(\text{OH})_2$ respectively. In this work a slightly modified synthetic procedure, but an identical literature separation method¹¹, has been used to prepared compound 6, as described in Chapter 4. By using a comparatively short reaction time, the proportion of $\text{Cy}_6\text{Si}_6\text{O}_9$ is maximised at the expense of the octa-sesquisiloxane in the initial solid mixture, so facilitating purification of the hexamer, albeit at the expense of an overall reduced yield. The other two products containing 7- and 8-silicon centres both contain silanol groups and have been structurally characterized previously¹¹. The chemistry of the 7-silicon centre compound in particular has been developed extensively by Feher¹².

Compound 6, $\text{Cy}_6\text{Si}_6\text{O}_9$ has a cage structure in which two six-membered Si_3O_3 rings are joined co-facially by Si-O-Si bridges, generating three further Si_4O_4 heterocycles (Figure 5.1). The final fractional atomic coordinates and isotropic thermal parameters are listed in Table 5.1, and selected bond length and angles are shown in Table 5.2. The bond length and angle data for the Si_3O_3 rings [mean Si-O: 1.640(6) Å; mean Si-O-Si angles: 129.5(5)°] are essentially unchanged from those of the virtually planar $\text{Ph}_6\text{Si}_3\text{O}_3$ compound [1.640(6) Å; 132-133°]¹³. Indeed collective data available for such ring compounds, including $\text{Me}_6\text{Si}_3\text{O}_3$, show a remarkable geometric consistency [Si-O: 1.635-1.654 Å; Si-O-Si angles: 125-135°]⁴. The Si_3O_3 rings in the two iso-structural silicate anions $[\text{cation}]_n[\text{Si}_6\text{O}_{15}]^{6-}$; {cation = Et_4N^+ , $n = 6$; $\text{Ni}(\text{en}^{2+})_3$, $n = 3$ }^{8,9}, also follow these geometric trends (Table 5.3), though the spread of Si-O bond lengths and Si-O-Si angles is somewhat wider, possibly due to distortions brought about by extensive hydrogen-bonding within the lattices. However, in contrast to $\text{R}_6\text{Si}_3\text{O}_3$ species in which the Si_3O_3 six-membered siloxane rings are invariably near-planar, with the maximum observed deviation from the mean plane being 0.1 Å¹³, the two Si_3O_3 units in compound 6 each adopt a chair conformation (Figure 5.2). This conformation is also apparent in

$[\text{Et}_4\text{N}^+]_6[\text{Si}_6\text{O}_{15}^{6-}]^8$, though in the $[\text{Ni}(\text{en})_3]^{2+}$ salt of this anion, the components of the six-membered ring are described as lying approximately in one plane⁹. In the title compound $\text{Cy}_6\text{Si}_6\text{O}_9$, the O-Si-O and C-Si-O bond angles [mean 109.2 and 110.5° respectively] are within the ranges of 105.8-112.2° found in most siloxanes, and show only minor deviations from the ideal tetrahedral value. The three eight-membered Si_4O_4 rings in $\text{Cy}_6\text{Si}_6\text{O}_9$ adopt a crown configuration, with the four oxygen atoms lying above an Si_4 plane. The two oxygen atoms which are solely part of the Si_4O_4 ring are significantly nearer to the Si_4 plane than the two oxygens which are also integral to the Si_3O_3 rings. Thus, O_5 and O_6 lie 0.32, 0.25 Å above the $\text{Si}_1\text{-Si}_4$ plane respectively, while the corresponding displacements for O_1 and O_3 are 0.65 Å (Figure 5.2). The Si-O bonds are somewhat shorter in this part of the molecule [mean: 1.625 Å] and are associated with slightly more open Si-O-Si angles [mean: 142.3°] (Table 5.2), a trend which has been commented on previously^{14,15}. The data for the Si_4O_4 rings in the two salts of the $[\text{Si}_6\text{O}_{15}^{6-}]$ anions discussed earlier are consistent with the trends noted in the Si_3O_3 heterocycles; that is the mean bond length and angles are identical to those in the title organometallic species, as indicated in Table 5.3.

Interestingly, the eight-membered Si_4O_4 rings in higher sesquisiloxanes, where the heterocycle is fused to other Si_4O_4 , ($\text{R}_8\text{Si}_8\text{O}_{12}$) or a larger ring, ($\text{R}_{10}\text{Si}_{10}\text{O}_{15}$), incorporate yet larger Si-O-Si angles (148-153°) and correspondingly shorter Si-O bonds (1.610 Å) as noted in Table 5.3. This feature is consistent with the relationship between these two parameters discussed earlier in Chapter 2 section 2.3.3. These data approach those for the parent molecule $\text{Ph}_8\text{Si}_4\text{O}_4$ [mean Si-O: 1.615 Å; mean Si-O-Si angles: 159.8°]¹⁶, which has been variously described as adopting a shallow boat or a planar structure¹⁷. Collectively, the structure of compound 6 reflects the increasing strain induced in Si_4O_4 rings when fused to other siloxane rings of decreasing nuclearity, and particularly when attached to an Si_3O_3 ring as in the title compound $\text{Cy}_6\text{Si}_6\text{O}_9$.

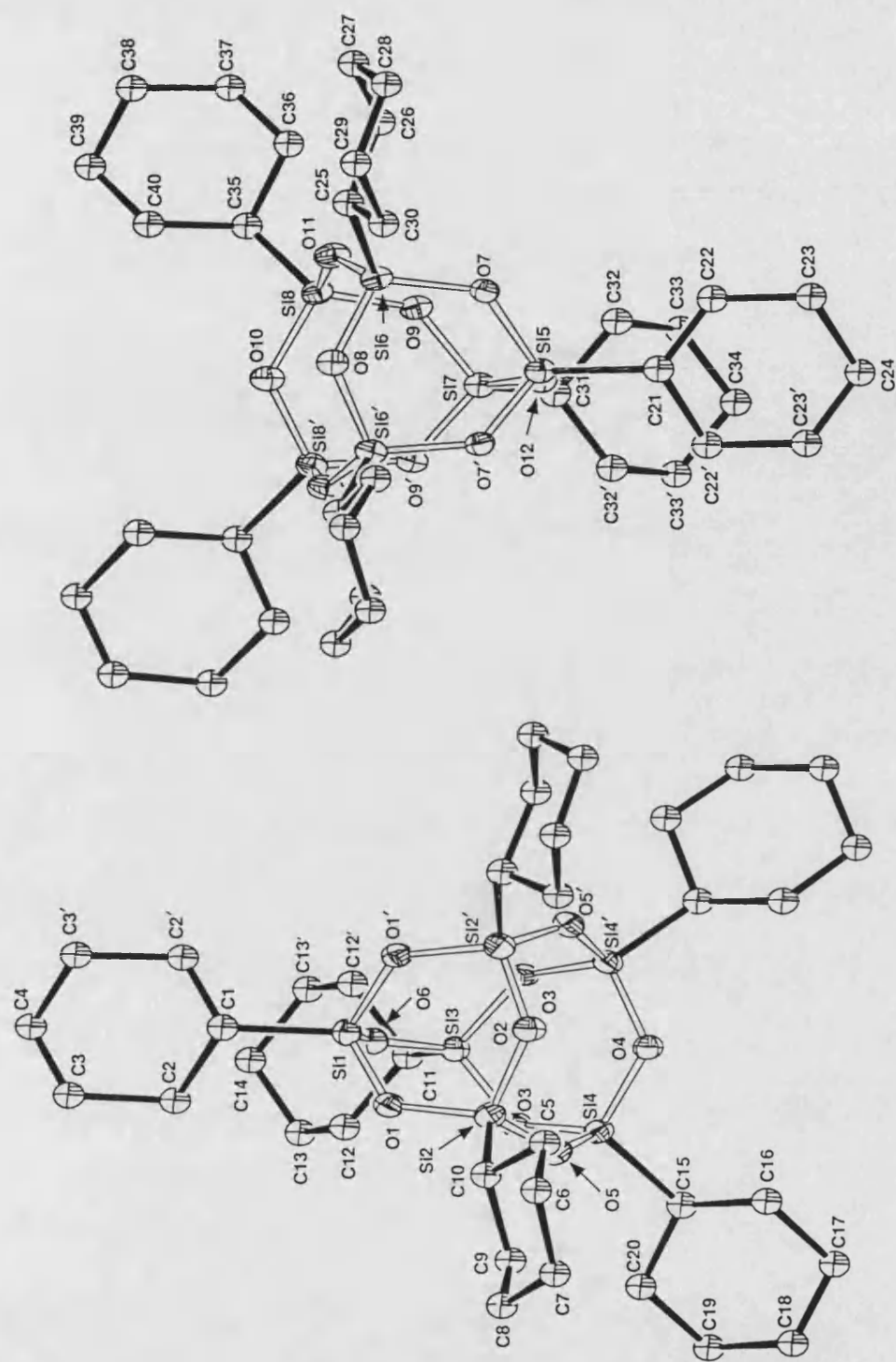


Figure 5.1

The asymmetric unit of $\text{Cy}_6\text{Si}_6\text{O}_9$, showing the two independent molecular halves. primed atoms are related to their unprimed counterparts by mirror planes through $\text{Si}_1, \text{Si}_3, \text{O}_2, \text{O}_6, \text{C}_1, \text{C}_4, \text{C}_{11}$ and C_{14} in molecule 1, and $\text{Si}_5, \text{Si}_7, \text{O}_8, \text{O}_{10}, \text{O}_{12}, \text{C}_{21}, \text{C}_{24}, \text{C}_{31}$ and C_{34} in molecule 2

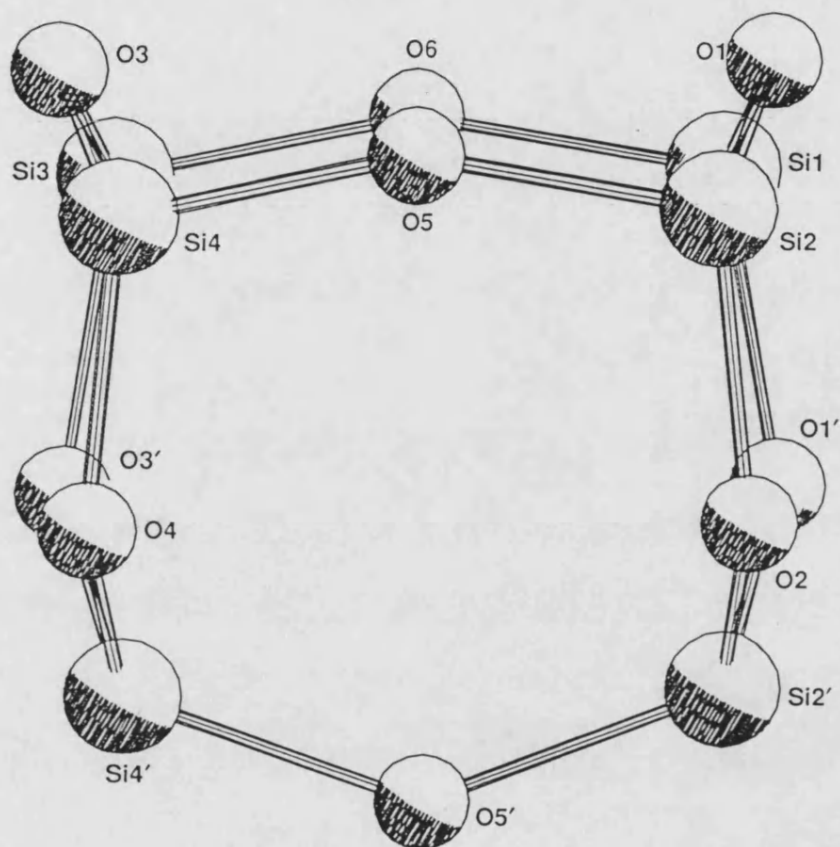


Figure 5.2

The sesquisiloxanes cage of $\text{Cy}_6\text{Si}_6\text{O}_9$, showing the crown configuration of the Si_4O_4 rings (top of molecule) and the chair configuration adopted by the Si_3O_3 rings (left and right edges of molecule)

Table 5.1

Fractional atomic coordinates and thermal parameters (\AA) for
 $\text{Cy}_6\text{Si}_6\text{O}_9$, compound 6

Atom	x	y	z	u_{eq}
Si1	0.5251(3)	0.2500	0.3230(1)	0.038(2) *
Si2	0.6201(2)	0.1703(1)	0.2174	0.040(1) *
Si3	0.2629(3)	0.2500	0.2559	0.037(2) *
Si4	0.3615(2)	0.1705(1)	0.1508(1)	0.037(2) *
O1	0.5835(5)	0.1797(3)	0.2893(2)	0.041(3) *
O2	0.6580(7)	0.2500	0.1929(4)	0.043(5) *
O3	0.2773(5)	0.1799(3)	0.2105(2)	0.039(3) *
O4	0.3720(7)	0.2500	0.1197(3)	0.041(5) *
O5	0.4994(5)	0.1429(3)	0.1744(2)	0.043(3) *
O6	0.3746(7)	0.2500	0.3096(3)	0.036(2) *
Si5	0.0153(3)	-0.2500	0.1938(1)	0.036(2) *
Si6	0.1098(2)	-0.1707(1)	0.3060(1)	0.037(1) *
Si7	-0.2474(3)	-0.2500	0.2435(1)	0.036(1) *
Si8	-0.1491(2)	-0.1708(1)	0.3553(1)	0.038(1) *
O7	0.0728(5)	-0.1797(3)	0.2317(2)	0.037(3) *
O8	0.1507(7)	-0.2500	0.3331(4)	0.041(5) *
O9	-0.2321(5)	-0.1799(3)	0.2892(2)	0.041(3) *
O10	-0.1398(7)	-0.2500	0.3879(4)	0.044(5) *
O11	-0.0109(5)	-0.1436(3)	0.3410(3)	0.043(3) *
O12	-0.1352(6)	-0.2500	0.1975(3)	0.038(4) *
C1	0.5610(10)	0.2500	0.4081(6)	0.054(3) *
C2	0.5112(10)	0.1828(6)	0.4394(5)	0.076(3) *
C3	0.5443(12)	0.1841(8)	0.5111(6)	0.099(4) *
C4	0.4977(12)	0.2500	0.5408(7)	0.102(6)
C5	0.7530(8)	0.1080(5)	0.2137(4)	0.054(2)
C6	0.8502(11)	0.1337(7)	0.1715(6)	0.090(4)
C7	0.9637(12)	0.0838(7)	0.1719(6)	0.093(4)
C8	0.9293(10)	0.0084(6)	0.1571(5)	0.071(3)
C9	0.8314(11)	-0.0172(7)	0.1954(6)	0.094(4)
C10	0.7154(10)	0.0307(6)	0.1949(5)	0.076(3)
C11	0.1162(10)	0.2500	0.2934(5)	0.039(3)
C12	0.1003(8)	0.1829(5)	0.3347(4)	0.058(2)
C13	-0.0202(10)	0.1827(6)	0.3691(5)	0.077(3)
C14	-0.0285(11)	0.2500	0.4068(7)	0.086(5)
C15	0.2915(7)	0.1074(4)	0.0927(4)	0.041(2)
C16	0.3613(9)	0.1090(5)	0.0320(4)	0.058(2)
C17	0.3048(10)	0.0548(6)	-0.0155(5)	0.068(3)
C18	0.0310(9)	-0.0193(6)	0.0106(5)	0.066(3)
C19	0.2315(9)	-0.0216(5)	0.0706(4)	0.058(2)
C20	0.2881(8)	0.0304(5)	0.1181(4)	0.048(2)
C21	0.0521(11)	-0.2500	0.1110(5)	0.039(3)
C22	0.0043(8)	-0.1828(5)	0.0770(4)	0.055(2)
H211	-0.0952(8)	-0.1804(5)	0.0786(4)	0.079(6)
C23	0.0375(10)	-0.1825(6)	0.0076(5)	0.069(3)
C24	-0.0094(15)	-0.2500	-0.0268(7)	0.071(4)
C25	0.2393(7)	-0.1076(4)	0.3228(4)	0.041(2)
C26	0.2106(9)	-0.0311(6)	0.3034(5)	0.064(3)
C27	0.3217(10)	0.0178(6)	0.3194(5)	0.076(3)
C28	0.4381(8)	-0.0075(5)	0.2924(4)	0.055(2)
C29	0.4671(9)	-0.0826(5)	0.3110(5)	0.059(3)

Cont. Table 5.1

C30	0.3584(9)	-0.1329(6)	0.2942(5)	0.066(3)
C31	-0.3962(11)	-0.2500	0.1961(5)	0.041(3)
C32	-0.4129(9)	-0.1826(5)	0.1560(4)	0.059(3)
C33	-0.5379(10)	-0.1837(6)	0.1159(5)	0.077(3)
C34	-0.5505(18)	-0.2500	0.0765(8)	0.089(5)
C35	-0.2164(8)	-0.1061(5)	0.4078(4)	0.043(2)
C36	-0.2149(9)	-0.0300(5)	0.3802(5)	0.062(3)
C37	-0.2702(10)	0.0246(7)	0.4238(5)	0.077(3)
C38	-0.2064(12)	0.0204(7)	0.4890(6)	0.093(4)
C39	-0.2090(12)	-0.0521(17)	0.5157(6)	0.091(4)
C40	-0.1525(10)	-0.1081(6)	0.4730(5)	0.074(3)

Table 5.2

Selected bond lengths (\AA) and bond angles ($^\circ$) for $\text{Cy}_6\text{Si}_6\text{O}_9$, compound 6

Bond	Bond Lengths	Bond	Bond Lengths
Si1-O1	1.649(6)	Si1-O6	1.633(8)
Si2-O2	1.645(4)	Si2-O1	1.625(6)
Si2-O5	1.630(6)	Si3-O3	1.648(6)
Si3-O6	1.612(8)	Si4-O3	1.629(6)
Si4-O4	1.641(4)	Si4-O5	1.627(6)
Si5-O7	1.648(5)	Si5-O12	1.634(8)
Si6-O7	1.626(5)	Si6-O8	1.647(4)
Si6-O11	1.628(6)	Si7-O9	1.640(6)
Si7-O12	1.611(8)	Si8-O9	1.634(6)
Si8-O10	1.643(4)	Si8-O11	1.626(6)
Si1-C1	1.839(13)	Si2-C5	1.858(10)
Si3-C11	1.825(11)	Si4-C15	1.842(8)
Si5-C21	1.844(12)	Si6-C25	1.849(8)
Si7-C31	1.845(12)	Si8-C35	1.837(9)
Bond	Bond Angles	Bond	Bond Angles
O6-Si1-O1	109.2(3)	C1-Si1-O1	111.9(3)
C1-Si1-O6	108.5(5)	O1-Si1-O1'	106.2(4)
O2-Si2-O1	106.6(3)	C5-Si2-O5	111.7(4)
O5-Si2-O1	109.5(3)	O5-Si2-O2	108.3(3)
C5-Si2-O1	110.2(4)	C5-Si2-O2	110.4(4)
O6-Si3-O3	109.0(3)	C11-Si3-O3	112.2(3)
C11-Si3-O6	108.5(5)	O3-Si3-O3'	105.8(4)
O4-Si4-O3	106.1(3)	C15-Si4-O5	109.5(3)
O5-Si4-O3	109.8(3)	O5-Si4-O4	109.2(4)
C15-Si4-O3	112.0(3)	C15-Si4-O4	110.3(4)
O12-Si5-O7	108.7(3)	C21-Si5-O7	112.0(3)
C21-Si5-O12	109.0(5)	O7-Si5-O7'	106.3(4)
O8-Si6-O7	107.1(3)	C25-Si6-O11	109.3(3)
O11-Si6-O7	109.3(3)	O11-Si6-O8	108.9(4)
C25-Si6-O7	113.1(3)	C25-Si6-O8	109.1(4)
O12-Si7-O9	108.3(3)	C31-Si7-O9	112.2(3)
C31-Si7-O12	109.2(5)	O9-Si7-O9'	106.4(4)
O10-Si8-O9	106.8(3)	C35-Si8-O11	108.3(3)
O11-Si8-O9	109.2(3)	O11-Si8-O10	109.4(4)
C35-Si8-O9	112.5(3)	C35-Si8-O10	110.6(4)
Si2-O1-Si1	128.8(4)	Si2-O2-Si2'	130.6(5)
Si4-O3-Si3	129.0(4)	Si4-O4-Si4'	130.8(5)
Si4-O5-Si2	139.3(4)	Si3-O6-Si1	144.7(5)
Si6-O7-Si5	128.7(4)	Si6-O8-Si6'	129.3(5)
Si8-O9-Si7	129.0(4)	Si8-O10-Si8''	129.5(5)
Si8-O11-Si6	139.8(4)	Si7-O12-Si5	145.2(5)

Compound	$R_3Si_3O_6$		$R_4Si_4O_8$		Ref.
	d(Si-O) Å Range Mean	Si-O-Si ° Range Mean	d(Si-O) Å Range Mean	Si-O-Si ° Range Mean	
$Cy_6Si_6O_9$	1.625(6)-1.649(6) 1.640	128.7(4)-130.8(5) 129.5	1.611(8)-1.634(8) 1.625	139.3(4)-145.2(5) 142.3	This work
$[Et_4N^+]_6[Si_6O_{15}^{6-}]$	1.620(2)-1.670(2) 1.640	128(1)-132(2) 130.7	1.611(3)-1.662(3) 1.630	138.3(2)-146.1(1) 141.0	8
$[Ni(en)_3^{2+}]_3[Si_6O_{15}^{6-}]$	1.630(2)-1.661(2) 1.650	128(3)-136(3) 132.0	1.602(2)-1.680(2) 1.640	137.7	9
$R_8Si_8O_{12}^a$			1.604(4)-1.633(4) 1.610	145.0(2)-150.7(2) 148.1	3,4
$Ph_{12}Si_{12}O_{18}$			1.609(5)-1.618(5) 1.614	149.9(4)-158.1(5) 153.6	6
$Ph_6Si_3O_3$	1.632(6)-1.654(7) 1.640	132.2(2)-133.1(3) 131.8			13
$Ph_8Si_4O_4$			1.604(3)-1.623(4) 1.615	152.3(2)-167.4(2) 159.8	16

^a Average data for 7 structures

Table 5.3 Comparative geometric data for organosesquisiloxanes and related compounds

5.3 THE STRUCTURE OF HEXAPHENYL-1,3,5-TRISILOXANE-1,5-DIOL

Siloxane diols and triols have attracted much recent interest. These materials can be used as models for macromolecular Si-O species. For example organosilane triols RSi(OH)_3 have been used as synthetic precursors for metasiloxanes which mimic surface adsorbed metal-centred fragments, and so replicate the surface of silica¹⁸. In addition silanols are important intermediates in siloxane bond formation. The structural chemistry of these materials is focused on the beginning of the series, with the majority of reports devoted to the initial hydrolysis products, $\text{R}_2\text{Si(OH)}_2$. For a variety of substituents R [Et, ⁱPr, ^tBu, *c*-C₅Me₅, *c*-C₆H₁₁, (Me₃Si)₃C, allyl and Ph], the geometric parameters within the repeat unit are remarkably consistent, with Si-O bond distances and Si-O-Si angles in the ranges 1.637-1.659 Å and 106-110°, respectively⁴. The main structural differences arise through the wide variety of hydrogen-bonding networks that are adopted, with 3-D and layer structures evident for compounds with small substituents on silicon, whilst self-association into chain or discrete oligomers is favoured by diols with bulky substituents on silicon¹⁸. Recently, the structures of a smaller range of linear 1,3-siloxanes diols, $\text{R}_2(\text{HO})\text{SiOSi(OH)R}_2$, R = Me, ⁿPr, ⁱPr, Ph) have also been studied^{4,19}. The main structural differences lie in the patterns of solid-state hydrogen-bonding and hence intermolecular associations. Double-stranded chains dominate (R = Me, ⁱPr, ⁿPr, Ph) though a sheet structure is preferred by $\text{Me(3-C}_4\text{H}_3\text{S)(HO)SiOSi(OH)(3-C}_4\text{H}_3\text{S)Me}$. The structure of $\text{Me}_2(\text{HO})\text{SiOSi(OH)Me}_2$ consists of molecules hydrogen-bonded together to form chains which are further linked by hydrogen-bonds to form double chains.

The only structure reported previously for a trisiloxane-1,5-diol is that of $(\text{HO})^t\text{Bu}_2\text{SiOSiMe}_2\text{OSi}^t\text{Bu}_2(\text{OH})$, prepared by the reaction of $^t\text{Bu}_2\text{Si(OH)(OLi)}$ with Me_2SiCl_2 ²⁰. Crystals of compound 3, $\text{Ph}_2(\text{HO})\text{SiOSi(Ph}_2\text{)OSi(OH)Ph}_2$, were obtained in this study by fractional crystallisation of the combined extracts of $[\text{Ph}_2(\text{HO})\text{SiOSi(OH)Ph}_2]_n$, $n < 2$ as described in Chapter 4, and the structure was

determined. Final fractional atomic coordinates and isotropic thermal parameters are shown in Table 5.4. Selected bond lengths and angles are given in Table 5.5, and the molecular structure of compound 3 together with the atom numbering scheme is shown in Figure 5.3. The silanol contains a novel almost planar eight-membered HSi_3O_4 heterocyclic ring, with the two ends of the nominally acyclic array linked through a hydrogen bond, $\text{O}_4\text{-H}_4\cdots\text{O}_3$. This hydrogen bond is by no means symmetrical [$\text{Si}_3\text{-H}_4$: 1.03 Å; $\text{Si}_3\text{-O}_4$: 1.78 Å, though the intramolecular $\text{O}\cdots\text{O}$ separation (2.74 Å) is typical of analogous intermolecular hydrogen bonds^{19,20}. The angle at the hydrogen (155.9°) causes this atom to sit above the $\text{Si}_1\text{Si}_3\text{O}_3\text{O}_4$ plane (Figure 5.4a). For comparison, the $\text{O-H}\cdots\text{O}$ angle which forms part of a five-membered CSi_2O_2 ring in $(\text{Me}_3\text{Si})_2\text{C}(\text{SiMe}_2\text{OH})_2$ is 137.1°²¹. In the title compound the non-terminal Si-O bond lengths are uniform, the spread over the four values being less than the standard deviation in the measurement [mean: 1.617(6) Å]. The Si-O-Si angles are 155.7(4) and 163.1(5)°, and accommodate the ring strain, while the angles at silicon vary only marginally from their ideal tetrahedral value (109.1-110.4°) as indicated in Table 5.5. The analogous Si-O distances and Si-O-Si angles in the related, unsymmetrical compound $(\text{HO})^i\text{Bu}_2\text{SiOSiMe}_2\text{OSi}^i\text{Bu}_2(\text{OH})$, are similar to those of compound 3 (mean: 1.612 Å, 161.6°, respectively)²⁰. In both compounds short Si-O bonds are associated with rather wide Si-O-Si angles, a trend which has been noted previously^{14,22}. For comparison the more acute angle at oxygen (141.4°) in tetramethylsiloxane-1,3-diol is accompanied by longer Si-O bonds (1.627 Å)¹⁹. The terminal Si-O(H) bonds in the title compound [1.631(6) Å and 1.651(5) Å] are considerably longer than the internal Si-O bond lengths [1.614(6)-1.618(5) Å], and fall towards the top of the range noted in a series of $\text{R}_2\text{Si}(\text{OH})_2$ compounds [1.63-1.66 Å]. Similar Si(OH) bond lengths are evident in $(\text{HO})^i\text{Bu}_2\text{SiOSiMe}_2\text{OSi}^i\text{Bu}_2(\text{OH})$ [mean: 1.630 Å]²⁰.

The structure of the title compound differs from that of $(\text{HO})^i\text{Bu}_2\text{SiOMe}_2\text{OSi}^i\text{Bu}_2(\text{OH})$, even though the dimeric nature of both compounds is their most striking feature (Figures 5.5a and 5.5b respectively). In compound 3 the square

consisting of the four oxygen atoms O_3 , O_4 , O_3 and O_4 in which the intermolecular $O_4...O_3$ separation (2.72 Å) is similar to the intramolecular $O_4...O_3$ distance (2.74 Å) noted earlier^{19,20,23}. The compound $(HO)^tBu_2SiOSiMe_2OSi^iBu_2(OH)$ also contains an O_4 square which is less regular, but the distances involved are similar (2.57-2.82 Å). In this latter compound, however none of the available hydrogen atoms on the four terminal hydroxyl groups appears to hydrogen bond internally to generate the HSi_3O_4 ring of compound 3, and the deviation from planarity of the molecule is considerably greater (Figures 5.4a and 5.4b). Furthermore, the open-jaws orientation of pairs of H-bonded $(HO)^tBu_2SiOSiMe_2OSi^iBu_2(OH)$ molecules, Figure 5.4b and 5.5b, suggests that the intermolecular bonding is somewhat weaker than the $O...O$ separation suggests. Although the position of the hydrogen atom of the second hydroxyl group in compound 3 was not located, the short intermolecular $O...O$ separation suggests that dimer formation is real. The overall structure therefore can be described as dimeric, in which two eight-membered HSi_3O_4 rings are linked through an eight-membered H_4O_4 heterocycle (Figure 5.5a), as is common in silanol chemistry¹⁹. The structure can thus be described as being a two-step section of a "staircase", no further contacts having been detected between these dimer units to produce a more extended array (Figure 5.4a). The parallel stacking of relatively planar ring in compound 3 is in contrast to that in $(HO)^tBu_2SiOMe_2OSi^iBu_2(OH)$, where the two rings are twisted with respect to each other (Figure 5.4c).

The silane-1,4-diol, $(HO)(Ph_2Si)_4(OH)$, adopts a cyclic seven-membered Si_4O_2H ring structure, in which the termini of the silane are also linked through an O-H...O hydrogen bond [2.804(4) Å], and prefers to form a chair conformation rather than a planar ring as in the title compound²³. Furthermore, this molecule dimerises through a pair of hydrogen bonds with an $O...O$ separation of 2.74 Å, though as with compound 3, difficulty was experienced in locating the exact position of the intermolecularly-bonded hydrogen atom. However, from the relative disposition of the two halves of the silane dimer about its inversion centre, the unit holding the two molecules together is a four-membered O_2H_2 ring²³, as occurs in $(HO)^tBu_2SiOMe_2OSi^iBu_2(OH)$, and not an O_4H_4 heterocycle as found

in the title compound (Figures 5.5a and 5.5b).

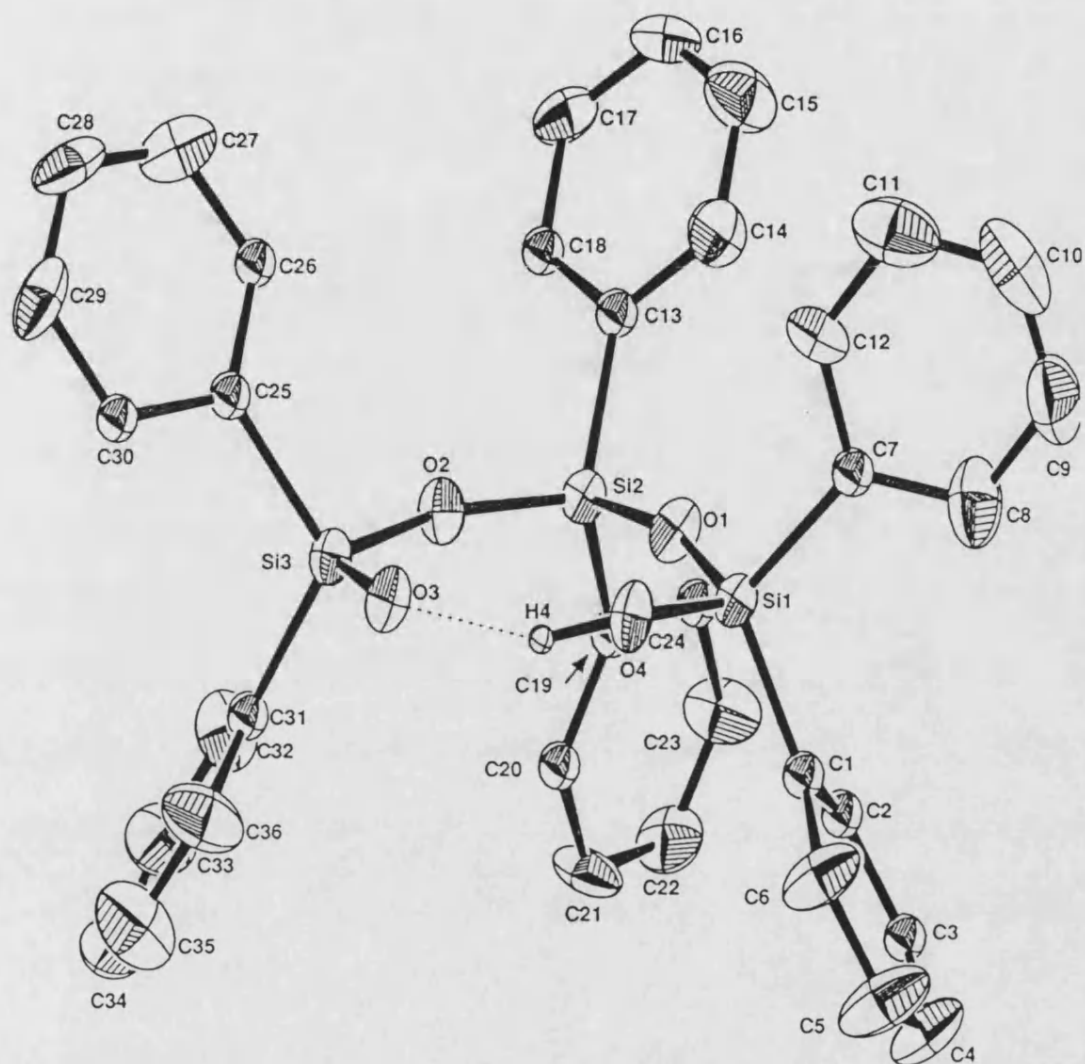


Figure 5.3 The asymmetric unit of compound 3,
 $\text{Ph}_2(\text{HO})\text{SiOSi}(\text{Ph}_2)\text{OSi}(\text{OH})\text{Ph}_2$

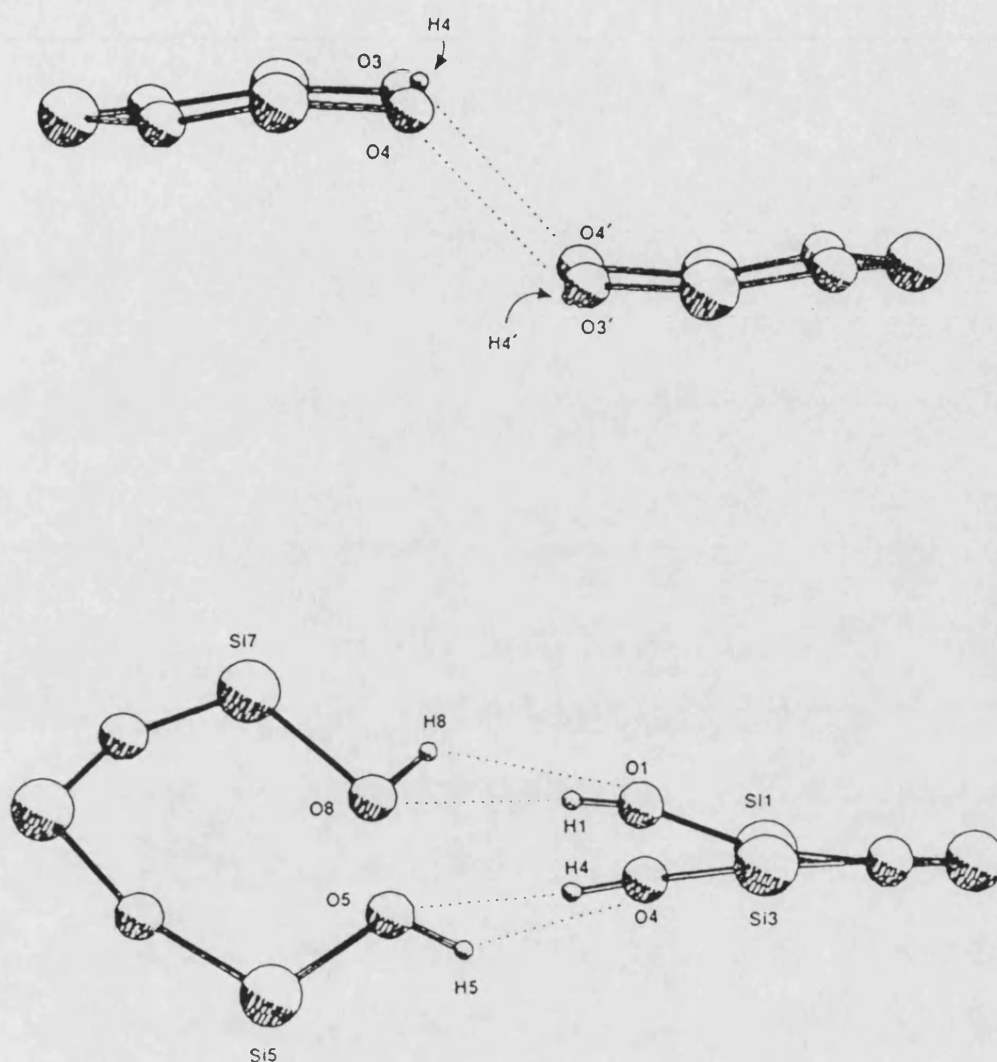


Figure 5.4

The dimer arrangements in $\text{Ph}_2(\text{HO})\text{SiOSi}(\text{Ph}_2)\text{OSi}(\text{OH})\text{Ph}_2$ and ${}^t\text{Bu}_2(\text{HO})\text{SiOSi}(\text{Me}_2)\text{OSi}(\text{OH}){}^t\text{Bu}_2$ (a and b respectively) viewed orthogonal to the approximate planes of the individual molecules. Organic substituents on silicon have been omitted for clarity

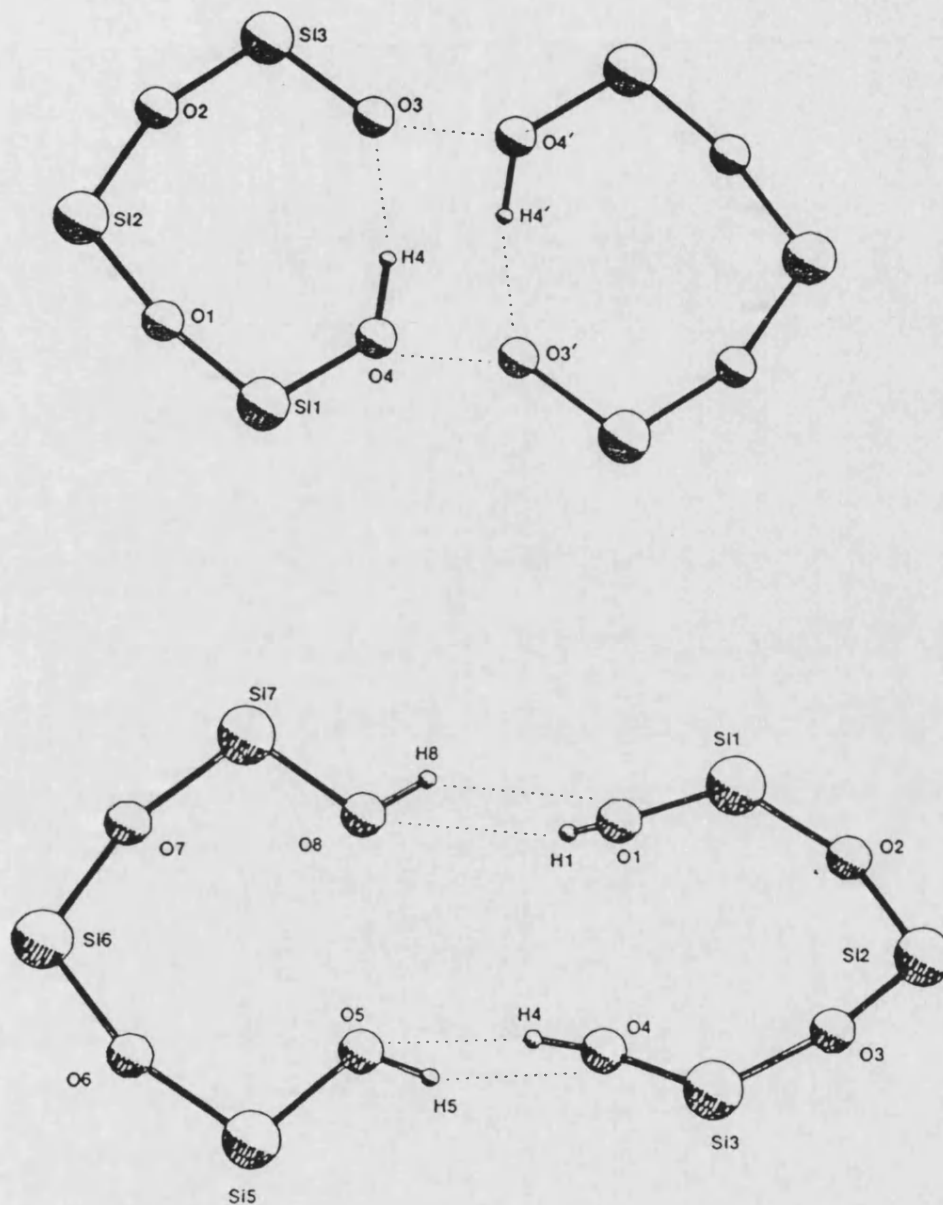


Figure 5.5

The dimer arrangements in $\text{Ph}_2(\text{HO})\text{SiOSi}(\text{Ph}_2)\text{OSi}(\text{OH})\text{Ph}_2$ and ${}^t\text{Bu}_2(\text{HO})\text{SiOSi}(\text{Me}_2)\text{OSi}(\text{OH}){}^t\text{Bu}_2$ (a and b respectively) viewed perpendicular to the approximate planes of the individual molecules. Organic substituents on silicon have been omitted for clarity

Table 5.4

Fractional atomic coordinates and thermal parameters (\AA) for
 $\text{Ph}_2(\text{HO})\text{SiOSi}(\text{Ph}_2)\text{OSi}(\text{OH})\text{Ph}_2$, compound 3

Atom	x	y	z	U_{eq}
Si1	0.5097(3)	0.3525(2)	0.2458(2)	0.044(1) *
Si2	0.5105(3)	0.1275(2)	0.2151(2)	0.041(1) *
Si3	0.3758(3)	0.2768(2)	-0.0020(2)	0.046(2) *
O1	0.5322(7)	0.2304(4)	0.2387(4)	0.059(4) *
O2	0.4479(7)	0.1780(4)	0.1022(4)	0.052(4) *
O3	0.3785(7)	0.4034(4)	-0.0095(4)	0.055(4) *
O4	0.4679(7)	0.4541(5)	0.1342(4)	0.059(4) *
C4	0.1846(14)	0.4034(11)	0.4908(9)	0.107(10) *
C5	0.2102(16)	0.4959(11)	0.4096(11)	0.124(12) *
C6	0.3010(13)	0.4822(9)	0.3332(8)	0.090(9) *
C8	0.7031(16)	0.3690(10)	0.3625(8)	0.104(10) *
C9	0.8326(20)	0.3725(13)	0.3842(12)	0.121(12) *
C10	0.9432(20)	0.3601(12)	0.3189(15)	0.124(15) *
C11	0.9244(16)	0.3490(12)	0.2336(13)	0.107(13) *
C12	0.7941(12)	0.3453(8)	0.2171(8)	0.072(8) *
C14	0.7981(12)	0.0250(9)	0.2652(8)	0.082(8) *
C15	0.9225(14)	-0.0599(11)	0.2767(10)	0.104(11) *
C16	0.9330(12)	-0.1473(9)	0.2489(8)	0.073(9) *
C17	0.8194(13)	-0.1526(9)	0.2095(8)	0.079(8) *
C21	0.1444(11)	0.0625(10)	0.3701(8)	0.070(8) *
C22	0.1936(15)	-0.0283(10)	0.4563(8)	0.083(9) *
C23	0.3307(14)	-0.0734(10)	0.4707(8)	0.077(9) *
C27	0.6803(15)	0.1533(11)	-0.1791(11)	0.103(11) *
C28	0.6301(14)	0.2149(12)	-0.2755(11)	0.103(11) *
C29	0.5059(15)	0.2950(11)	-0.2892(8)	0.098(10) *
C32	0.1511(14)	0.1764(10)	0.0310(8)	0.089(9) *
C33	0.0201(17)	0.1736(15)	0.0240(11)	0.123(13) *
C34	-0.0866(17)	0.2729(19)	-0.0194(13)	0.159(17) *
C35	-0.0420(19)	0.3686(14)	-0.0566(12)	0.137(15) *
C36	0.0892(14)	0.3735(11)	-0.0481(10)	0.107(11) *
C1	0.3737(10)	0.3722(7)	0.3387(6)	0.055(2)
C2	0.3381(10)	0.2821(8)	0.4192(7)	0.064(3)
C3	0.2474(12)	0.2969(9)	0.4948(8)	0.073(3)
C7	0.6800(10)	0.3580(7)	0.2792(6)	0.051(2)
C13	0.6811(9)	0.0215(6)	0.2261(6)	0.041(2)
C18	0.6952(12)	-0.0693(8)	0.1994(7)	0.069(3)
C19	0.3814(9)	0.0626(6)	0.3082(5)	0.041(2)
C20	0.2412(11)	0.1064(8)	0.2959(7)	0.069(3)
C24	0.4304(12)	-0.0301(8)	0.3981(7)	0.071(3)
C25	0.4830(10)	0.2494(7)	-0.1095(6)	0.048(2)
C26	0.6066(12)	0.1692(9)	-0.0979(8)	0.073(3)
C30	0.4262(11)	0.3150(8)	-0.2083(7)	0.063(3)
C31	0.1902(10)	0.2762(8)	-0.0058(6)	0.051(2)
H4	0.409(7)	0.449(6)	0.084(4)	0.05

Table 5.5

Selected bond lengths (Å) and bond angles (°) for
 $\text{Ph}_2(\text{HO})\text{SiOSi}(\text{Ph}_2)\text{OSi}(\text{OH})\text{Ph}_2$, compound 3

Bond	Bond Lengths	Bond	Bond Lengths
Si1-O1	1.618(6)	Si1-O4	1.631(6)
Si1-C1	1.827(9)	Si1-C7	1.847(9)
Si2-O1	1.614(6)	Si2-O2	1.618(6)
Si2-C13	1.839(9)	Si2-C19	1.863(8)
Si3-O2	1.617(6)	Si3-O3	1.651(5)
Si3-C25	1.875(9)	Si3-C31	1.854(10)
Bond	Bond Angles	Bond	Bond Angles
O4-Si-O1	109.1(3)	C1-Si1-O1	111.0(4)
C1-Si1-O4	110.5(4)	C7-Si1-O1	107.9(4)
C7-Si1-O4	106.9(4)	C7-Si1-C1	111.2(4)
O2-Si2-O1	109.3(3)	C13-Si2-O1	108.8(4)
C13-Si2-O2	110.6(3)	C19-Si2-O1	108.4(3)
C19-Si2-O2	108.9(4)	C19-Si2-C13	110.8(4)
O3-Si3-O2	110.4(3)	C25-Si3-O2	107.5(4)
C25-Si3-O3	108.3(3)	C31-Si3-O2	109.8(4)
C31-Si3-O3	108.5(4)	C31-Si3-C25	112.4(4)
Si2-O1-Si1	163.1(5)	Si3-O2-Si2	155.7(4)

5.4 THE STRUCTURE OF 1,1,1,3,5,5,5-HEPTAPHENYL-3-BORA-1,5-SILOXANE

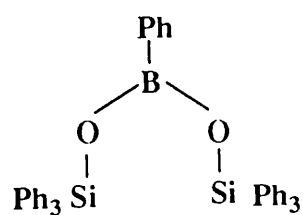
The chemistry of metallasiloxanes, containing one or more metal-oxygen-silicon linkages has been explored in order (i) to prepare siloxane polymers with modified properties resulting from the incorporation of different metal atoms in the siloxane chain, (ii) to compare the properties of metal siloxides with metal alkoxides, and (iii) to explore the catalytic activity of such materials. Although there is a considerable literature on cyclic borosiloxanes⁴, $\text{PhB(OSiPh}_3)_2$ and $\text{B(OSiPh}_3)_3$ are the only known linear compounds containing Si-O-B linkages. These were prepared via the reaction of Ph_3SiOH and PhB(OH)_2 in a 2:1 molar ratio, and of Ph_3SiOH and $\text{B(O}^i\text{Pr)}_3$ in a 3:1 ratio respectively²⁴. In this work a modified procedure has been used to prepare such compounds with the structural formula $\text{R}^*_{3-n}\text{B(OSiR}_n\text{H}_{3-n})$, ($\text{R}, \text{R}^* = \text{Ph}$ and $\text{R} = \text{Ph}, \text{R}^* = \text{Me}$; $n = 2$ or 3). To the best of our knowledge no structures have been reported for linear borosiloxanes until during the writing of this thesis when a publication in December 1993 appeared²⁵ which will be discussed later. Therefore, the structure of $\text{PhB(OSiPh}_3)_2$ was determined in the course of this study in order to provide a comparison with cyclic Si-O-B systems which exhibit ring strain¹⁴. Final fractional atomic coordinates and isotropic thermal parameters for compound 16 are given in Table 5.6, with selected bond lengths and angles shown in Table 5.7.

The molecular structure of the title compound together with the atom numbering scheme is given in Figure 5.6, The structure contains a central trigonal planar BO_2C unit bound through the oxygen atom to two tetrahedral $-\text{SiPh}_3$ groups. It contains a linear, coplanar Si-O-B-O-Si skeleton which maximizes π -overlaps, and in addition the phenyl ring attached to the boron atom approaches co-planarity with the Si_2BO_2 backbone, the dihedral angle $\text{C}_{24}\text{-C}_{19}\text{-B}_1\text{-O}_2$ and $\text{C}_{20}\text{-C}_{19}\text{-B}_1\text{-O}_1$ being 10.4° and 13.9° respectively. However, the B-C bond [$1.577(2) \text{ \AA}$] is slightly longer than the B-C separation in *cyclo*- $\text{PhB(OSiPh}_2)_2$ [$1.543(15) \text{ \AA}$]¹⁴, PhB(OH)_2 [$1.562(3) \text{ \AA}$]²⁶, or *cyclo*- $\text{Ph}_3\text{B}_3\text{O}_3$ [$1.540(3) \text{ \AA}$]²⁷. Key geometric data for compound 16 are compared in Table 5.8 with those

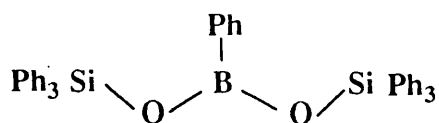
of related structures. Comparison can be made with *cyclo*-Et₃B₃O₃ [B-C: 1.565(1) Å]²⁸ in which stacking of B₃O₃ rings suggests inter-molecular B..O interactions rather than any significant π (B-C) overlap, and with the sum of the respective covalent radii [1.591(2) Å]. For the strained six-membered ring compound PhBO(Ph₂SiO)₂, the normal valence angles at tetrahedral silicon and trigonal boron [mean: 106.3(3)° and 120.2(9)°, respectively] are accommodated at the expense of distortions of the angles about oxygen [127.3(4) and 129.3(5)°]¹⁴. In the title compound, the valence angles at unstrained tetrahedral silicon and trigonal boron centres are as expected, similar to those in the cyclic compound [mean: 108.2° and 118.1°, respectively], Table 5.8 The most remarkable feature in compound 16 is the difference in the B-O-Si bond angles with the B₁-O₁-Si₁ angle being 153.1(3) and the B₁-O₂-Si₂ angle only 136.9(3). These differences can be related to a combination of two effects within the linear molecule. Firstly, unlike the cyclic borosiloxanes, there is no ring strain to distort the angles about oxygen, and secondly the bulky substituents on silicon will prevent a coplanar arrangement in which the Si-O-B angles are equal and acute, and related by a plane of symmetry as shown in (A) below. Hence a structure based on (B) or (C) is expected from steric considerations. Despite the differences in B-O-Si angles the pair Si-O and B-O bond distances are not significantly different, [Si₁-O₁, 1.637(3); Si₂-O₂, 1.647(3) Å] and [B₁-O₁, 1.360(5); B₁-O₂, 1.361(5) Å], indicating little difference in Si-O or B-O bond energies.

While writing this thesis a paper appeared²⁵ in which the structure of the linear borasiloxane compound 16 is described. The data are in complete agreement with those determined at Bath. In addition a calculation was carried out by Spalding and his coworkers²⁵ on H₂B-O-SiX₃ (X = H, OH) investigating the effects of substituents on B-O and Si-O bond lengths and on the B-O-Si angle. Replacement of H by OH on both boron and silicon atoms had little or no effect on the calculated minimum-energy B-O-Si angle. Comparison of the bond distances from the calculations suggests that while B-O_{Si} distances increase slightly with substitution of H by OH, Si-O_B distances decrease. From these calculations it was also noteworthy these species had approximately the same large

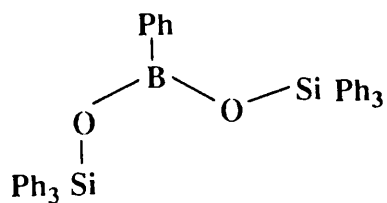
range of B-O-Si angle variation (ca 30°) within 5 kJ mol⁻¹ of the minimum energies of the molecules. Thus in unstrained bora-siloxanes fairly large variations in Si-O-B angles can be accommodated without significant changes in Si-O or B-O bond energies, as is evident in the structure of compound 16.



A



B



C

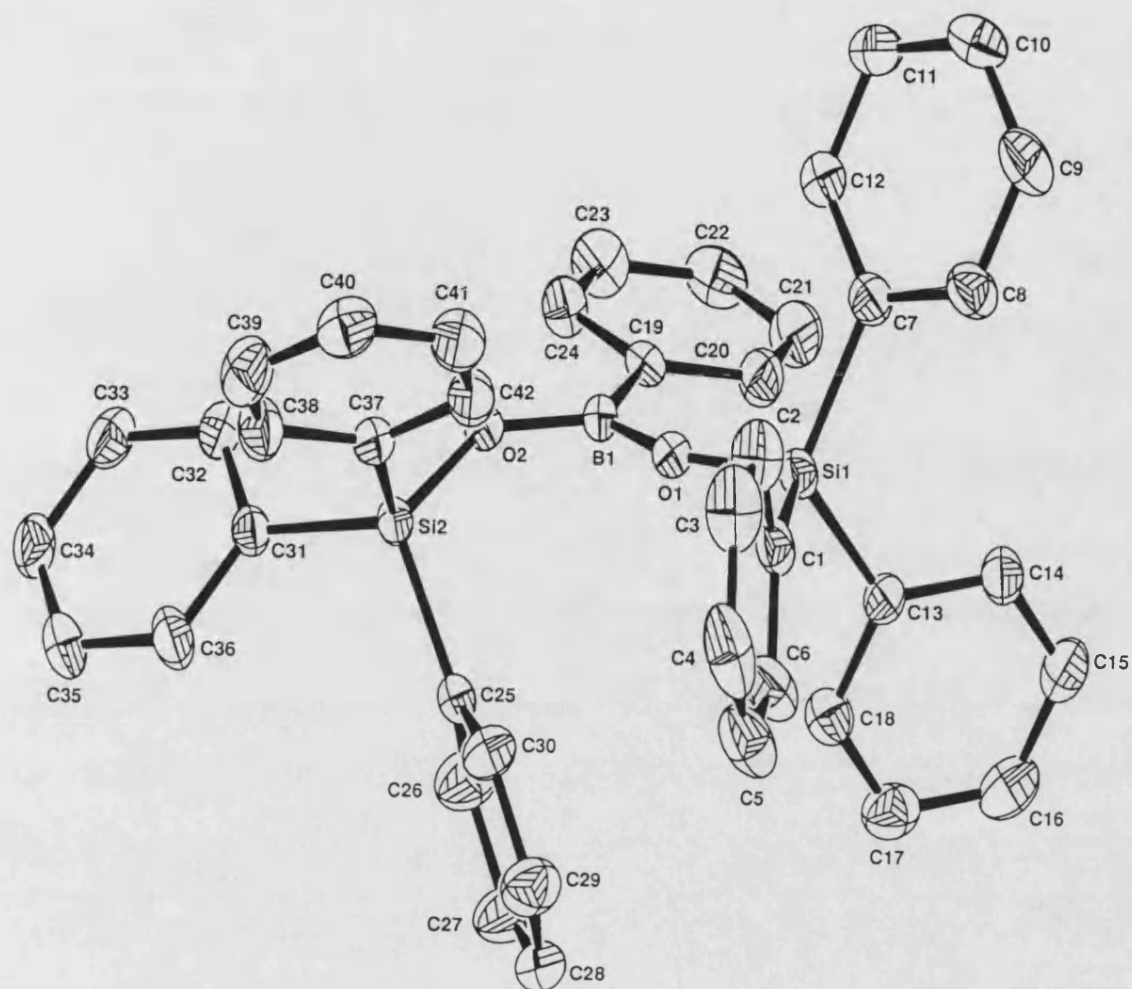


Figure 5.6 The asymmetric unit of $\text{PhB}(\text{Ph}_3\text{SiO})_2$, compound 16

Table 5.6

Fractional atomic coordinates and thermal parameters (Å) for
PhB(Ph₃SiO)₂, compound 16

Atom	x	y	z	U _{eq}
Si1	0.67897(6)	0.03017(11)	0.58477(5)	0.0461(6) ***
Si2	0.84668(5)	0.11470(11)	0.78621(5)	0.0421(6) ***
B1	0.8010(2)	0.1965(4)	0.6505(2)	0.041(2) ***
C2	0.6821(2)	-0.2534(3)	0.6220(2)	0.0779(3) ***
C3	0.6635(2)	-0.3684(3)	0.6578(2)	0.092(4) ***
C4	0.6123(2)	-0.3561(3)	0.7012(2)	0.101(5) ***
C5	0.5797(2)	-0.2288(3)	0.7090(2)	0.098(4) ***
C6	0.5983(2)	-0.1138(3)	0.6733(2)	0.080(3) ***
C1	0.6495(2)	-0.1261(3)	0.6298(2)	0.055(2) ***
C8	0.6603(1)	-0.1117(3)	0.4590(1)	0.065(3) ***
C9	0.6812(1)	-0.1637(3)	0.3996(1)	0.078(3) ***
C10	0.7500(1)	-0.1338(3)	0.3848(1)	0.076(3) ***
C11	0.7979(1)	-0.0519(3)	0.4293(1)	0.072(3) ***
C12	0.7770(1)	0.0001(3)	0.4887(1)	0.058(2) ***
C7	0.7082(1)	-0.0298(3)	0.5053(1)	0.053(2) ***
C14	0.5613(1)	0.1779(3)	0.5061(1)	0.059(3) ***
C15	0.5052(1)	0.2748(3)	0.4967(1)	0.070(3) ***
C16	0.4908(1)	0.3531(3)	0.5520(1)	0.079(3) ***
C17	0.5305(1)	0.3346(3)	0.6165(1)	0.079(3) ***
C18	0.5886(1)	0.2377(3)	0.2659(1)	0.070(3) ***
C13	0.6030(1)	0.1594(3)	0.5706(1)	0.049(2) ***
C20	0.7579(1)	0.3614(3)	0.5486(1)	0.063(3) ***
C21	0.7677(1)	0.4778(3)	0.5097(1)	0.078(3) ***
C22	0.8311(1)	0.5558(3)	0.5253(1)	0.078(3) ***
C23	0.8847(1)	0.5176(3)	0.5798(1)	0.076(3) ***
C24	0.8749(1)	0.4012(3)	0.6187(1)	0.059(3) ***
C19	0.8115(1)	0.3231(3)	0.6031(1)	0.046(2) ***
C26	0.7287(2)	0.2707(2)	0.8164(2)	0.084(3) ***
C27	0.6604(2)	0.2916(2)	0.8344(2)	0.101(4) ***
C28	0.6166(2)	0.1787(2)	0.8436(2)	0.081(3) ***
C29	0.6412(2)	0.0449(2)	0.8347(2)	0.085(4) ***
C30	0.7095(2)	0.0240(2)	0.8167(2)	0.067(3) ***
C25	0.7533(2)	0.1370(2)	0.8076(2)	0.046(2) ***
C32	0.9707(1)	0.2866(3)	0.8281(1)	0.053(2) ***
C33	1.0208(1)	0.0356(3)	0.8763(1)	0.063(3) ***
C34	1.0360(1)	0.3537(3)	0.9452(1)	0.070(3) ***
C35	0.9564(1)	0.2815(3)	0.9659(1)	0.080(3) ***
C36	0.9062(1)	0.2119(3)	0.9177(1)	0.068(3) ***
C31	0.9134(1)	0.2144(3)	0.8488(1)	0.044(2) ***
C38	0.9125(1)	-0.1287(3)	0.8409(1)	0.065(3) ***
C39	0.9378(1)	-0.2692(3)	0.8414(1)	0.076(3) ***
C40	0.9047(1)	-0.3541(3)	0.7884(1)	0.073(3) ***
C41	0.8552(1)	-0.2983(3)	0.7349(1)	0.073(3) ***
C42	0.8388(1)	-0.1578(3)	0.7344(1)	0.062(3) ***
C37	0.8388(1)	-0.1578(3)	0.7344(1)	0.048(2) ***
O1	0.7481(1)	0.0996(3)	0.63499(1)	0.053(1)
O2	0.8482(1)	0.1824(3)	0.7103(1)	0.049(1)

Table 5.7

Selected bond lengths (Å) and bond angles (°) for PhB(Ph₃SiO)₂, compound 16

Bond	Bond Lengths	Bond	Bond Lengths
Si1-O1	1.637(3)	Si1-C1	1.885(3)
Si1-C7	1.877(3)	Si1-C13	1.877(3)
Si2-O2	1.647(3)	Si2-C25	1.874(3)
Si2-C31	1.874(2)	Si2-C37	1.876(3)
O1-B1	1.360(5)	O2-B1	1.361(5)
B1-C19	1.577(5)	C2-C3	1.395(1)
C2-C1	1.395(1)		
Bond	Bond Angles	Bond	Bond Angles
C1-Si1-O1	107.8(1)	C7-Si1-O1	109.6(1)
C7-Si1-C1	107.9(1)	C13-Si1-O1	108.5(1)
C13-Si1-C1	109.5(1)	C13-Si1-C7	113.5(1)
C25-Si2-O2	108.6(1)	C31-Si2-O2	110.7(1)
C31-Si2-C25	109.4(1)	C37-Si2-C31	110.7(1)
C37-Si2-C25	110.5(1)	B1-O2-Si2	136.9(3)
B1-O1-Si1	153.1(3)	C19-B1-O1	123.9(3)
O2-B1-O1	118.0(3)	C1-C2-C3	120.0(1)
C19-B1-O2	118.1(3)	C24-C19-B1	118.3(2)
C2-C1-Si1	119.4(1)	C36-C31-Si2	118.6(1)
C14-C13-Si1	121.0(1)	C42-C37-Si2	118.8(1)
C20-C19-B1	121.6(2)	C32-C31-Si2	121.4(1)

Compound	Bond distances				Bond angles			Ref.
	B-O (Å)	Si-O(B) (Å)	Si-O(Si) (Å)	O-B-O (°)	O-Si-O (°)	B-O-Si (°)	Si-O-Si (°)	
Ph ₇ Si ₂ BO ₂ (3)	1.361(5) 1.360(5)	1.637(3) 1.647(3)		118.0(3)		153.1(2) 136.9(3)		This work
Ph ₆ Si ₂ BO ₂ (10)	1.374(7) 1.370(2)	1.639(1) 1.655(1)	1.644(2) 1.636(9)	120.2(9) 120.8(2)	106.3(3) 106.5(8)	129.3(5) 128.9(1)	127.3(4) 127.1(1)	14
Ph ₆ Si ₃ O ₃			1.640(1)		107.7(8)		131.8(8)	13
Ph ₃ B ₃ O ₃	1386(2)			121.7(2)		118.0(4) ^a		26
^a <B-O-B								

Table 5.8 Comparative geometric data for PhB(Ph₃SiO)₂ (compound 16) and related compounds

5.5 THE STRUCTURE OF 2,2-DIMETHYL-4,6-DIPHENYL -1,3,5-TRIAZA-2-SILA-4,6-DIBORACYCLOHEXANE

A model cyclic compound containing Si-N-B linkages has been synthesised during the course of this work, using a procedure described previously²⁹ for possible use as a preceramic polymer precursor in the formation of Si_3N_4 ceramic materials. The structure of $\text{Me}_2\text{Si}(\text{PhBNH})_2\text{NH}$, compound 19, has been determined by x-ray crystallography, and structural data compared with those of the only two known analogues, $\text{Ph}_2\text{Si}(\text{Me}_2\text{BN})_2\text{NMe}$ and $\text{MeB}(\text{Ph}_2\text{SiMeN})_2\text{NMe}$, which contain 2:1 and 1:2 boron to silicon ratios respectively²⁹. Final fractional atomic coordinates and isotropic thermal parameters for compound 19 are given in Table 5.9, and selected bond lengths and angles are shown in Table 5.10. Figure 5.7 shows the molecular structure of compound 19 together with the atom numbering scheme.

The central six-membered SiB_2N_3 heterocyclic ring in compound 19 is almost planar, the maximum deviations from the least squares planes through all the ring atoms being 0.0087° (Si_1), -0.0637° (N_1), 0.022° (B_1), 0.0504° (N_2), -0.0370° (N_3) and -0.218° (B_2). These data are similar to those described in the literature for the other two structures²⁹ which also contain essentially planar heterocyclic ring systems.

The valence angles of the title compound at tetrahedral silicon [$102.2(1)^\circ$] and trigonal boron [$119.1(3)^\circ$ and $117.3(3)^\circ$] are less by $\sim 4^\circ$ and $\sim 2^\circ$ respectively than those in $[\text{PhB}(\text{Ph}_2\text{SiO})_2\text{O}]$. The final sum of the internal angles of the heterocycle Si-N-B in compound 19 is close to ideal [$\Sigma = 719.4^\circ$], as it is all planar six-membered ring compounds spanning the spectrum of Si, B and N combinations i.e. $(\text{Me}_3\text{C})_6\text{Si}_3\text{N}_3\text{H}_3$ [$\Sigma = 718.5^\circ$]³⁰, $\text{Ph}_2\text{SiB}_2\text{N}_3\text{Me}_5$ [$\Sigma = 719.5^\circ$]²⁹ and $\text{Ph}_4\text{Si}_2\text{BN}_3\text{Me}_4$ [$\Sigma = 718.9^\circ$]²⁹. In the title compound the internal angles of an idealized hexagon [120°] are not much changed from ideal by the slightly smaller tetrahedral and trigonal angles at silicon and boron respectively, as the angles at nitrogen increase slightly [$127.0(2)^\circ$, $125.6(2)$, $128.2(2)^\circ$] as found in related six-membered ring systems, Table 5.11.

The bulky substituents attached to nitrogen have a considerable effect on the planarity of the ring in cyclic silazanes and cause significant deviations from planarity. For example, $(\text{Me}_2\text{SiNR})_3$, ($\text{R} = \text{SiMe}_3$) has a boat conformation³¹, but $(\text{CMe}_3\text{FSiNR})_3$, ($\text{R} = \text{H}$ or Me) has a planar conformation^{32,33}. By contrast bulky silicon substituents do not greatly affect the planar conformation. Geometric data for compound 19 are compared with those of related structures in Table 5.11. these reveal that the mean B-N bond length in the unit B-N(B) of the title compound [1.425 Å] is shorter than that in the B-N(B) unit in $\text{Ph}_2\text{SiB}_2\text{N}_3\text{Me}_5$ [1.441 Å], this could be attributed to the nature of the substituents on nitrogen. The mean Si-N bond length in the unit Si-N(Si) of $\text{Ph}_4\text{Si}_2\text{BN}_3\text{Me}_4$ [1.719 Å]²⁹ is noticeably shorter than the mean Si-N(B) unit in the same compound [1.732 Å], or in the title compound [1.728 Å]. This could be due to the lone pair electrons of nitrogen (N:) being more involved in the $p(\pi)$ - $p(\pi)$ bonding to the adjacent boron atom in the Si-N(B) unit than in π -bonding in the Si-N(Si) units. Short bond Si-N(Si) bond lengths are combined with a wide Si-N-Si bond angles, Table 5.11, as occurs in siloxane chemistry. However, for few crystal structures are available for borasilazanes, and hence no firm conclusions concerning ring strain can be drawn with certainty at this stage.

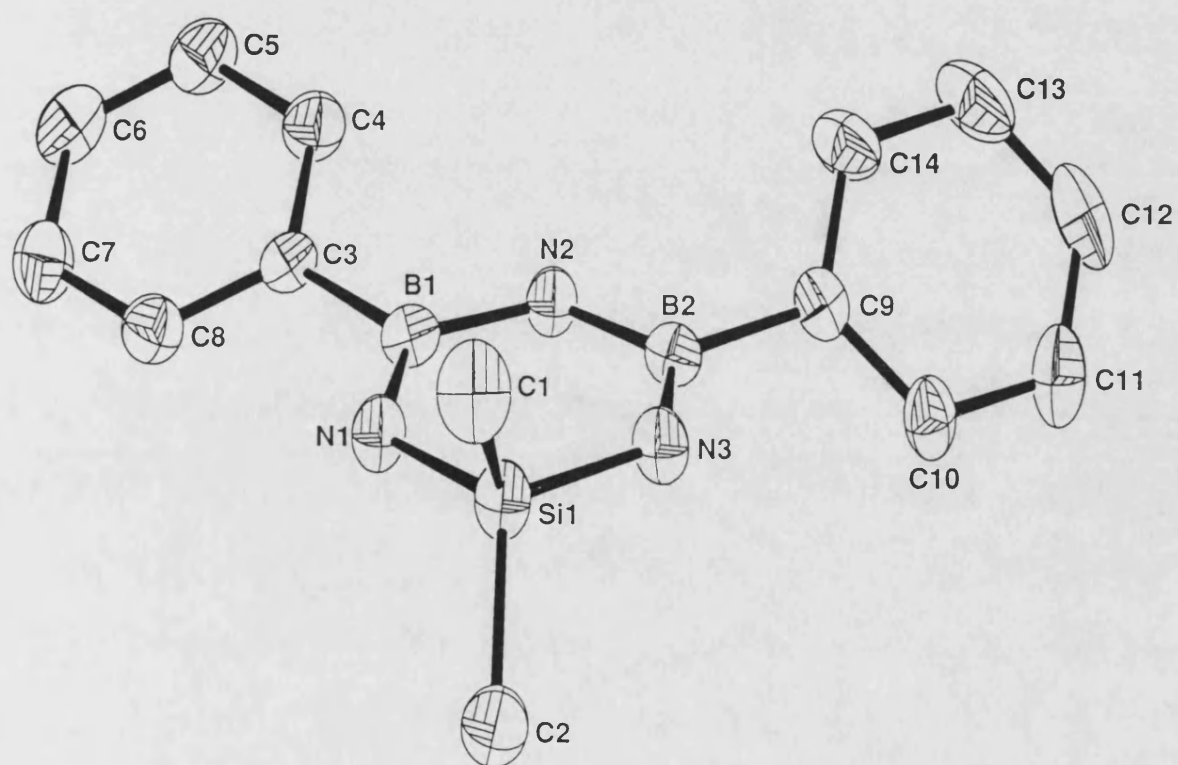


Figure 5.7

The asymmetric unit of $\text{Me}_2\text{Si}(\text{PhBNH})_2\text{NH}$, compound 19

Table 5.9 Fractional atomic coordinates and thermal parameters (Å) for
 $\text{Me}_2\text{Si}(\text{PhBNH})_2\text{NH}$, compound 19

Atom	x	y	z	U_{eq}
Si1	0.13113(9)	0.68818(6)	0.48043(10)	0.0684(7)
N1	0.2965(2)	0.7203(2)	0.5210(3)	0.67(2)
N2	0.2441(2)	0.8723(2)	0.4099(2)	0.062(2)
N3	0.0431(3)	0.7885(2)	0.4007(3)	0.068(2)
B1	0.3432(4)	0.8027(2)	0.4809(3)	0.057(2)
B2	0.1011(4)	0.8695(2)	0.3717(3)	0.057(2)
C1	0.0866(4)	0.5816(3)	0.3778(4)	0.101(3)
C2	0.0964(4)	0.6634(3)	0.6182(4)	0.102(3)
C3	0.4967(3)	0.8178(2)	0.5095(3)	0.056(3)
C4	0.5347(3)	0.8798(2)	0.4382(3)	0.072(2)
C5	0.6707(4)	0.8922(2)	0.4614(4)	0.081(2)
C6	0.7699(4)	0.8438(3)	0.5577(4)	0.079(2)
C7	0.7358(3)	0.7817(3)	0.6317(3)	0.076(2)
C8	0.6011(3)	0.7697(2)	0.6067(3)	0.068(2)
C9	0.0098(3)	0.9547(2)	0.2933(3)	0.055(2)
C10	-0.0914(3)	0.9929(2)	0.3215(3)	0.071(2)
C11	-0.1688(3)	1.0706(3)	0.2566(4)	0.091(3)
C12	-0.1461(5)	1.01095(3)	0.1595(4)	0.089(3)
C13	-0.0456(5)	1.0735(3)	0.1291(3)	0.095(3)
C14	0.0314(4)	0.9979(2)	0.1966(3)	0.079(2)
H1	0.3683(31)	0.6780(25)	0.5755(33)	0.119(3)
H2	0.2774(37)	0.9300(19)	0.3887(34)	0.119(3)
H3	-0.0554(19)	0.7881(29)	0.3670(36)	0.119(3)

Table 5.10 Selected bond lengths (Å) and bond angles (°) for
 $\text{Me}_2\text{Si}(\text{PhBNH})_2\text{NH}$, compound 19

Bond	Bond Lengths	Bond	Bond Lengths
Si1-N1	1.720(3)	Si1-N3	1.741(3)
Si1-C1	1.855(4)	Si1-C2	1.844(4)
N1-B1	1.425(4)	N1-H1	0.976(18)
N2-B1	1.435(4)	N2-B2	1.430(4)
N2-H2	0.965(18)	N3-B2	1.412(4)
N3-H3	0.977(18)	B1-C3	1.576(5)
B2-C9	1.582(5)	C3-C4	1.389(4)
C3-C8	1.399(4)	C12-C13	1.385(6)
Bond	Bond Angles	Bond Angles	Bond Angles
N3-Si1-N1	102.2(1)	C1-Si1-N1	110.4(2)
C1-Si1-N3	111.8(2)	C2-Si1-N1	112.8(2)
C2-Si1-N3	110.7(2)	C2-Si1-C1	108.8(2)
B1-N1-Si1	127.0(2)	H1-N1-Si1	119(2)
H1-N1-B1	114(2)	B2-N2-B1	128.2(2)
H2-N2-B1	117(2)	H2-N2-B2	115(2)
B2-N3-Si1	125.6(2)	H3-N3-Si1	118(2)
H3-N3-B2	116(2)	N2-B1-N1	117.3(3)
C3-B1-N1	122.3(2)	C3-B1-N2	120.3(2)
N3-B2-N2	119.1(3)	C9-B2-N2	119.8(3)
C9-B2-N3	121.0(3)	C4-C3-B1	121.1(3)
C8-C3-B1	122.4(3)	C10-C9-B2	121.5(3)

Compound	d B-N(B) (Å) Range Mean	d Si-N(B) (Å) Range Mean	Si-N-B (°) Range Mean	B-N-B (°) Range Mean	N-Si-N (°) Range Mean	N-B-N (°) Range Mean	Ref.
R ₂ Si(R ¹ BNR ²) ₂ NR ² (a)	1.412(4)-1.435(4) 1.425	1.720(3)-1.741(3) 1.728	125.6(2)-127.0(2) 126.3	128.2(2)	102.2(1)	117.3(3)-119.1(3) 118.2	This work
R ₂ Si(R ¹ BNR ²) ₂ NR ² (b)	1.431(5)-1.451(5) 1.441	1.727(3)-1.729(3) 1.728	124.7(2)-124.5(2) 124.6	126.6(3)	104.4(1)	120.1(3)-119.3(3)	29
RB(R ¹ SiNR ²)NR ² (b)		1.731(3)-1.733(3) 1.732 1.718(3)-1.737(5) ^e 1.726 ^e	128.7(3)-128.8(3) 128.7 126.7(2) ^f		107.0(1)-107.2(1) 107.1(1)	121.1(3)	29
(RR ¹ SiNR ²) ₃ (c)		1.705(9)-1.696(9) ^e 1.700 ^e	129.8(5) ^f		110.1		33
(R ₂ SiNR ¹) ₃ (d)		1.737(4)-1.750(4) ^e 1.744 ^e	115.8(3)-122.1(3) ^f 119.6 ^f		108.4(17)-109.0(17) 108.3		31

(a) R=Me, R¹=Ph, R²=H (b) R=Ph, R¹=R²=Me (c) R=Ph, R¹=F, R²=Me
 (d) R=Me, R¹=SiMe₃ ^e d Si-N(Si) ^f Si-N-Si angle

Table 5.11 Comparative geometric data for Me₂Si(PhBNH)₂NH (compound 19) and related compounds

5.6 REFERENCES

1. D W Scott, J Am Chem Soc, 1946, **68**, 356.
2. J F Brown, L H Vogt and P I Prescott, J Am Chem Soc, 1964, **86**, 1120.
3. F J Feher and T A Budzichowski, J Organomet Chem, 1989, **373**, 153.
4. E Lukevics, O Pudova and R Sturkovich, Molecular Structure of Organosilicon Compounds, Ellis Horwood, Chichester, UK, 1989, Chap.3,196 (and references therein).
5. N A Baidina, Zh Strukt Khim, 1980, **21**, 125.
6. W Glegg, G M Sheldrick and N Vater, Acta Crystallog Sect, 1980, **B36**, 3162.
7. P A Agaskar, V W Day and W G Klemperer, J Am Chem Soc, 1987, **109**, 5554.
8. Yu I Smolin, Sov Phys Crystallogr, 1984, **29**, 421.
9. Yu I Smolin, Sov Phys Crystallogr, 1970, **15**, 23.
10. D Hoebbel, G Engelhardt, A Samoson and K Uiszaszy, Z Anorg Allg Chem, 1987, **552**, 236.
11. F J Feher, D A Newman and J F Walzer, J Am Chem Soc, 1989, **111**, 1471.
12. F J Feher, T A Budzichowski, R L Blanski and K J Weller, Organometallics, 1991, **10**, 2526 and references therein.
13. P E Tomlins, J E Lydon, D Akrigg and G Sheldrick, Acta Crystallogr, 1985, **C41**, 292.
14. B J Brisdon, M F Mahon, K C Molloy and P J Schofield, J Organomet Chem, 1992, **436**, 11.
15. H Behbehani, B J Brisdon, M F Mahon and M Mazhar, J Organomet Chem, 1993, **463**, 41.
16. M A Hossain, M B Hursthouse and K M A Malik, Acta Crystallogr, 1979, **B 35**, 522.
17. D Braga and G Zanotti, Acta Crystallogr, 1980, **B36**, 950.

18. S S Al-Juaid, C Eaborn, P D Lickiss and P Jutizi, *J Organomet Chem*, 1990, **384**, 33; F J Feher, T A Budzichowski and J W Ziller, *Inorg Chem*, 1992, 31, 5100 (and references therein).
19. P D Lickiss, A D Redhouse, R J Thompson and K Rozga, *J Organometal Chem*, 1993, **453**, 13.
20. O Graalmann, U Klingebiel, W Clegg, M Haase and G M Sheldrick, *Chem Ber*, 1984, **117**, 2988.
21. N H Buttrus, C Eaborn, P B Hitchcock and A K Saxena, *J Organomet Chem*, 1986, **309**, 25.
22. H Behbehani, B J Brisdon, M F Mahon and K C Molloy, *J Organomet Chem*, in press.
23. Yu E Ovchinnikov, V E Shklover, Y T Struchkov, V V Dementev, T M Frunze and B A Antipova, *J Organomet Chem*, 1987, **335**, 157.
24. P N Bhardwaj and G Srivastava, *J Indian Chem Soc*, 1982, 300.
25. D Murphy, J P Sheehan, T R Spalding, G Ferguson, A Jhough and J F Gallagher, *J Mater Chem*, 1993, **3**, 1275.
26. S J Rettig and J Trotter, *Can J Chem*, 1977, **55**, 3071.
27. C P Brock, R P Minton and K Niedenzu, *Acta Crystallogr*, 1987, **C43**, 1775.
28. R Boese, M Polk and D Blaser, *Angew Chem Int Ed Eng*, 1987, **26**, 245.
29. E Hanecker and H Noth, *Z Naturforsch*, 1985, **40b**, 717.
30. W Clegg, G M Sheldrick and D Stalke, *Acta Crystallogr*, 1984, **C40**, 433.
31. G W Adamson and J J Daly, *J Chem Soc*, 1970, 2724.
32. W Clegg, *Acta Crystallogr*, 1983, **C39**, 387.
33. W Clegg, M Noltemeyer, G M Sheldrick and N Vater, *Acta Crystallogr*, 1980, **B** **36**, 2461.

CHAPTER SIX

THERMOLYSIS OF HETEROCYCLICSILOXANE AND RELATED MATERIALS

6.1 SUMMARY

The thermal decomposition of the model compounds whose synthesis was described in chapter 4, can be divided into three stages. The first stage involves low temperature isothermal heat treatment (up to 220°C) which shows the ring-opening polymerisation behaviour of compounds 6, 9, 10 and 14. Intermediate heat treatment (up to 1200°C) was studied by thermogravimetric analysis. The products at this stage were analysed by microelemental techniques, x-ray diffraction and scanning electron microscopy. Finally, the high temperature heat treatment (up to 1700°C) under an inert atmosphere produced solid residues which were analysed by several techniques, including x-ray diffraction, scanning electron microscopy with energy dispersive analysis and electron probe analysis.

6.2 EXPERIMENTAL

6.2.1 Low Temperature Heat Treatment

Low temperature pyrolyses of heterocyclic siloxanes containing eight- and six-membered rings with 1:1 and 2:1 silicon to boron ratio, compounds 9 and 10 respectively, were performed by placing weighed portions (300-500 mg) into an aluminium oxide boat (50 x 20 x 20 mm), which was placed in an oven at 220°C for up to 2 weeks, in contact with air at atmospheric pressure. The same procedure was carried out for compounds 6 and 14 which were heated to 300°C and 220°C respectively, for up to 3 days. The weight losses during those periods were recorded, and the residues were analysed by infrared and NMR spectroscopies. Volatilisation of compound 9 was followed by heating a sample of 100 mg to 220°C under a nitrogen gas flow for 4 hours, using a reactor fitted with a cold finger to condense volatiles. The volatiles and the final residues

were analysed by infrared, NMR spectroscopies and by mass spectrometry.

6.2.2 Intermediate Heat Treatment

Thermal gravimetric analyses were performed for a series of compounds on 40-100 mg samples using a Setaram TGA-92 (Appendix II). Samples were placed in an alumina crucible. Pyrolysis was carried out in the range of 25-1400°C under different atmospheres, He, N₂, or air, with a flow rate of 1 l/h, and a heating rate of 2, 5 and 10°C/min. A schematic diagram of the main components of the Setaram TGA-92 is in Figure 6.1. The final residues of the pyrolysed materials were subjected to C, H and N microelemental analysis, x-ray diffraction and scanning electron microscopy with energy dispersive analysis (Appendix II). Typical experimental conditions of the pyrolysis process are shown in Table 6.1.

6.2.3 High Temperature Heat Treatment

The high temperature pyrolyses were carried out in two steps, firstly by placing weighed amounts (200-400 mg) of the compounds 6, 9, 10 and 20 in an alumina crucible, which was placed into a tube furnace (Appendix II). Samples were pyrolyzed to 800°C in a flowing argon or air atmosphere at a maximum heating rate of 2°C/min. The residual materials were further pyrolyzed by heating in a flowing argon atmosphere at an average heating rate of 5°C/min to 1700°C which temperature was then maintained for 1 hour, using an graphite resistance furnace Astro Industrial Inc (Appendix II). The final residual solids were examined by x-ray diffraction and scanning electron microscopy with dispersive x-ray analysis for qualitative measurements and an electron probe analyser for quantitative measurements (Appendix II).

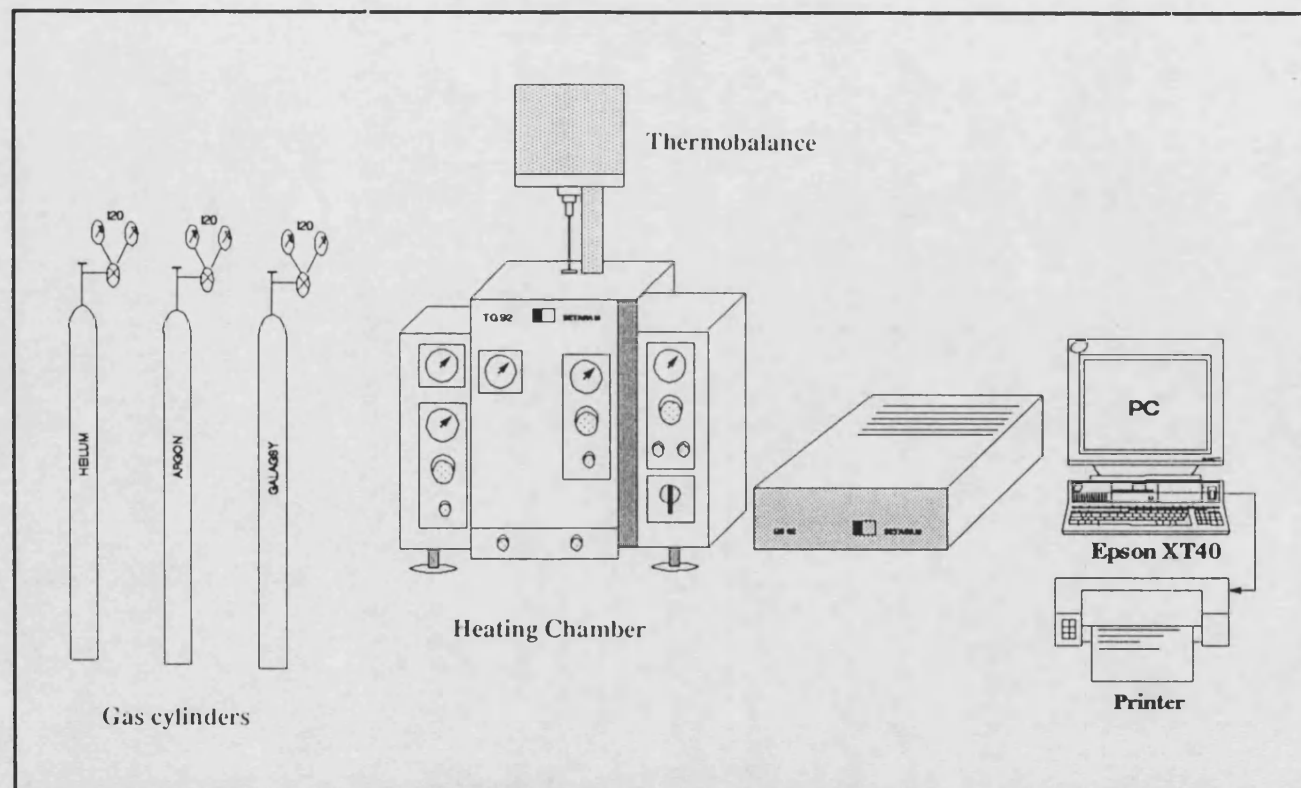


Figure 6.1

Schematic diagram of the main components of the Setaram
TGA-92

Table 6.1 Experimental conditions for the pyrolysis process using thermogravimetric analysis

Compound	Atmosphere	Test Conditions	Sample Wt.(mg)	Residue Wt%
4	He	pyrolysed to 600°C at 10°C/min	40.24	22.7
6	He	pyrolysed to 650°C at 10°C/min	43.45	36.2
7	He	pyrolysed to 650°C at 10°C/min	40.89	45.2
8	He	pyrolysed to 1200°C at 10°C/min	47.50	48.7
9	He	pyrolysed to 800°C at 10°C/min	77.17	41.0
9	He	pyrolysed to 1000°C at 10°C/min	69.19	37.4
9	He	pyrolysed to 1200°C at 10°C/min	79.33	36.1
9	He/Air	pyrolysed to 650°C under He, then isotherm for 2 h under air to 1200°C	53.83	38.2
9	N ₂	pyrolysed to 500°C at 10°C/min	57.43	65.0
9	N ₂	pyrolysed to 800°C at 10°C/min	50.26	39.2
9	N ₂	pyrolysed to 1200°C at 10°C/min	52.98	35.1
9	N ₂	pyrolysed to 1500°C at 10°C/min	57.81	30.3
9	Air	pyrolysed to 500°C at 10°C/min	50.82	68.4
9	Air	Pyrolysed to 800°C at 10°C/min	47.22	36.1
9	Air	pyrolysed to 1200°C at 10°C/min	88.49	30.3
9	Air	pyrolysed to 1000°C, then isotherm for 1 h and pyrolysed to 1400°C at 10°C/min	59.65	22.9
10	He	pyrolysed to 800°C at 10°C/min	57.96	38.9
10	He	pyrolysed to 1000°C at 10°C/min	51.86	32.1
10	He	pyrolysed to 1300°C at 10°C/min	59.38	20.9
10	Air	pyrolysed to 1000°C at 10°C/min, then isotherm for 1 h and pyrolysed to 1300°C	76.68	26.4

continued...

11	He	pyrolysed to 600°C at 10°C/min	54.79	no residue
12	He	pyrolysed to 300°C at 10°C/min	49.39	no residue
14	He	pyrolysed to 150°C at 10°C/min, then at 5°C/min to 650°C	40.90	47.9
14	He	pyrolysed to 150°C at 2°C/min, then pyrolysed to 900°C at 10°C/min	45.32	37.2
15	He	pyrolysed to 600°C at 10°C/min	49.17	no residue
15	He	pyrolysed to 600°C at 2°C/min	58.56	no residue
16	He	pyrolysed to 250°C at 10°C/min, then pyrolysed to 600°C at 5°C/min	48.67	no residue
16	He	pyrolysed to 600°C at 10°C/min	44.09	no residue
19	He	pyrolysed to 800°C at 10°C/min	40.32	no residue
20	He	pyrolysed to 800°C at 10°C/min	101.42	18.5
20	He	pyrolysed to 1200°C at 10°C/min, isotherm for 1 h	61.08	17.2
(Ph ₂ SiO) ₃	Air	pyrolysed to 1200°C at 10°C/min	61.95	no residue
(Ph ₂ SiO) ₃	He	pyrolysed to 800°C at 10°C/min	47.60	no residue
(Ph ₂ SiO) ₃	He	pyrolysed to 1000°C at 10°C/min	73.14	no residue
(Me ₂ SiO) ₃	He	pyrolysed to 600°C at 10°C/min	66.39	no residue

6.3 RESULTS AND DISCUSSION OF THE THERMOLYSIS PROCESSES

6.3.1 Low Temperature Heat Treatment of $[\text{PhB}(\text{SiOPh}_2)\text{O}]_2$ and $\text{PhB}[(\text{OSiPh}_2)_2\text{O}]$

Heterocyclosiloxanes are formally derived from conventional cyclosiloxanes via the replacement of a skeletal silicon atom by an atom of another main group element or transition metal, as was discussed earlier in chapter 2^{1,2}. Compared to the cyclic siloxanes, very few attempts to polymerise heterocyclosiloxanes have been reported³. Studies of these compounds should provide valuable insight into how the presence of different skeletal atoms, such as boron, influence polymerisability. Furthermore, successful ring-opening polymerisation of heterocyclosiloxanes would provide a route to new inorganic polymers which should display interesting and potentially useful properties⁴.

In this section the results will be discussed of the low temperature isothermal heat treatment of heterocyclosiloxanes containing boron with 1:1 and 2:1 silicon to boron atom ratios, compounds 9 and 10 respectively. The covalent radius of the boron atom (0.80 Å) is considerably smaller than that of silicon (1.17 Å) and so the replacement of silicon by boron in a siloxane ring might be expected to increase significantly the ring-strain present⁵ and hence the polymerisation behaviour detected⁶. Many cyclic siloxanes are known to undergo ring-opening polymerisation in the presence of acidic or basic catalysts. $\text{K}(\text{OSiMe}_3)$ has been used previously as an initiator in ring opening polymerisation⁷, with strained ring compounds particularly susceptible to Si-O bond breaking.

Polymerisation experiments were carried out for compounds 9 and 10. These involved thermally induced reactions in the melt and were carried out in the absence of externally added acid or base initiators. Figure 6.2 shows the weight losses versus time at 220°C for compounds 9 and 10. The final weight losses were about 40% and 35% respectively. These weight losses are due to the volatilisation of low molecular weight cyclic species formed by redistribution reactions. Significant quantities of volatilised materials were isolated when a sample of compound 9 was isothermally heated for 4 hours

at 220°C under an inert gas flow using the cold finger technique. No further volatilisation was noted after over-night isothermal heat treatments. The condensed volatile residue was identified by infrared, ^1H NMR spectroscopies and mass spectrometry, which show conclusively that the volatile is a cyclic boroxine species $(\text{PhBO})_3$. Figure 6.3 shows the mass spectrum of the condensed volatile, which is identical to that of $(\text{PhBO})_3$.

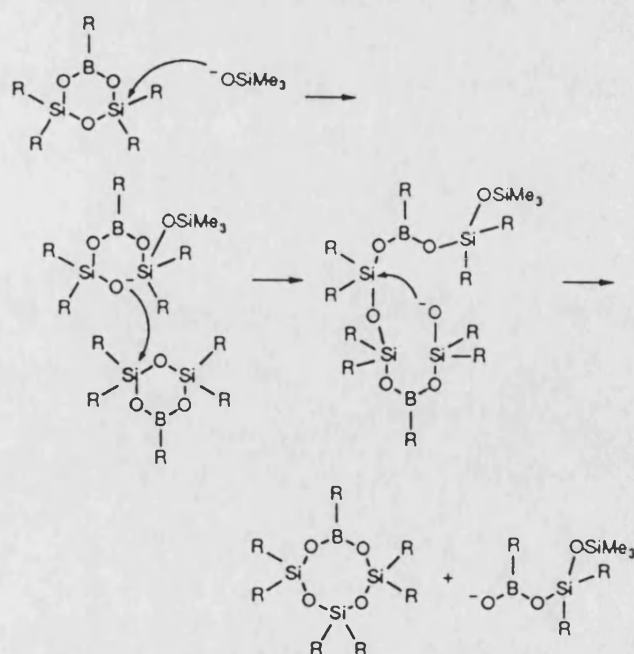
The final involatile solid residue from the low temperature isothermal heat treatment was examined by ^1H NMR spectroscopy which shows multiple broad peaks at 7.0-7.6 due to several phenyl-containing siloxanes or heterosiloxanes. The infrared spectrum of this residue, Figure 6.4, shows a broad peak at 3215 cm^{-1} indicative of Si-OH, B-OH or adsorbed moisture. Bands at $3074\text{-}3003\text{ cm}^{-1}$ and 1600 cm^{-1} represent aryl C-H and Ph ring modes. Other noticeable peaks at 1128 cm^{-1} and 1080 cm^{-1} represent $-\text{CH}_2\text{-Si-}$ deformation, and the peak at 1028 cm^{-1} represents the stretching frequency of Si-O-C and/or Si-O-Si open chain. The infrared spectrum contains a band at 1344 cm^{-1} which indicates that a significant amount of B-O is present in the final residue.

These results indicate that the final residue of the low temperature isothermal heat treatments has a lower boron content than the initial product and consists of large rings and/or chains of borasiloxanes. These rings and/or chains attain equilibrium only slowly and may be intermediates in the processes occurring during intermediate temperature heat treatment, as will be discussed later. The release of the ring strain in compounds 9 and 10 due to the presence of boron is clearly one of the driving forces behind the ring-opening polymerisation observed. The slow formation of volatile, stable $(\text{PhBO})_3$ provides another driving force for the redistribution reactions which are probably catalysed by traces of moisture initiating Si-OH formation.

Ring-ring transformation reactions have been detected previously in heterosiloxane chemistry. For example, treatment of TiCl_4 with $\text{LiOSiPh}_2\text{OSiPh}_2\text{OLi}$ resulted in eight-membered titanatetrasiloxane rings rather than the expected six-membered ring product⁸. The lack of stability of the smaller ring product has been attributed to the strain energy likely to be present in the expected six-membered ring. By contrast, ring-ring

transformations are dominant with many other inorganic ring systems⁹.

During the course of this work, Manners and his coworkers¹⁰ reported similar acid catalysed thermal behaviour for heterocyclicsiloxanes containing boron atoms. Samples of $\text{PhBO}(\text{R}_2\text{SiO})_2$ ($\text{R} = \text{Me}$ or Ph), were heat treated in the presence of 1.0 mol% of the initiator $\text{K}(\text{OSiMe}_3)$ at 200°C . The residual silicon-containing products consisted mainly of larger rings containing a single boron atom which was detected by NMR techniques. They also isolated a significant amount of $(\text{PhBO})_3$ during the polymerisation processes. In contrast, reaction of cycloborasiloxanes with 1.0 mol% of triflic acid in CH_2Cl_2 at -80°C , followed by warming to room temperature, yielded the cyclic siloxanes $(\text{R}_2\text{SiO})_x$, $x = 3, 4$ together with $(\text{PhBO})_3$ ¹¹. No larger borosiloxane rings and/or polymers were detected as intermediates during the polymerisation processes. This suggests that cationic initiation is more effective than initiation with base for the ring-ring transformation reaction, as the reaction proceeds cleanly and rapidly to the thermodynamically favoured siloxane and boroxane products. The mechanism for ring-ring transformation reaction for the formation of larger borasiloxane rings containing a single boron atom suggested by Manners is illustrated below¹⁰:



This mechanism involves initial attack of (OSiMe_3) at the silicon atom of the heterocyclosiloxane which induces ring-opening to generate an anionic open-chain species. A longer chain might then be formed by attack of another heterocyclosiloxane molecule. Cyclization of this species via a back-biting reaction could then afford a large boracyclosiloxane ring and would generate a new anionic species which might initiate further ring-ring transformation reactions. Because of the overall complexity of the equilibration process, no detailed mechanisms for siloxane and boroxane formation were proposed.

Thermally induced ring-ring transformation reaction mechanisms for the formation of larger borasiloxane rings or chains, similar to those suggested by Manners, can be proposed for the thermal decomposition of compounds 9 and 10 during low temperature isothermal heat treatments. If initiated by moisture, it would be expected to lead to the same type of products as those observed in the base catalysed route.

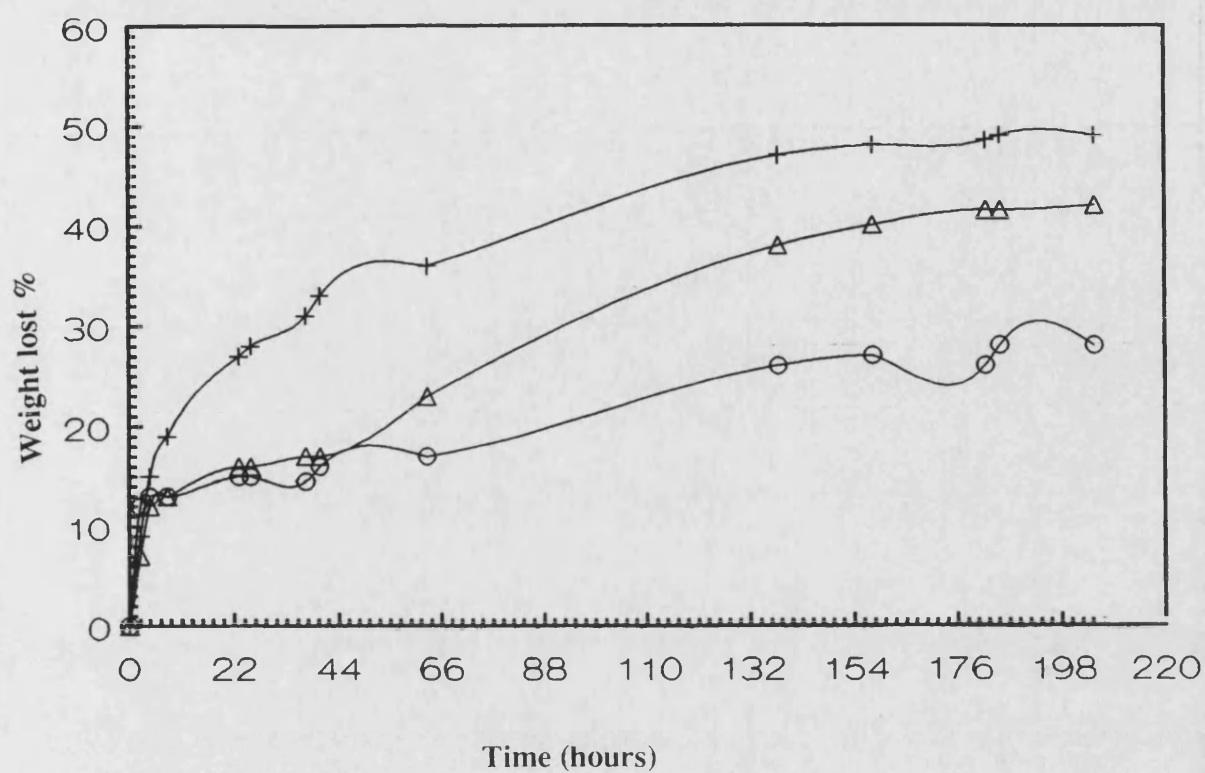
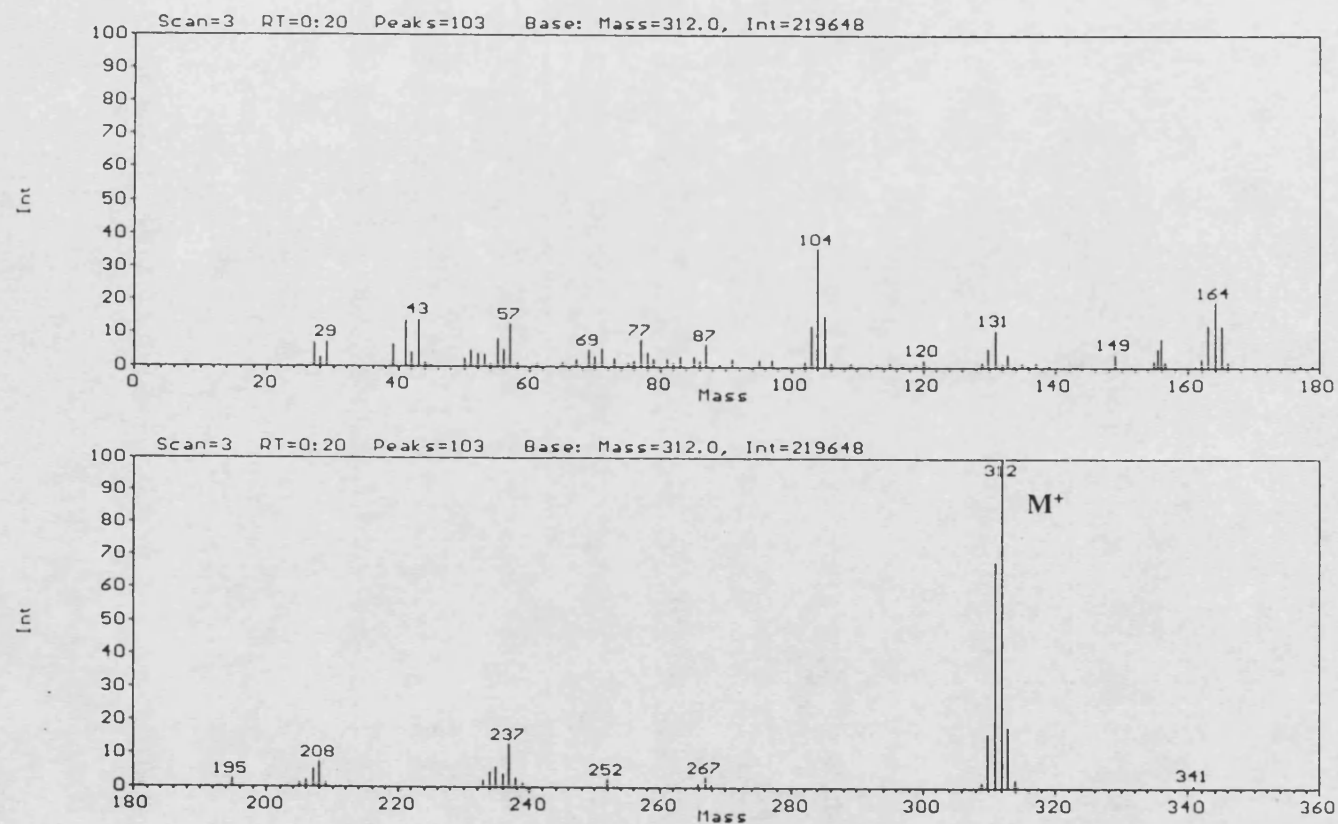


Figure 6.2

Weight losses versus time curves of $\text{Ph}_2\text{B}_2(\text{OSiPh}_2)_2\text{O}_2$, $\text{PhB}[(\text{OSiPh}_2)_2\text{O}]$ and $\text{PhB}(\text{OSiPh}_2\text{H})_2$ (compounds 9, 10 and 14 respectively) heated at 220°C for 3 days



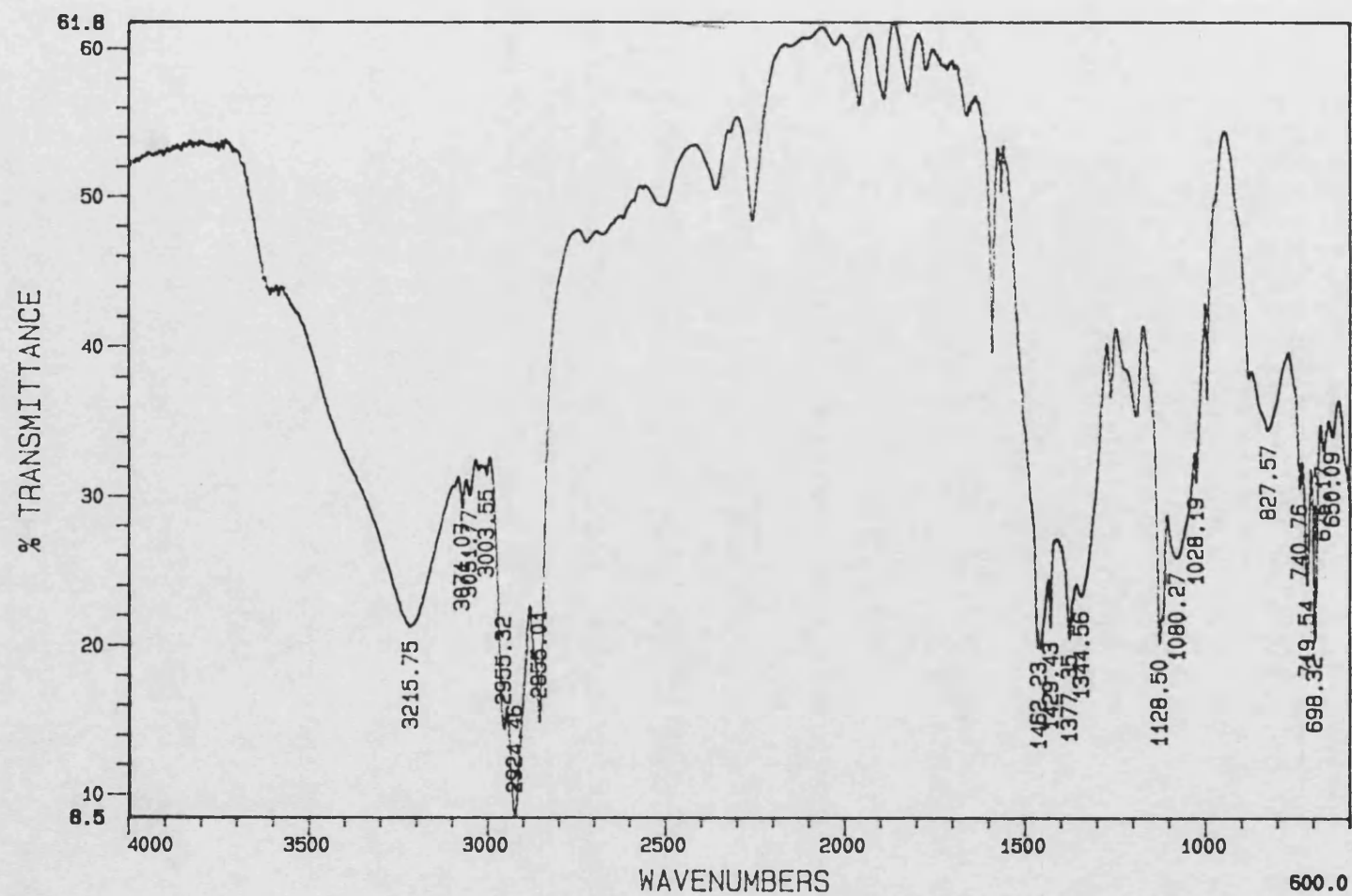


Figure 6.4

Infra-red spectrum of the final residue heated at 220°C from
 $\text{Ph}_2\text{B}_2(\text{OSiPh}_2)_2\text{O}_2$, compound 9

6.3.2 Intermediate Heat Treatment of $[\text{PhB}(\text{OSiPh}_2)\text{O}]_2$ and

$[\text{PhB}(\text{OSiPh}_2)_2\text{O}]$

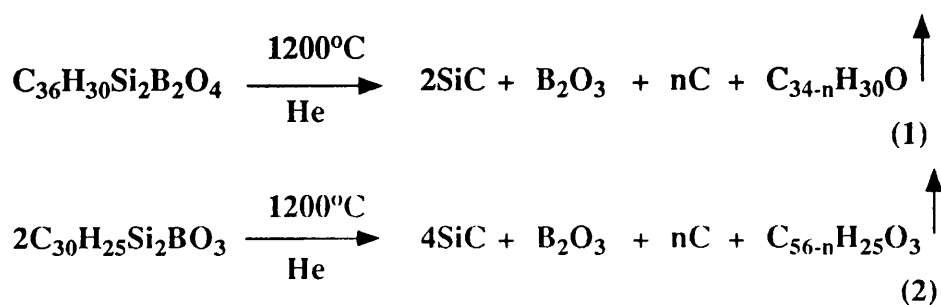
Pyrolysis of compound 9 and 10 under an inert atmosphere up to 1200°C.

The curves of weight loss versus temperature/time for compounds 9 and 10 from room temperature to up to 1200°C in a stream of inert gas (He or N₂) are shown in Figures 6.5a and 6.6a respectively. The initiation temperatures of the thermal decomposition of both compounds are about 250°C, and the thermal decomposition for both compounds under an inert atmosphere takes place in two main steps. The first step of the decomposition is in the 250-460°C range, and the second step is in the 460-680°C range. The first decomposition step of compounds 9 and 10 involves about 30% and 45% weight loss respectively, and the total weight loss at 1200°C is 65% and 70% respectively.

Scanning electron microscopy of the residual decomposition products at 1200°C from both compounds 9 and 10 indicates that the residues are black glassy amorphous solids, Figure 6.7. The structure of the solid residue suggests that during the course of the decomposition it has passed through a liquid phase, from which the glassy phase was formed. There is clear evidence in Figure 6.7 of bubbles presumably resulting from volatile products which were trapped in the solidifying glassy matrix. The mainly amorphous nature of the residue is confirmed by x-ray diffraction analysis. In some cases weak and broad peaks can be assigned to SiC at 2.51 Å and a strong peak at 3.18 Å assigned to B(OH)₃, Table 6.2. The broad and weak peaks of SiC may be due to the small crystal size and marginal crystallinity of SiC or both; the broad peaks also could be attributed to the presence of disorder in the SiC crystals, in other words, crystallinity is developing gradually on thermal treatment. The major peak at 3.18 Å indicates the presence of crystalline B(OH)₃ which presumably forms by hydration of B₂O₃ on exposure to humid air. The presence of Si, C and O atoms in the residual decomposition products at 1200°C for both compounds has been confirmed by scanning electron microscopy with energy dispersive x-ray analysis. Figure 6.8a and 6.9 show the intensity

and the position of the x-ray peaks for compound 9 and 10 respectively. Boron is difficult to detect by this technique, because it is a light element and the positions of the boron and carbon peaks are similar. Microelemental analyses of the solid residues of compounds 9 and 10 pyrolysed to 1200°C in an inert atmosphere reveal a concentration of carbon in the range 30-35%, Table 6.2. This suggests that free carbon is also present in the glassy solid for the following reasons.

Assuming that all B and Si atoms are retained in the solid residue of compounds 9 and 10 at 1200°C in inert atmosphere the decompositions can be represented for compounds 9 and 10 respectively as:



A free carbon content of 30-35 wt% implies that $n = 5-7$ and $n = 9-10$ for equation 1 and 2 respectively. These values of n translate to weight losses of 66-71 % for compound 9 and 65-66 % for compound 10 that are in reasonable agreement with the weight losses obtained by thermogravimetric analysis for compounds 9 and 10, of 68 and 70 % respectively, particularly when the uncertainty in these calculations due to possible volatilisation of B-containing species in the early stages of decomposition is considered

Considering the thermal decomposition of compounds 9 and 10 in an inert atmosphere to 1200°C, the cyclic borasiloxanes are ultimately converted to a glassy residue containing SiC, B₂O₃ and free carbon. An outline mechanism for this conversion process is sketched in Diagram 6.1. Thermogravimetric analysis shows that there are two main processes occurring at 250-460°C and 460-680°C. In the first decomposition step (250-460°C) for compounds 9 and 10, it is suggested that there is ring opening polymerisation and ring-ring transformation reactions of the central Si-O-B ring,

accompanied by slow volatilisation of boron containing species, as was detected in the low temperature studies. These will lead to the formation of polymer/chain intermediates containing different Si-O-B ratios. It is also possible that scission of substituent phenyl groups occurs followed by their condensation to form polyaromatic hydrocarbons (which are known to be precursors of free carbon).

The second step of decomposition (460-680°C) of the thermogravimetric analysis involves further decomposition of the polymer intermediates with the elimination of volatiles and the formation of amorphous solids rich in B, Si, C and O. At the same time polyaromatic hydrocarbons will condense to form free carbon. The formation of the glassy phase involves melting and it is significant that the melting point of B_2O_3 is about 460°C. Therefore, it is reasonable to suppose that the relatively low melting temperature of B_2O_3 facilitates the formation of the glassy phase. As the temperature increases towards 1200°C silicon-containing moieties react with carbon to form SiC which begins incipient crystallisation.

Pyrolysis of compound 9 and 10 in an air stream up to 1200°C.

The TG curves of compound 9 and 10 for pyrolysis from room temperature to 1200°C in a stream of air, Figure 6.5b and 6.6b respectively, are similar to those obtained on pyrolysis in an inert atmosphere, Figure, 6.5a and 6.6a, with the two distinct decomposition steps occurring in similar temperature ranges. Scanning electron microscopy with energy dispersive x-ray analysis show a considerable increase of oxygen in the final residue of compound 9 pyrolyzed to 1200°C in air compared with pyrolysis in an inert atmosphere, Figure 6.8a and 6.8b. Similar behaviour was also found for compound 10 comparing pyrolysis to 1200°C in air and inert atmosphere. Table 6.2 shows that the carbon contents of the solid decomposition products from both compounds heated in air to 1200°C are considerably lower than these obtained after pyrolysis in an inert atmosphere. This reduction in carbon content can be attributed to the reaction of free carbon with oxygen from the stream of air to form CO and/or CO_2 gases above 800°C.

Pyrolytic conditions have a considerable influence on the composition of the final

residue. Thus, changing the pyrolysis atmosphere from inert gas to air will lead to different residual products with different chemical compositions, Table 6.2 and Figures 6.8a and 6.8b. Thermogravimetric studies show that varying the heating rate in the range 2-10°C/min had no effect on the slope of the thermogravimetric curve. Therefore, nearly all of the thermogravimetric analyses have been carried at a constant heating rate of 10°C/min.

There have been few published studies exploring the potential of polymers containing Si-O-B linkages as preceramic polymers (Chapter 3). Poly(boradiphenylsiloxane) (PB)_p which contains B, Si O, C and H, has been synthesised previously by the reaction of boric acid and diphenyldichlorosilane, and its thermal decomposition compared with that of polycarbosilane (containing Si, C and H)¹². Formation of an intermediate amorphous state before formation of fine particles of SiC was detected for both systems¹³. Of the various organometallic polymers, boron polymers are generally heat resistant but not very moisture proof¹⁴. Vale reported the production of polyboradimethylsiloxane (PB)_m from boric acid and dimethyldichlorosilane¹⁵. The thermal decomposition processes of (PB)_p and (PB)_m were compared and Figure 6.10 shows the thermal analysis curves obtained by Vale for (PB)_p and (PB)_m from room temperature to 500°C under a stream of air¹². Thermogravimetric analysis of (PB)_p was examined up to 1200°C in a stream of N₂ gas, and the TG curve was almost the same as that obtained in air at 500°C. The thermal decomposition initiation temperature is about 150°C which is considerably lower than the initiation temperature of compounds 9 and 10 (*ca.* 250°C). Yajima suggested that in the pyrolysis of (PB)_p, the organic group is decomposed at 1000°C, and an amorphous phase containing many elements is obtained. By further pyrolysis the residual product contains crystalline SiC and graphite as confirmed by x-ray diffraction¹⁶. These thermolysis results are broadly consistent with those obtained for the thermolysis of compounds 9 and 10 after intermediate temperature heat treatment. In particular there are broad similarities with the present work and the mechanisms outlined earlier for the formation of the glassy phase. Diagram 6.1, may have

some relevance to the decomposition of $(PB)_p$ and $(PB)_m$.

It would be of great value to determine the identity, rate of evolution and total amount of the major volatile products across the entire range of the thermogravimetric analysis, for example, by gas-liquid chromatography (GLC), and/or mass spectrometry (MS) analysis of volatiles. This information, along with spectroscopic, elemental and microstructural analysis of the residue at various stages of the thermal conversion process, would enable more precise identification of the chemical mechanisms of degradation and microstructural evaluation. This type of information is greatly needed in order to understand and control the thermal conversion process and hence the chemical composition and microstructure of the final residue, and could usefully be undertaken in a future study.

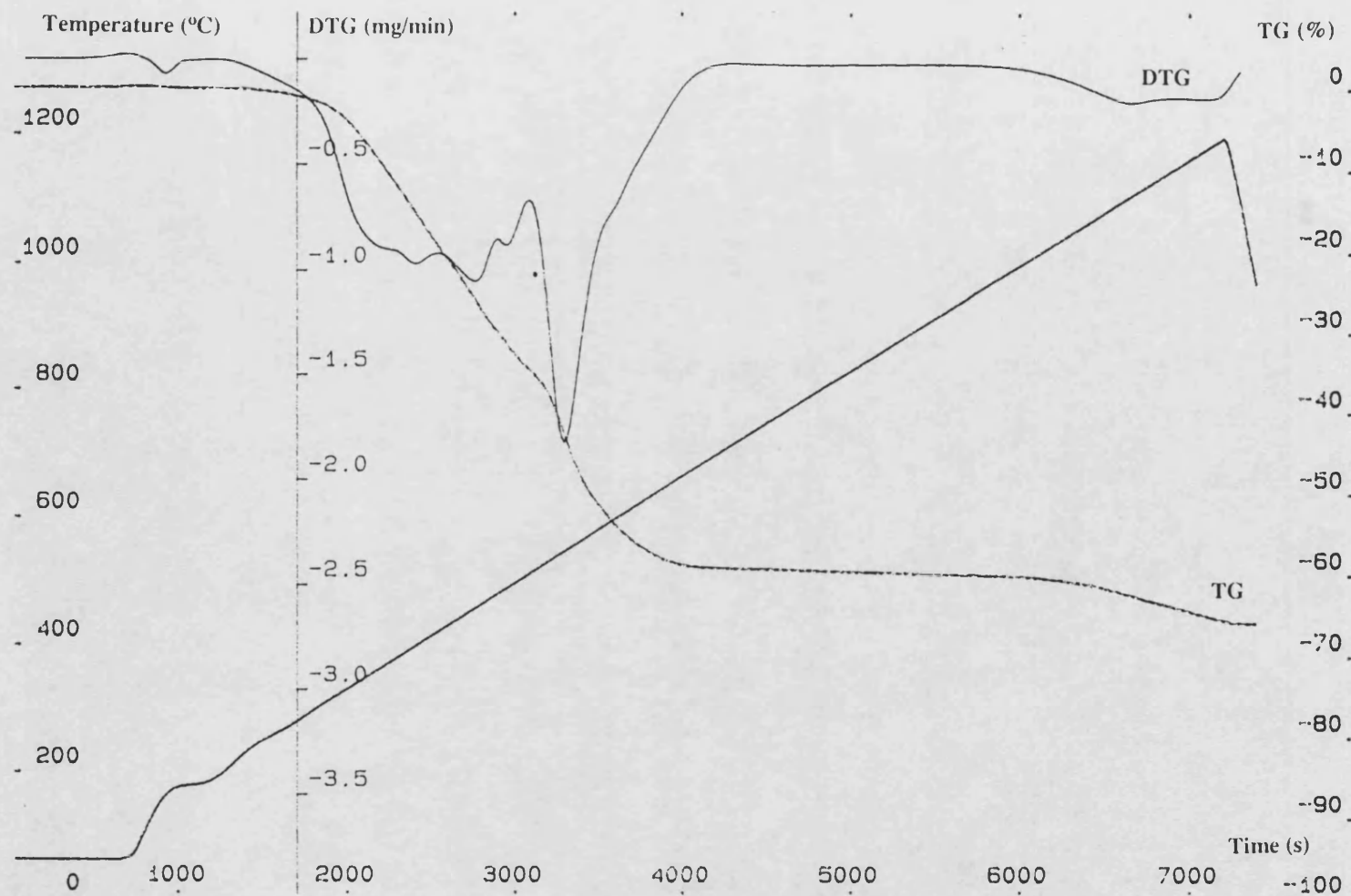


Figure 6.5a

Thermogravimetric analysis of $\text{Ph}_2\text{B}_2(\text{OSiPh}_2)_2\text{O}_2$, compound 9,
from room temperature to 1200°C in a stream of helium

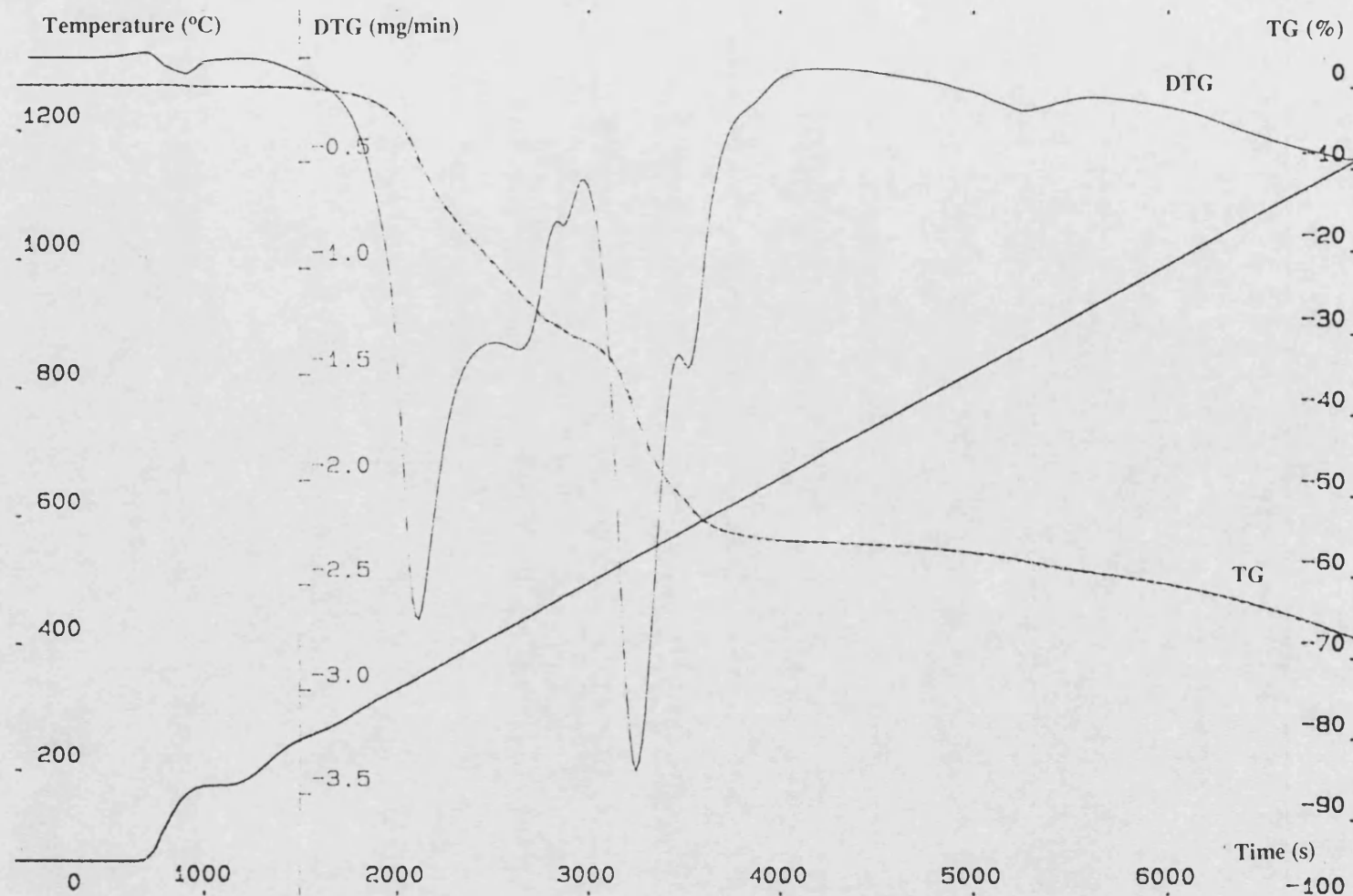


Figure 6.5b Thermogravimetric analysis of $\text{Ph}_2\text{B}_2(\text{OSiPh}_2)_2\text{O}_2$, compound 9, from room temperature to 1200°C in a stream of air

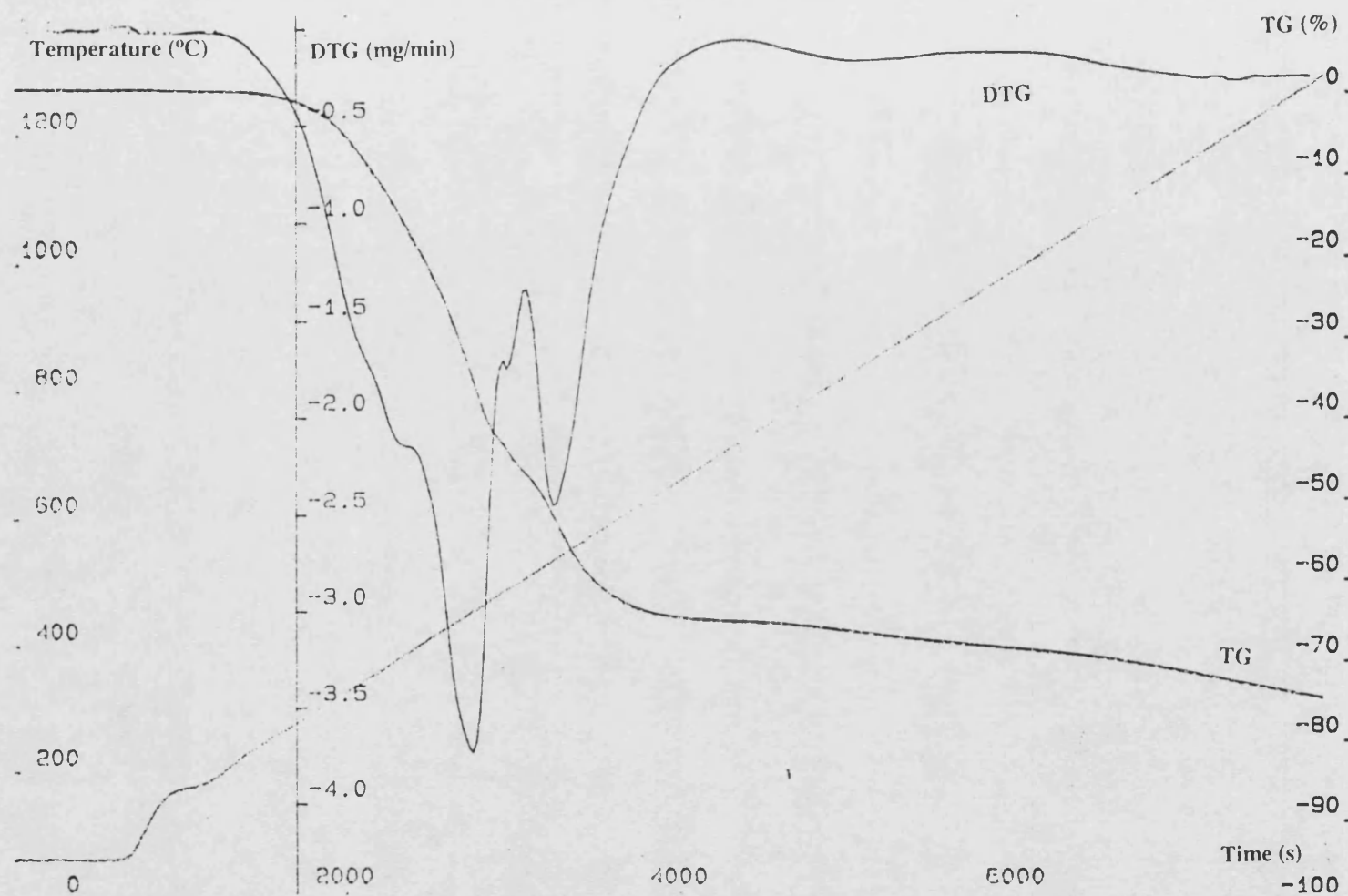


Figure 6.6a Thermogravimetric analysis of $\text{PhB}[(\text{OSiPh}_2)_2\text{O}]$, compound 10, from room temperature to 1200°C in a stream of helium

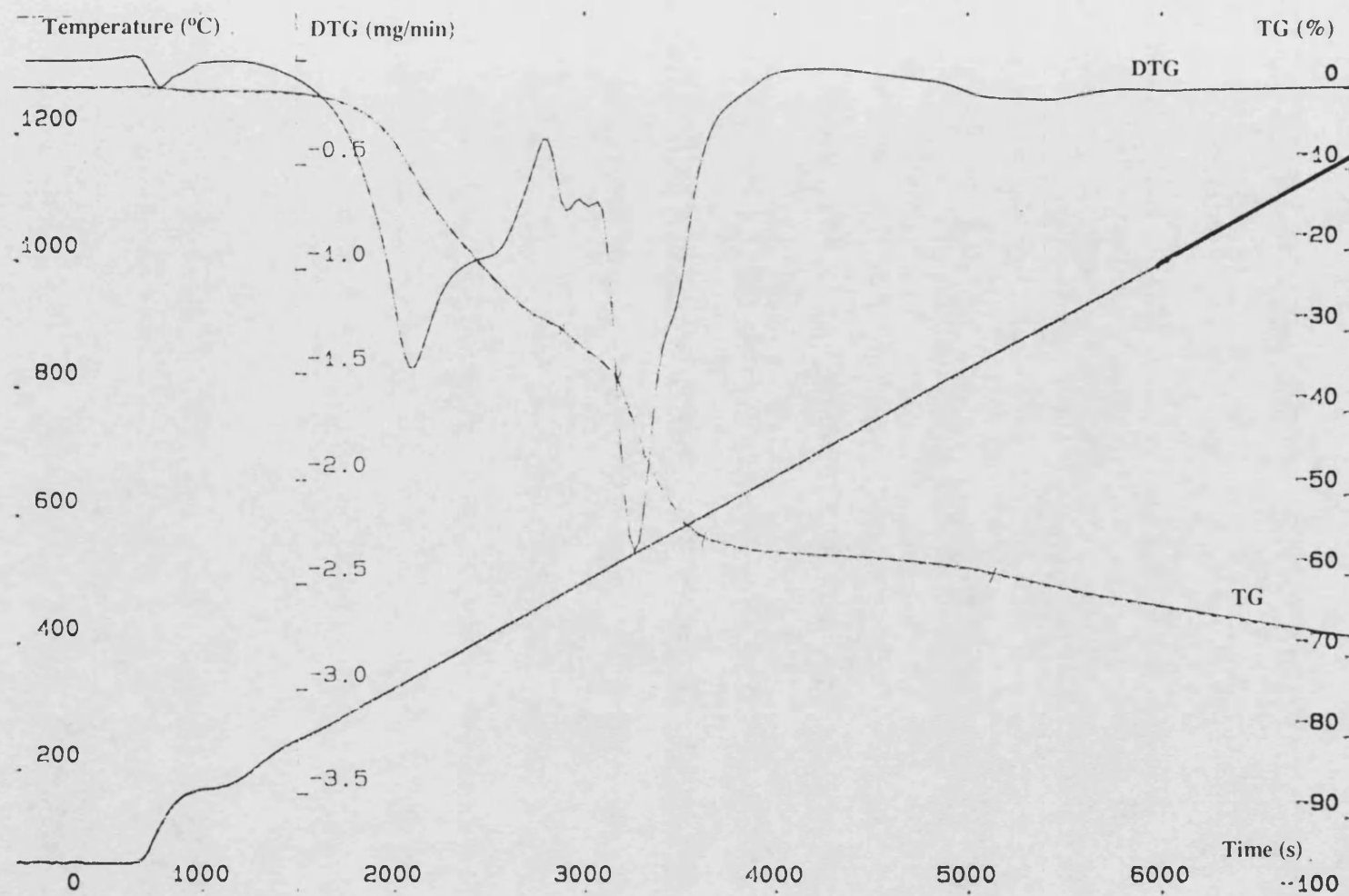


Figure 6.6b

Thermogravimetric analysis of $\text{PhB}[(\text{OSiPh}_2)_2\text{O}]$, compound 10,
from room temperature to 1200°C in a stream of air

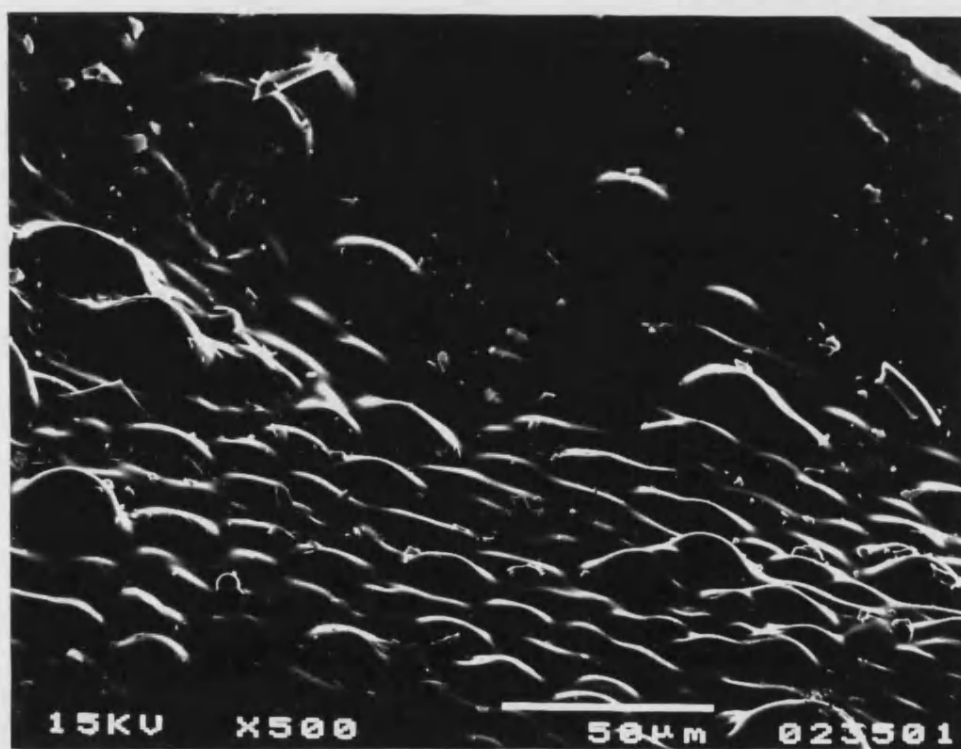
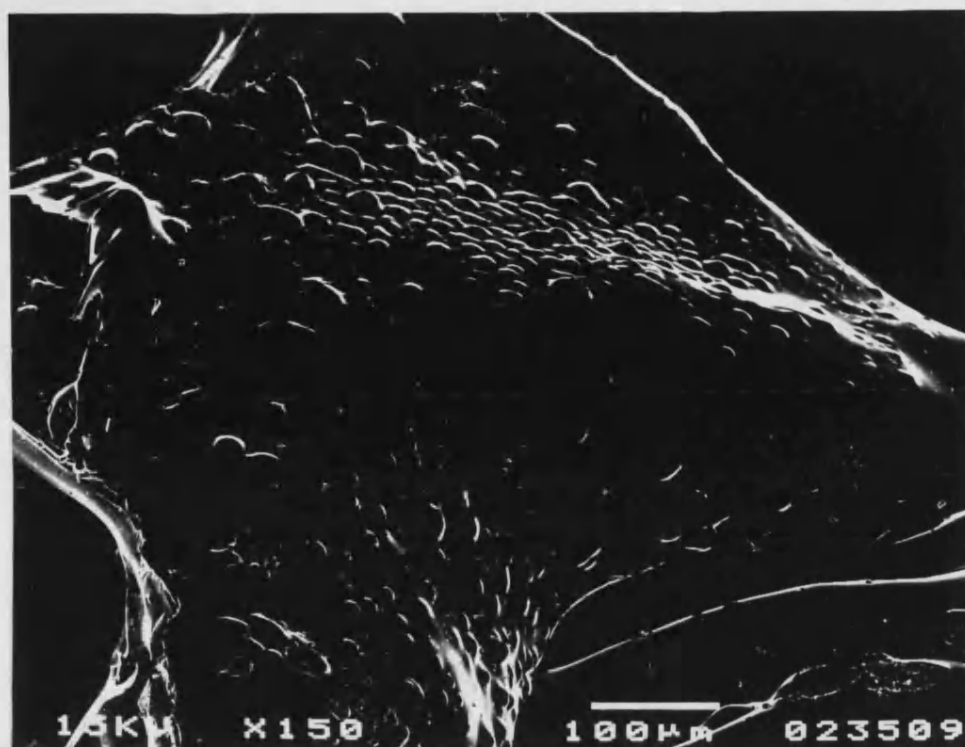


Figure 6.7 Scanning electron micrographs of amorphous residue from compound 9 pyrolysed to 1200°C under an inert atmosphere



Figure 6.8a

Energy dispersive x-ray analysis of the 1200°C solid residue formed under an inert atmosphere for $\text{Ph}_2\text{B}_2(\text{OSiPh}_2)_2\text{O}_2$, compound 9

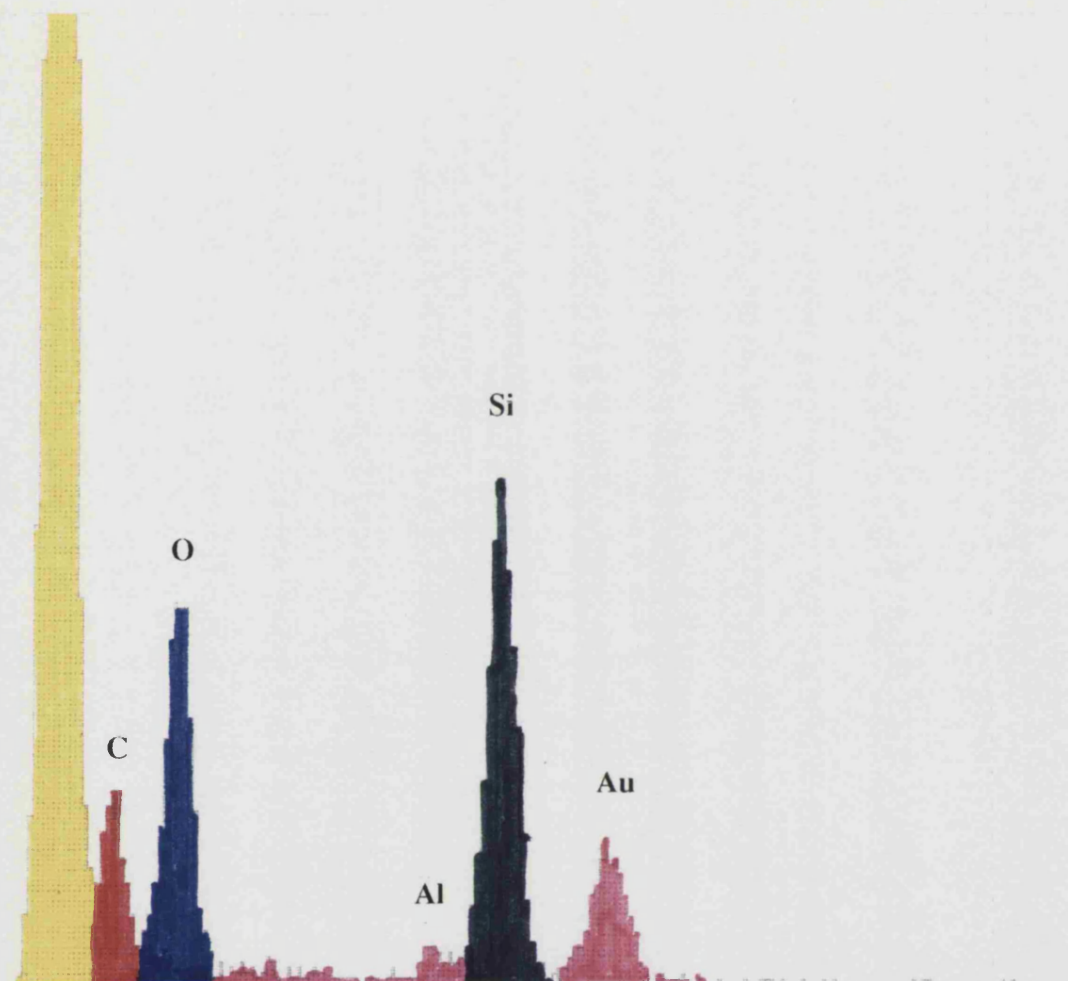


Figure 6.8b

Energy dispersive x-ray analysis of the 1200°C solid residue
formed under an air atmosphere for $\text{Ph}_2\text{B}_2(\text{OSiPh}_2)_2\text{O}_2$, compound
9

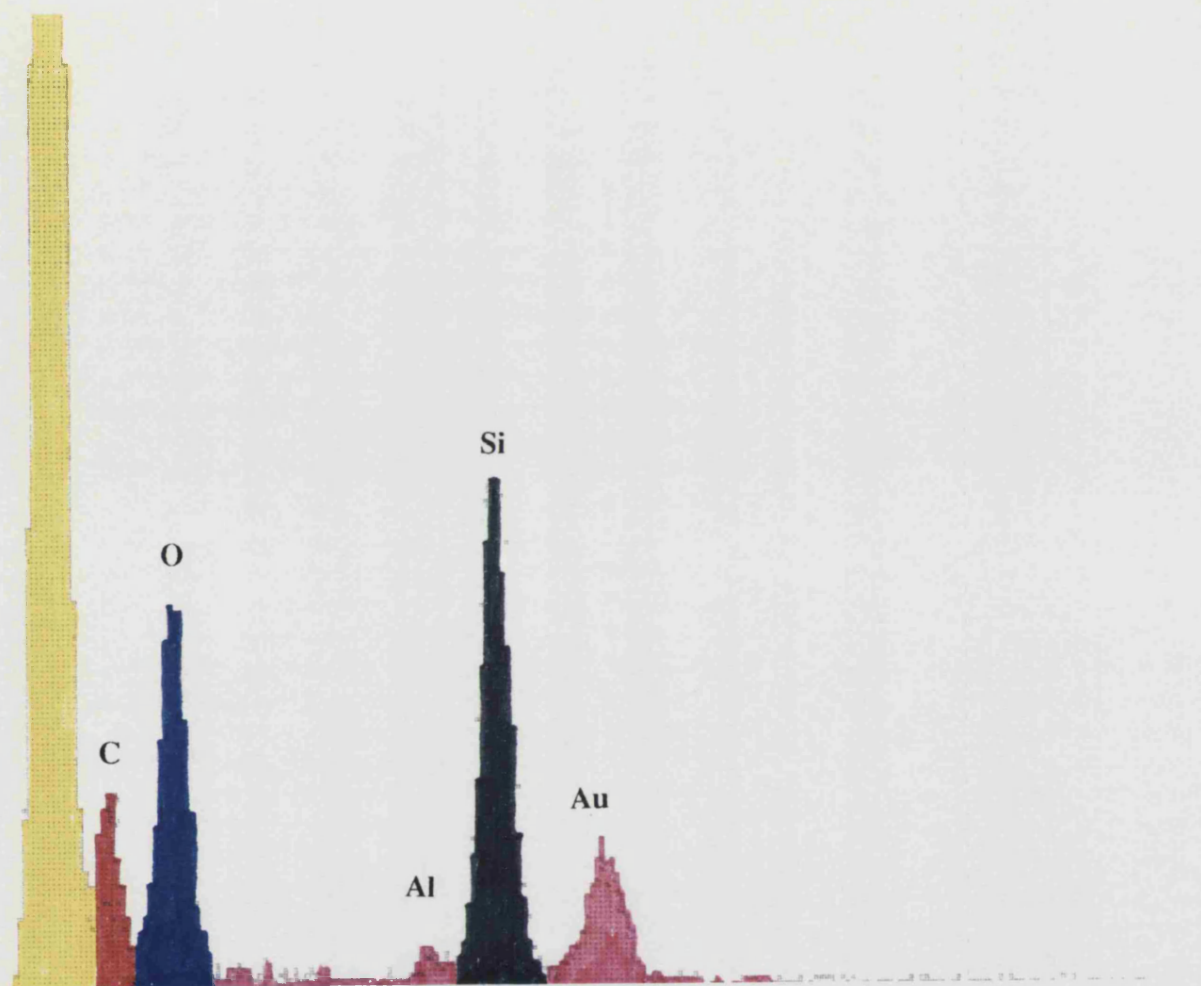


Figure 6.9

Energy dispersive x-ray analysis of the 1200°C solid residue formed under an inert atmosphere for $\text{PhB}[(\text{OSiPh}_2)_2\text{O}]$, compound 10

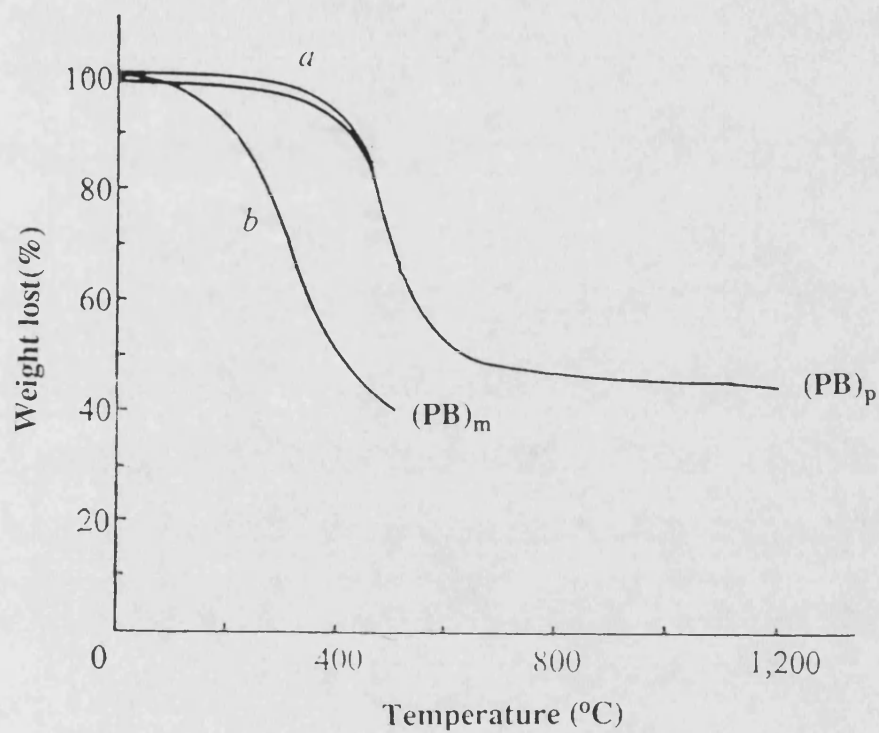
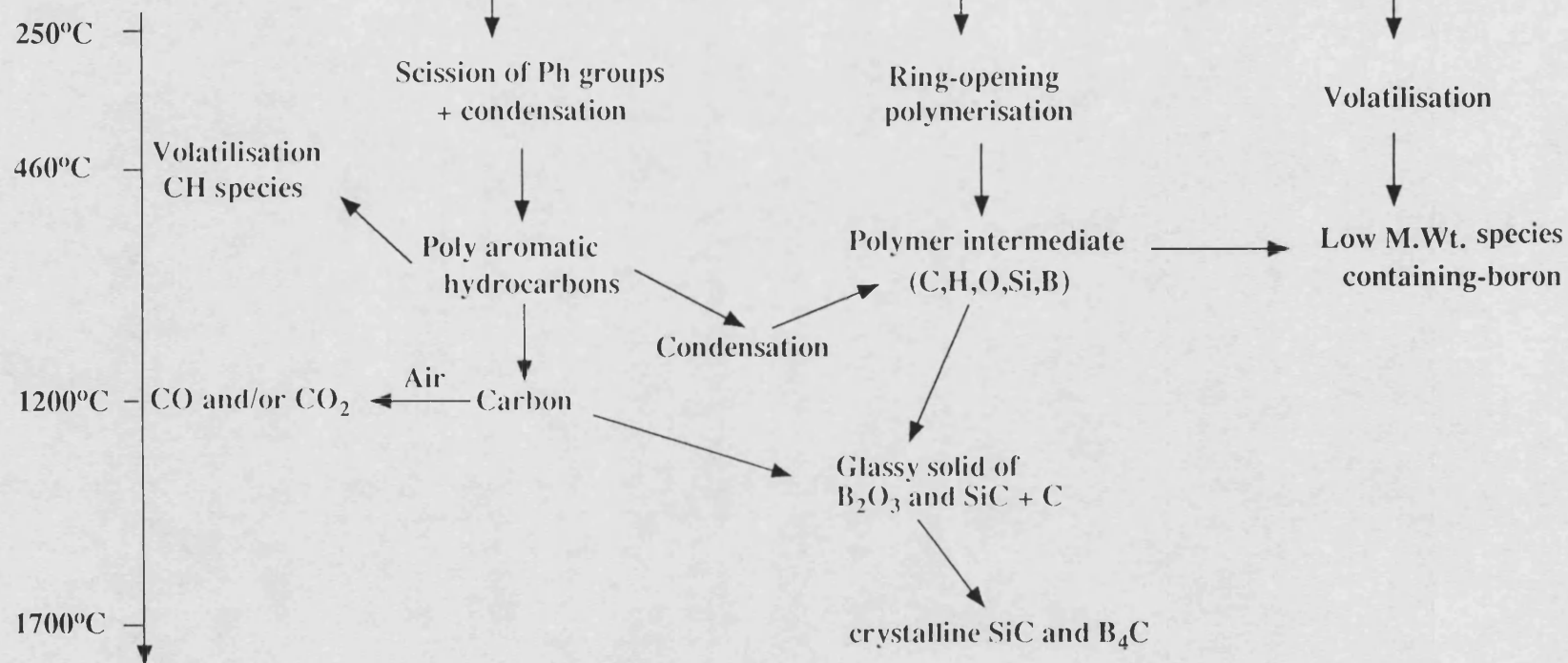


Figure 6.10 Thermogravimetric analysis of polyboradiphenylsiloxane and polyboradimethylsiloxane in a stream of nitrogen gas (from reference 13)

Compound	Pyrolysis Temperature and Atmosphere	Wt. Lost (%)	Elemental Analysis			X-Ray Diffraction (Principal Peaks (Å) and assignments)
			C (%)	H (%)	N (%)	
9	1200°C/Air	67.9	8.10	0.5	0.0	6.08, 5.94, 3.18 [B(OH) ₃]
9	1200°C/He	65.1	30.5	0.1	0.0	6.08, 5.94, 3.18 [B(OH) ₃] 2.51, 1.54 [SiC]
9	1200°C/N ₂	65.8	32.1	0.1	0.2	6.08, 5.94, 3.18 [B(OH) ₃]
9	800°C/Air 1700°C/Ar	85.1	27.2	0.1	0.0	2.52, 2.18, 1.54, 1.31, 0.89 [SiC]
9	800°C/Ar	86.4	29.8	0.0	0.0	2.52, 2.18, 1.54, 1.31, 0.89 [SiC]
	1700°C/Ar 1200°C/Air	89.5	5.61	0.0	0.0	4.05, 3.14, 2.49 [SiO ₂]
10	1200°C/Air	73.6	9.10	0.3	0.0	6.08, 5.94, 3.18 [B(OH) ₃]
10	1200°C/He	72.2	35.2	0.2	0.0	6.08, 5.94, 3.18 [B(OH) ₃]
10	800°C/Air 1700°C/Ar	82.4	30.1	0.1	0.0	2.52, 2.18, 1.54, 1.31, 0.89 [SiC]
10	800°C/Ar 1700°C/Ar	83.1	29.5	0.1	0.0	2.52, 2.18, 1.54, 1.31, 0.89 [SiC]

Table 6.2 Analysis of the solid residue from the heat treatment up to 1400°C of Ph₂B₂(OSiPh₂)₂O₂ and PhB[(OSiPh₂)₂O] (compounds 9 and 10 respectively)

Compound 9 or 10



6.3.3 High Temperature Heat Treatment of $[\text{PhB}(\text{OSiPh}_2)\text{O}]_2$ and $[\text{PhB}(\text{OSiPh}_2)_2\text{O}]$

Both $[\text{PhB}(\text{SiOPh}_2)\text{O}]_2$ and $\text{PhB}[(\text{OSiPh}_2)_2\text{O}]$, compounds 9 and 10 respectively, were pyrolysed up to 1700°C in two stages in different furnaces: stage 1 from ambient temperature to about 800°C in a tube furnace under argon or air atmosphere and, stage 2 from ambient temperature to 1700°C in a graphite resistance furnace under an argon atmosphere. The two-stage procedure was adopted to minimize contamination of the graphite resistance furnace by decomposition products, as most of the weight loss occurs between 250-650°C, as indicated by thermogravimetric analysis, Figures 6.5 and 6.6

Scanning electron micrographs of the solid residues after heat treatment of compounds 9 and 10 to 1700°C show a matrix of well formed microcrystals of silicon carbide, Figure 6.11 and 6.12 respectively. A comparison of Figures 6.11 and 6.12 with Figure 6.7 clearly shows that on heat treatment from 1200°C to 1700°C there is a transformation of the solid residues from an amorphous form to a crystalline form. Chemical elements present in the residual product were detected by scanning electron microscopy with energy dispersive x-ray analysis. Figures 6.13 and 6.14 show the position and intensities of the Si and C x-ray peaks for compound 9 and 10 respectively, obtained from the microcrystalline matrix of silicon carbide formed on heat treatment to 1700°C. The intensities and positions of the x-ray peaks are similar to a standard SiC sample, Figure 6.15. The solid residues of the high temperature heat treatment of compounds 9 and 10 were analysed by x-ray diffraction which shows major peaks at 2.51, 1.54 and 1.31 Å, attributed to SiC, Table 6.2.

Interestingly, some whiskers were detected in the solid residue formed from compound 9 at 1700°C, Figure 6.20. Although the whiskers could not be positively identified they are possibly SiC. Several workers^{17,18} have shown that whiskers of SiC can be grown under special conditions. The characteristic of spiral growth on the surface of SiC crystals was first reported by Tone in 1907¹⁹.

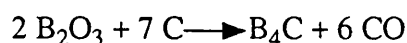
A few large crystals (size *ca* 10 µm) embedded in the crystalline SiC matrix were

detected by scanning electron microscopy for compounds 9 and 10, Figures 6.16 and 6.17 respectively. These micrographs also show the well-developed microcrystalline matrix of SiC with crystals ranging from sub-micron size to a width of about 3-4 μm . Also some whiskers of different thicknesses up to *ca* 2 μm are seen, Figure 6.16. Scanning electron microscopy with energy dispersive x-ray analysis of the large crystals show two peaks corresponding to B and C (i.e a boron carbide) which were detected for both compounds 9 and 10, Figures 6.18 and 6.19. No x-ray diffraction evidence for crystalline boron or silicon oxides was found in the solid residues formed on pyrolysis to 1700°C.

Large single crystals were detected when a sample of compound 9 was pyrolysed to 1700° under an inert atmosphere, Figure 6.21. These were identified as B₄C crystals by computer modelling using a "Growth and Equilibrium Morphology" program (Miller Index) to generate model B₄C of space group R₃-MH, Figure 6.21. The programme was run by Dr S Parker in the School of Chemistry, University of Bath. The large size of the B₄C crystals, compared to the SiC crystals, suggests that nucleation of B₄C crystals is more difficult, but once they are nucleated, the embryonic crystals grow quickly as a result of rapid diffusion of B and C. The later stages of the pyrolysis process, from 1200° to 1700°C seem to be quite insensitive to the processes occurring in the early stages of decomposition, since pyrolysis of both compounds 9 and 10 results in similar products at 1200°C. Similar products at 1700°C are also obtained if the compounds are heated in an air atmosphere to 800°C (rather than in inert atmosphere) and then subsequently heat treated in an inert atmosphere to 1700°C.

The pyrolysis processes occurring during heat treatment of compounds 9 and 10 to 1200°C were discussed in section 6.3.2, Diagram 6.1. For both compounds it was concluded that the solid residue is a glassy phase containing SiC, B₂O₃ and free carbon. The reactions occurring on further heat treatment from 1200° to 1700°C are similar for both compounds and appear to involve two processes. The first process is further crystallisation of SiC (some evidence for crystallisation of SiC was seen at 1200°C), Table 6.2. The second process can be attributed to the carbothermal reduction of B₂O₃ by free

carbon. It is well known that carbothermal reduction of B_2O_3 can occur at temperatures above 1400°C , particularly if the carbon is finely divided¹⁷.



The phase diagrams for silicon and boron carbides are illustrated in Figures 6.22. Both B_4C and SiC are solid to temperatures considerably higher than 1700°C . SiC exists in stoichiometric form with 30 wt% C; B_4C can be found in a wide non-stoichiometric range from close to the stoichiometric value of 21.7 wt% C, to 10 wt% C, i.e. with a considerable excess of B over the stoichiometric value. It is well known that boron can replace carbon in the B_4C lattice to a considerable extent¹⁷. The large crystals of B_4C were studied using quantitative electron probe microanalysis. Table 6.3 shows the quantitative results for a standard reference sample of B_4C with the corresponding results for the B_4C crystals embedded in the SiC crystalline matrix for compounds 9 and 10, The results for the standard crystal and the B_4C crystals formed from compounds 9 and 10 lie within the non-stoichiometric range found for B_4C .

Table 6.3 Quantitative results of B_4C microcrystals present in the solid residue from the heat treatment at 1700°C of $Ph_2B_2(OSiPh_2)_2O_2$ and $PhB[(OSiPh_2)_2O]$ (compounds 9 and 10 respectively) with standard B_4C crystals by SEM probe analyser

	B	B_4C C	Total
Standard	83.1	9.50	92.7
Compound 9	85.5	14.2	99.7
Compound 10	78.8	20.9	99.8

Some evidence for segregation was found in the solid residue of compound 9 heat

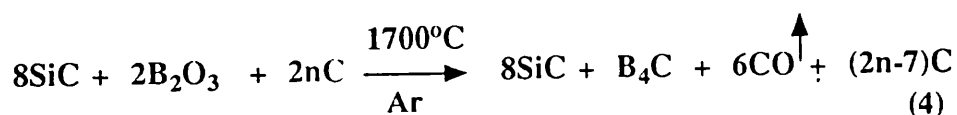
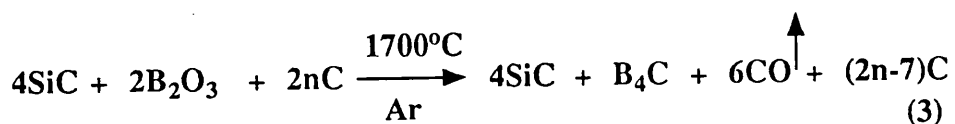
treated to 1700°C in an inert atmosphere, Figure 6.23, in the form of a dark centre line in transverse section of the solid residue. It is possible that this results from a segregation process accompanying solidification. The glassy appearance of the solid residue produced at 1200°C suggests that the material is in the liquid state at high temperature (see earlier). On cooling, solidification will proceed from the outside surface towards the centre line of the solid. Any impurities and/or insoluble species will be precipitated in the centre line on final solidification. The EDX line spectrum for oxygen, Figure 6.24, from the dark centre line and the edge profiles suggests that there is a some oxygen depletion at the centre line. Figure 6.25 show the corresponding line spectrum for carbon. Carbon content increases at the centre line. It has been shown that the solid residues fired at 1200°C from compounds 9 and 10 contain free carbon. Thus it is possible that the dark centre line results from segregation of some of the free carbon during the solidification process.

The residue of compound 9 which was pyrolysed to 1700°C under an inert atmosphere, was subsequently heat treated to 1200°C in air in the thermobalance, Figure 6.26. The thermogravimetric curve shows that the decomposition of the residue is initiated at a temperature of about 500°C, and involves about 40% weight loss in the 500-700°C range, followed by a weight gain of 10% at temperatures above 700°C. X-ray diffraction peaks for the residue are found at 4.05 (100), 3.14, 2.84, 2.48, 1.61 and 1.53 Å, which correspond to microcrystalline SiO₂. These results were supported by scanning electron microscopy with energy dispersive x-ray analysis which confirms the presence of Si and O, together with small amounts of C, Figure 6.27.

Reactions 1 and 2 described earlier indicate that there are substantial amounts of free carbon after heat treatment to 1200°C in an inert atmosphere and it is reasonable to suppose that significant amounts of free carbon remain after carbothermal reduction of B₂O₃. Therefore, the most likely reason for the initial weight loss on heating compound 9 in air is removal of free carbon as CO and/or CO₂. The 10% weight gain may correspond to the partial formation of SiO₂ in the 700°-1200°C temperature range. This suggestion is consistent with the experimental results, and it is known that SiC can form a layer of SiO₂

on the surface which is protective of further oxidation. The SiO₂ film is stable up to 1550°C²⁰.

The weight losses for compounds 9 and 10 on heat treatment above 1200°C are small (15 and 19% respectively), the total weight losses were 85% and 89% respectively for compounds 9 and 10 pyrolysed to 1700°C under an inert atmosphere. Equations 3 and 4 show how the solid products (SiC, B₂O₃ and free C) formed by intermediate heat treatment of compounds 9 and 10, (see equations 1 and 2) are transferred to crystalline SiC and B₄C.



The yield of the final residues in equation (3) above corresponds closely with the value expected for quantitative conversion of compound 9 to SiC plus B₄C (83%) in the molar ratio of 4:1, Equation 3. Thermolysis of compound 10 under similar conditions followed a very similar pattern with quantitative conversion to a mixture of SiC and B₄C (81%) in the molar ratio 8:1 Equation 4. These values for the total weight losses are consistent with the molecular composition of the final residues containing SiC and B₄C. The low temperature heat treatment shows that some B is volatilised as (PhBO)₃, but no further volatilisation of B-containing species occurs under intermediate and higher heat treatment pyrolysis conditions.

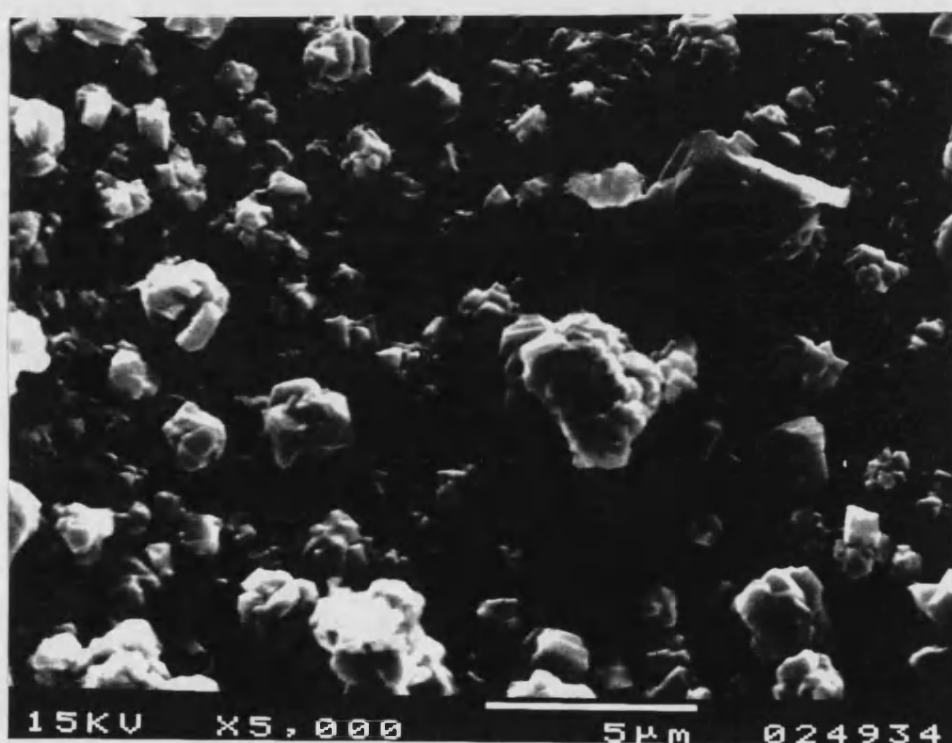
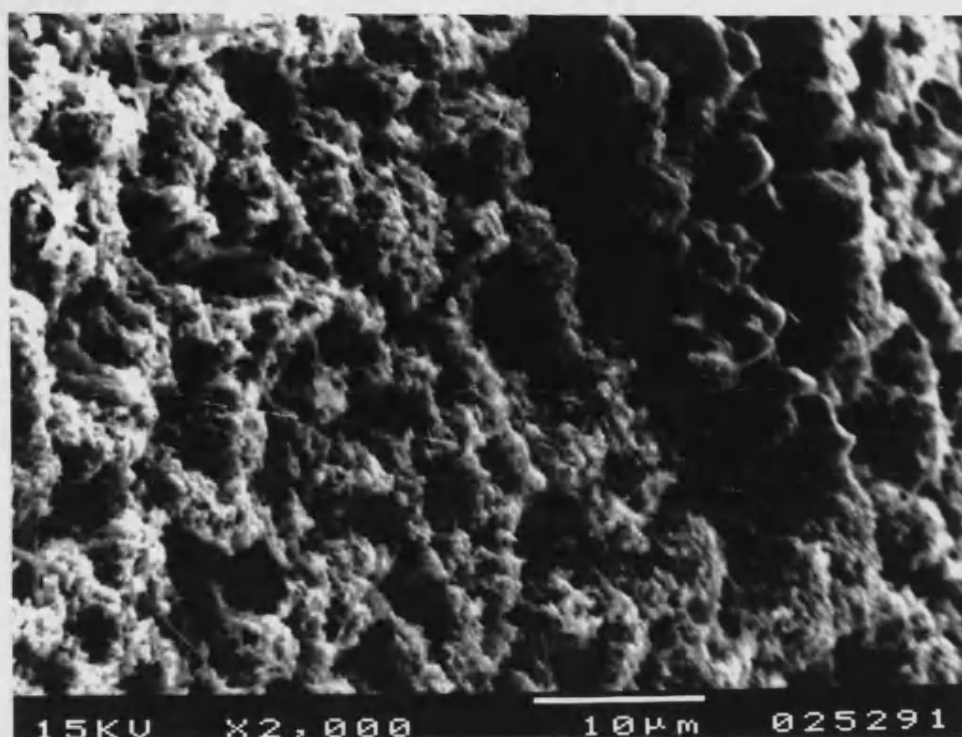


Figure 6.11 Scanning electron micrographs of microcrystalline SiC from $\text{Ph}_2\text{B}_2(\text{OSiPh}_2)_2\text{O}_2$, compound 9, pyrolysed to 1700°C under an inert atmosphere

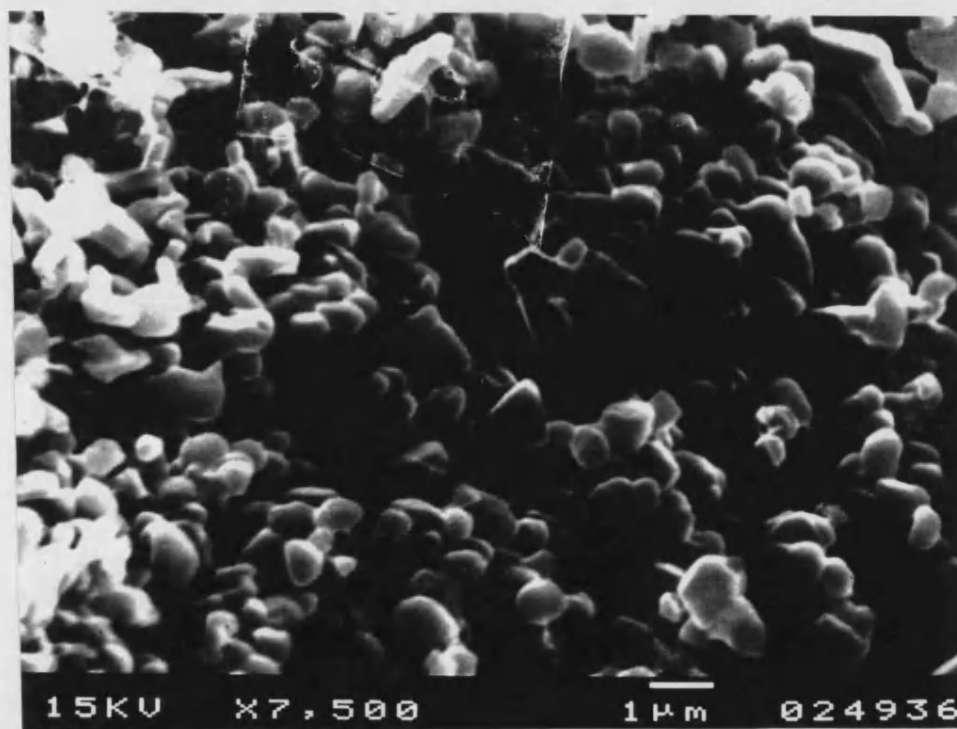
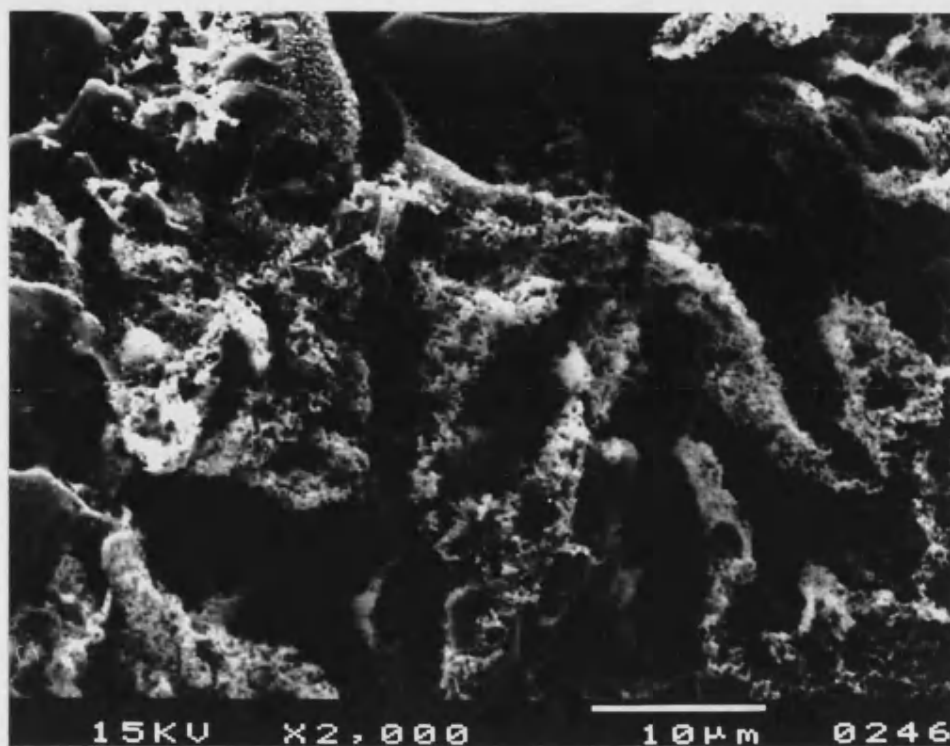


Figure 6.12 Scanning electron micrographs of microcrystalline SiC from $\text{PhB}[(\text{OSiPh}_2)_2\text{O}]$, compound 10, pyrolysed to 1700°C under an inert atmosphere

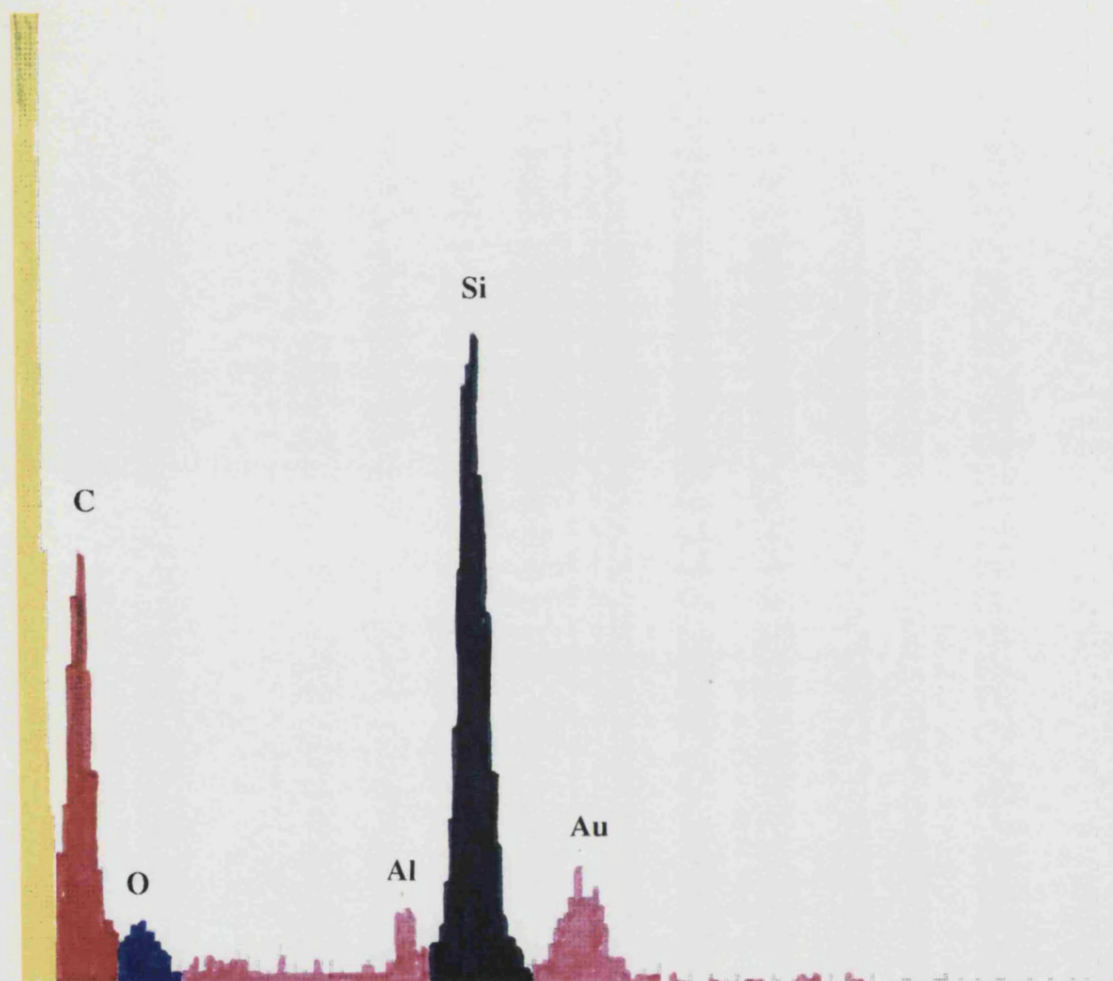


Figure 6.13 Energy dispersive x-ray analysis of the microcrystalline SiC present in the final solid residue from $\text{Ph}_2\text{B}_2(\text{OSiPh}_2)_2\text{O}_2$, compound 9, at 1700°C

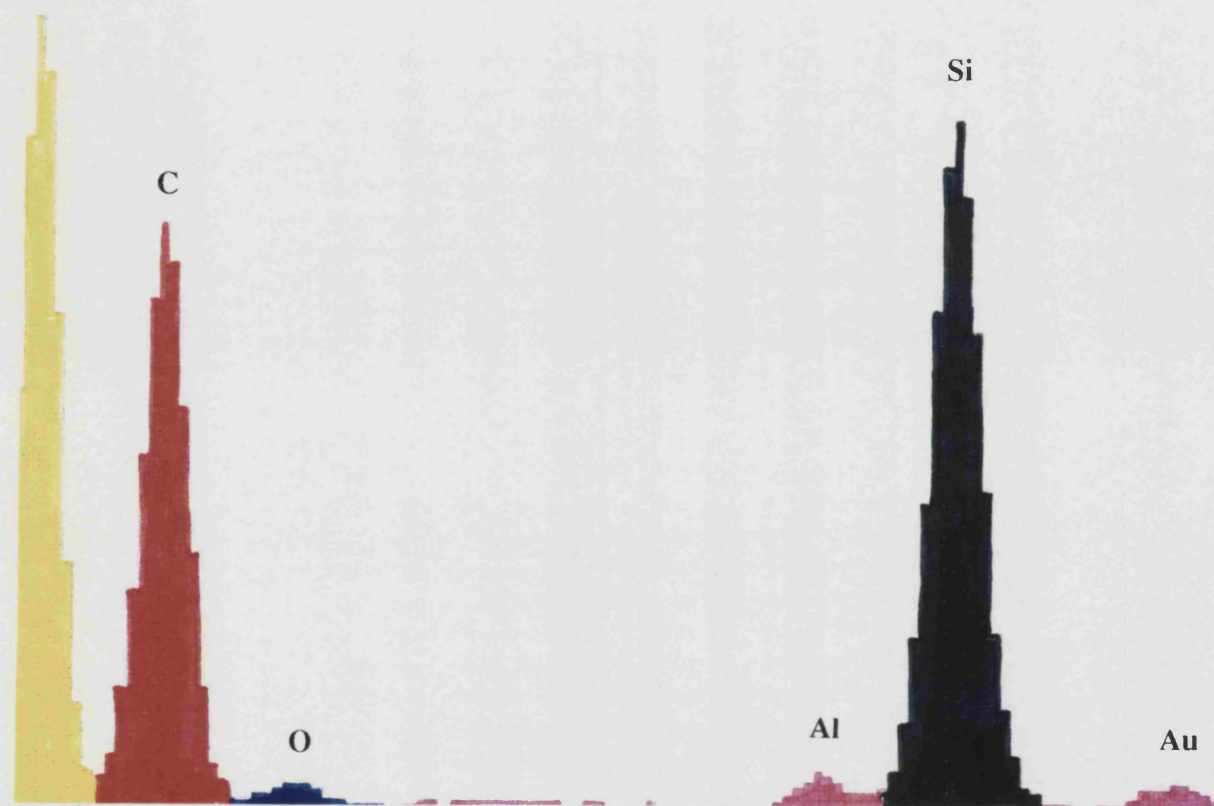


Figure 6.14 Energy dispersive x-ray analysis of the microcrystalline SiC present in the final solid residue from $\text{PhB}[(\text{OSiPh}_2)_2\text{O}]$, compound 10, at 1700°C

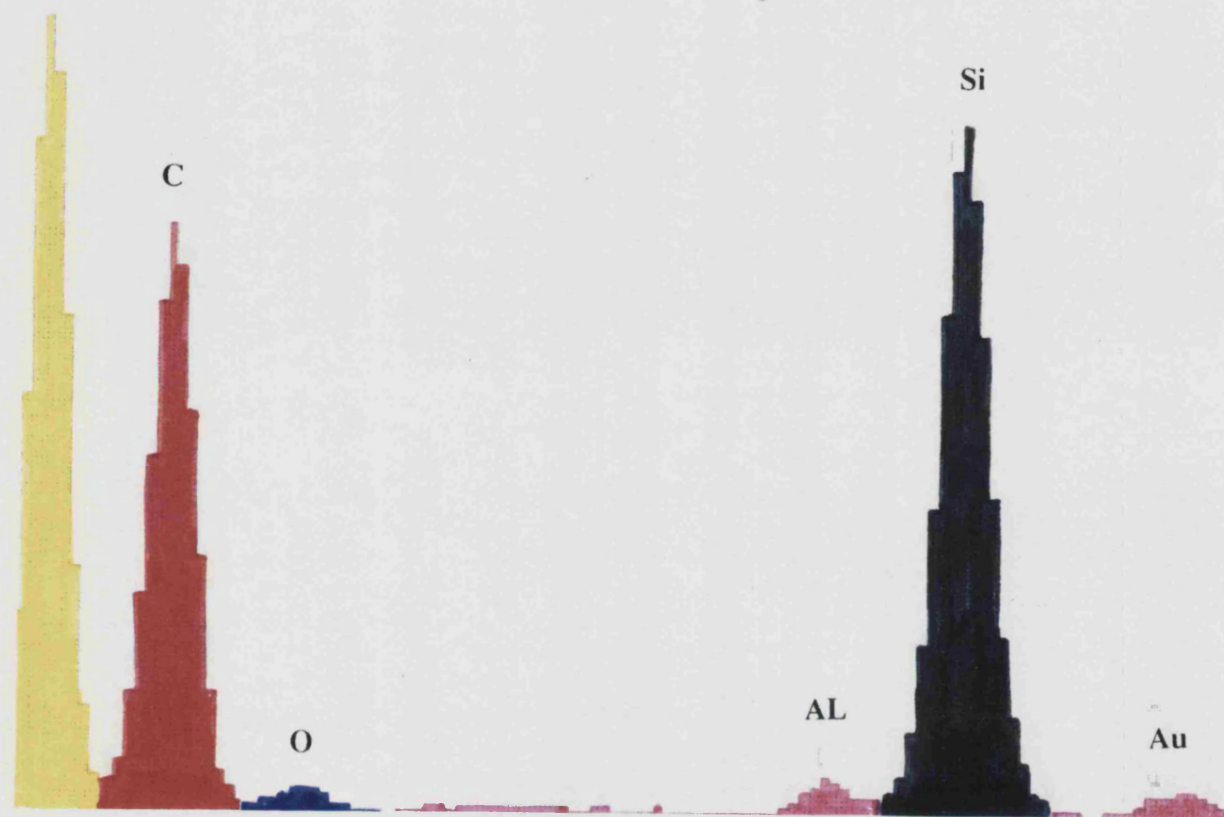


Figure 6.15 Energy dispersive x-ray analysis of standard SiC

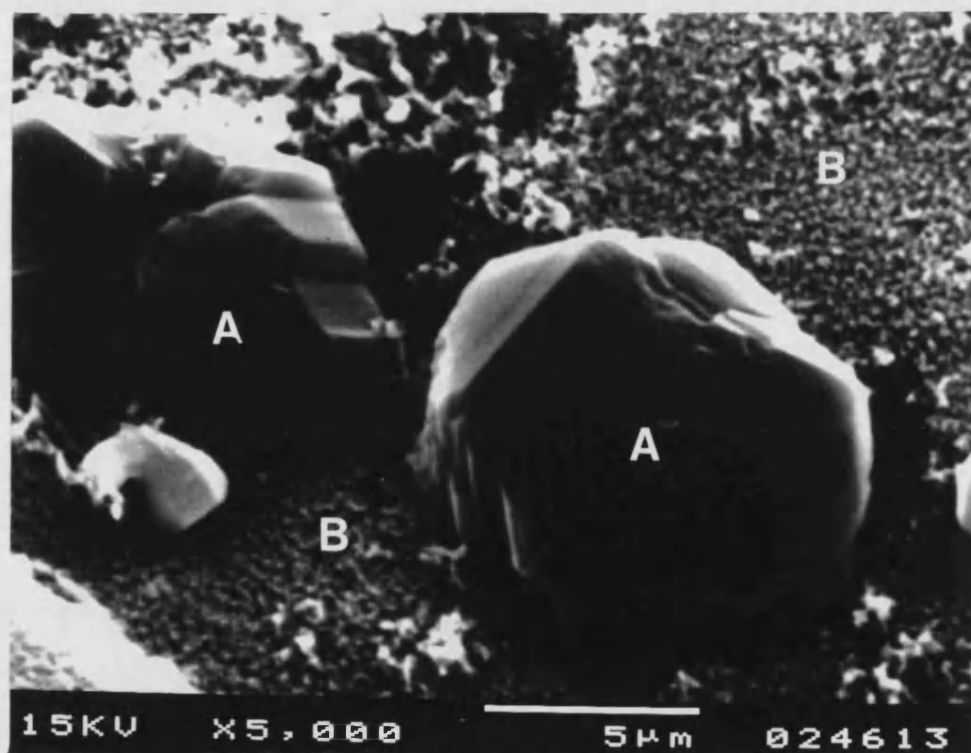


Figure 6.16 Scanning electron micrographs of large crystals of B_4C (A) over microcrystalline SiC matrix (B) and whiskers at (C) from $Ph_2B_2(OSiPh_2)_2O_2$, compound 9, pyrolysed to 1700°C

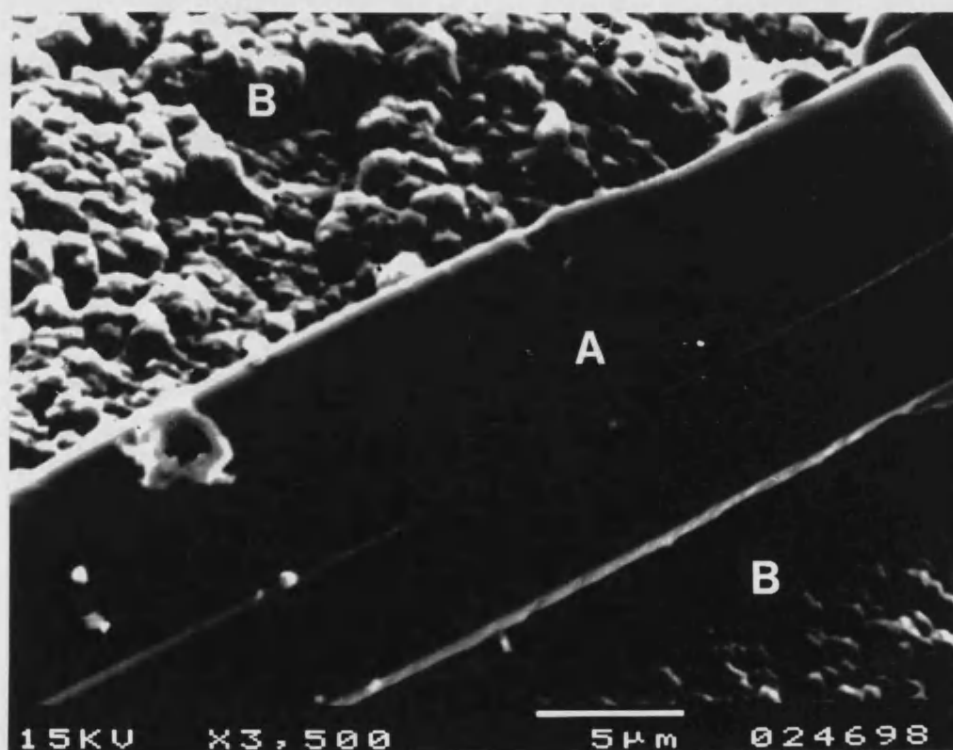
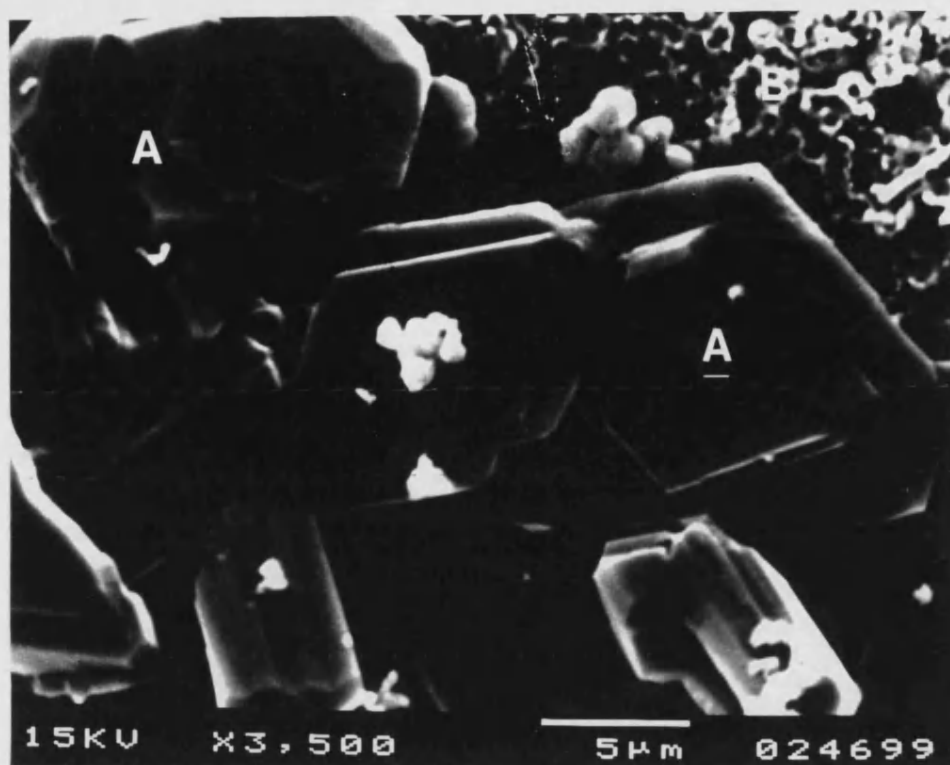


Figure 6.17 Scanning electron micrographs of large crystals of B_4C (A) embedded over microcrystalline SiC matrix (B) from $PhB[(OSiPh_2)_2O]$, compound 10, pyrolysed to $1700^\circ C$

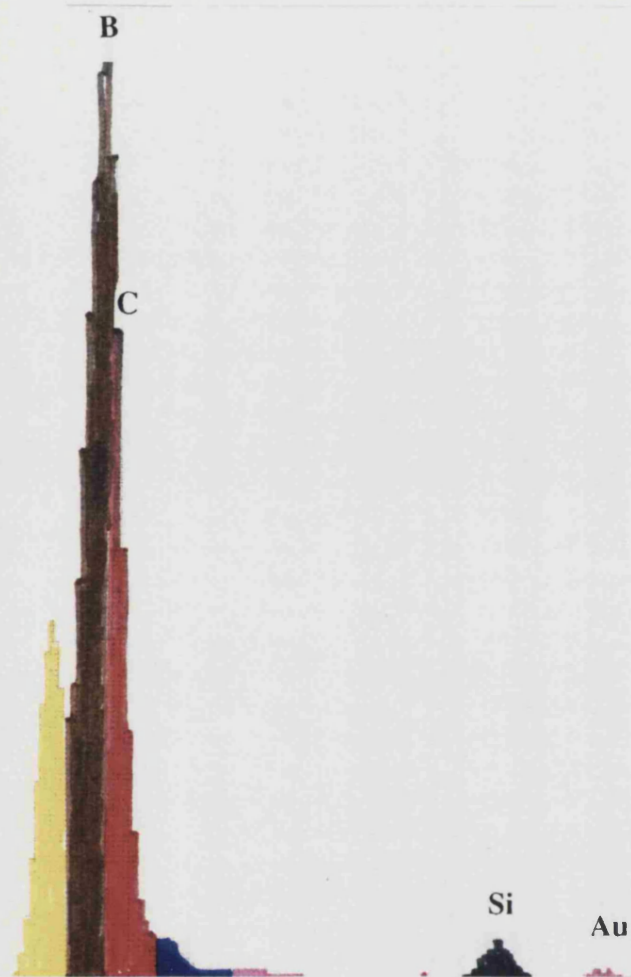


Figure 6.18

Energy dispersive x-ray analysis of the large crystals of B_4C embedded on a microcrystalline matrix of SiC in the residual decomposition product of $Ph_2B_2(OSiPh_2)_2O_2$, compound 9, pyrolysed to $1700^\circ C$

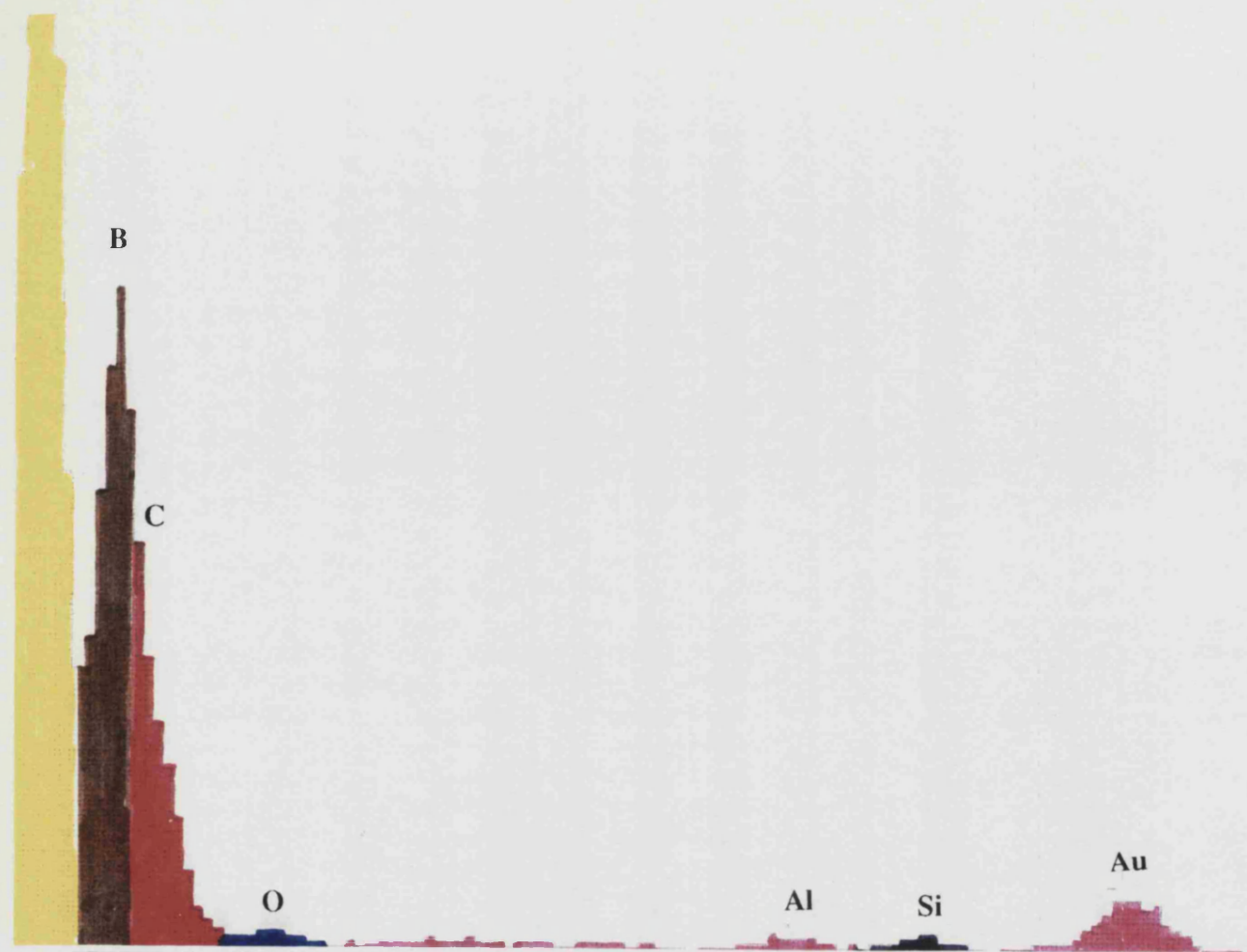


Figure 6.19

Energy dispersive x-ray analysis of the large crystals of B_4C embedded on a microcrystalline matrix of SiC in the residual decomposition product of $PhB[(OSiPh_2)_2O]$, compound 10, pyrolysed to $1700^\circ C$

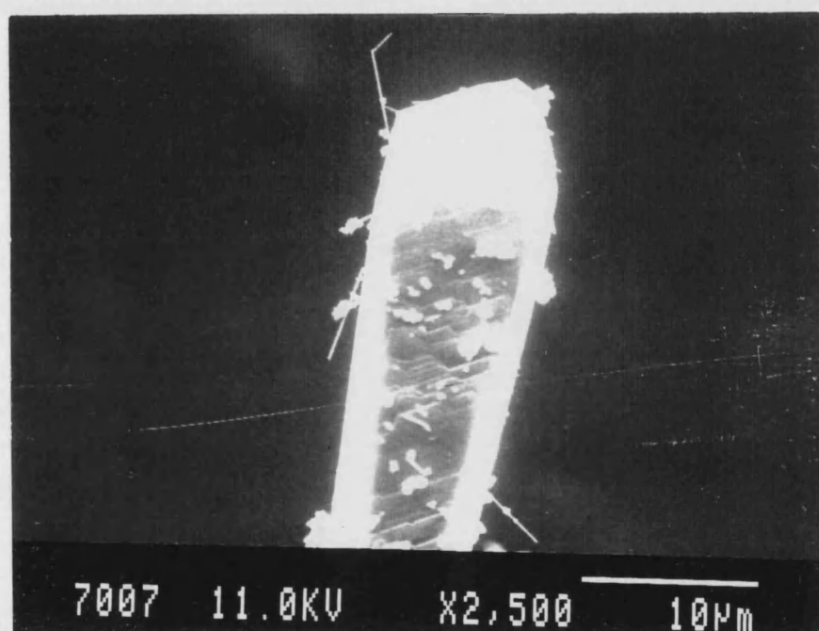


Figure 6.20

Whisker present in the solid residue of $\text{Ph}_2\text{B}_2(\text{OSiPh}_2)_2\text{O}_2$,
compound 9, heated at 1700°C

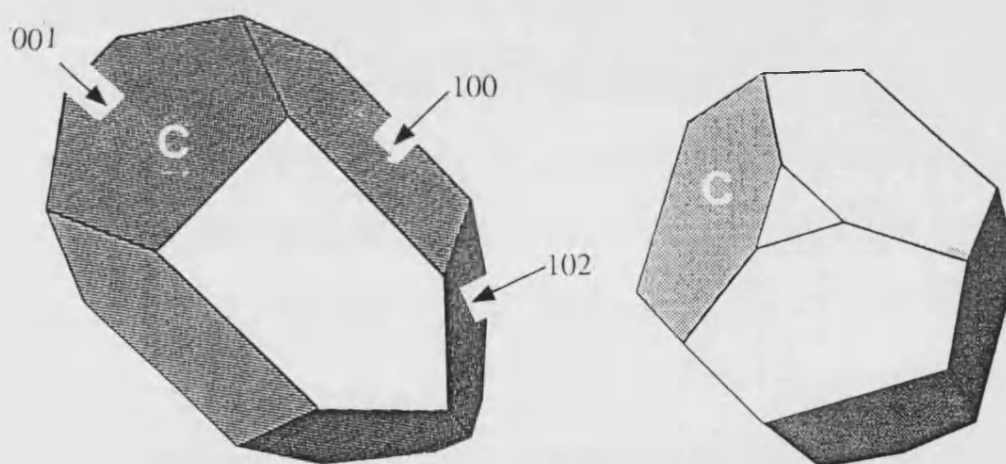
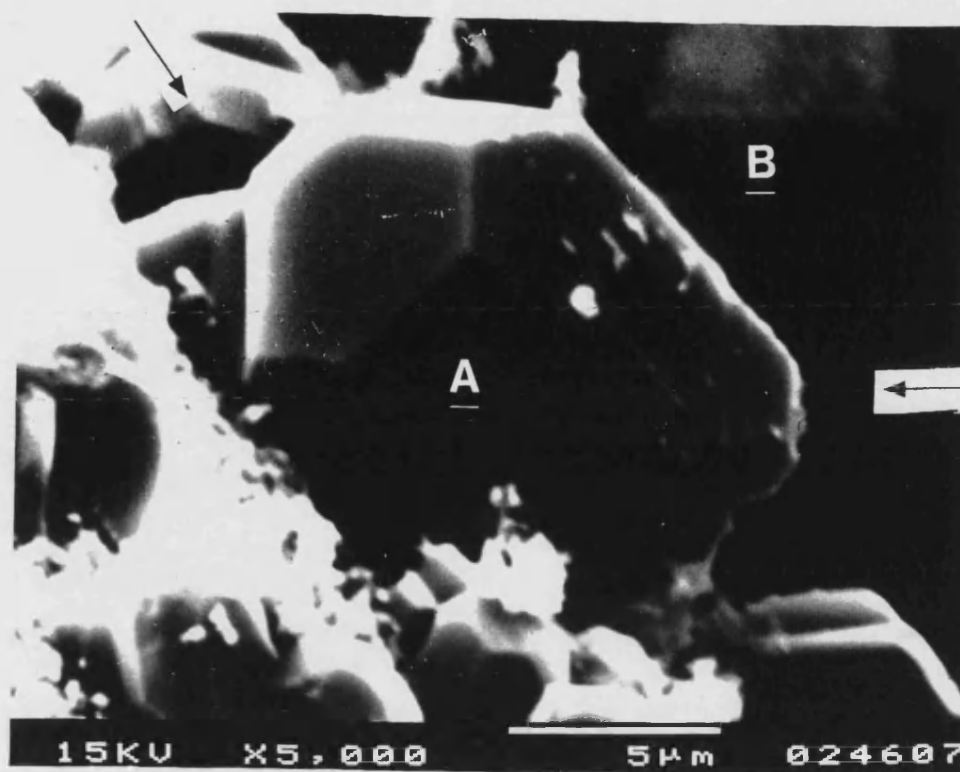


Figure 6.21 Scanning electron micrograph of large crystals of B_4C (A) in a SiC matrix (B) driven from $Ph_2B_2(OSiPh_2)_2O_2$, compound 9, and a computer generated model of B_4C of space group R_3-MH (C)

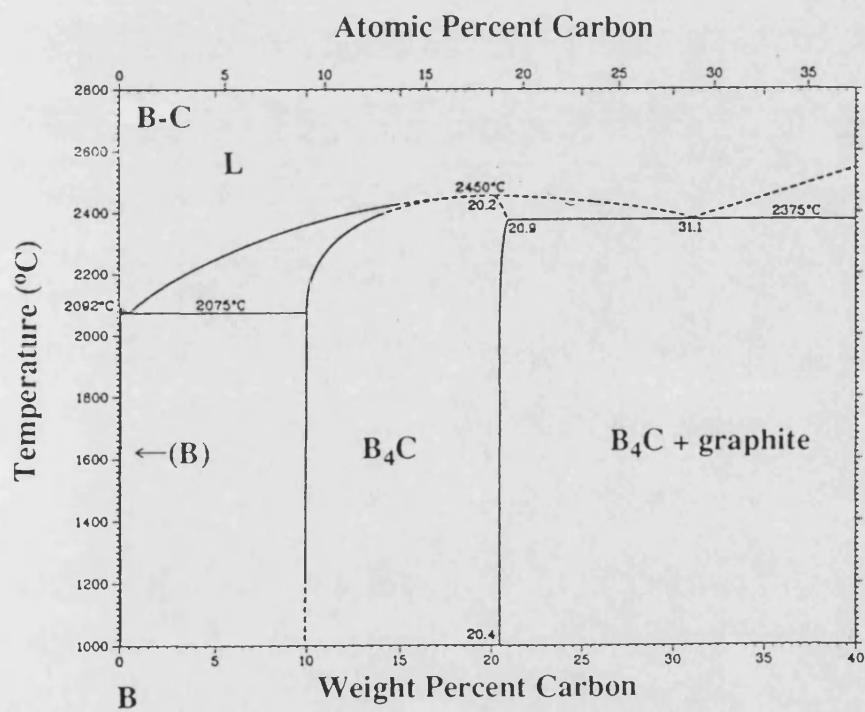
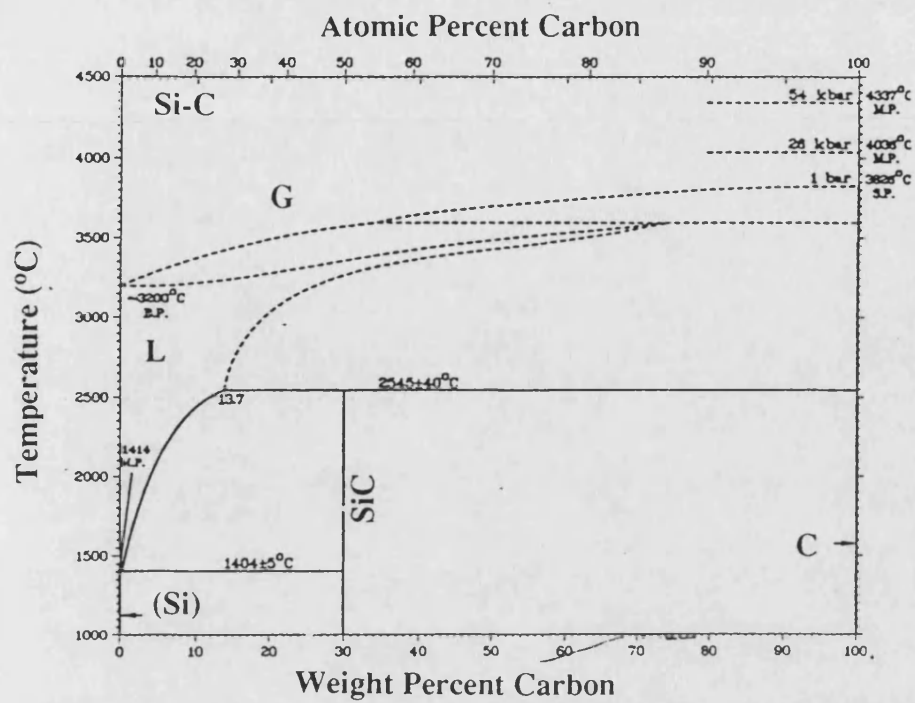


Figure 6.22 Phase diagrams of Si-C and B-C

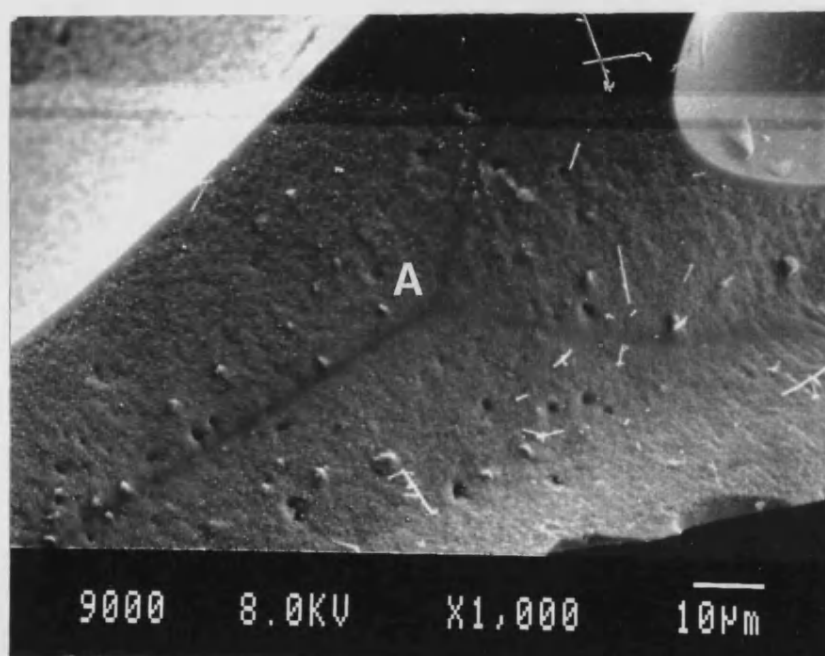
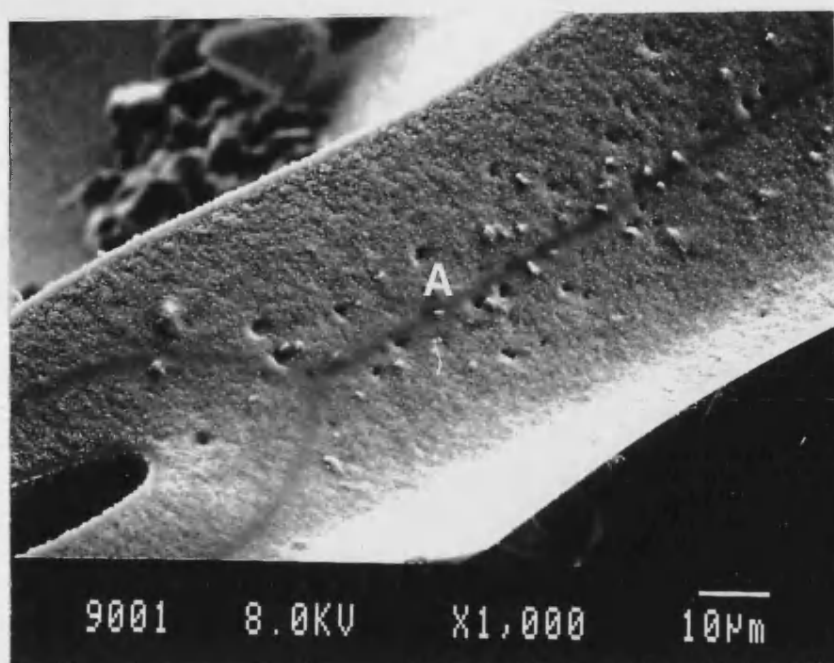


Figure 6.23 Evidence for centre line segregation (A) in the solid residue of $\text{Ph}_2\text{B}_2(\text{OSiPh}_2)_2\text{O}_2$, compound 9, heated at 1700°C

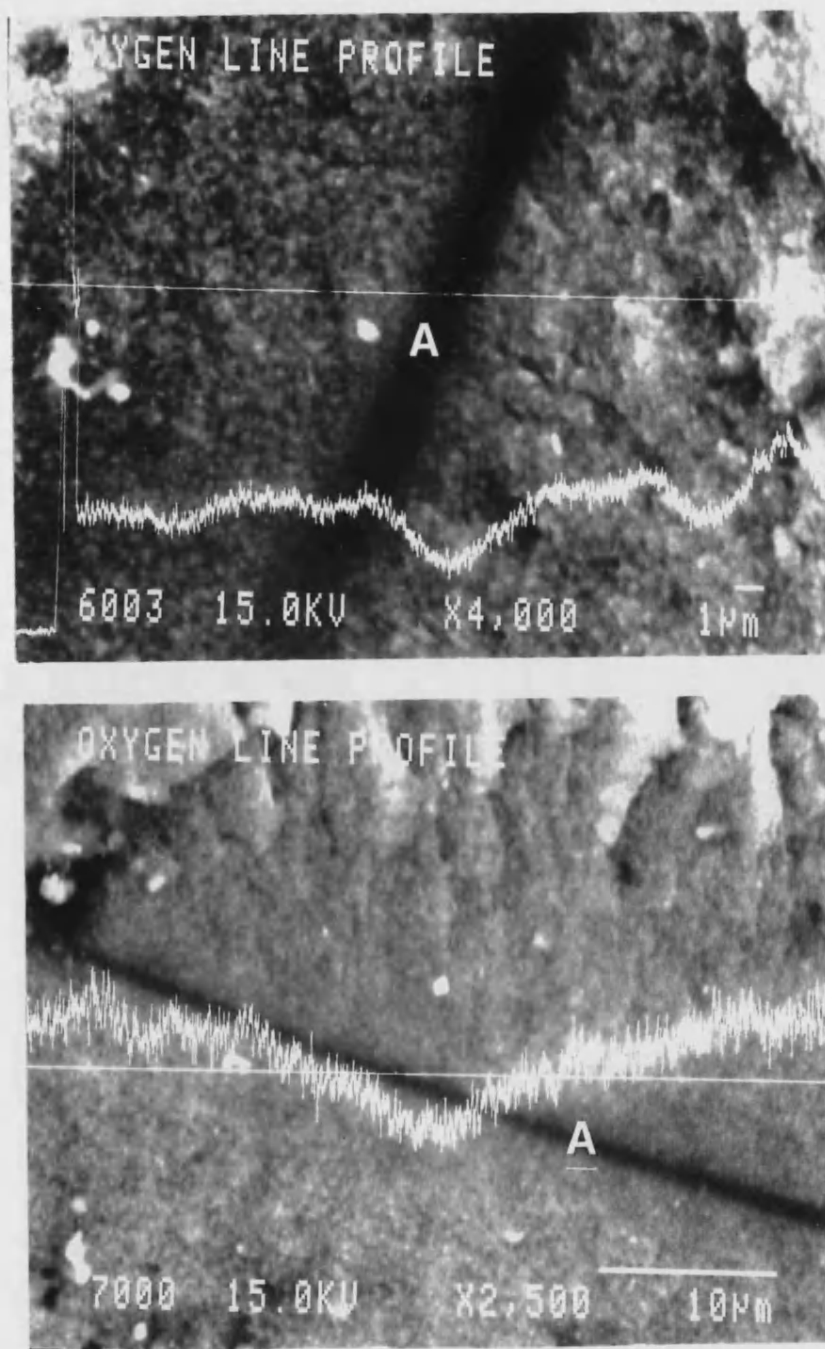


Figure 6.24 EDX line spectra showing the oxygen concentration through the centre line segregation in the solid residue from $\text{Ph}_2\text{B}_2(\text{OSiPh}_2)_2\text{O}_2$, compound 9, heated at 1700°C

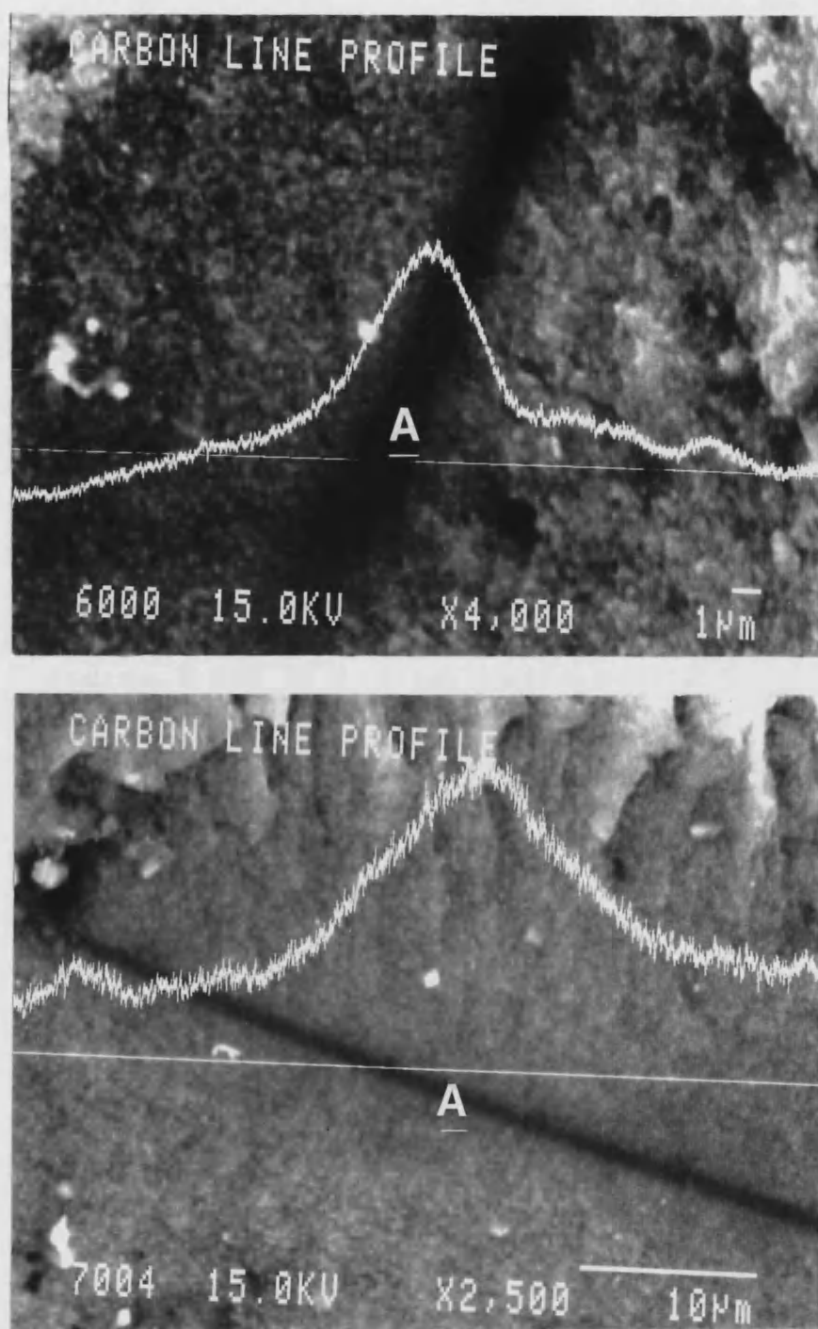


Figure 6.25 EDX line spectra showing the carbon concentration through the centre line segregation in the final residue from $\text{Ph}_2\text{B}_2(\text{OSiPh}_2)_2\text{O}_2$, compound 9, heated at 1700°C

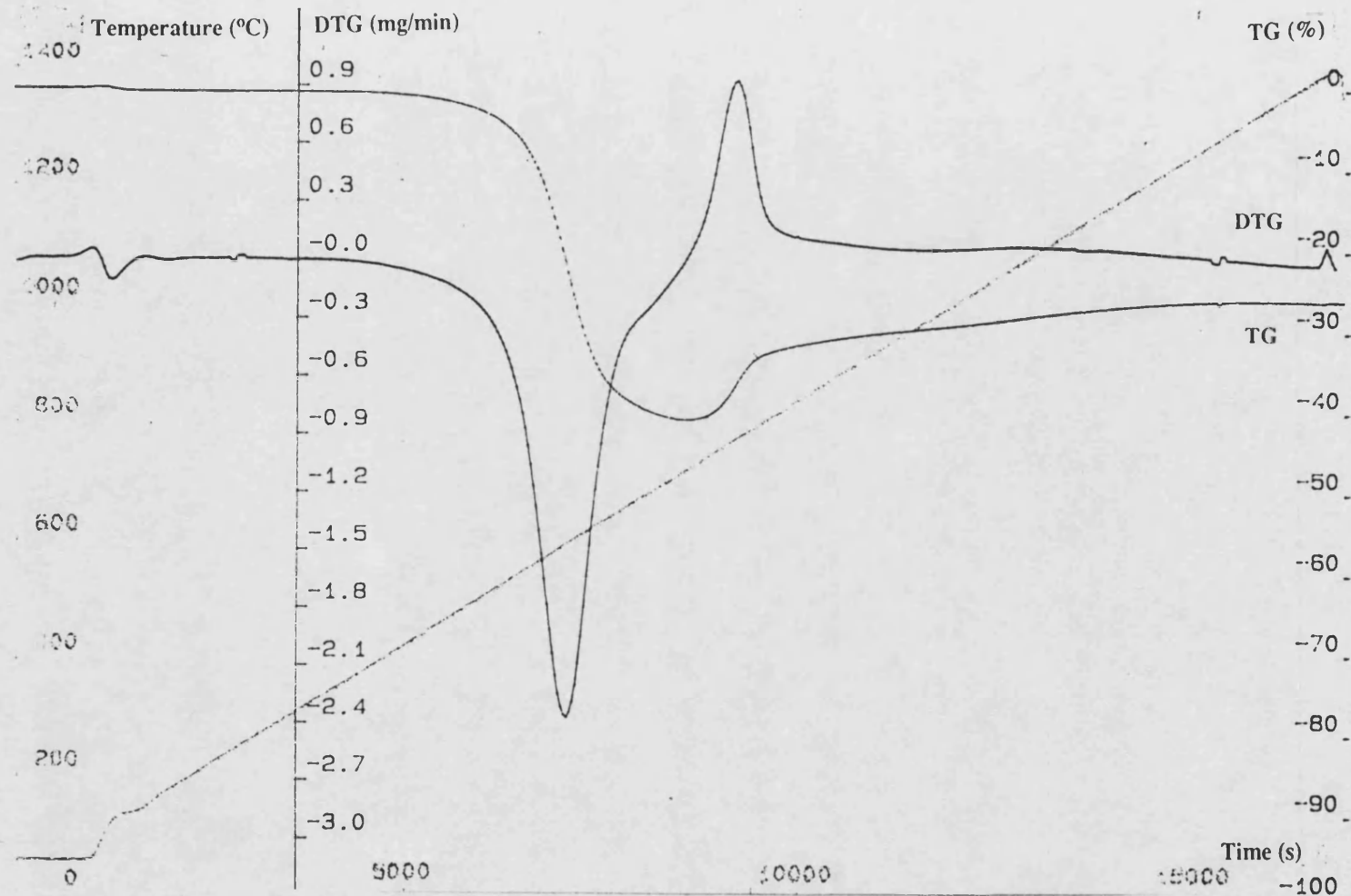


Figure 6.26

Thermogravimetric analysis of the solid residue heated at 1700°C from $\text{Ph}_2\text{B}_2(\text{OSiPh}_2)_2\text{O}_2$, compound 9, then heated to 1200°C in an air stream

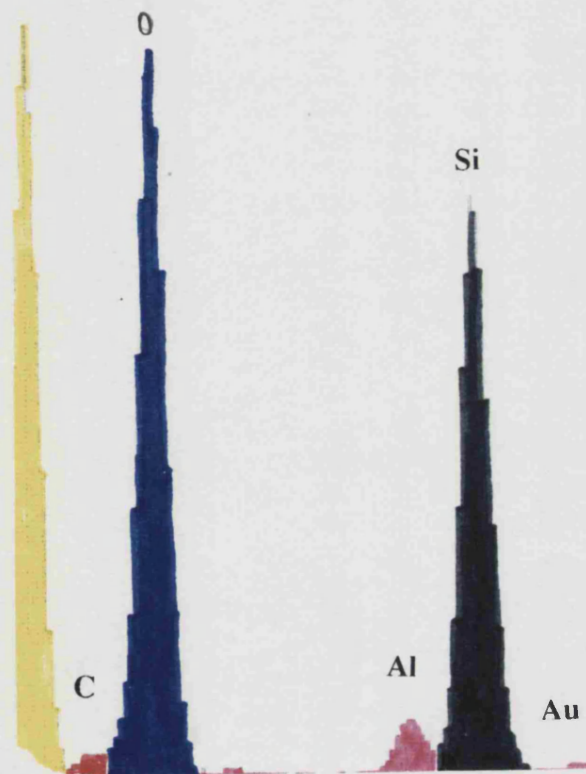


Figure 6.27

Energy dispersive x-ray analysis of the solid residue heated at 1700°C from $\text{Ph}_2\text{B}_2(\text{OSiPh}_2)_2\text{O}_2$, compound 9, then heated to 1200°C in an air stream

6.4 THERMOLYSIS OF OTHER COMPOUNDS CONTAINING Si, C, B and O or N

Thermogravimetric analyses of other cyclic compounds (Me_2SiO)₃, (Ph_2SiO)₃ and (PhBO)₃ were carried out. The curves of weight loss versus temperature/time for (Me_2SiO)₃ and (Ph_2SiO)₃, Figures 6.28 and 6.29 respectively, show that complete volatilisation occurs for both cyclosiloxanes by 300° and 500°C respectively. It was shown in chapter 5 that the ring strain in the small ring cycloborasiloxanes contributes to ring-opening and polymerisation. The amount of ring strain in the cyclosiloxanes, (RSiO)₃ is expected to be considerably lower than in the cycloborasiloxanes, compounds 9 and 10, as been discussed in chapter 5. Consequently, volatilisation of the cyclosiloxanes takes place before ring-opening and polymerisation can occur.

The cycloboroxane (PhBO)₃ decomposed and lost about 77 wt % when it was pyrolysed to 800°C under an inert atmosphere, Figure 6.30. X-ray diffraction of the solid residual product shows major x-ray absorptions for B(OH)_3 at 6.08, 3.18 (100), 2.95 and 1.59 Å. The bond strengths of B-O and B-C (808 and 448 kJ mol⁻¹ respectively), suggest that scission of the B-C bonds occurs first, which facilitates the formation of the boron oxide B_2O_3 , which readily forms B(OH)_3 when subsequently exposed to humid air.

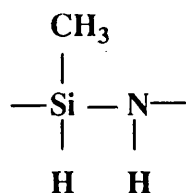
Other linear borosiloxanes synthesised during the course of this study, compounds 15-18, were also thermally analysed, and the thermal treatment resulted in their almost complete volatilisation by *ca* 500°C. Figure 6.31 shows the thermogravimetric analysis curve for $\text{PhB(OSiPh}_3)_2$ (compound 16). This behaviour may be attributed to their linear unstrained structures, which therefore show no tendency to polymerise, Chapter 5, compared with their cyclic analogues, such as $\text{Ph}_2\text{B}_2(\text{OSiPh})_2\text{O}_2$ and $\text{PhB[(OSiPh}_2)_2\text{O]}$ (compound 9 and 10 respectively). The single exception is $\text{PhB(OSiPh}_2\text{H})_2$, compound 14 that contains silicon hydride bonds (Si-H), and which decomposes under an inert atmosphere on heating to 800°C to yield 40 wt% solid residue. The initiation temperature for thermal decomposition of compound 14 is about 200°C, and the thermal

decomposition takes place in two major steps; the first step is in the 220-450°C range, and the second step in the 400-550°C range, Figure 6.32. The first decomposition step involves about 35% weight loss, and the total weight lost is 60%. The decomposition of compound 14 may be linked to the presence of the silicon hydride groups, which are thermally unstable and facilitate polymerisation on heat treatment via Si-H to Si-Si and/or (in the presence of traces of air) Si-O-Si linkages. A sample of compound 14 was also heated for 3 days at 220°C in an oven. Figure 6.2 shows its weight loss versus time curve compared with those of compounds 9 and 10. The total weight loss for compound 14 occurs in two stages, a 10% weight loss after 2.5 hours and a 15% loss after 40 hours. A yellowish residue was formed during this isothermal heat treatment whose infrared spectrum shows a very significant reduction of the Si-H absorptions at 2150 and 1010 cm⁻¹, due to elimination of hydrogen. The thermal decomposition of compound 14 is worthy of a more extensive examination than was possible in the time available at the end of this study.

In the final stages of this work attempts were made to pyrolyse a model compound Me₂Si(NHBPh)₂NH, (compound 19) containing a cyclic Si-N-B ring with a 2:1 boron to silicon ratio. The thermogravimetric analysis of compound 19 shows that the sample is completely volatilised when a temperature of 300°C is reached, Figure 6.33. A single crystal structure determination of compound 19 was carried out during the course of this study in order to investigate the nature of ring-strain in heterosilazane rings containing boron atoms for comparison with heterocyclic siloxanes containing boron, Chapter 5. Complete volatilisation of this compound indicates that ring-ring transformation reactions of the Si-N-B ring system are not fast at elevated temperatures and so no cross-linking occurs before volatilisation. This is an interesting result as two boron atoms per ring would be expected to exert a strong destabilising effect and it would be worth examining the effect of heat treatment with a ring-opening catalyst.

Previous work has shown that the ammonolysis of organochlorosilicon hydrides, RSiHCl₂ and diorganodichlorosilane, R₂SiCl₂ (R= alkyl and aryl), gives cyclic products, (RSiH₂NH)_n and (R₂SiNH)_n, respectively²¹. The product from MeSiHCl₂ consists mainly

of cyclic species $(\text{MeSiHNNH})_n$, $n = 3$ and larger, with $n = 4$ being the major constituent, and possibly some linear products as well. To be utilized effectively in pyrolytic preceramic synthesis, these cyclic compounds must be converted to products of higher molecular weight. Attempted pyrolysis of these materials gives mainly a cyclic species. The residue consists of a structural repeating unit of



The adjacent NH and SiH groups provide the functionality which permits the molecular weight to be increased by dehydrogenation followed by condensation.

By pyrolysis up to 1400°C under nitrogen atmosphere, a residue containing $\alpha\text{-Si}_3\text{N}_4$ was detected²².

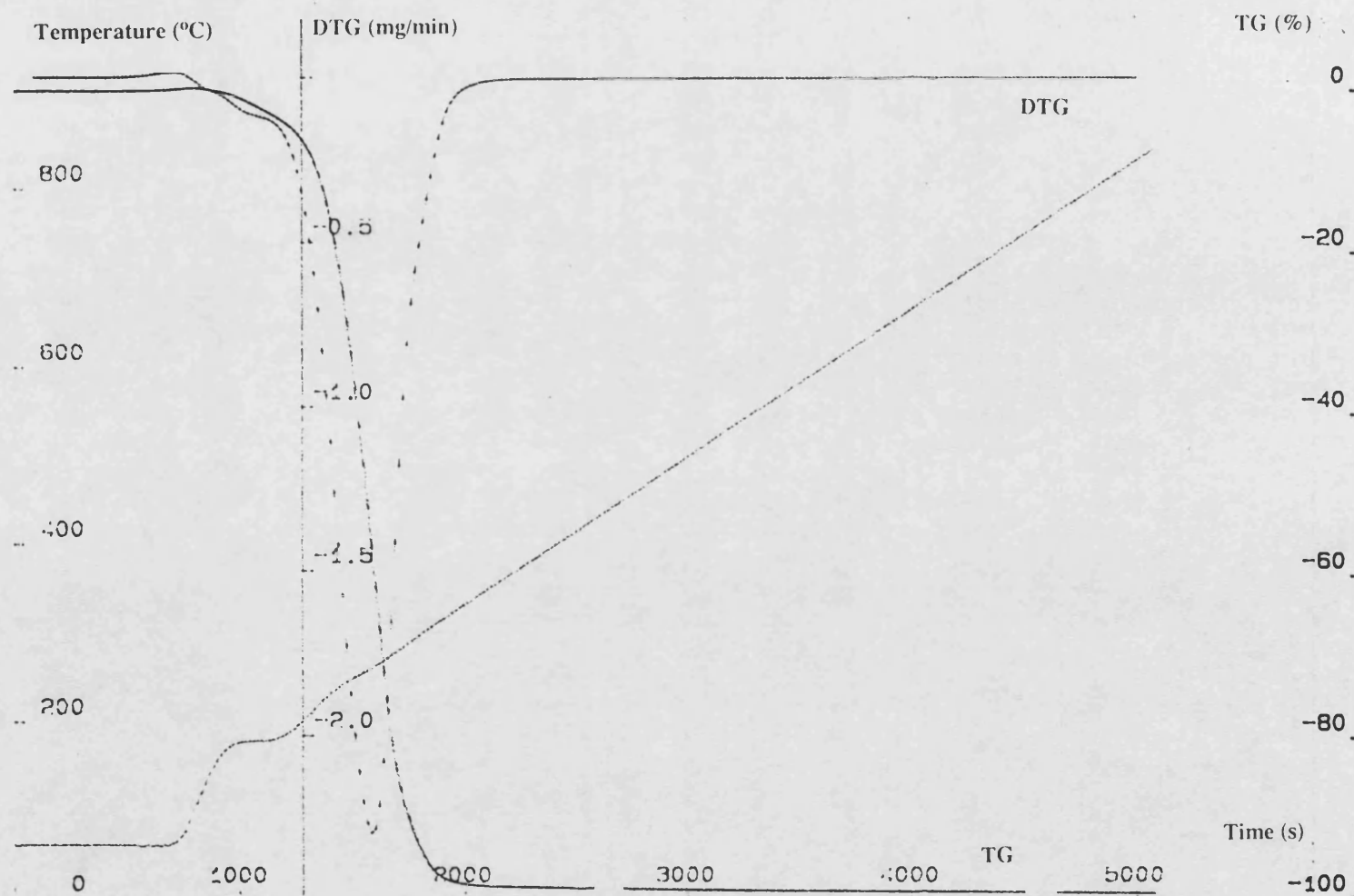


Figure 6.28 Thermogravimetric analysis of $(\text{Me}_2\text{SiO})_3$ in a stream of He

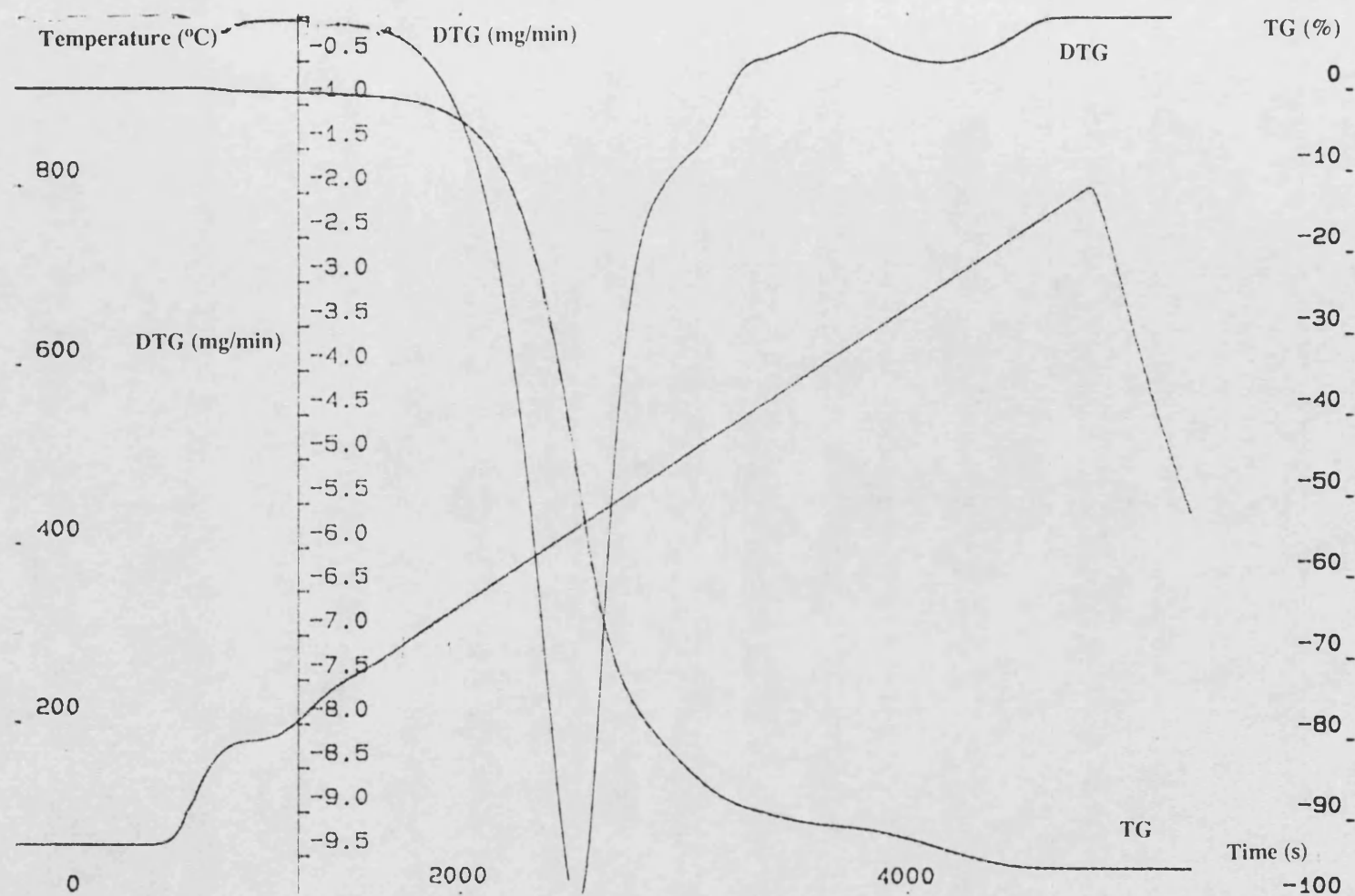


Figure 6.29 Thermogravimetric analysis of $(\text{Ph}_2\text{SiO})_3$ in a stream of He

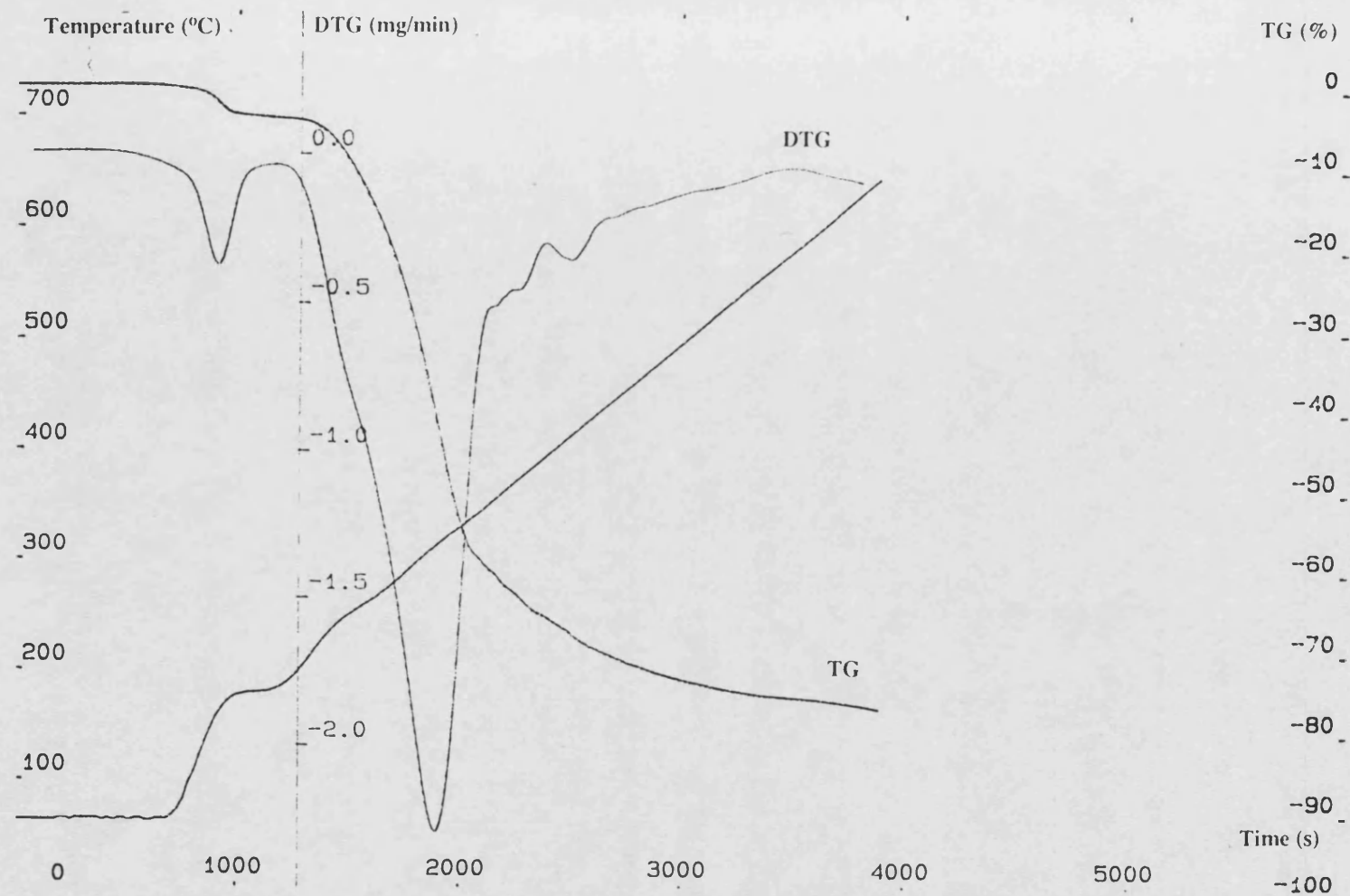


Figure 6.30

Thermogravimetric analysis of $(\text{PhBO})_3$, compound 4, in a stream of He

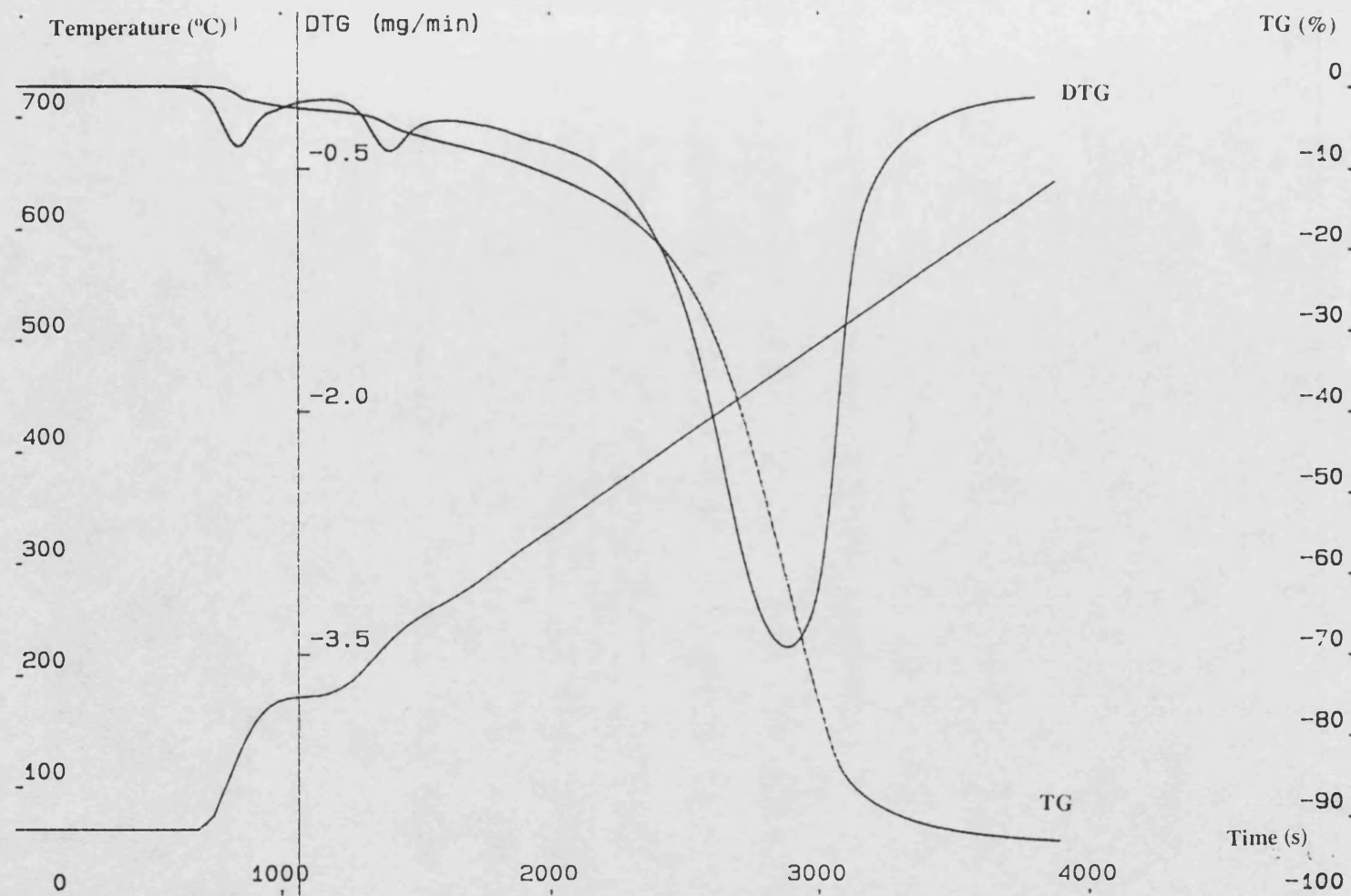


Figure 6.31

Thermogravimetric analysis of $\text{PhB(OSiPh}_3)_2$, compound 16, to 600°C in a stream of He

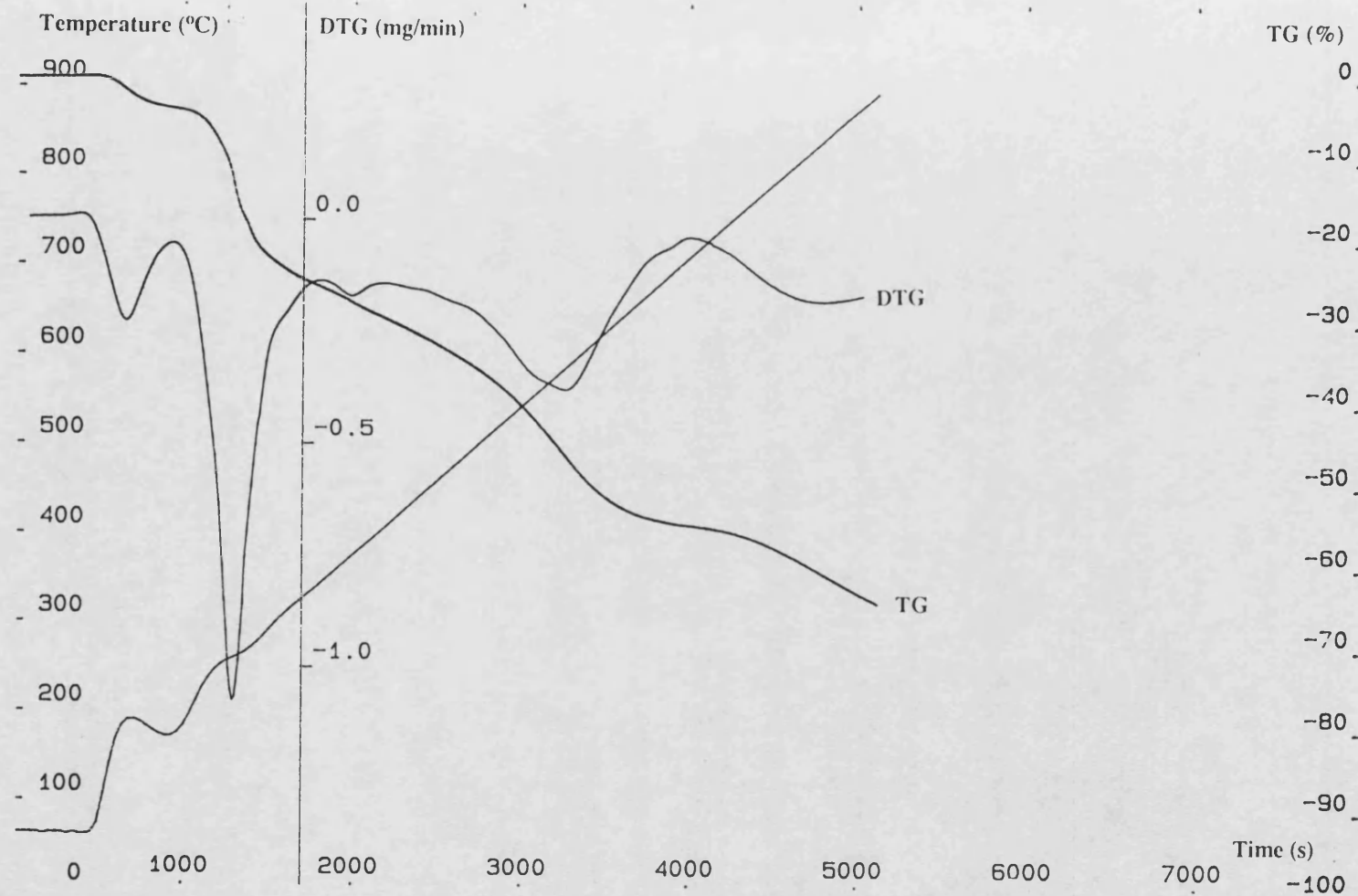


Figure 6.32 Thermogravimetric analysis of $\text{PhB(OSiPh}_2\text{H)}_2$, compound 14, to 800 $^{\circ}\text{C}$ in a stream of He

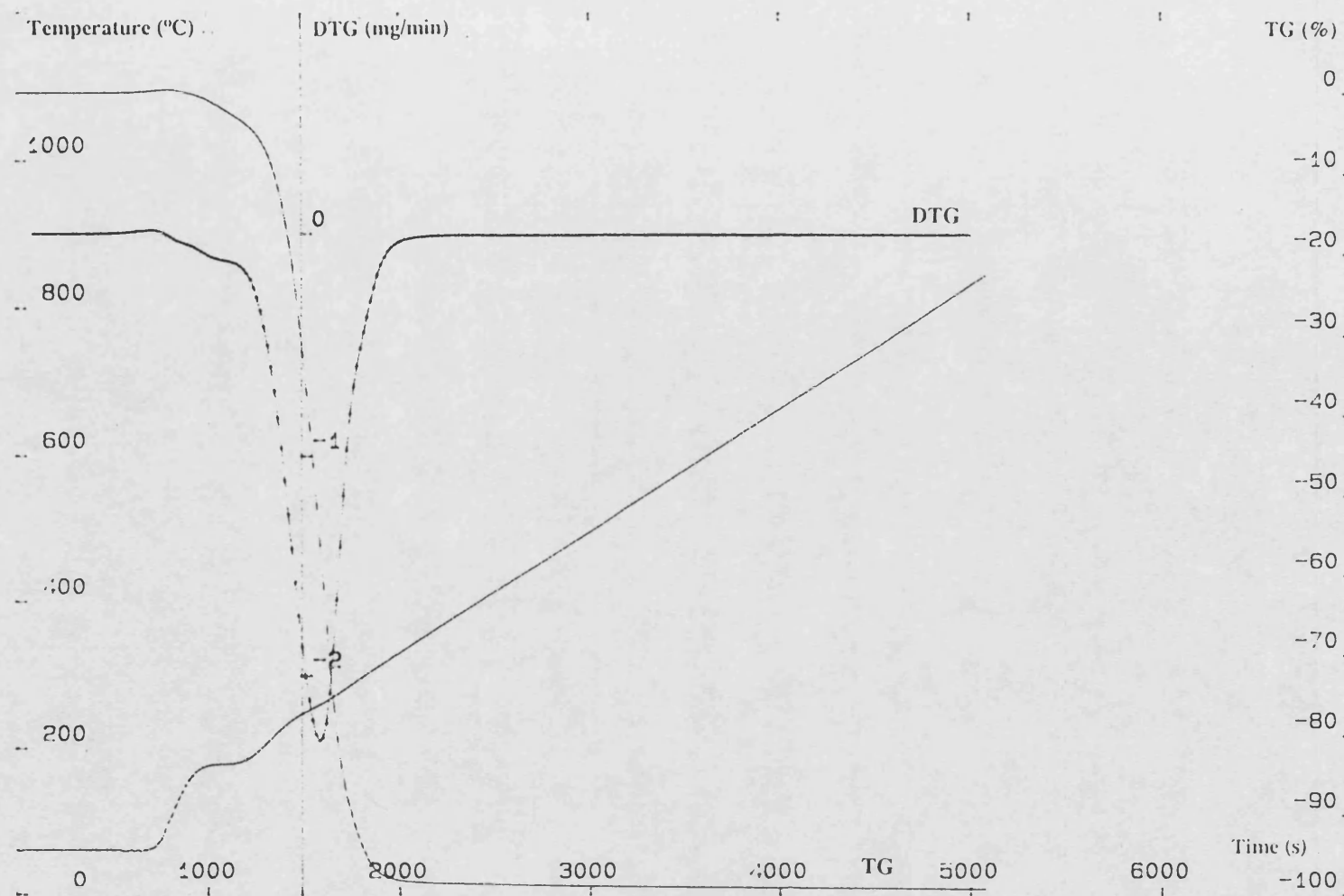


Figure 6.33

Thermogravimetric analysis of $\text{Me}_2\text{Si}(\text{PhBNH})_2\text{NH}$, compound 19,
to 800°C in a stream of He

6.5 THERMOLYSIS OF PHENYLMETHYLSILANE-DIMETHYLSILANE COPOLYMER

For comparison purposes a phenylmethylsilane copolymer was also thermolysed and briefly examined as a precursor for silicon carbide. Thermogravimetric analysis was performed on samples of $(\text{MePhSi})_n(\text{Me}_2\text{Si})_m$, (compound 20) prepared using the method of Burkhard²³. The curve of weight loss versus temperature/time for this compound is shown in Figure 6.34. The copolymer loses 80% of its weight upon heating under He at 10°C/min up to 800°C. The initial thermal decomposition started at 130°C, and it takes place in three major steps. The first step occurs in the 130-380°C temperature range, the second in the 380-520°C range, and the third decomposition step is in the 600-720°C range. The percentage weight losses were 40, 30 and 10% of the total weight lost, respectively.



The theoretical weight loss according to the equation above yielding pure SiC as the final product is 55%, so 25% of the sample must have been driven off as volatile silicon species. These are likely to be small ring cyclics, but it would be of great interest to determine the exact identity of the volatile Si products produced during the thermogravimetric analysis, which would help in identifying the chemical mechanism of degradation.

The solid residue from the thermal decomposition up to 800°C of compound 20 was a shiny black amorphous glass as indicated by x-ray diffraction. Scanning electron microscopy with energy dispersive x-ray analysis shows the presence of both Si and C atoms, as shown in Figure 6.35. Pyrolysis of the compound 20 up to 1700°C under an argon atmosphere yielded crystalline silicon carbide, as detected by x-ray diffraction

which shows major peaks at 2.51 (100), 1.54 and 1.31 Å attributable to ^{considerable} ~~octahedral~~ SiC. Scanning electron micrographs of the silicon carbide formed at 1700°C are shown in Figure 6.36. This type of polymer shows considerable promise as a precursor of SiC. West²⁴ has reported the thermal decomposition of (Me₂Si)_n, and found that 90% of the sample was volatilised at 400°C and the residue volatilised completely at 650°C. He has also used the same copolymer as in this work, i.e phenylmethylsilane-dimethylsilane as a precursor for forming silicon carbide fibres. He showed that the copolymer was easily drawn into fibres by hand with a metal spatula, from a sample with M_n= 12000. Some of the fibres formed hollow tubes because they tended to curl when drawn²⁴.

Wesson and Williams showed that block copolymers containing (Me₂Si)_n and (Ph₂Si)_n blocks can be made²⁵, and Trujillo published the synthesis of the (PhMeSi)_n homopolymer²⁶. Other possible precursors to SiC reported recently include the 3-dimensional polysilanes made by Baney and coworkers²⁷, polycarbosilanes obtained from vinylsilanes¹³. West and Davide reported that copolymers of phenylmethylsilylene and dimethylsilylene units, with Me₂Si/PhMeSi ratios varying from 3:1 to 20:1, were less crystalline and could be softened to viscous liquids at high temperatures. These materials proved useful in strengthening silicon nitride ceramics. The Si₃N₄ ceramic body was soaked in polysilane and refired, leading to the formation of silicon carbide in the pore spaces and a resultant increase in strength²⁸.

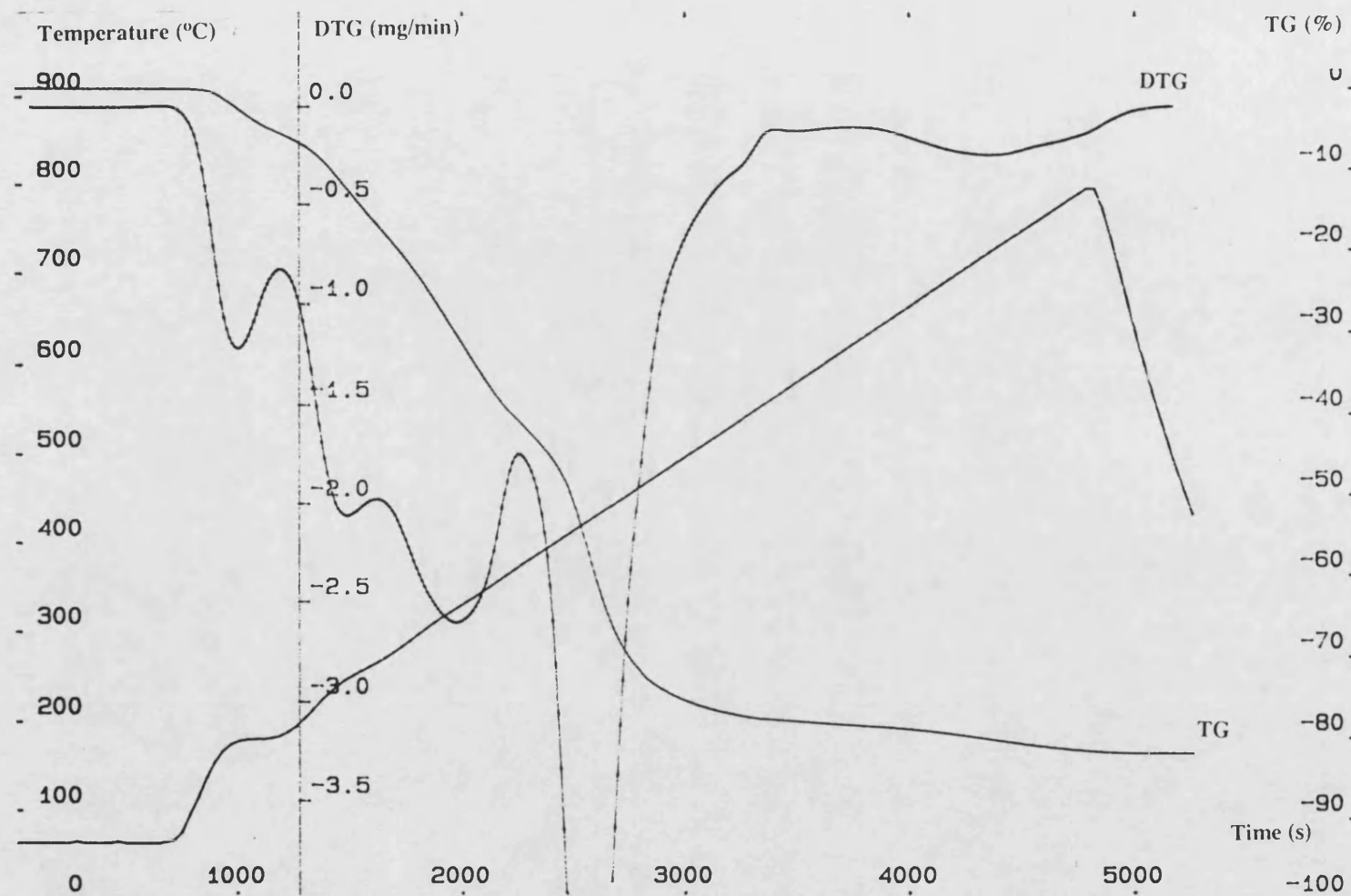


Figure 6.34

Thermogravimetric analysis of $(\text{MePhSi})_n(\text{Me}_2\text{Si})_m$, compound 20, to 800°C in a stream of He

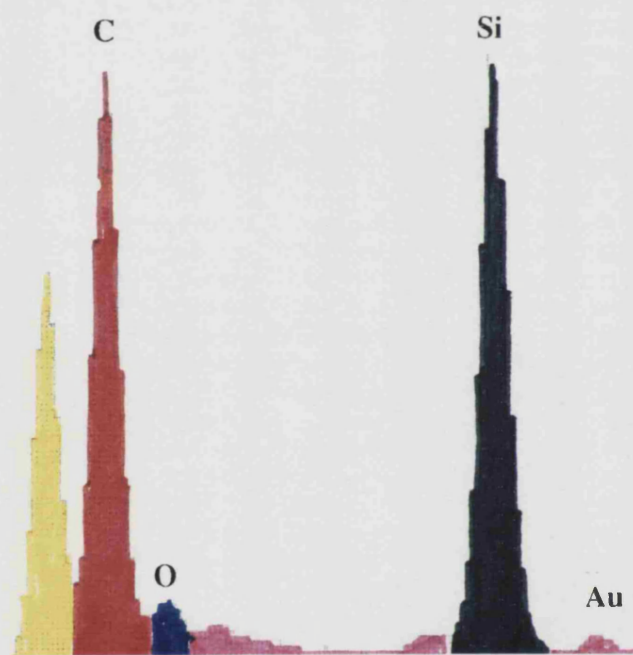


Figure 6.35

Energy dispersive x-ray analysis of the solid residue from $(\text{MePhSi})_n(\text{Me}_2\text{Si})_m$, compound 20, heated to 800°C in an inert atmosphere

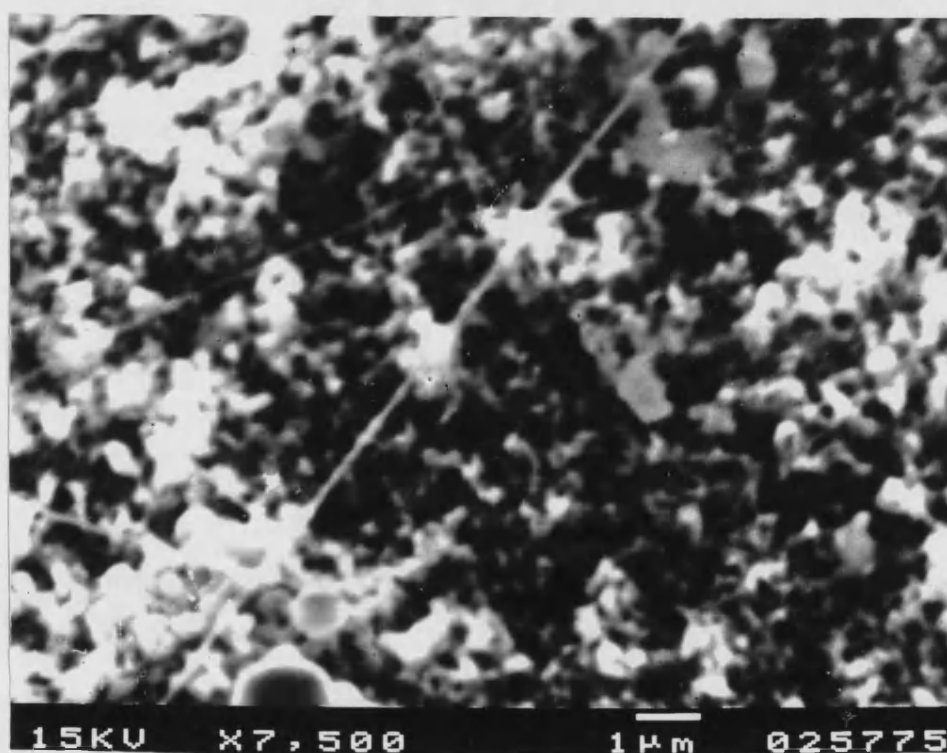
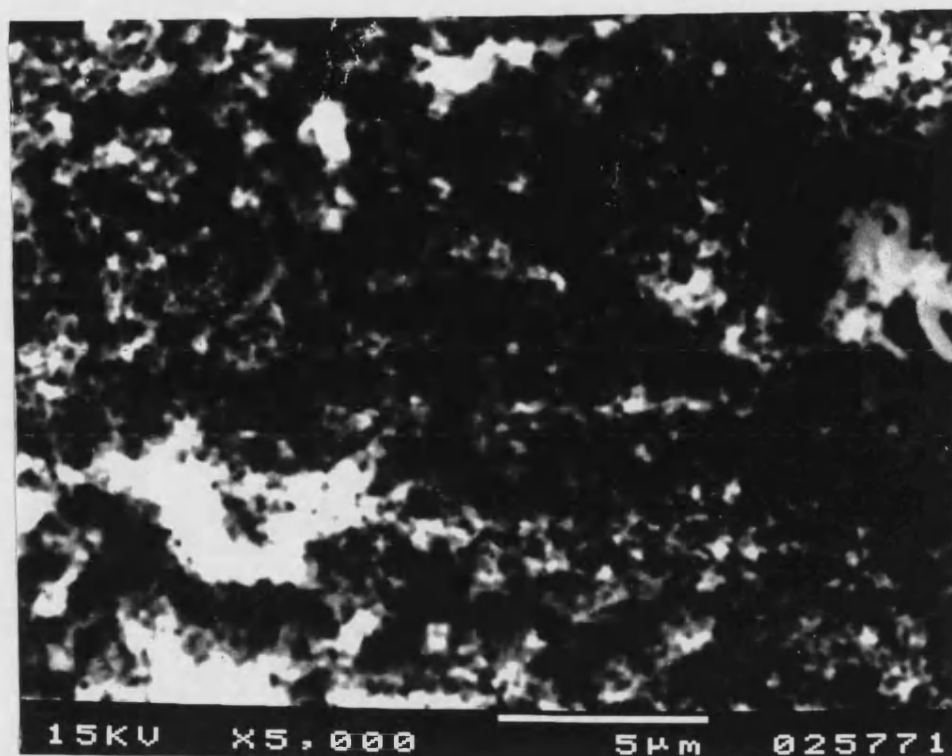


Figure 6.36 Scanning electron micrographs of microcrystalline SiC for $(\text{MePhSi})_n(\text{Me}_2\text{Si})_m$, compound 20, pyrolysed to 1700°C under an argon atmosphere

6.6 THERMOLYSIS OF SILSESQUIOXANES

Thermogravimetric analysis from room temperature to 700°C of $\text{Cy}_6\text{Si}_6\text{O}_9$ (compound 6), which represents a non-volatile model compound of the silsesquioxane series containing Si, O and C, showed that the decomposition occurs gradually above 250°C and it is complete at 600°C, Figure 6.37. A total of 40 wt % of the material is left in the solid residue in the form of an amorphous solid, as indicated by x-ray diffraction. Scanning electron microscopy with energy dispersive x-ray analysis shows peaks for Si, C and O which may be attributed to the formation of amorphous silica and free carbon, and possibly amorphous SiC, Figures 6.38. Further pyrolysis of compound 6 up to 1700°C was carried out in two stages as described for the pyrolysis of compound 9 and 10. The major weight loss occurs in the temperature range 400-600°C, and a further 15% weight loss occurs above 800°C. Scanning electron microscopy with energy dispersive x-ray analysis of the residual product of decomposition at 1700°C shows the presence of Si and O. The carbon atom intensity is significantly reduced during the high temperature heat treatment (1700°C), Figure 6.39. Scanning electron micrographs of microcrystalline SiO_2 as the final residual product of decomposition at 1700°C under an inert atmosphere of compound 6 is shown in Figure 6.40. X-ray diffraction, peaks at 4.05 (100), 3.14 and 2.49 Å are attributed to microcrystalline SiO_2 . On the assumption that all the oxygen reacted with silicon to form microcrystalline SiO_2 , the remaining oxygen reacts with the free carbon forming CO and/or CO_2 gas which volatilized during the high temperature pyrolysis. No evidence of crystalline SiC at high temperature heat treatment of compound 6 was found. This is a fundamentally different situation than that found for the other cyclic borasiloxane compounds 9 and 10 discussed earlier. This situation clearly show the role of boron in these systems, where the boron reacts with oxygen in the early stages of the thermolysis forming B_2O_3 and this facilitates the formation of SiC rather than silica.

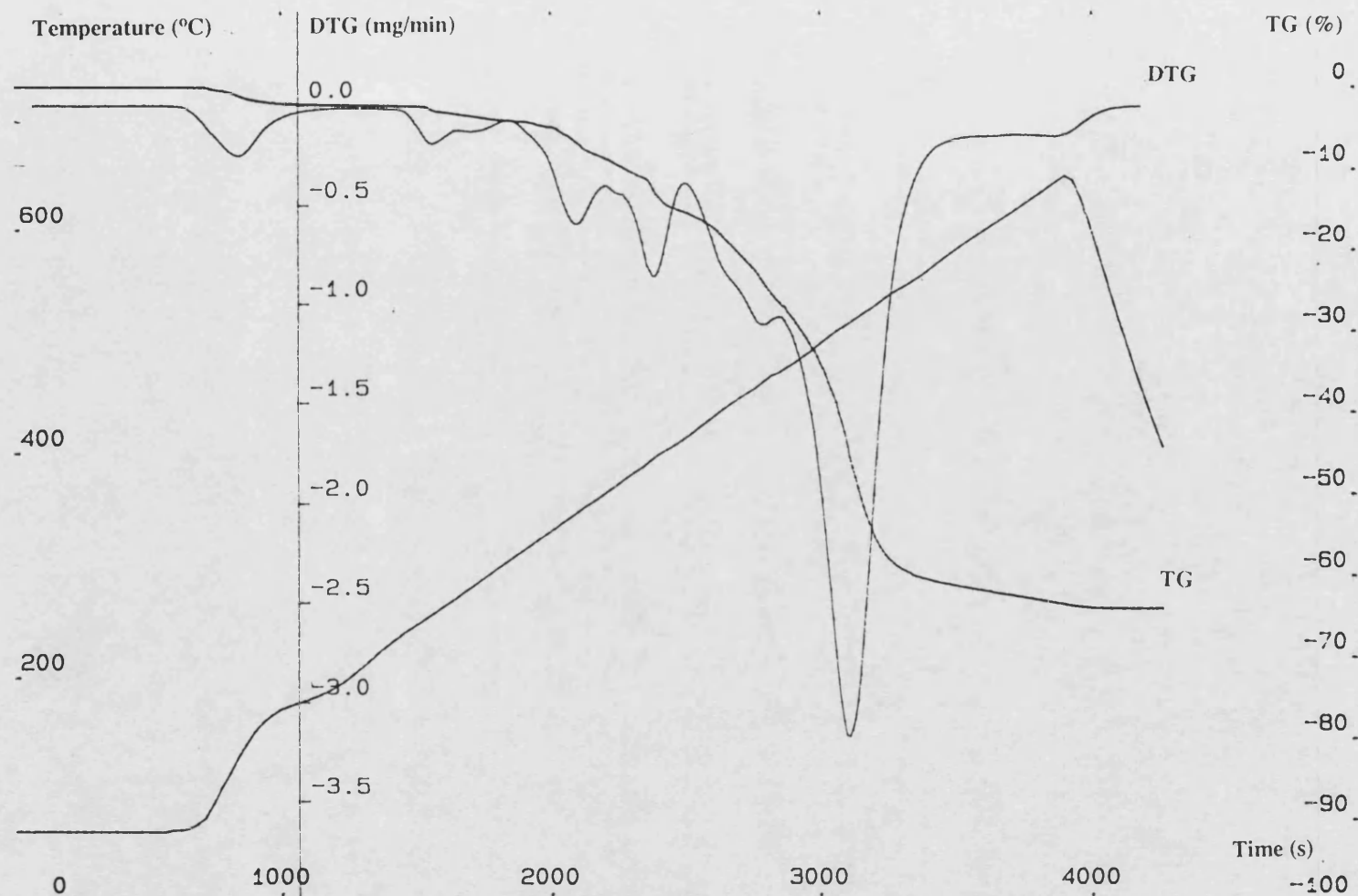


Figure 6.37

Thermogravimetric analysis of $\text{Cy}_6\text{Si}_6\text{O}_9$, compound 6, from room temperature to 600 $^{\circ}\text{C}$ in a stream of He



Figure 6.38 Energy dispersive x-ray analysis of the residue present after heating of $\text{Cy}_6\text{Si}_6\text{O}_9$, compound 6, at 700°C

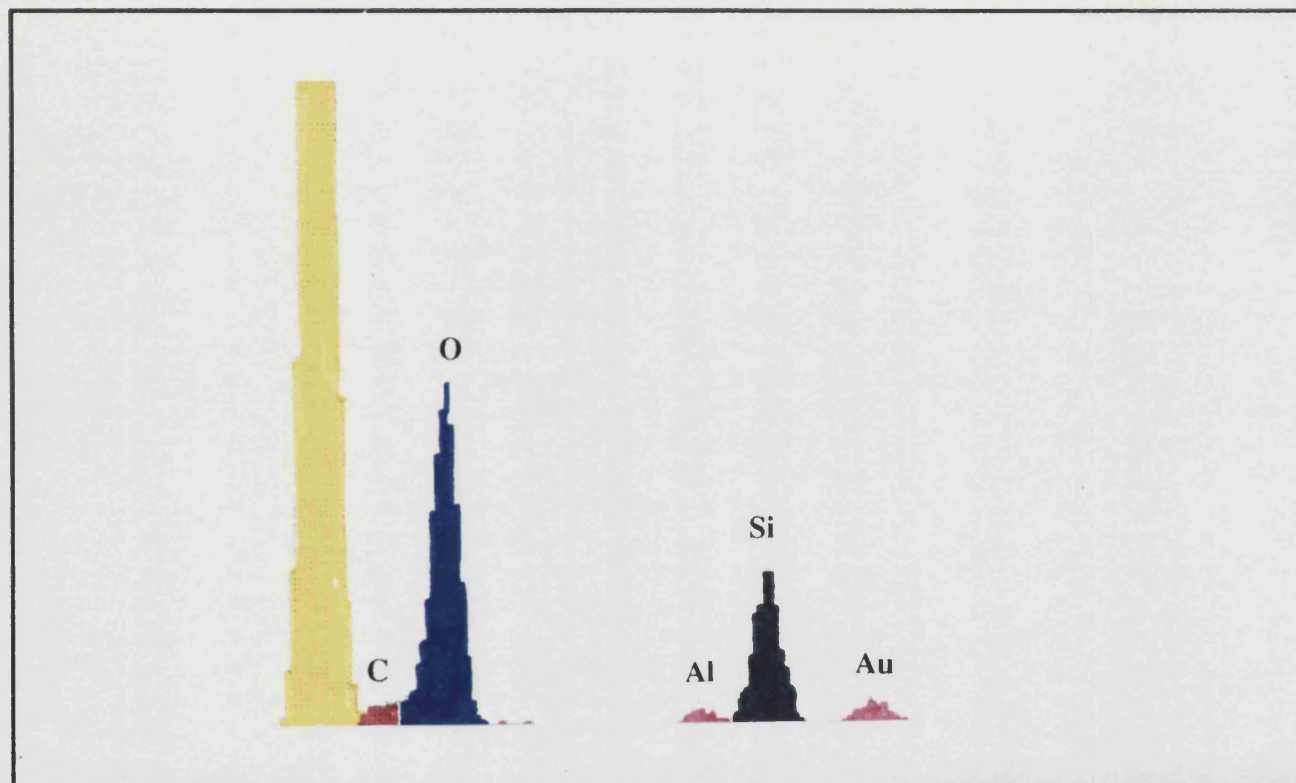


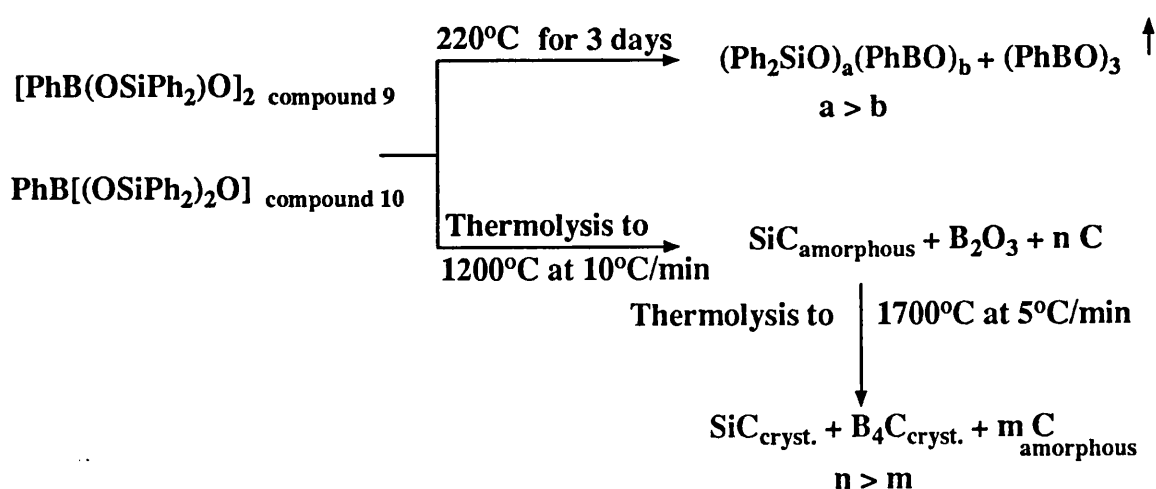
Figure 6.39 Energy dispersive x-ray analysis of microcrystalline SiO_2 from $\text{Cy}_6\text{Si}_6\text{O}_9$, compound 6, pyrolysed to 1700°C under an inert atmosphere



Figure 6.40 Scanning electron micrograph from $\text{Cy}_6\text{Si}_6\text{O}_9$, compound 6, pyrolysed to 1700°C under an inert atmosphere

6.7 CONCLUSIONS

The eight- and six-membered cycloborasiloxanes $[\text{PhB}(\text{OSiPh}_2)\text{O}]_2$ and $\text{PhB}[(\text{OSiPh}_2)_2\text{O}]$ with 1:1 and 2:1 silicon to boron ratios respectively which were synthesised via the reaction of $\text{PhB}(\text{OH})_2$ with diphenylsilandiol and 1,1,3,3-tetraphenyl-1,3-dihydroxy-1,3-disiloxane respectively, contain highly strained rings due mainly to the presence of the small boron atom(s), and both compounds undergo ring-opening polymerisation and ring-ring transformation reactions on thermolysis. Prolonged heat treatment at 220°C , results in volatilisation of the cyclic boroxane $(\text{PhBO})_3$, and the formation of a boron depleted polymeric residue, whereas rapid heating of either compound at a rate of $10^\circ\text{C}/\text{min}$ to 1400°C in an inert atmosphere does not result in significant loss of boron, but affords instead an amorphous residue containing silicon carbide, boron oxide and free carbon. Upon further pyrolysis at 1700°C the final product consists of a microcrystalline α -silicon carbide matrix in which are embedded large crystals of boron carbide.



The linear heteroborasiloxanes $\text{RB(OSiPh}_n\text{H}_{3-n})_2$; ($\text{R} = \text{Ph}$, or Me $n = 2$ or 3) and $\text{B(OSiPh}_3)_3$, containing 1:2 or 1:3 boron to silicon ratios respectively, were prepared by the reaction of B(OMe)_3 or PhB(OH)_2 with triphenylsilanol or diphenylchlorosilane. These were shown via an x-ray crystal structure determination on compound 16, $\text{PhB(OSiPh}_3)_2$, to possess a non-strained configuration, and with the exception of compound 14, $\text{PhB(OSiPh}_2\text{H)}_2$, which contains reactive silicon hydride bonds, they volatilise on heating. Compound 14 thermolyses to a residue containing Si, C and O, presumably via the intermediacy of cross-linked materials formed by hydrogen loss. The most remarkable feature in the structure of compound 16 is the difference in the B-O-Si bond angles being $153.1(3)$ and $136.9(3)^\circ$. These differences arise from a combination of two effects within the linear molecule. Firstly, unlike the cyclic borasiloxanes, there is no ring strain to distort the angles about oxygen, and secondly the phenyl substituents on silicon will prevent a coplanar arrangement around boron in which the Si-O-B angles are equal and acute. No significant changes in the Si-O bond lengths were detected, in agreement with theoretical calculations on Si-O-B containing compounds which indicate that deformation of high angle Si-O-B systems occurs with little change in overall energy²⁹.

These studies show that boron has two main roles in borasiloxanes. In the small ring cyclic compounds it induces ring strain so facilitating ring-opening polymerisation, and at high temperatures it scavenges oxygen and is finally reduced to boron carbide by carbothermal reduction, so minimizing the Si-O content of the final residue. The high temperature behaviour is consistent with thermodynamic considerations.

Hydrolysis of Ph_2SiCl_2 in diethyl ether yields $\text{Ph}_2\text{Si(OH)}_2$ as the major product, which can be separated from higher oligomers by extraction of the mixture. The minor products $\text{Ph}_2(\text{HO})\text{SiOSi(OH)Ph}_2$ and $\text{Ph}_2(\text{HO})\text{SiOSi(Ph}_2\text{)OSi(OH)Ph}_2$ were separated by repeated fractional crystallisation and the structure of the latter compound was shown to contain a novel eight-membered HSi_3O_4 heterocycle, with the two ends of the nominally acyclic array linked through a hydrogen bond. H-bonding between monomers, as inferred

from the short intermolecular O...O separation suggests that dimers are formed in the solid state, consisting of two eight-membered rings linked through an eight-membered O_4H_4 assembly. Although association via H-bonding is common in silanol chemistry³⁰, this compound affords a unique structural arrangement.

The silsesquioxane $c\text{-Cy}_6\text{Si}_6\text{O}_9$ was isolated as one of the products on hydrolysis of $c\text{-CySiCl}_3$ in acetone. The major product is a trisilanol which Feher and co-workers have investigated extensively as a model for silica surface chemistry. By using a comparatively short reaction time, the proportion of $\text{Cy}_6\text{Si}_6\text{O}_9$ is maximised at the expense of the other minor product, a octa-sesquisiloxane in the initial solid mixture, so facilitating purification of the hexamer, albeit at the expense of an overall reduced yield. The $c\text{-Cy}_6\text{Si}_6\text{O}_9$ structure, which had not been determined previously, contains two Si_3O_3 which are linked co-facially by Si-O-Si bridges, generating three further Si_4O_4 heterocycles. A consideration of bond length and bond angle data indicates that the fused Si_3O_3 rings are strained (as in analogous mononuclear siloxane rings), and on thermolysis to 700°C, this compound yields an amorphous solid containing Si, O and C. It was not possible to determine the exact constituents of the solid residue at that stage, but on further heating crystalline SiO_2 is formed with no evidence of crystalline SiC. This behaviour confirms the very important effect boron has on the thermal behaviour of heterosiloxane species.

These studies were extended to a cycloborasilazane $\text{Me}_2\text{Si}(\text{PhBNH})_2\text{NH}$, which was isolated from the reaction of $(\text{Me}_2\text{SiNH})_3$ with PhBCl_2 , in order to determine whether ring-opening polymerisation and subsequent thermolysis would produce Si_3N_4 . Unexpectedly this compound volatilised completely at low temperatures. A structure determination was carried out to further characterise this compound, but in view of the lack of comparative structural data for Si-N-B analogues it is not possible to deduce from these data whether this compound is strained. Even if it does possess ring strain, it may be slow to undergo ring-opening reactions in the absence of a catalyst, which would explain its volatility. It is interesting to note that other routes to Si-N and Si-N-B ceramic materials employ labile or/and reactive substituents on Si or B to facilitate cross-linking.

6.8 FUTURE WORK

The use of preceramic polymers based on hetero-, homo-polymers or ceramers in the synthesis of ceramic materials is currently an active area of research, with considerable attention being focused on silicon-containing materials as precursors to SiC and Si₃N₄. A critical challenge in the design of inorganic-organic composites or polymers for use as precursors is control of their precise stoichiometry. The work described in this thesis shows that preceramic polymers can be produced by the ring-opening polymerisation of simple, strained ring heterosiloxanes of well defined composition, and that ceramic materials are formed on pyrolysis at very high temperatures. Thus the term 'preceramic polymers' should be extended to 'preceramic compounds' to include materials such as those described in this thesis. For future work on these preceramic compounds, the following proposals are suggested.

One practical role for preceramic compounds is as a possible binder to form a green body with ceramic filler particles. an ideal binder would totally fill the open pores present in a body formed from dry powder and it should be converted to a ceramic materials in high yield on pyrolysis. Also, the associated removal of volatiles should occur without damaging the body. In practice, preceramic compounds fall short of this ideal. For example, the yields of the solid residue obtained on heating the heteroborasiloxane, compounds 9 and 10 to 1200°C in inert atmosphere were 35 and 28% respectively, whereas Yajima¹² has shown that the thermal decomposition of poly(borodiphenylsiloxane) in a N₂ atmosphere to 1000°C results in a 47% yield of solid residue. By introducing less bulky substituent on Si such as vinyl groups which could be cross-linked, high ceramic yields would be obtained.

There has been very little work on developing methods for incorporating preceramic compounds as binders in green bodies so as to optimise density. Nor has the transformation of such green bodies to ceramic bodies by firing been studied in any detail. Thus a study of these processes, coupled with measurements of the physical, thermal and

mechanical properties of the bodies would be useful practical development from the present work.

A further development would be to study the thermal decomposition of the preceramic compounds under nitriding conditions to explore the potential for producing Si_3N_4 . It is known that SiO_2 can be converted in the presence of carbon to Si_3N_4 in N_2 or NH_3 containing atmospheres by two-step process involving carbothermal reduction to SiC followed by nitridation to Si_3N_4 ³¹. Thus, the potential to produce Si_3N_4 from the decomposition products of the preceramic compounds studied in this work should be explored.

Finally, this work has provided some useful information on the initial stages of decomposition of the preceramic compounds and on the later stages of decomposition for example, the growth of the SiC and B_4C crystals from compounds 9 and 10. However, the important but very complex processes occurring during the main part of the thermal decomposition are not clear. It would add greatly to our understanding of the transformation of the preceramic compounds if future studies would be directed to this fundamental area.

6.9 REFERENCES

1. M Haoudi, H Schmid, M Noltemeyer and H Roesky, *Z Naturforsch*, 1991, **46b**, 587, and references therein.
2. M M Levitsky, O I Schegolikhina, A A Zhdanov, A V Igonin, Yu Eovchinnikov, V E Shklover and Yu T Struckov, *J Organomet Chem*, 1991, **401**, 199.
3. N S Borisov, G M Voronkov and Y E Lukevits, *Organosilicon Heteropolymers and Heterocompounds*; Plenum: New York, 1970.
4. H R Allcock, M S Coley and I Manners, *Macromolecules*, 1991, **24**, 2024.
5. A D Foucher, J A Lough and I Manners, *J Organomet Chem*, 1991, **414**, C1.
6. H Behbehani, B J Brisdon and B McEnaney, *J Polym Adv Techno*, in press.
7. C J Saam, *Silicon Based Polymer Science*; M J Zeigler and W F G Fearon, Eds.; *Advances in Chemistry* **224**, Am Chem Soc, Washington DC, 1990, 565.
8. M A Hossain, B M Hursthouse, A Ibrahim, M Mazid and A C Sullivan, *J Chem Soc, Dalton Trans*, 1989, 2347 and references therein.
9. I Manners, H G Riding, A J Dodge and H R Allock, *J Am Chem Soc*, 1989, **111**, 3067; I Manners H G Riding, A J Dodge and H R Allock, *J Am Chem Soc*, 1991, **113**, 9596.
10. D A Foucher, A J Lough and I Manners, *Inorg Chem*, 1992, **31**, 3034.
11. K Matyjaszewski, J Hrkach, K H Kim and K Ruehl, *Adv Chem Ser*, 1990, **224**, 285.
12. S Yajima, J Hayashi and K Okamura, *Nature*, 1977, **266**, 521.
13. C L Schilling, J P Wesson and T C Williams, *Am Ceram Soc Bull*, 1983, **62**, 912.
14. A Stone and G Graham, *Inorganic Polymers*, Academic, New York, 1962, 185.
15. L R Vale, *J Chem Soc*, 1960, 2252.
16. S Yajima, *Am Ceram Soc Bull*, 1983, **62**, 893.
17. J Boone, In *Encyclopedia of Chemical Technology*, Wiley Press, 1964, **3**, 676 and **4**, 117.

18. D Hamilton, J Appl Phys, 1960, **31**, 112.
19. F Tone, The Mineral Industry, Hill Publishing Co, New York, 1907, 154.
20. J R Strife and J E Sheehan, Am Ceram Soc Bull, 1988, **67**, 369.
21. D Seyferth and G H Wiseman, J Am Ceram Soc, 1984, **67**, 132.
22. R Fossenden and J S Fossenden, Chem Rev, 1961, **61**, 361.
23. C A Burkhard, J Am Chem Soc, 1949, **71**, 963.
24. R West, L David, P Djurovich and R Sinclar, Am Ceram Soc Bull, 1983, **62**, 899.
25. J P Wesson and T C Williams, J Polymer Sci Polymer Chem Ed, 1981, **19**, 65.
26. R E Trujillo, J Organomet Chem, 1980, **198**, C27.
27. R Baney, UK. Pat. Appl. 2,021,545, Dec 5, 1979.
28. K S Mazdiyasni, R West and L D David, J Am Ceram Soc, 1978, **61**, 504.
29. S Shambayati, J F Blake, S G Wierschke, W L Jorgensen and S L Schreiber, J Am Chem Soc, 1990, **112**, 697.
30. E Lukevics, O Pudova and R Sturkovich, Molecular Structure of Organosilicon Compounds, Ellis Horwood, Chichester, UK, 1989, Chap.3,196 (and references therein); P D Lickiss, A D Redhouse, R J Thompson and K Rozga, J Organometal Chem, 1993, **453**, 13.
31. H Hada and L Wang, Ceram Eng Sci Proc, 1990, **11**, 1463.

APPENDIX (I)

Safety

The toxicological properties of silane and heterosiloxanes have not been fully investigated, and all necessary precaution were taken when using these materials. Thus all synthesis were carried out in high toxicity fume cupboards. Toxic and flammable gases were handled in closed systems within the laboratory and finally vented to atmosphere. The reagents involved in this research are commonly used materials, and the precautions taken when handling them were in accordance with their known hazards. A safety hazard sheet have been used for each reaction contain all the hazard details of the materials involved. A standard safety sheet is attached.

Reagents

All chemicals employed were standard laboratory reagents (BDH or Analar grade) which were used without further purification unless otherwise stated. Benzene and toluene were normally dried over sodium wire for at least 24 hours, and dry solvents were deoxygenated under an atmosphere of dry nitrogen gas prior to use. Diphenylsilanediol, phenylboronic acid, methylboronic acid, dichlorodiphenylsilane, diphenylchlorosilane, triphenylsilanol, trimethylborate, borontriiodide, phenylborondichloride, cyclohexyltrichlorosilane, hexamethylcyclotrisiloxane, hexaphenylcyclotrisiloxane and hexamethylcyclotrisilazane were purchased from Aldrich or from Lancaster, and were used without any further purification unless otherwise stated.

University of Bath

SCHOOL OF CHEMISTRY

COSHH

CHEMICAL AND GENERAL RISK ASSESSMENT

Project Title/Research Area.....

Name of Supervisor.....

Location of Work.....Start Date.....

Hazardous Substance(s)	Class*	Quantity in use	Data Sheet attached /consulted?

*According to *Classification, Packaging & Labelling Regulations, 1988*:

Cg: Carcinogenic; C: Corrosive; H: Harmful; I: Irritant; T: Toxic;

O: Oxidant; F: Flammable; HF: Highly flammable; E: Explosive.

Experimental procedures/system of work to be followed. Indicate transformation under investigation and literature reference, if available.

Full Nature of Reactive Hazards involved (if no Safety Data Sheets attached)
Indicate other general hazards (high pressure/vacuum/high temperatures etc.).

Fume Cupboard Classification
required (tick)

Any special containment
required (specify)

Low toxicity

Medium toxicity

High toxicity

Other safeguards/protective clothing required:

NOTE: Safety glasses MUST be worn at ALL times.

Waste Disposal (tick as appropriate)

Chlorinated Solvent Bottle Non-Chlorinated Solvent Bottle

Chlorinated & Other Solvent Bottle

Waste water drainage Solid waste disposal

Special action in case of spillage/service (power/water) failure.

Include any other precautions that have not been recorded above.

Personnel who carried out the assessment:

Staff Member (block caps)

Signature:

.

Date:

Researcher (block caps)

Signature:

.

Date:

APPENDIX (II)

Instrumentation

Microelemental Analysis:

Carbon, hydrogen and nitrogen analyses were determined by microelemental techniques by the Analytical Services, School of Chemistry, University of Bath.

Infrared Spectroscopy (IR):

Infrared spectra were recorded on a Nicolet 510P infrared spectrophotometer in the region of 4000-600 cm^{-1} , samples were prepared as mulls using paraffin and held between NaCl discs.

Nuclear Magnetic Resonance (NMR):

Samples for ^1H and ^{13}C NMR measurements were prepared using deuterated chloroform as solvent unless otherwise stated. Spectra were recorded on JEOL GX 270 FT NMR spectrometer (operating at 67.80 and 270.05 MHz for ^{13}C and ^1H measurements respectively) and were referenced to TMS. ^{29}Si NMR samples were dissolved in deuterated chloroform with TMS as internal standard in some cases. ^{29}Si NMR spectra were recorded using a JEOL GX 400 spectrometer housed at the School of Chemistry, University of Bristol and a JEOL GXE 400 spectrometer housed at the school of Chemistry, University of Bath.

Mass Spectroscopy (MS):

Mass spectra data were recorded using a VG 7070E spectrometer housed at the School of Chemistry, University of Bath.

X-Ray Powder Diffraction (XRD):

X-Ray powder diffraction studies were carried out on various samples which resulted from thermally treated siloxanes and borasiloxane.

X-Ray Crystallography:

X-ray single crystal structure determinations were carried out at room temperature using A Hilger and Watts Y290 Four-Circle diffractometer and more recently a CAD4 automatic four circle diffractometer.

Scanning Electron Microscopy (SEM):

samples were mounted on aluminium discs and were gold coated for 1 minute. A list of the SEM equipments are listed below:

JEOL T330 Scanning Electron Microscopy

JEOL JSM 35C Scanning Electron microscopy with oxford instrument link A 10000 energy dispersive x-ray analyser.

JEOL 8600 Electron probe microanalyser.

All SEM facilities were placed at the School of Material Science, University of Bath.

Thermal Heat Treatments:

Thermogravimetric analysis (TGA):

TGA were carried out on ca 70 mg samples loaded into an alumina crucible using a SETARAM TGA-92, with argon as a carrier gas. Tests were carried out under different atmospheres of helium, nitrogen or air, with a heating rate of either 5°C/min. or 10°C/min. to a maximum temperature of 1500°C.

Tube furnace experiments:

A tubular Carbolite furnace was used to pyrolyse samples of ca 0.1g to 800°C under an argon or air atmosphere at a heating rate of 2°C/min.

High temperature heat treatment:

An Astro industries INC, USA furnace were used to pyrolyse samples to 1700 or 1750°C under an argon atmosphere after the pre-heat treatment with the tube furnace. A holder made of carbon was used to hold the alumina crucibles in the astro furnace.

APPENDIX (III)

X-ray crystallography supplementary tables for hexa(cyclohexylsesquioxane),
compound 6

Table 1 Fractional atomic coordinates and thermal parameters (Å) for
Cy₆Si₆O₉ compound 6

Atom	x	y	z	Uiso or Ueq (***)	
Si1	0.5251 (3)	0.2500	0.3230 (1)	0.038 (2)	***
Si2	0.6201 (2)	0.1703 (1)	0.2174 (1)	0.040 (1)	***
Si3	0.2629 (3)	0.2500	0.2559 (1)	0.037 (2)	***
Si4	0.3615 (2)	0.1705 (1)	0.1508 (1)	0.037 (1)	***
O1	0.5835 (5)	0.1797 (3)	0.2893 (2)	0.041 (3)	***
O2	0.6580 (7)	0.2500	0.1929 (4)	0.043 (5)	***
O3	0.2773 (5)	0.1799 (3)	0.2105 (2)	0.039 (3)	***
O4	0.3720 (7)	0.2500	0.1197 (3)	0.041 (5)	***
O5	0.4994 (5)	0.1429 (3)	0.1744 (2)	0.043 (3)	***
O6	0.3746 (7)	0.2500	0.3096 (3)	0.039 (5)	***
Si5	0.0153 (3)	-0.2500	0.1938 (1)	0.036 (2)	***
Si6	0.1098 (2)	-0.1707 (1)	0.3060 (1)	0.037 (1)	***
Si7	-0.2474 (3)	-0.2500	0.2435 (1)	0.036 (2)	***
Si8	-0.1491 (2)	-0.1708 (1)	0.3552 (1)	0.038 (1)	***
O7	0.0728 (5)	-0.1797 (3)	0.2317 (2)	0.037 (3)	***
O8	0.1507 (7)	-0.2500	0.3331 (4)	0.041 (5)	***
O9	-0.2321 (5)	-0.1799 (3)	0.2892 (2)	0.041 (3)	***
O10	-0.1398 (7)	-0.2500	0.3879 (4)	0.044 (5)	***
O11	-0.0109 (5)	-0.1436 (3)	0.3410 (3)	0.043 (3)	***
O12	-0.1352 (6)	-0.2500	0.1975 (3)	0.038 (4)	***
C1	0.5610 (10)	0.2500	0.4081 (6)	0.054 (3)	
C2	0.5112 (10)	0.1828 (6)	0.4394 (5)	0.076 (3)	
C3	0.5443 (12)	0.1841 (8)	0.5111 (6)	0.099 (4)	
C4	0.4977 (12)	0.2500	0.5408 (7)	0.102 (6)	
C5	0.7530 (8)	0.1080 (5)	0.2137 (4)	0.054 (2)	
C6	0.8502 (11)	0.1337 (7)	0.1715 (6)	0.090 (4)	

Table 1 **continued...**

C7	0.9637 (12)	0.0838 (7)	0.1719 (6)	0.093 (4)
C8	0.9293 (10)	0.0084 (6)	0.1571 (5)	0.071 (3)
C9	0.8314 (11)	-0.0172 (7)	0.1954 (6)	0.094 (4)
C10	0.7154 (10)	0.0307 (6)	0.1949 (5)	0.076 (3)
C11	0.1162 (10)	0.2500	0.2934 (5)	0.039 (3)
C12	0.1003 (8)	0.1829 (5)	0.3347 (4)	0.058 (2)
C13	-0.0202 (10)	0.1827 (6)	0.3691 (5)	0.077 (3)
C14	-0.0285 (11)	0.2500	0.4068 (7)	0.086 (5)
C15	0.2915 (7)	0.1074 (4)	0.0927 (4)	0.041 (2)
C16	0.3613 (9)	0.1090 (5)	0.0320 (4)	0.058 (2)
C17	0.3048 (10)	0.0548 (6)	-0.0155 (5)	0.068 (3)
C18	0.3010 (9)	-0.0193 (6)	0.0106 (5)	0.066 (3)
C19	0.2315 (9)	-0.0216 (5)	0.0706 (4)	0.058 (2)
C20	0.2881 (8)	0.0304 (5)	0.1181 (4)	0.048 (2)
C21	0.0521 (11)	-0.2500	0.1110 (5)	0.039 (3)
C22	0.0043 (8)	-0.1828 (5)	0.0770 (4)	0.055 (2)
H211	-0.0952 (8)	-0.1804 (5)	0.0786 (4)	0.079 (6)
C23	0.0375 (10)	-0.1825 (6)	0.0076 (5)	0.069 (3)
C24	-0.0094 (15)	-0.2500	-0.0268 (7)	0.071 (4)
C25	0.2393 (7)	-0.1076 (4)	0.3228 (4)	0.041 (2)
C26	0.2106 (9)	-0.0311 (6)	0.3034 (5)	0.064 (3)
C27	0.3217 (10)	0.0178 (6)	0.3194 (5)	0.076 (3)
C28	0.4381 (8)	-0.0075 (5)	0.2924 (4)	0.055 (2)
C29	0.4671 (9)	-0.0826 (5)	0.3110 (5)	0.059 (3)
C30	0.3584 (9)	-0.1329 (6)	0.2942 (5)	0.066 (3)
C31	-0.3962 (11)	-0.2500	0.1961 (5)	0.041 (3)
C32	-0.4129 (9)	-0.1826 (5)	0.1560 (4)	0.059 (3)
C33	-0.5379 (10)	-0.1837 (6)	0.1159 (5)	0.077 (3)
C34	-0.5505 (18)	-0.2500	0.0765 (8)	0.089 (5)
C35	-0.2164 (8)	-0.1061 (5)	0.4078 (4)	0.043 (2)
C36	-0.2149 (9)	-0.0300 (5)	0.3802 (5)	0.062 (3)

Table 1 continued...

C37	-0.2702 (10)	0.0246 (7)	0.4238 (5)	0.077 (3)
C38	-0.2064 (12)	0.0204 (7)	0.4890 (6)	0.093 (4)
C39	-0.2090 (12)	-0.0521 (7)	0.5157 (6)	0.091 (4)
C40	-0.1525 (10)	-0.1081 (6)	0.4730 (5)	0.074 (3)
H41	0.3988 (21)	0.2500	0.5433 (58)	0.121 (17)
H42	0.5401 (104)	0.2500	0.5877 (23)	0.121 (17)
H111	0.0466 (107)	0.2500	0.2550 (49)	0.121 (17)
H141	0.0445 (78)	0.2500	0.4436 (40)	0.121 (17)
H142	-0.1158 (56)	0.2500	0.4284 (53)	0.121 (17)
H211	0.1500 (37)	-0.2500	0.1044 (75)	0.121 (17)
H311	-0.4602 (116)	-0.2500	0.2329 (52)	0.121 (17)
H341	-0.4812 (82)	-0.2500	0.0423 (46)	0.121 (17)
H342	-0.6401 (52)	-0.2500	0.0510 (52)	0.121 (17)
H11	0.6581 (41)	0.2500	0.4236 (72)	0.121 (17)
H241	-0.1084 (25)	-0.2500	-0.0355 (59)	0.121 (17)
H242	0.0322 (106)	-0.2500	-0.0712 (32)	0.121 (17)

Table 2 **Fractional atomic coordinates for the hydrogen atoms for**
Cy₆Si₆O₉ compound 6

Atom	x	y	z
H21	0.5514	0.1359	0.4197
H22	0.4117	0.1812	0.4309
H31	0.6440	0.1823	0.5190
H32	0.5042	0.1378	0.5320
H51	0.7938	0.1071	0.2611
H61	0.8093	0.1370	0.1242
H62	0.8809	0.1860	0.1868
H71	1.0101	0.0851	0.2181
H72	1.0259	0.1030	0.1382
H81	1.0106	-0.0247	0.1651
H82	0.8965	0.0052	0.1085
H91	0.8038	-0.0698	0.1793
H92	0.8699	-0.0203	0.2431
H101	0.6702	0.0306	0.1484
H102	0.6524	0.0103	0.2277
H121	0.1770	0.1812	0.3696
H122	0.1018	0.1359	0.3057
H131	-0.0220	0.1369	0.3995
H132	-0.0982	0.1806	0.3350
H151	0.1971	0.1249	0.0828
H161	0.4574	0.0957	0.0430
H162	0.3551	0.1618	0.0118
H171	0.3592	0.0544	-0.0560
H172	0.2111	0.0711	-0.0293
H181	0.2550	-0.0540	-0.0237
H182	0.3949	-0.0375	0.0210
H191	0.2368	-0.0748	0.0899
H192	0.1356	-0.0076	0.0598

Table 2 **continued...**

H201	0.2346	0.0297	0.1590
H202	0.3820	0.0137	0.1310
H222	0.0456	-0.1367	0.1002
H231	0.1370	-0.1796	0.0059
H232	-0.0044	-0.1365	-0.0156
H251	0.2538	-0.1075	0.3732
H261	0.1876	-0.0293	0.2536
H262	0.1325	-0.0125	0.3279
H271	0.3372	0.0206	0.3696
H272	0.3000	0.0703	0.3011
H281	0.5138	0.0265	0.3093
H282	0.4272	-0.0043	0.2420
H291	0.5465	-0.1002	0.2870
H292	0.4888	-0.0846	0.3609
H301	0.3815	-0.1855	0.3117
H302	0.3425	-0.1349	0.2439
H321	-0.4105	-0.1366	0.1863
H322	-0.3380	-0.1793	0.1251
H331	-0.5427	-0.1377	0.0855
H332	-0.6129	-0.1817	0.1468
H351	-0.3118	-0.1214	0.4121
H361	-0.2686	-0.0297	0.3359
H362	-0.1203	-0.0152	0.3730
H371	-0.3678	0.0138	0.4266
H372	-0.2583	0.0775	0.4054
H381	-0.2523	0.0564	0.5192
H382	-0.1109	0.0364	0.4865
H391	-0.1572	-0.0521	0.5606
H392	-0.3042	-0.0665	0.5219
H401	-0.1635	-0.1605	0.4927
H402	-0.0551	-0.0968	0.4701

Table 3 **Anisotropic thermal parameters (Å) for $\text{Cy}_6\text{Si}_6\text{O}_9$ compound 6**

Atom	U11	U22	U33	U23	U13	U12
Si1	0.037 (2)	0.041 (2)	0.036 (2)	0.000 (1)	0.003 (1)	0.000 (1)
Si2	0.038 (1)	0.041 (1)	0.043 (1)	-0.003 (1)	0.006 (1)	0.004 (1)
Si3	0.037 (2)	0.037 (2)	0.037 (2)	0.000 (1)	0.007 (1)	0.000 (1)
Si4	0.041 (1)	0.034 (1)	0.038 (1)	-0.004 (1)	0.007 (1)	-0.001 (1)
O1	0.049 (3)	0.034 (3)	0.040 (3)	0.002 (3)	0.009 (2)	-0.001 (3)
O2	0.043 (5)	0.037 (5)	0.048 (5)	0.000 (1)	0.015 (4)	0.000 (1)
O3	0.050 (3)	0.029 (3)	0.038 (3)	-0.003 (2)	0.011 (2)	-0.008 (3)
O4	0.050 (5)	0.035 (5)	0.038 (4)	0.000 (1)	0.015 (4)	0.000 (1)
O5	0.049 (3)	0.039 (3)	0.042 (3)	-0.006 (3)	0.007 (3)	0.004 (3)
O6	0.037 (4)	0.040 (5)	0.041 (5)	0.000 (1)	0.001 (3)	0.000 (1)
Si5	0.033 (2)	0.035 (2)	0.039 (2)	0.000 (1)	0.007 (1)	0.000 (1)
Si6	0.033 (1)	0.034 (1)	0.044 (1)	-0.004 (1)	0.007 (1)	-0.002 (1)
Si7	0.030 (2)	0.035 (2)	0.043 (2)	0.000 (1)	0.002 (1)	0.000 (1)
Si8	0.036 (1)	0.034 (1)	0.044 (1)	-0.005 (1)	0.008 (1)	0.002 (1)
O7	0.041 (3)	0.031 (3)	0.039 (3)	0.002 (2)	0.004 (2)	0.000 (3)
O8	0.040 (5)	0.038 (5)	0.045 (5)	0.000 (1)	0.003 (4)	0.000 (1)
O9	0.043 (3)	0.032 (3)	0.047 (3)	-0.005 (3)	0.005 (2)	0.001 (3)
O10	0.046 (5)	0.035 (5)	0.052 (5)	0.000 (1)	0.007 (4)	0.000 (1)
O11	0.037 (3)	0.034 (3)	0.056 (4)	-0.003 (3)	0.012 (3)	-0.004 (3)
O12	0.030 (4)	0.042 (5)	0.042 (4)	0.000 (1)	0.009 (3)	0.000 (1)

Table 4 **Bond lengths (Å) for Cy₆Si₆O₉ compound 6**

Si1 -O1	1.649 (6)	Si1 -O6	1.633 (8)
Si1 -C1	1.839 (13)	Si2 -O1	1.625 (6)
Si2 -O2	1.645 (4)	Si2 -O5	1.630 (6)
Si2 -C5	1.858 (10)	Si3 -O3	1.648 (6)
Si3 -O6	1.612 (8)	Si3 -C11	1.825 (11)
Si4 -O3	1.629 (6)	Si4 -O4	1.641 (4)
Si4 -O5	1.627 (6)	Si4 -C15	1.842 (8)
C1 -C2	1.541 (14)	C1 -H11	1.08 (6)
C2 -C3	1.553 (16)	C3 -C4	1.493 (16)
C4 -H41	1.07 (3)	C4 -H42	1.08 (6)
C5 -C6	1.511 (16)	C5 -C10	1.552 (15)
C6 -C7	1.543 (18)	C7 -C8	1.491 (17)
C8 -C9	1.461 (17)	C9 -C10	1.542 (17)
C11 -C12	1.554 (12)	C11 -H111	1.08 (10)
C12 -C13	1.538 (15)	C13 -C14	1.504 (14)
C14 -H141	1.08 (8)	C14 -H142	1.08 (8)
C15 -C16	1.547 (13)	C15 -C20	1.544 (12)
C16 -C17	1.537 (14)	C17 -C18	1.500 (15)
C18 -C19	1.531 (14)	C19 -C20	1.511 (13)
Si5 -O7	1.648 (5)	Si5 -O12	1.634 (8)
Si5 -C21	1.844 (12)	Si6 -O7	1.626 (5)
Si6 -O8	1.647 (4)	Si6 -O11	1.628 (6)
Si6 -C25	1.849 (8)	Si7 -O9	1.640 (6)
Si7 -O12	1.611 (8)	Si7 -C31	1.845 (12)
Si8 -O9	1.634 (6)	Si8 -O10	1.643 (4)
Si8 -O11	1.626 (6)	Si8 -C35	1.837 (9)
C21 -C22	1.528 (11)	C21 -H211	1.08 (5)
C22 -H211	1.080 (13)	C22 -C23	1.553 (14)
C23 -C24	1.533 (14)	C24 -H241	1.07 (3)

Table 4 **continued...**

C24 -H242	1.08 (8)	C25 -C26	1.521 (13)
C25 -C30	1.537 (13)	C26 -C27	1.531 (15)
C27 -C28	1.495 (15)	C28 -C29	1.492 (14)
C29 -C30	1.531 (14)	C31 -C32	1.533 (12)
C31 -H311	1.08 (12)	C32 -C33	1.553 (14)
C33 -C34	1.504 (15)	C34 -H341	1.08 (10)
C34 -H342	1.08 (7)	C35 -C36	1.545 (13)
C35 -C40	1.517 (13)	C36 -C37	1.535 (16)
C37 -C38	1.517 (16)	C38 -C39	1.476 (19)
C39 -C40	1.546 (17)		

Table 5 **Bond angles (°) for Cy₆Si₆O₉ compound 6**

O6	-Si1	-O1	109.2 (3)	C1	-Si1	-O1	111.9 (3)
C1	-Si1	-O6	108.5 (5)	O2	-Si2	-O1	106.6 (3)
O5	-Si2	-O1	109.5 (3)	O5	-Si2	-O2	108.3 (3)
C5	-Si2	-O1	110.2 (4)	C5	-Si2	-O2	110.4 (4)
C5	-Si2	-O5	111.7 (4)	Si2	-O2	-Si2	130.6 (5)
O6	-Si3	-O3	109.0 (3)	C11	-Si3	-O3	112.2 (3)
C11	-Si3	-O6	108.5 (5)	O4	-Si4	-O3	106.1 (3)
O5	-Si4	-O3	109.8 (3)	O5	-Si4	-O4	109.2 (4)
C15	-Si4	-O3	112.0 (3)	C15	-Si4	-O4	110.3 (4)
C15	-Si4	-O5	109.5 (3)	Si4	-O4	-Si4	130.8 (5)
Si2	-O1	-Si1	128.8 (4)	O1	-Si1	-O1	106.2 (4)
Si4	-O3	-Si3	129.0 (4)	O3	-Si3	-O3	105.8 (4)
Si4	-O5	-Si2	139.3 (4)	Si3	-O6	-Si1	144.7 (5)
C2	-C1	-Si1	112.0 (6)	H11	-C1	-Si1	116 (8)
H11	-C1	-C2	103 (4)	C3	-C2	-C1	111 (1)
C2	-C1	-C2	110 (1)	C4	-C3	-C2	112 (1)
C3	-C4	-C3	112 (1)	H41	-C4	-C3	113 (3)
H42	-C4	-C3	105 (3)	H42	-C4	-H41	108 (9)
C6	-C5	-Si2	113.3 (7)	C10	-C5	-Si2	114.1 (7)
C10	-C5	-C6	108.8 (9)	C7	-C6	-C5	113 (1)
C8	-C7	-C6	113 (1)	C9	-C8	-C7	112 (1)
C10	-C9	-C8	115 (1)	C9	-C10	-C5	110.1 (9)
C12	-C11	-Si3	112.5 (6)	H111-C11	-Si3		104 (6)
H111-C11	-C12		110 (3)	C13	-C12	-C11	113.8 (8)
C12	-C11	-C12	108 (1)	C14	-C13	-C12	109.8 (9)
C13	-C14	-C13	114 (1)	H141-C14	-C13		109 (2)
H142-C14	-C13		108 (3)	H142-C14	-H141		108 (7)
C16	-C15	-Si4	110.7 (6)	C20	-C15	-Si4	112.4 (5)
C20	-C15	-C16	109.8 (7)	C17	-C16	-C15	110.5 (8)

Table 5 continued...

C18 -C17 -C16	112.6 (8)	C19 -C18 -C17	111.5 (9)
C20 -C19 -C18	110.4 (8)	C19 -C20 -C15	112.6 (7)
O12 -Si5 -O7	108.7 (3)	C21 -Si5 -O7	112.0 (3)
C21 -Si5 -O12	109.0 (5)	O8 -Si6 -O7	107.1 (3)
O11 -Si6 -O7	109.3 (3)	O11 -Si6 -O8	108.9 (4)
C25 -Si6 -O7	113.1 (3)	C25 -Si6 -O8	109.1 (4)
C25 -Si6 -O11	109.3 (3)	Si6 -O8 -Si6	129.3 (5)
O12 -Si7 -O9	108.3 (3)	C31 -Si7 -O9	112.2 (3)
C31 -Si7 -O12	109.2 (5)	O10 -Si8 -O9	106.8 (3)
O11 -Si8 -O9	109.2 (3)	O11 -Si8 -O10	109.4 (4)
C35 -Si8 -O9	112.5 (3)	C35 -Si8 -O10	110.6 (4)
C35 -Si8 -O11	108.3 (3)	Si8 -O10 -Si8	129.5 (5)
Si6 -O7 -Si5	128.7 (4)	O7 -Si5 -O7	106.3 (4)
Si8 -O9 -Si7	129.0 (4)	O9 -Si7 -O9	106.4 (4)
Si8 -O11 -Si6	139.8 (4)	Si7 -O12 -Si5	145.2 (5)
C22 -C21 -Si5	111.8 (6)	H211-C21 -Si5	114 (8)
H211-C21 -C22	104 (4)	H211-C22 -C21	109 (1)
C23 -C22 -C21	111.6 (8)	C23 -C22 -H211	108.9 (9)
C22 -C21 -C22	111 (1)	C24 -C23 -C22	111 (1)
C23 -C24 -C23	111 (1)	H241-C24 -C23	112 (3)
H242-C24 -C23	106 (3)	H242-C24 -H241	108 (9)
C26 -C25 -Si6	114.3 (6)	C30 -C25 -Si6	111.6 (6)
C30 -C25 -C26	110.0 (8)	C27 -C26 -C25	111.1 (8)
C28 -C27 -C26	113.1 (9)	C29 -C28 -C27	111.3 (9)
C30 -C29 -C28	112.0 (8)	C29 -C30 -C25	111.5 (8)
C32 -C31 -Si7	112.0 (6)	H311-C31 -Si7	100 (6)
H311-C31 -C32	111 (3)	C33 -C32 -C31	111.4 (9)
C32 -C31 -C32	111 (1)	C34 -C33 -C32	111 (1)
C33 -C34 -C33	112 (1)	H341-C34 -C33	110 (2)
H342-C34 -C33	109 (3)	H342-C34 -H341	107 (7)
C36 -C35 -Si8	111.1 (6)	C40 -C35 -Si8	111.9 (7)

Table 5 **continued...**

C40 -C35 -C36	111.1 (8)	C37 -C36 -C35	111.6 (8)
C38 -C37 -C36	110.7 (9)	C39 -C38 -C37	113 (1)
C40 -C39 -C38	112 (1)	C39 -C40 -C35	110.8 (9)

Table 6 Intermolecular distances (Å) for $\text{Cy}_6\text{Si}_6\text{O}_9$ compound 6

Si2 ...Si2	2.99	-2	0.0	1.0	0.0
Si2 ...O2	1.65	-2	0.0	1.0	0.0
Si4 ...Si4	2.98	-2	0.0	1.0	0.0
Si4 ...O4	1.64	-2	0.0	1.0	0.0
O1 ...O1	2.64	-2	0.0	1.0	0.0
O1 ...O2	2.62	-2	0.0	1.0	0.0
O1 ...O6	2.68	-2	0.0	1.0	0.0
O1 ...C1	2.89	-2	0.0	1.0	0.0
O3 ...O3	2.63	-2	0.0	1.0	0.0
O3 ...O4	2.61	-2	0.0	1.0	0.0
O3 ...O6	2.65	-2	0.0	1.0	0.0
O3 ...C11	2.88	-2	0.0	1.0	0.0
C2 ...C2	2.52	-2	0.0	1.0	0.0
C2 ...H22	2.77	-2	0.0	1.0	0.0
C2 ...C3	2.94	-2	0.0	1.0	0.0
C2 ...C4	2.52	-2	0.0	1.0	0.0
C2 ...H41	2.89	-2	0.0	1.0	0.0
C2 ...H11	2.07	-2	0.0	1.0	0.0
H21 ...C37	2.84	1	-1.0	0.0	0.0
H21 ...H11	2.43	-2	0.0	1.0	0.0
H22 ...C4	2.79	-2	0.0	1.0	0.0
C3 ...C3	2.47	-2	0.0	1.0	0.0
C3 ...H31	2.73	-2	0.0	1.0	0.0
C3 ...C4	1.49	-2	0.0	1.0	0.0
C3 ...H41	2.15	-2	0.0	1.0	0.0
C3 ...H42	2.06	-2	0.0	1.0	0.0
C3 ...H11	2.62	-2	0.0	1.0	0.0
H31 ...C4	2.10	-2	0.0	1.0	0.0
H31 ...H42	2.29	-2	0.0	1.0	0.0

Table 6 **continued...**

H31 ...H11	2.42	-2	0.0	1.0	0.0
H32 ...C4	2.11	-2	0.0	1.0	0.0
H32 ...H41	2.41	-2	0.0	1.0	0.0
H32 ...H42	2.44	-2	0.0	1.0	0.0
H62 ...H111	2.54	1	-1.0	0.0	0.0
H62 ...H111	2.54	-2	-1.0	1.0	0.0
C12 ...C12	2.52	-2	0.0	1.0	0.0
C12 ...H121	2.77	-2	0.0	1.0	0.0
C12 ...C13	2.95	-2	0.0	1.0	0.0
C12 ...C14	2.49	-2	0.0	1.0	0.0
C12 ...H111	2.17	-2	0.0	1.0	0.0
C12 ...H141	2.75	-2	0.0	1.0	0.0
H121...C14	2.73	-2	0.0	1.0	0.0
H121...H141	2.56	-2	0.0	1.0	0.0
H122...H111	2.46	-2	0.0	1.0	0.0
C13 ...C13	2.52	-2	0.0	1.0	0.0
C13 ...H132	2.78	-2	0.0	1.0	0.0
C13 ...C14	1.50	-2	0.0	1.0	0.0
C13 ...H111	2.89	-2	0.0	1.0	0.0
C13 ...H141	2.12	-2	0.0	1.0	0.0
C13 ...H142	2.11	-2	0.0	1.0	0.0
H131...C14	2.13	-2	0.0	1.0	0.0
H131...H141	2.41	-2	0.0	1.0	0.0
H131...H142	2.45	-2	0.0	1.0	0.0
H132...C14	2.12	-2	0.0	1.0	0.0
H132...H142	2.41	-2	0.0	1.0	0.0
H162...H341	2.48	-1	0.0	0.0	0.0
H162...H341	2.48	2	0.0	-1.0	0.0
H172...H211	2.59	-1	0.0	0.0	0.0
Si6 ...Si6	2.98	-2	0.0	0.0	0.0
Si6 ...O8	1.65	-2	0.0	0.0	0.0

Table 6 **continued...**

Si8	...Si8	2.97	-2	0.0	0.0	0.0
Si8	...O10	1.64	-2	0.0	0.0	0.0
O7	...O7	2.64	-2	0.0	0.0	0.0
O7	...O8	2.63	-2	0.0	0.0	0.0
O7	...O12	2.67	-2	0.0	0.0	0.0
O7	...C21	2.90	-2	0.0	0.0	0.0
O9	...H291	2.82	1	1.0	0.0	0.0
O9	...O9	2.63	-2	0.0	0.0	0.0
O9	...O10	2.63	-2	0.0	0.0	0.0
O9	...O12	2.64	-2	0.0	0.0	0.0
O9	...C31	2.90	-2	0.0	0.0	0.0
O9	...H311	2.98	-2	0.0	0.0	0.0
C22	...C22	2.52	-2	0.0	0.0	0.0
C22	...H211	2.78	-2	0.0	0.0	0.0
C22	...C23	2.97	-2	0.0	0.0	0.0
C22	...C24	2.55	-2	0.0	0.0	0.0
C22	...H211	2.07	-2	0.0	0.0	0.0
C22	...H241	2.91	-2	0.0	0.0	0.0
H211	...H211	2.61	-2	0.0	0.0	0.0
H211	...C24	2.82	-2	0.0	0.0	0.0
H222	...H211	2.41	-2	0.0	0.0	0.0
C23	...C23	2.53	-2	0.0	0.0	0.0
C23	...H231	2.80	-2	0.0	0.0	0.0
C23	...C24	1.53	-2	0.0	0.0	0.0
C23	...H211	2.66	-2	0.0	0.0	0.0
C23	...H241	2.18	-2	0.0	0.0	0.0
C23	...H242	2.11	-2	0.0	0.0	0.0
H231	...C24	2.14	-2	0.0	0.0	0.0
H231	...H211	2.48	-2	0.0	0.0	0.0
H231	...H242	2.35	-2	0.0	0.0	0.0
H232	...C24	2.14	-2	0.0	0.0	0.0
H232	...H241	2.43	-2	0.0	0.0	0.0

Table 6 continued...

H232...H242	2.48	-2	0.0	0.0	0.0
H271...C39	2.96	-1	0.0	0.0	1.0
H301...H42	2.57	-1	1.0	0.0	1.0
H301...H42	2.57	2	1.0	0.0	1.0
C32 ...C32	2.53	-2	0.0	0.0	0.0
C32 ...H322	2.81	-2	0.0	0.0	0.0
C32 ...C33	2.95	-2	0.0	0.0	0.0
C32 ...C34	2.52	-2	0.0	0.0	0.0
C32 ...H311	2.16	-2	0.0	0.0	0.0
C32 ...H341	2.80	-2	0.0	0.0	0.0
H321...H311	2.43	-2	0.0	0.0	0.0
H322...C34	2.79	-2	0.0	0.0	0.0
H322...H341	2.63	-2	0.0	0.0	0.0
C33 ...C33	2.49	-2	0.0	0.0	0.0
C33 ...H332	2.75	-2	0.0	0.0	0.0
C33 ...C34	1.50	-2	0.0	0.0	0.0
C33 ...H311	2.87	-2	0.0	0.0	0.0
C33 ...H341	2.13	-2	0.0	0.0	0.0
C33 ...H342	2.12	-2	0.0	0.0	0.0
H331...C34	2.12	-2	0.0	0.0	0.0
H331...H341	2.41	-2	0.0	0.0	0.0
H331...H342	2.45	-2	0.0	0.0	0.0
H332...C34	2.12	-2	0.0	0.0	0.0
H332...H342	2.42	-2	0.0	0.0	0.0
H401...H141	2.47	-1	0.0	0.0	1.0
H401...H141	2.47	2	0.0	0.0	1.0
H142...H11	2.44	1	1.0	0.0	0.0
H211...H342	2.61	1	-1.0	0.0	0.0

Table 7 **Intramolecular distances (Å) for Cy₆Si₆O₉ compound 6**

Si1 ...Si2	2.95	Si1 ...C2	2.81
Si1 ...H21	2.98	Si1 ...H22	2.98
Si1 ...H11	2.51	Si2 ...H51	2.36
Si2 ...C6	2.82	Si2 ...H62	2.95
Si2 ...C10	2.87	Si3 ...Si4	2.96
Si3 ...C12	2.81	Si3 ...H121	2.96
Si3 ...H122	3.00	Si3 ...H111	2.34
Si4 ...H151	2.38	Si4 ...C16	2.79
Si4 ...H161	2.95	Si4 ...H162	2.98
Si4 ...C20	2.82	Si4 ...H201	2.99
Si4 ...H202	2.98	O1 ...O2	2.62
O1 ...O5	2.66	O1 ...O6	2.68
O1 ...C1	2.89	O1 ...H21	2.95
O1 ...C5	2.86	O1 ...H51	2.75
O2 ...O5	2.65	O2 ...C5	2.88
O2 ...H62	2.70	O3 ...O4	2.61
O3 ...O5	2.66	O3 ...O6	2.65
O3 ...C11	2.88	O3 ...H122	2.99
O3 ...C15	2.88	O3 ...H151	3.00
O3 ...H272	2.83	O4 ...O5	2.66
O4 ...C15	2.86	O4 ...H162	2.84
O5 ...C5	2.89	O5 ...H101	2.88
O5 ...C15	2.84	O5 ...H161	2.96
O5 ...H202	2.86	O6 ...C1	2.82
O6 ...H22	2.91	O6 ...C11	2.79
O6 ...H121	2.87	C1 ...H21	2.16
C1 ...H22	2.15	C1 ...C3	2.55
C1 ...H31	2.79	C1 ...C4	2.97
C2 ...H31	2.15	C2 ...H32	2.16

Table 7 **continued...**

C2	...C4	2.52	C2	...H41	2.89
C2	...H11	2.07	H21	...C3	2.16
H21	...H11	2.43	H22	...C3	2.16
H22	...C4	2.79	C3	...H41	2.15
C3	...H42	2.06	C3	...H11	2.62
H31	...C4	2.10	H31	...H42	2.29
H31	...H11	2.42	H32	...C4	2.11
H32	...H41	2.41	H32	...H42	2.44
C5	...H61	2.12	C5	...H62	2.12
C5	...C7	2.54	C5	...H71	2.81
C5	...C8	2.98	C5	...C9	2.54
C5	...H92	2.77	C5	...H101	2.17
C5	...H102	2.16	H51	...C6	2.11
H51	...C7	2.77	H51	...C9	2.77
H51	...C10	2.15	C6	...H71	2.14
C6	...H72	2.15	C6	...C8	2.53
C6	...H82	2.82	C6	...C9	2.89
C6	...C10	2.49	C6	...H101	2.76
H61	...C7	2.15	H61	...C8	2.81
H61	...C10	2.74	H62	...C7	2.15
C7	...H81	2.10	C7	...H82	2.10
C7	...C9	2.44	C7	...H92	2.71
C7	...C10	2.94	H71	...C8	2.10
H71	...C9	2.74	H72	...C8	2.11
C8	...H91	2.07	C8	...H92	2.06
C8	...C10	2.53	C8	...H101	2.83
H81	...C9	2.09	H82	...C9	2.07
H82	...C10	2.82	C9	...H101	2.15
C9	...H102	2.16	H91	...C10	2.15
H92	...C10	2.13	H102...	C28	2.80
C11	...H121	2.15	C11	...H122	2.16

Table 7 **continued...**

C11 ...C13	2.59	C11 ...H132	2.85
C11 ...C14	2.98	C12 ...H131	2.16
C12 ...H132	2.15	C12 ...C14	2.49
C12 ...H111	2.17	C12 ...H141	2.75
H121...C13	2.13	H121...C14	2.73
H121...H141	2.56	H122...C13	2.14
H122...H111	2.46	C13 ...H111	2.89
C13 ...H141	2.12	C13 ...H142	2.11
H131...C14	2.13	H131...H141	2.41
H131...H142	2.45	H132...C14	2.12
H132...H142	2.41	C15 ...H161	2.16
C15 ...H162	2.16	C15 ...C17	2.53
C15 ...H172	2.78	C15 ...C18	2.96
C15 ...C19	2.54	C15 ...H192	2.80
C15 ...H201	2.15	C15 ...H202	2.15
H151...C16	2.16	H151...C17	2.80
H151...C19	2.79	H151...C20	2.14
C16 ...H171	2.15	C16 ...H172	2.14
C16 ...C18	2.53	C16 ...H182	2.78
C16 ...C19	2.97	C16 ...C20	2.53
C16 ...H202	2.77	H161...C17	2.15
H161...C18	2.80	H161...C20	2.80
H162...C17	2.15	C17 ...H181	2.12
C17 ...H182	2.11	C17 ...C19	2.51
C17 ...H192	2.78	C17 ...C20	2.92
H171...C18	2.11	H172...C18	2.11
H172...C19	2.76	C18 ...H191	2.15
C18 ...H192	2.15	C18 ...C20	2.50
C18 ...H202	2.74	H181...C19	2.14
H182...C19	2.14	H182...C20	2.76
C19 ...H201	2.12	C19 ...H202	2.12
H191...C20	2.13	H192...C20	2.13

Table 7 **continued...**

Si5 ...Si6	2.95	Si5 ...C22	2.80
Si5 ...H211	2.97	Si5 ...H222	2.96
Si5 ...H211	2.48	Si6 ...H251	2.37
Si6 ...C26	2.84	Si6 ...C30	2.81
Si6 ...H301	2.94	Si6 ...H302	3.00
Si7 ...Si8	2.96	Si7 ...C32	2.81
Si7 ...H321	2.98	Si7 ...H322	2.97
Si7 ...H311	2.30	Si8 ...H351	2.39
Si8 ...C36	2.80	Si8 ...H361	2.96
Si8 ...H362	2.96	Si8 ...C40	2.78
Si8 ...H401	2.97	Si8 ...H402	2.95
O7 ...O8	2.63	O7 ...O11	2.65
O7 ...O12	2.67	O7 ...C21	2.90
O7 ...H222	2.93	O7 ...C25	2.90
O8 ...O11	2.66	O8 ...C25	2.85
O8 ...H251	3.00	O8 ...H301	2.84
O9 ...O10	2.63	O9 ...O11	2.66
O9 ...O12	2.64	O9 ...C31	2.90
O9 ...H321	2.95	O9 ...C35	2.89
O9 ...H311	2.98	O10 ...O11	2.67
O10 ...C35	2.86	O10 ...H401	2.83
O11 ...C25	2.84	O11 ...H251	2.98
O11 ...H262	2.93	O11 ...C35	2.81
O11 ...H362	2.79	O11 ...H402	2.97
O12 ...C21	2.83	O12 ...H211	2.92
O12 ...C31	2.82	O12 ...H322	2.92
C21 ...H211	2.14	C21 ...H222	2.14
C21 ...C23	2.55	C21 ...H231	2.82
C21 ...C24	2.98	C22 ...H231	2.16
C22 ...H232	2.16	C22 ...C24	2.55
C22 ...H211	2.07	C22 ...H241	2.91

Table 7 **continued...**

H211...H222	1.76	H211...C23	2.16
H211...H232	2.44	H211...C24	2.82
H222...C23	2.16	H222...H211	2.41
C23 ...H211	2.66	C23 ...H241	2.18
C23 ...H242	2.11	H231...C24	2.14
H231...H211	2.48	H231...H242	2.35
H232...C24	2.14	H232...H241	2.43
H232...H242	2.48	C25 ...H261	2.14
C25 ...H262	2.13	C25 ...C27	2.52
C25 ...H271	2.79	C25 ...C28	2.96
C25 ...C29	2.54	C25 ...H292	2.80
C25 ...H301	2.15	C25 ...H302	2.15
H251...C26	2.10	H251...C27	2.74
H251...C29	2.78	H251...C30	2.15
C26 ...H271	2.14	C26 ...H272	2.14
C26 ...C28	2.52	C26 ...H282	2.81
C26 ...C29	2.93	C26 ...C30	2.51
C26 ...H302	2.77	H261...C27	2.14
H261...C28	2.81	H261...C30	2.78
H262...C27	2.14	C27 ...H281	2.11
C27 ...H282	2.11	C27 ...C29	2.47
C27 ...H292	2.74	C27 ...C30	2.91
H271...C28	2.11	H271...C29	2.74
H272...C28	2.10	C28 ...H291	2.10
C28 ...H292	2.11	C28 ...C30	2.51
C28 ...H302	2.78	H281...C29	2.11
H282...C29	2.11	H282...C30	2.78
C29 ...H301	2.14	C29 ...H302	2.14
H291...C30	2.14	H292...C30	2.14
C31 ...H321	2.14	C31 ...H322	2.14
C31 ...C33	2.55	C31 ...H332	2.81
C31 ...C34	2.96	C32 ...H331	2.16

Table 7 **continued...**

C32 ...H332	2.16	C32 ...C34	2.52
C32 ...H311	2.16	C32 ...H341	2.80
H321...C33	2.16	H321...H311	2.43
H322...C33	2.16	H322...C34	2.79
H322...H341	2.63	C33 ...H311	2.87
C33 ...H341	2.13	C33 ...H342	2.12
H331...C34	2.12	H331...H341	2.41
H331...H342	2.45	H332...C34	2.12
H332...H342	2.42	C35 ...H361	2.15
C35 ...H362	2.15	C35 ...C37	2.55
C35 ...H371	2.82	C35 ...C38	2.94
C35 ...C39	2.52	C35 ...H392	2.78
C35 ...H401	2.13	C35 ...H402	2.13
H351...C36	2.14	H351...C37	2.78
H351...C39	2.74	H351...C40	2.11
C36 ...H371	2.15	C36 ...H372	2.15
C36 ...C38	2.51	C36 ...H382	2.77
C36 ...C39	2.93	C36 ...C40	2.52
C36 ...H402	2.80	H361...C37	2.14
H362...C37	2.15	H362...C38	2.79
H362...C40	2.80	C37 ...H381	2.13
C37 ...H382	2.12	C37 ...C39	2.49
C37 ...H392	2.75	C37 ...C40	2.96
H371...C38	2.13	H371...C39	2.77
H372...C38	2.13	C38 ...H391	2.09
C38 ...H392	2.09	C38 ...C40	2.51
C38 ...H402	2.78	H381...C39	2.09
H382...C39	2.09	H382...C40	2.76
C39 ...H401	2.16	C39 ...H402	2.15
H391...C40	2.15	H392...C40	2.15
H41 ...H42	1.74	H141...H142	1.74

**X-ray crystallography supplementary tables for
hexaphenyl-1,3,5-trisiloxane-1,5-diol, compound 3**

Table 8 Fractional atomic coordinates and thermal parameters (Å) for
Ph₂(HO)SiOSi(Ph₂)OSi(OH)Ph₂ (compound 3)

Atom	x	y	z	U _{eq}	
Si1	0.5097 (3)	0.3525 (2)	0.2458 (2)	0.044 (1)	*
Si2	0.5105 (3)	0.1275 (2)	0.2151 (2)	0.041 (1)	*
Si3	0.3758 (3)	0.2768 (2)	-0.0020 (2)	0.046 (2)	*
O1	0.5322 (7)	0.2304 (4)	0.2387 (4)	0.059 (4)	*
O2	0.4479 (7)	0.1780 (4)	0.1022 (4)	0.052 (4)	*
O3	0.3785 (7)	0.4034 (4)	-0.0095 (4)	0.055 (4)	*
O4	0.4679 (7)	0.4541 (5)	0.1342 (4)	0.059 (4)	*
C4	0.1846 (14)	0.4034 (11)	0.4908 (9)	0.107 (10)	*
C5	0.2102 (16)	0.4959 (11)	0.4096 (11)	0.124 (12)	*
C6	0.3010 (13)	0.4822 (9)	0.3332 (8)	0.090 (9)	*
C8	0.7031 (16)	0.3690 (10)	0.3652 (8)	0.104 (10)	*
C9	0.8362 (20)	0.3725 (13)	0.3842 (12)	0.121 (13)	*
C10	0.9432 (20)	0.3601 (12)	0.3189 (15)	0.124 (15)	*
C11	0.9244 (16)	0.3490 (12)	0.2336 (13)	0.107 (13)	*
C12	0.7941 (12)	0.3453 (8)	0.2171 (8)	0.072 (8)	*
C14	0.7981 (12)	0.0250 (9)	0.2652 (8)	0.082 (8)	*
C15	0.9225 (14)	-0.0599 (11)	0.2767 (10)	0.104 (11)	*
C16	0.9330 (12)	-0.1473 (9)	0.2489 (8)	0.073 (9)	*
C17	0.8194 (13)	-0.1526 (9)	0.2095 (8)	0.079 (8)	*
C21	0.1444 (11)	0.0625 (10)	0.3701 (8)	0.070 (8)	*
C22	0.1936 (15)	-0.0283 (10)	0.4563 (8)	0.083 (9)	*
C23	0.3307 (14)	-0.0734 (10)	0.4707 (8)	0.077 (9)	*
C27	0.6802 (15)	0.1533 (11)	-0.1791 (11)	0.103 (11)	*
C28	0.6301 (14)	0.2149 (12)	-0.2755 (11)	0.103 (11)	*
C29	0.5059 (15)	0.2950 (11)	-0.2892 (8)	0.098 (10)	*

Table 8 continued...

C32	0.1511 (14)	0.1764 (10)	0.0310 (8)	0.089 (9)	*
C33	0.0201 (17)	0.1736 (15)	0.0240 (11)	0.123 (13)	*
C34	-0.0866 (17)	0.2729 (19)	-0.0194 (13)	0.159 (17)	*
C35	-0.0420 (19)	0.3686 (14)	-0.0566 (12)	0.137 (15)	*
C36	0.0892 (14)	0.3735 (11)	-0.0481 (10)	0.107 (11)	*
C1	0.3737 (10)	0.3722 (7)	0.3387 (6)	0.055 (2)	
C2	0.3381 (10)	0.2821 (8)	0.4192 (7)	0.064 (3)	
C3	0.2474 (12)	0.2969 (9)	0.4948 (8)	0.073 (3)	
C7	0.6800 (10)	0.3580 (7)	0.2795 (6)	0.051 (2)	
C13	0.6811 (9)	0.0215 (6)	0.2261 (6)	0.041 (2)	
C18	0.6957 (12)	-0.0692 (8)	0.1994 (7)	0.069 (3)	
C19	0.3814 (9)	0.0626 (6)	0.3082 (5)	0.041 (2)	
C20	0.2412 (11)	0.1064 (8)	0.2959 (7)	0.069 (3)	
C24	0.4304 (12)	-0.0301 (8)	0.3981 (7)	0.071 (3)	
C25	0.4830 (10)	0.2494 (7)	-0.1095 (6)	0.048 (2)	
C26	0.6066 (12)	0.1692 (9)	-0.0979 (8)	0.073 (3)	
C30	0.4262 (11)	0.3150 (8)	-0.2083 (7)	0.063 (3)	
C31	0.1902 (10)	0.2762 (8)	-0.0058 (6)	0.051 (2)	
H4	0.409 (7)	0.449 (6)	0.084 (4)	0.05	

Table 9 **Fractional atomic coordinates for the hydrogen atoms for**
Ph₂(HO)SiOSi(Ph₂)OSi(OH)Ph₂ compound 3

Atom	x	y	z
H21	0.3829	0.1965	0.4223
H31	0.2252	0.2241	0.5575
H41	0.1159	0.4154	0.5515
H51	0.1585	0.5806	0.4068
H61	0.3134	0.5566	0.2678
H81	0.6179	0.3761	0.4182
H91	0.8516	0.3857	0.4507
H101	1.0462	0.3587	0.3369
H111	1.0099	0.3428	0.1806
H121	0.7797	0.3333	0.1498
H141	0.7943	0.0947	0.2865
H151	1.0134	-0.0582	0.3094
H161	1.0304	-0.2131	0.2576
H171	0.8261	-0.2207	0.1851
H181	0.6053	-0.0752	0.1693
H201	0.2029	0.1783	0.2265
H211	0.0326	0.0997	0.3581
H221	0.1212	-0.0645	0.5137
H231	0.3663	-0.1444	0.5413
H241	0.5419	-0.0682	0.4109
H261	0.6479	0.1165	-0.0226
H271	0.7815	0.0918	-0.1690
H281	0.6865	0.1996	-0.3393
H291	0.4677	0.3458	-0.3656
H301	0.3252	0.3770	-0.2198

Table 9 **continued...**

H321	0.2286	0.0964	0.0666
H331	-0.0060	0.0926	0.0538
H341	-0.1950	0.2746	-0.0237
H351	-0.1166	0.4482	-0.0981
H361	0.1116	0.4554	-0.0735

^a Code for numbering of hydrogen atoms: H361 is hydrogen 1 on carbon 36

Table 10 Anisotropic thermal parameters (Å) Ph ₂ (HO)SiOSi(Ph ₂)OSi(OH)Ph ₂ compound 3						
Atom	U11	U22	U33	U23	U13	U12
Si1	0.055 (2)	0.039 (1)	0.038 (1)	-0.015 (1)	0.005 (1)	-0.018 (1)
Si2	0.052 (2)	0.033 (1)	0.040 (1)	-0.011 (1)	0.004 (1)	-0.019 (1)
Si3	0.056 (2)	0.044 (1)	0.037 (1)	-0.011 (1)	0.002 (1)	-0.020 (1)
O1	0.078 (5)	0.046 (3)	0.053 (3)	-0.022 (3)	0.014 (3)	-0.031 (3)
O2	0.075 (5)	0.041 (3)	0.041 (3)	-0.002 (3)	-0.008 (3)	-0.020 (3)
O3	0.081 (5)	0.040 (3)	0.043 (3)	-0.015 (3)	-0.002 (3)	-0.022 (3)
O4	0.088 (5)	0.049 (3)	0.038 (3)	-0.013 (3)	-0.003 (3)	-0.034 (3)
C4	0.118 (12)	0.125 (11)	0.077 (8)	-0.055 (8)	0.053 (8)	-0.033 (9)
C5	0.154 (15)	0.082 (9)	0.135 (12)	-0.062 (9)	0.059 (11)	-0.002 (9)
C6	0.124 (12)	0.057 (7)	0.088 (8)	-0.031 (6)	0.044 (8)	-0.013 (7)
C8	0.126 (13)	0.108 (10)	0.079 (8)	-0.033 (7)	-0.009 (7)	-0.060 (9)
C9	0.121 (16)	0.125 (12)	0.117 (13)	-0.057 (10)	-0.034 (10)	-0.033 (11)
C10	0.101 (16)	0.102 (11)	0.170 (19)	-0.026 (12)	-0.065 (13)	-0.022 (10)
C11	0.073 (13)	0.107 (11)	0.140 (14)	-0.017 (10)	0.017 (9)	-0.027 (9)
C12	0.043 (9)	0.076 (7)	0.096 (8)	-0.028 (6)	-0.004 (6)	-0.013 (6)
C14	0.079 (10)	0.066 (7)	0.101 (8)	-0.047 (6)	-0.006 (7)	-0.017 (7)
C15	0.070 (11)	0.089 (9)	0.154 (12)	-0.058 (9)	-0.010 (8)	-0.022 (8)
C16	0.044 (9)	0.069 (7)	0.105 (9)	-0.031 (7)	0.010 (6)	0.001 (6)
C17	0.078 (10)	0.067 (7)	0.091 (8)	-0.051 (6)	0.020 (7)	-0.011 (7)
C21	0.032 (8)	0.093 (8)	0.084 (8)	-0.005 (7)	0.006 (5)	-0.016 (6)
C22	0.086 (11)	0.095 (9)	0.068 (8)	-0.019 (7)	0.031 (7)	-0.044 (8)
C23	0.074 (10)	0.096 (9)	0.061 (7)	0.029 (6)	0.023 (6)	-0.023 (8)
C27	0.105 (12)	0.093 (9)	0.111 (10)	-0.052 (9)	0.038 (9)	-0.022 (8)
C28	0.083 (12)	0.117 (11)	0.111 (11)	-0.076 (9)	0.059 (9)	-0.046 (9)
C29	0.133 (13)	0.113 (10)	0.048 (6)	-0.039 (7)	0.029 (7)	-0.057 (10)
C32	0.097 (11)	0.078 (8)	0.091 (8)	-0.019 (6)	-0.004 (7)	-0.050 (8)
C33	0.076 (13)	0.151 (14)	0.141 (12)	-0.075 (11)	0.032 (9)	-0.078 (11)
C34	0.051 (13)	0.259 (23)	0.167 (15)	-0.144 (17)	0.041 (10)	-0.082 (14)
C35	0.107 (17)	0.122 (13)	0.181 (17)	-0.050 (12)	-0.036 (12)	-0.016 (12)
C36	0.063 (11)	0.083 (9)	0.175 (14)	-0.044 (9)	-0.002 (9)	-0.027 (8)

Table 11 Bond lengths (Å) for **Ph₂(HO)SiOSi(Ph₂)OSi(OH)Ph₂**
compound 3

Si1 -O1	1.618 (6)	Si1 -O4	1.631 (6)
Si1 -C1	1.827 (9)	Si1 -C7	1.847 (9)
Si2 -O1	1.614 (6)	Si2 -O2	1.618 (6)
Si2 -C13	1.839 (9)	Si2 -C19	1.863 (8)
Si3 -O2	1.617 (6)	Si3 -O3	1.651 (5)
Si3 -C25	1.875 (9)	Si3 -C31	1.854 (10)
C1 -C2	1.387 (11)	C1 -C6	1.405 (13)
C2 -C3	1.370 (12)	C3 -C4	1.352 (14)
C4 -C5	1.372 (15)	C5 -C6	1.376 (14)
C7 -C8	1.358 (13)	C7 -C12	1.375 (13)
C8 -C9	1.400 (18)	C9 -C10	1.352 (20)
C10 -C11	1.341 (19)	C11 -C12	1.363 (16)
C13 -C14	1.374 (13)	C13 -C18	1.375 (11)
C14 -C15	1.384 (15)	C15 -C16	1.350 (15)
C16 -C17	1.358 (14)	C17 -C18	1.372 (14)
C19 -C20	1.348 (12)	C19 -C24	1.394 (11)
C20 -C21	1.406 (13)	C21 -C22	1.353 (14)
C22 -C23	1.324 (15)	C23 -C24	1.414 (13)
C25 -C26	1.348 (12)	C25 -C30	1.420 (12)
C26 -C27	1.363 (14)	C27 -C28	1.365 (16)
C28 -C29	1.351 (16)	C29 -C30	1.403 (13)
C31 -C32	1.366 (12)	C31 -C36	1.344 (14)
C32 -C33	1.331 (16)	C33 -C34	1.392 (20)
C34 -C35	1.347 (20)	C35 -C36	1.346 (18)

Table 12 Bond angles (°) for Ph₂(HO)SiOSi(Ph₂)OSi(OH)Ph₂ compound

3

O4	-Si1	-O1	109.1 (3)	C1	-Si1	-O1	111.0 (4)
C1	-Si1	-O4	110.5 (4)	C7	-Si1	-O1	107.9 (4)
C7	-Si1	-O4	106.9 (4)	C7	-Si1	-C1	111.2 (4)
O2	-Si2	-O1	109.3 (3)	C13	-Si2	-O1	108.8 (4)
C13	-Si2	-O2	110.6 (3)	C19	-Si2	-O1	108.4 (3)
C19	-Si2	-O2	108.9 (4)	C19	-Si2	-C13	110.8 (4)
O3	-Si3	-O2	110.4 (3)	C25	-Si3	-O2	107.5 (4)
C25	-Si3	-O3	108.3 (3)	C31	-Si3	-O2	109.8 (4)
C31	-Si3	-O3	108.5 (4)	C31	-Si3	-C25	112.4 (4)
Si2	-O1	-Si1	163.1 (5)	Si3	-O2	-Si2	155.7 (4)
C6	-C1	-C2	116.0 (9)	C3	-C2	-C1	123 (1)
C4	-C3	-C2	120 (1)	C5	-C4	-C3	120 (1)
C6	-C5	-C4	121 (1)	C5	-C6	-C1	120 (1)
C8	-C7	-Si1	124.4 (9)	C12	-C7	-Si1	118.9 (8)
C12	-C7	-C8	117 (1)	C9	-C8	-C7	120 (1)
C10	-C9	-C8	120 (2)	C11	-C10	-C9	122 (2)
C12	-C11	-C10	117 (1)	C11	-C12	-C7	124 (1)
C14	-C13	-Si2	122.6 (7)	C18	-C13	-Si2	120.9 (7)
C18	-C13	-C14	116.4 (9)	C15	-C14	-C13	120 (1)
C16	-C15	-C14	121 (1)	C17	-C16	-C15	119 (1)
C18	-C17	-C16	119 (1)	C17	-C18	-C13	123 (1)
C20	-C19	-Si2	122.7 (7)	C24	-C19	-Si2	119.1 (7)
C24	-C19	-C20	118.0 (9)	C21	-C20	-C19	122 (1)
C22	-C21	-C20	119 (1)	C23	-C22	-C21	120 (1)
C24	-C23	-C22	122 (1)	C23	-C24	-C19	118 (1)
C26	-C25	-Si3	124.1 (7)	C30	-C25	-Si3	117.0 (7)
C30	-C25	-C26	118.8 (9)	C27	-C26	-C25	121 (1)
C28	-C27	-C26	122 (1)	C29	-C28	-C27	118 (1)

**X-ray crystallography supplementary tables for
1,1,1,3,5,5,5-heptaphenyl-3-bora1,5-siloxane, compound 16**

Table 13 Fractional atomic coordinates and thermal parameters (Å) for
PhB(Ph₃SiO)₂ compound 16

Atom	x	y	z	Uiso or Ueq (***	
Si1	0.67897 (6)	0.03017 (11)	0.58477 (5)	0.0461 (6)	***
Si2	0.84668 (5)	0.11470 (11)	0.78621 (5)	0.0421 (6)	***
B1	0.8010 (2)	0.1965 (4)	0.6505 (2)	0.041 (2)	***
C2	0.6821 (2)	-0.2534 (3)	0.6220 (2)	0.077 (3)	***
C3	0.6635 (2)	-0.3684 (3)	0.6578 (2)	0.092 (4)	***
C4	0.6123 (2)	-0.3561 (3)	0.7012 (2)	0.101 (5)	***
C5	0.5797 (2)	-0.2288 (3)	0.7090 (2)	0.098 (4)	***
C6	0.5983 (2)	-0.1138 (3)	0.6733 (2)	0.080 (3)	***
C1	0.6495 (2)	-0.1261 (3)	0.6298 (2)	0.055 (2)	***
C8	0.6603 (1)	-0.1117 (3)	0.4590 (1)	0.065 (3)	***
C9	0.6812 (1)	-0.1637 (3)	0.3996 (1)	0.078 (3)	***
C10	0.7500 (1)	-0.1338 (3)	0.3848 (1)	0.076 (3)	***
C11	0.7979 (1)	-0.0519 (3)	0.4293 (1)	0.072 (3)	***
C12	0.7770 (1)	0.0001 (3)	0.4887 (1)	0.058 (2)	***
C7	0.7082 (1)	-0.0298 (3)	0.5035 (1)	0.053 (2)	***
C14	0.5613 (1)	0.1779 (3)	0.5061 (1)	0.059 (3)	***
C15	0.5052 (1)	0.2748 (3)	0.4967 (1)	0.070 (3)	***
C16	0.4908 (1)	0.3531 (3)	0.5520 (1)	0.079 (3)	***
C17	0.5325 (1)	0.3346 (3)	0.6165 (1)	0.079 (3)	***
C18	0.5886 (1)	0.2377 (3)	0.6259 (1)	0.070 (3)	***
C13	0.6030 (1)	0.1594 (3)	0.5706 (1)	0.049 (2)	***
C20	0.7579 (1)	0.3614 (3)	0.5486 (1)	0.063 (3)	***
C21	0.7677 (1)	0.4778 (3)	0.5097 (1)	0.078 (3)	***
C22	0.8311 (1)	0.5558 (3)	0.5253 (1)	0.078 (3)	***
C23	0.8847 (1)	0.5176 (3)	0.5798 (1)	0.076 (3)	***
C24	0.8749 (1)	0.4012 (3)	0.6187 (1)	0.059 (3)	***

Table 13 **continued...**

C19	0.8115 (1)	0.3231 (3)	0.6031 (1)	0.046 (2)	***
C26	0.7287 (2)	0.2707 (2)	0.8164 (2)	0.084 (3)	***
C27	0.6604 (2)	0.2916 (2)	0.8344 (2)	0.101 (4)	***
C28	0.6166 (2)	0.1787 (2)	0.8436 (2)	0.081 (3)	***
C29	0.6412 (2)	0.0449 (2)	0.8347 (2)	0.085 (4)	***
C30	0.7095 (2)	0.0240 (2)	0.8167 (2)	0.067 (3)	***
C25	0.7533 (2)	0.1370 (2)	0.8076 (2)	0.046 (2)	***
C32	0.9707 (1)	0.2866 (3)	0.8281 (1)	0.053 (2)	***
C33	1.0208 (1)	0.3562 (3)	0.8763 (1)	0.062 (3)	***
C34	1.0136 (1)	0.3537 (3)	0.9452 (1)	0.070 (3)	***
C35	0.9564 (1)	0.2815 (3)	0.9659 (1)	0.080 (3)	***
C36	0.9062 (1)	0.2119 (3)	0.9177 (1)	0.068 (3)	***
C31	0.9134 (1)	0.2114 (3)	0.8488 (1)	0.044 (2)	***
C38	0.9215 (1)	-0.1287 (3)	0.8409 (1)	0.065 (3)	***
C39	0.9378 (1)	-0.2692 (3)	0.8414 (1)	0.076 (3)	***
C40	0.9047 (1)	-0.3541 (3)	0.7884 (1)	0.073 (3)	***
C41	0.8552 (1)	-0.2983 (3)	0.7349 (1)	0.073 (3)	***
C42	0.8388 (1)	-0.1578 (3)	0.7344 (1)	0.062 (3)	***
C37	0.8719 (1)	-0.0729 (3)	0.7873 (1)	0.048 (2)	***
O1	0.7481 (1)	0.0996 (3)	0.6349 (1)	0.052 (1)	
O2	0.8482 (1)	0.1824 (3)	0.7103 (1)	0.049 (1)	

Table 14 Fractional atomic coordinates for the hydrogen atoms for
PhB(Ph₃SiO)₂ compound 16

Atom	x	y	z
H2	0.7218	-0.2629	0.5884
H3	0.6887	-0.4670	0.6518
H4	0.5979	-0.4452	0.7289
H5	0.5400	-0.2193	0.7426
H6	0.5731	-0.0152	0.6793
H8	0.6070	-0.1349	0.4705
H9	0.6441	-0.2271	0.3652
H10	0.7661	-0.1740	0.3388
H11	0.8511	-0.0287	0.4178
H12	0.8140	0.0635	0.5232
H14	0.5725	0.1173	0.4633
H15	0.4729	0.2891	0.4468
H16	0.4474	0.4281	0.5447
H17	0.5213	0.3952	0.6593
H18	0.6209	0.2233	0.6758
H20	0.7088	0.3010	0.5366
H21	0.7262	0.5074	0.4675
H22	0.8387	0.6459	0.4952
H23	0.9338	0.5780	0.5919
H24	0.9163	0.3716	0.6609
H26	0.7626	0.3582	0.8093
H27	0.6414	0.3952	0.8412
H28	0.5637	0.1948	0.8575
H29	0.6073	-0.0425	0.8418
H30	0.7285	-0.0795	0.8099
H32	0.9763	0.2885	0.7748
H33	1.0652	0.4121	0.8603
H34	1.0524	0.4076	0.9825

Table 14 **continued...**

H36	0.8619	0.1561	0.9337
H38	0.9471	-0.0630	0.8819
H39	0.9762	-0.3124	0.8828
H40	0.9174	-0.4629	0.7888
H41	0.8296	-0.3640	0.6939
H42	0.8005	-0.1146	0.6929

Table 15 continued...

C26	0.074 (3)	0.066 (3)	0.113 (4)	-0.017 (3)	0.025 (3)	0.005 (2)
C27	0.081 (4)	0.087 (4)	0.135 (5)	-0.024 (4)	0.038 (4)	0.018 (3)
C28	0.054 (3)	0.119 (4)	0.070 (3)	-0.020 (3)	0.015 (2)	0.008 (3)
C29	0.066 (3)	0.091 (4)	0.097 (4)	-0.013 (3)	0.028 (3)	-0.017 (3)
C30	0.053 (2)	0.069 (3)	0.078 (3)	0.002 (2)	0.020 (2)	-0.005 (2)
C25	0.047 (2)	0.054 (2)	0.038 (2)	-0.008 (2)	0.004 (2)	-0.002 (2)
C32	0.046 (2)	0.053 (2)	0.060 (2)	-0.001 (2)	-0.001 (2)	0.002 (2)
C33	0.045 (2)	0.058 (3)	0.082 (3)	-0.011 (2)	0.002 (2)	-0.002 (2)
C34	0.058 (3)	0.082 (3)	0.071 (3)	-0.032 (3)	-0.011 (2)	0.001 (2)
C35	0.080 (3)	0.110 (4)	0.049 (2)	-0.022 (3)	-0.003 (2)	-0.007 (3)
C36	0.070 (3)	0.092 (4)	0.042 (2)	-0.004 (2)	-0.001 (2)	-0.013 (3)
C31	0.046 (2)	0.048 (2)	0.039 (2)	0.000 (2)	0.002 (2)	0.003 (2)
C38	0.070 (3)	0.068 (3)	0.056 (3)	0.003 (2)	-0.003 (2)	0.008 (2)
C39	0.070 (3)	0.075 (3)	0.083 (3)	0.022 (3)	0.002 (3)	0.011 (3)
C40	0.072 (3)	0.056 (3)	0.090 (3)	0.012 (3)	0.021 (3)	0.014 (2)
C41	0.081 (3)	0.058 (3)	0.081 (3)	-0.016 (2)	0.011 (3)	0.010 (2)
C42	0.062 (3)	0.061 (3)	0.063 (3)	-0.010 (2)	0.005 (2)	0.009 (2)
C37	0.043 (2)	0.057 (2)	0.044 (2)	0.001 (2)	0.008 (2)	0.002 (2)

Table 16 **Bond lengths (Å) for PhB(Ph₃SiO)₂ compound 16**

Si1 -O1	1.637 (3)	Si1 -C1	1.885 (3)
Si1 -C7	1.877 (3)	Si1 -C13	1.877 (3)
Si2 -O2	1.647 (3)	Si2 -C25	1.874 (3)
Si2 -C31	1.874 (2)	Si2 -C37	1.876 (3)
O1 -B1	1.360 (5)	O2 -B1	1.361 (5)
B1 -C19	1.577 (5)	C2 -C3	1.395 (1)
C2 -C1	1.395 (1)	C3 -C4	1.395 (1)
C4 -C5	1.395 (1)	C5 -C6	1.395 (1)
C6 -C1	1.395 (1)	C8 -C9	1.395 (1)
C8 -C7	1.395 (1)	C9 -C10	1.395 (1)
C10 -C11	1.395 (1)	C11 -C12	1.395 (1)
C12 -C7	1.395 (1)	C14 -C15	1.395 (1)
C14 -C13	1.395 (1)	C15 -C16	1.395 (1)
C16 -C17	1.395 (1)	C17 -C18	1.395 (1)
C18 -C13	1.395 (1)	C20 -C21	1.395 (1)
C20 -C19	1.395 (1)	C21 -C22	1.395 (1)
C22 -C23	1.395 (1)	C23 -C24	1.395 (1)
C24 -C19	1.395 (1)	C26 -C27	1.395 (1)
C26 -C25	1.395 (1)	C27 -C28	1.395 (1)
C28 -C29	1.395 (1)	C29 -C30	1.395 (1)
C30 -C25	1.395 (1)	C32 -C33	1.395 (1)
C32 -C31	1.395 (1)	C33 -C34	1.395 (1)
C34 -C35	1.395 (1)	C35 -C36	1.395 (1)
C36 -C31	1.395 (1)	C38 -C39	1.395 (1)
C38 -C37	1.395 (1)	C39 -C40	1.395 (1)
C40 -C41	1.395 (1)	C41 -C42	1.395 (1)
C42 -C37	1.395 (1)		

Table 17 **Bond angles (°) for PhB(Ph₃SiO)₂ compound 16**

C1	-Si1	-O1	107.8 (1)	C7	-Si1	-O1	109.6 (1)
C7	-Si1	-C1	107.9 (1)	C13	-Si1	-O1	108.5 (1)
C13	-Si1	-C1	109.5 (1)	C13	-Si1	-C7	113.5 (1)
C25	-Si2	-O2	108.6 (1)	C31	-Si2	-O2	106.9 (1)
C31	-Si2	-C25	109.4 (1)	C37	-Si2	-O2	110.7 (1)
C37	-Si2	-C25	110.5 (1)	C37	-Si2	-C31	110.7 (1)
B1	-O1	-Si1	153.1 (3)	B1	-O2	-Si2	136.9 (3)
O2	-B1	-O1	118.0 (3)	C19	-B1	-O1	123.9 (3)
C19	-B1	-O2	118.1 (3)	C1	-C2	-C3	120.0 (1)
C4	-C3	-C2	120.0 (1)	C5	-C4	-C3	120.0 (1)
C6	-C5	-C4	120.0 (1)	C1	-C6	-C5	120.0 (1)
C2	-C1	-Si1	119.4 (1)	C6	-C1	-Si1	120.5 (1)
C6	-C1	-C2	120.0 (1)	C7	-C8	-C9	120.0 (1)
C10	-C9	-C8	120.0 (1)	C11	-C10	-C9	120.0 (1)
C12	-C11	-C10	120.0 (1)	C7	-C12	-C11	120.0 (1)
C8	-C7	-Si1	118.2 (1)	C12	-C7	-Si1	121.7 (1)
C12	-C7	-C8	120.0 (1)	C13	-C14	-C15	120.0 (1)
C16	-C15	-C14	120.0 (1)	C17	-C16	-C15	120.0 (1)
C18	-C17	-C16	120.0 (1)	C13	-C18	-C17	120.0 (1)
C14	-C13	-Si1	121.0 (1)	C18	-C13	-Si1	119.0 (1)
C18	-C13	-C14	120.0 (1)	C19	-C20	-C21	120.0 (1)
C22	-C21	-C20	120.0 (1)	C23	-C22	-C21	120.0 (1)
C24	-C23	-C22	120.0 (1)	C19	-C24	-C23	120.0 (1)
C20	-C19	-B1	121.6 (2)	C24	-C19	-B1	118.3 (2)
C24	-C19	-C20	120.0 (1)	C25	-C26	-C27	120.0 (1)
C28	-C27	-C26	120.0 (1)	C29	-C28	-C27	120.0 (1)
C30	-C29	-C28	120.0 (1)	C25	-C30	-C29	120.0 (1)
C26	-C25	-Si2	118.2 (1)	C30	-C25	-Si2	121.8 (1)
C30	-C25	-C26	120.0 (1)	C31	-C32	-C33	120.0 (1)
C34	-C33	-C32	120.0 (1)	C35	-C34	-C33	120.0 (1)
C36	-C35	-C34	120.0 (1)	C31	-C36	-C35	120.0 (1)

Table 17 **continued...**

C32 -C31 -Si2	121.4 (1)	C36 -C31 -Si2	118.6 (1)
C36 -C31 -C32	120.0 (1)	C37 -C38 -C39	120.0 (1)
C40 -C39 -C38	120.0 (1)	C41 -C40 -C39	120.0 (1)
C42 -C41 -C40	120.0 (1)	C37 -C42 -C41	120.0 (1)
C38 -C37 -Si2	121.1 (1)	C42 -C37 -Si2	118.8 (1)
C42 -C37 -C38	120.0 (1)		

Table 18 Intermolecular distances (Å) for PhB(Ph₃SiO)₂ compound 16

C4	...H17	2.98	1	0.0	1.0	0.0
C5	...H28	2.88	2	1.0	0.0	1.0
C1	...H15	2.98	-1	1.0	0.0	1.0
C9	...H27	2.89	-2	0.0	1.0	1.0
H8	...C15	2.66	-1	1.0	0.0	1.0
H8	...C16	2.78	-1	1.0	0.0	1.0
H10	...C40	2.94	-2	0.0	0.0	1.0
H10	...C41	2.87	-2	0.0	0.0	1.0
C21	...H36	2.82	-2	0.0	1.0	1.0
C22	...H36	2.86	-2	0.0	1.0	1.0
C23	...H41	2.88	1	0.0	-1.0	0.0
C24	...H41	2.92	1	0.0	-1.0	0.0
H21	...C29	2.89	-2	0.0	1.0	1.0
H21	...C30	2.97	-2	0.0	1.0	1.0
H23	...C32	2.97	2	2.0	-1.0	1.0
H23	...C33	2.86	2	2.0	-1.0	1.0
H23	...C34	2.98	2	2.0	-1.0	1.0
C32	...H40	2.69	1	0.0	-1.0	0.0
C33	...H40	2.95	1	0.0	-1.0	0.0
H33	...C42	2.88	2	2.0	-1.0	1.0

Table 19 **Intramolecular distances (Å) for PhB(Ph₃SiO)₂ compound 16**

Si1 ...B1	2.91	Si1 ...C2	2.84
Si1 ...C6	2.86	Si1 ...H2	2.95
Si1 ...H6	2.97	Si1 ...C8	2.82
Si1 ...C12	2.87	Si1 ...H8	2.91
Si1 ...H12	3.00	Si1 ...C14	2.86
Si1 ...C18	2.83	Si1 ...H14	2.98
Si1 ...H18	2.93	Si1 ...H20	2.88
Si2 ...B1	2.80	Si2 ...C26	2.82
Si2 ...C30	2.86	Si2 ...H26	2.91
Si2 ...H30	2.99	Si2 ...C32	2.86
Si2 ...C36	2.82	Si2 ...H32	2.99
Si2 ...H36	2.92	Si2 ...C38	2.86
Si2 ...C42	2.83	Si2 ...H38	2.98
Si2 ...H42	2.93	O1 ...O2	2.33
O1 ...C1	2.85	O1 ...C7	2.87
O1 ...H12	2.73	O1 ...C13	2.85
O1 ...H18	2.90	O1 ...C19	2.59
O1 ...H20	2.77	O1 ...H42	2.49
O2 ...C24	2.89	O2 ...C19	2.52
O2 ...H24	2.52	O2 ...C25	2.86
O2 ...C31	2.83	O2 ...H32	2.72
O2 ...C37	2.90	B1 ...H12	2.88
B1 ...C20	2.60	B1 ...C24	2.55
B1 ...H20	2.79	B1 ...H24	2.72
C2 ...C4	2.42	C2 ...C5	2.79
C2 ...C6	2.42	C2 ...H3	2.15
C2 ...H42	2.76	C3 ...C5	2.42
C3 ...C6	2.79	C3 ...C1	2.42
C3 ...H2	2.15	C3 ...H4	2.15

Table 19 continued...

C4	...C6	2.42	C4	...C1	2.79
C4	...H3	2.15	C4	...H5	2.15
C5	...C1	2.42	C5	...H4	2.15
C5	...H6	2.15	C6	...H5	2.15
C1	...H2	2.15	C1	...H6	2.15
C1	...H42	2.89	H2	...C7	2.80
H6	...C18	2.70	H6	...C13	2.87
C8	...C10	2.42	C8	...C11	2.79
C8	...C12	2.42	C8	...H9	2.15
C8	...H14	2.77	C9	...C11	2.42
C9	...C12	2.79	C9	...C7	2.42
C9	...H8	2.15	C9	...H10	2.15
C10	...C12	2.42	C10	...C7	2.79
C10	...H9	2.15	C10	...H11	2.15
C11	...C7	2.42	C11	...H10	2.15
C11	...H12	2.15	C12	...H11	2.15
C7	...H8	2.15	C7	...H12	2.15
C7	...H14	2.90	H12	...C19	2.98
C14	...C16	2.42	C14	...C17	2.79
C14	...C18	2.42	C14	...H15	2.15
C14	...H20	2.97	C15	...C17	2.42
C15	...C18	2.79	C15	...C13	2.42
C15	...H14	2.15	C15	...H16	2.15
C16	...C18	2.42	C16	...C13	2.79
C16	...H15	2.15	C16	...H17	2.15
C17	...C13	2.42	C17	...H16	2.15
C17	...H18	2.15	C18	...H17	2.15
C13	...H14	2.15	C13	...H18	2.15
C13	...H20	2.59	C20	...C22	2.42
C20	...C23	2.79	C20	...C24	2.42
C20	...H21	2.15	C21	...C23	2.42

Table 19 continued...

C21 ...C24	2.79	C21 ...C19	2.42
C21 ...H20	2.15	C21 ...H22	2.15
C22 ...C24	2.42	C22 ...C19	2.79
C22 ...H21	2.15	C22 ...H23	2.15
C23 ...C19	2.42	C23 ...H22	2.15
C23 ...H24	2.15	C24 ...H23	2.15
C19 ...H20	2.15	C19 ...H24	2.15
C26 ...C28	2.42	C26 ...C29	2.79
C26 ...C30	2.42	C26 ...H27	2.15
C27 ...C29	2.42	C27 ...C30	2.79
C27 ...C25	2.42	C27 ...H26	2.15
C27 ...H28	2.15	C28 ...C30	2.42
C28 ...C25	2.79	C28 ...H27	2.15
C28 ...H29	2.15	C29 ...C25	2.42
C29 ...H28	2.15	C29 ...H30	2.15
C30 ...H29	2.15	C25 ...H26	2.15
C25 ...H30	2.15	C25 ...H36	2.95
H30 ...C42	2.84	H30 ...C37	2.79
C32 ...C34	2.42	C32 ...C35	2.79
C32 ...C36	2.42	C32 ...H33	2.15
C33 ...C35	2.42	C33 ...C36	2.79
C33 ...C31	2.42	C33 ...H32	2.15
C33 ...H34	2.15	C34 ...C36	2.42
C34 ...C31	2.79	C34 ...H33	2.15
C34 ...H35	2.15	C35 ...C31	2.42
C35 ...H34	2.15	C35 ...H36	2.15
C36 ...H35	2.15	C36 ...H38	2.89
C31 ...H32	2.15	C31 ...H36	2.15
C31 ...H38	2.81	C38 ...C40	2.42
C38 ...C41	2.79	C38 ...C42	2.42
C38 ...H39	2.15	C39 ...C41	2.42
C39 ...C42	2.79	C39 ...C37	2.42

Table 19 **continued...**

C39 ...H38	2.15	C39 ...H40	2.15
C40 ...C42	2.42	C40 ...C37	2.79
C40 ...H39	2.15	C40 ...H41	2.15
C41 ...C37	2.42	C41 ...H40	2.15
C41 ...H42	2.15	C42 ...H41	2.15
C37 ...H38	2.15	C37 ...H42	2.15

X-ray crystallography supplementary tables for

2,2-dimethyl-4,6-diphenyl-1,3,5-triaza-2-sila-4,6-diboracyclohexane, compound 19

Table 20 **Fractional atomic coordinates and thermal parameters (Å) for**
Me₂Si(PhBNH)₂NH compound 19

Atom	x	y	z	Uiso or Ueq (***)	
Si1	0.13113 (9)	0.68818 (6)	0.48043 (10)	0.0684 (7)	***
N1	0.2965 (2)	0.7203 (2)	0.5210 (3)	0.067 (2)	***
N2	0.2441 (2)	0.8723 (2)	0.4099 (2)	0.062 (2)	***
N3	0.0431 (3)	0.7885 (2)	0.4007 (3)	0.068 (2)	***
B1	0.3432 (4)	0.8027 (2)	0.4809 (3)	0.057 (2)	***
B2	0.1011 (4)	0.8695 (2)	0.3717 (3)	0.057 (2)	***
C1	0.0866 (4)	0.5816 (3)	0.3778 (4)	0.101 (3)	***
C2	0.0964 (4)	0.6634 (3)	0.6182 (4)	0.102 (3)	***
C3	0.4967 (3)	0.8178 (2)	0.5095 (3)	0.056 (2)	***
C4	0.5347 (3)	0.8798 (2)	0.4382 (3)	0.072 (2)	***
C5	0.6707 (4)	0.8922 (2)	0.4615 (4)	0.081 (2)	***
C6	0.7699 (4)	0.8438 (3)	0.5577 (4)	0.079 (2)	***
C7	0.7358 (3)	0.7817 (3)	0.6317 (3)	0.076 (2)	***
C8	0.6011 (3)	0.7697 (2)	0.6067 (3)	0.068 (2)	***
C9	0.0098 (3)	0.9547 (2)	0.2933 (3)	0.055 (2)	***
C10	-0.0914 (3)	0.9929 (2)	0.3215 (3)	0.071 (2)	***
C11	-0.1688 (4)	1.0706 (3)	0.2566 (4)	0.091 (3)	***
C12	-0.1461 (5)	1.1095 (3)	0.1595 (4)	0.089 (3)	***
C13	-0.0456 (5)	1.0735 (3)	0.1291 (3)	0.095 (3)	***
C14	0.0314 (4)	0.9979 (2)	0.1966 (3)	0.079 (2)	***
H1	0.3683 (31)	0.6780 (25)	0.5755 (33)	0.119 (3)	
H2	0.2774 (37)	0.9300 (19)	0.3887 (34)	0.119 (3)	
H3	-0.0554 (19)	0.7881 (29)	0.3670 (36)	0.119 (3)	

Table 21 Fractional atomic coordinates for the hydrogen atoms for $\text{Me}_2\text{Si}(\text{PhBNH})_2\text{NH}$ compound 19

Atom	x	y	z
H11	-0.0175	0.5625	0.3527
H12	0.1515	0.5231	0.4268
H13	0.0998	0.5974	0.2936
H21	0.1521	0.6010	0.6660
H22	-0.0105	0.6513	0.5885
H23	0.1279	0.7235	0.6813
H41	0.4575	0.9186	0.3624
H51	0.6976	0.9401	0.4039
H61	0.8745	0.8537	0.5753
H71	0.8141	0.7439	0.7078
H81	0.5753	0.7216	0.6648
H101	-0.1118	0.9606	0.3952
H111	-0.2438	1.1011	0.2831
H121	-0.2091	1.1670	0.1047
H131	-0.0256	1.1059	0.0552
H141	0.1099	0.9703	0.1727

Table 22 Anisotropic thermal parameters (\AA) for $\text{Me}_2\text{Si}(\text{PhBNH})_2\text{NH}$ compound 19

Atom	U11	U22	U33	U23	U13	U12
Si1	0.059 (1)	0.051 (1)	0.095 (1)	0.016 (1)	0.034 (1)	-0.006 (1)
N1	0.054 (2)	0.057 (2)	0.092 (2)	0.020 (1)	0.031 (1)	-0.001 (1)
N2	0.057 (2)	0.050 (1)	0.080 (2)	0.009 (1)	0.033 (1)	-0.008 (1)
N3	0.056 (2)	0.056 (2)	0.091 (2)	0.016 (1)	0.030 (1)	-0.006 (1)
B1	0.063 (2)	0.048 (2)	0.059 (2)	-0.002 (2)	0.029 (2)	-0.004 (2)
B2	0.060 (2)	0.050 (2)	0.060 (2)	-0.001 (2)	0.027 (2)	-0.008 (2)
C1	0.099 (3)	0.062 (2)	0.141 (4)	-0.002 (2)	0.036 (3)	-0.018 (2)
C2	0.092 (3)	0.086 (3)	0.126 (3)	0.043 (2)	0.063 (3)	0.010 (2)
C3	0.058 (2)	0.048 (2)	0.062 (2)	-0.005 (1)	0.033 (2)	-0.011 (1)
C4	0.067 (2)	0.067 (2)	0.083 (2)	0.007 (2)	0.041 (2)	-0.008 (2)
C5	0.065 (2)	0.078 (2)	0.098 (2)	0.002 (2)	0.046 (2)	-0.015 (2)
C6	0.057 (2)	0.082 (2)	0.097 (3)	-0.026 (2)	0.040 (2)	-0.022 (2)
C7	0.052 (2)	0.092 (3)	0.084 (2)	0.002 (2)	0.020 (2)	-0.006 (2)
C8	0.061 (2)	0.073 (2)	0.069 (2)	0.005 (2)	0.027 (2)	-0.006 (2)
C9	0.053 (2)	0.052 (2)	0.061 (2)	0.005 (1)	0.016 (2)	-0.011 (1)
C10	0.048 (2)	0.070 (2)	0.095 (2)	0.024 (2)	0.022 (2)	0.000 (2)
C11	0.066 (3)	0.082 (3)	0.124 (3)	0.016 (3)	0.022 (2)	0.001 (2)
C12	0.098 (3)	0.070 (2)	0.098 (3)	0.022 (2)	0.001 (3)	0.008 (2)
C13	0.144 (4)	0.068 (3)	0.073 (2)	0.022 (2)	0.031 (3)	0.002 (3)
C14	0.112 (3)	0.061 (2)	0.065 (2)	0.005 (2)	0.039 (2)	-0.003 (2)

Table 23 **Bond lengths (Å) for Me₂Si(PhBNH)₂NH compound 19**

Si1 -N1	1.720 (3)	Si1 -N3	1.741 (3)
Si1 -C1	1.855 (4)	Si1 -C2	1.844 (4)
N1 -B1	1.425 (4)	N1 -H1	0.976 (18)
N2 -B1	1.435 (4)	N2 -B2	1.430 (4)
N2 -H2	0.965 (18)	N3 -B2	1.412 (4)
N3 -H3	0.977 (18)	B1 -C3	1.576 (5)
B2 -C9	1.582 (5)	C3 -C4	1.389 (4)
C3 -C8	1.399 (4)	C4 -C5	1.402 (5)
C5 -C6	1.371 (5)	C6 -C7	1.388 (5)
C7 -C8	1.382 (5)	C9 -C10	1.388 (4)
C9 -C14	1.392 (4)	C10 -C11	1.395 (5)
C11 -C12	1.378 (6)	C12 -C13	1.385 (6)
C13 -C14	1.379 (5)		

Table 24 **Bond angles (°) for Me₂Si(PhBNH)₂NH compound 19**

N3	-Si1	-N1	102.2 (1)	C1	-Si1	-N1	110.4 (2)
C1	-Si1	-N3	111.8 (2)	C2	-Si1	-N1	112.8 (2)
C2	-Si1	-N3	110.7 (2)	C2	-Si1	-C1	108.8 (2)
B1	-N1	-Si1	127.0 (2)	H1	-N1	-Si1	119 (2)
H1	-N1	-B1	114 (2)	B2	-N2	-B1	128.2 (2)
H2	-N2	-B1	117 (2)	H2	-N2	-B2	115 (2)
B2	-N3	-Si1	125.6 (2)	H3	-N3	-Si1	118 (2)
H3	-N3	-B2	116 (2)	N2	-B1	-N1	117.3 (3)
C3	-B1	-N1	122.3 (3)	C3	-B1	-N2	120.3 (3)
N3	-B2	-N2	119.1 (3)	C9	-B2	-N2	119.8 (3)
C9	-B2	-N3	121.0 (3)	C4	-C3	-B1	121.1 (3)
C8	-C3	-B1	122.4 (3)	C8	-C3	-C4	116.5 (3)
C5	-C4	-C3	121.4 (3)	C6	-C5	-C4	120.1 (3)
C7	-C6	-C5	120.0 (3)	C8	-C7	-C6	119.1 (3)
C7	-C8	-C3	122.8 (3)	C10	-C9	-B2	121.5 (3)
C14	-C9	-B2	121.6 (3)	C14	-C9	-C10	116.8 (3)
C11	-C10	-C9	122.1 (3)	C12	-C11	-C10	119.0 (4)
C13	-C12	-C11	120.4 (4)	C14	-C13	-C12	119.4 (4)
C13	-C14	-C9	122.2 (4)				

Table 25 **Intermolecular distances (Å) for Me₂Si(PhBNH)₂NH compound**
19

N2	...H81	2.99	-2	1.0	2.0	1.0
N3	...H81	2.94	-2	1.0	2.0	1.0
B2	...H81	2.65	-2	1.0	2.0	1.0
H13	...C8	2.89	-2	1.0	2.0	1.0
H21	...C10	2.93	-2	0.0	2.0	0.0
H23	...C11	2.97	-1	0.0	2.0	1.0
H23	...C12	2.95	-1	0.0	2.0	1.0
C5	...H101	2.95	1	-1.0	0.0	0.0
C5	...H2	2.97	-1	1.0	2.0	1.0
H51	...C10	2.94	1	-1.0	0.0	0.0
C8	...H131	2.88	2	0.0	0.0	0.0

Table 26 Intramolecular distances (Å) for Me₂Si(PhBNH)₂NH compound
19

Si1 ...B1	2.82	Si1 ...B2	2.81
Si1 ...H11	2.44	Si1 ...H12	2.44
Si1 ...H13	2.43	Si1 ...H21	2.42
Si1 ...H22	2.43	Si1 ...H23	2.42
Si1 ...H1	2.35	Si1 ...H3	2.37
N1 ...N2	2.44	N1 ...N3	2.69
N1 ...B2	2.98	N1 ...C1	2.94
N1 ...C2	2.97	N1 ...C3	2.63
N1 ...H81	2.79	N2 ...N3	2.45
N2 ...C3	2.61	N2 ...H41	2.69
N2 ...C9	2.61	N2 ...H141	2.89
N3 ...C1	2.98	N3 ...C2	2.95
N3 ...C9	2.61	N3 ...H101	2.94
B1 ...B2	2.58	B1 ...C4	2.58
B1 ...H41	2.76	B1 ...C8	2.61
B1 ...H81	2.79	B1 ...H1	2.03
B1 ...H2	2.06	B2 ...C10	2.59
B2 ...H101	2.77	B2 ...C14	2.60
B2 ...H141	2.77	B2 ...H2	2.03
B2 ...H3	2.04	C3 ...H41	2.13
C3 ...C5	2.43	C3 ...C6	2.81
C3 ...C7	2.44	C3 ...H81	2.14
C3 ...H1	2.71	C3 ...H2	2.71
C4 ...H51	2.16	C4 ...C6	2.40
C4 ...C7	2.77	C4 ...C8	2.37
C4 ...H2	2.71	H41 ...C5	2.15
H41 ...H2	2.12	C5 ...H61	2.12
C5 ...C7	2.39	C5 ...C8	2.75
H51 ...C6	2.13	C6 ...H71	2.14

C6	...C8	2.39
C7	...H81	2.12
C8	...H1	2.73
C9	...H101	2.13
C9	...C12	2.80
C9	...H141	2.13
C9	...H3	2.70
C10	...C12	2.39
C10	...C14	2.37
H101...	C11	2.14
C11	...H121	2.13
C11	...C14	2.76
C12	...H131	2.14
H121...	C13	2.14
H131...	C14	2.14
H141...	H2	2.48

H61	...C7	2.15
H71	...C8	2.15
H81	...H1	2.14
C9	...C11	2.44
C9	...C13	2.43
C9	...H2	2.67
C10	...H111	2.16
C10	...C13	2.76
C10	...H3	2.93
H101...	H3	2.56
C11	...C13	2.40
H111...	C12	2.14
C12	...C14	2.39
C13	...H141	2.12
C14	...H2	2.84